Understanding Melt Behavior of Ice Cream: Influence of the Microstructure and Composition on Drip-Through Rate of Ice Cream Products

By

Maya M. Warren

A dissertation submitted in partial fulfillment of the requirements for the degree of

Doctor of Philosophy

(Food Science)

at the

UNIVERSITY OF WISCONSIN-MADISON

2015

Date of final oral examination: 9/18/2015

The dissertation is approved by the following members of the Final Oral Committee:

Richard W. Hartel, Professor, Food Science

Scott A. Rankin, Professor, Food Science

Shinya Ikeda, Assistant Professor, Food Science

Hans Zoerb, Lecture, Food Science

Mark P. Richards, Professor, Animal Science

©Copyright by Maya M. Warren 2015
All Rights Reserved

ABSTRACT

Ice cream is a complex, partially frozen food with a microstructure composed of ice crystals, air cells, fat globules, and partially-coalesced fat globules all dispersed in an unfrozen serum phase (sugars, proteins, stabilizers). The effect of the microstructure on drip-through rate has been of great interest. Much of the literature attributes a decrease in drip-through rate to an increase in partially-coalesced fat.

It was hypothesized that as dasher speed, overrun, emulsifiers (MDG and PS80), and fat content increased, partial coalescence would increase while drip-through rate would decrease across all experiments. In addition, it was hypothesized that the microstructure components could be used to predict the drip-through rate of ice cream products.

In this current work two main studies were carried out. The first study was a survey on the microstructure, compositional, and sensorial properties of United States commercial ice cream products. In the second study (controlled ice cream study), experiments were carried out to control partial coalescence and drip-through rate through varying processing conditions (dasher speed (250 RPM, 500 RPM, 750 RPM) and overrun (50%, 75%, 100%)) and formulation parameters (emulsifier ratios (100:0, 90:10, 80:20 – mono- and diglyceride:polysorbate 80 (MDG:PS80)) and fat content (6%, 9%, 12%, 15%)). Experiments were also run with no added emulsifiers.

From the survey, commercial ice cream products varied widely in composition, structure, behavior, and sensory properties. From a multivariate pairwise comparison test, it was determined that ice crystal size, percent destabilized fat, total fat, and total solids inversely

correlated with drip-through rate. No statistically significant correlation was determined between instrumental analysis of drip-through rate and sensorial melt rate. Furthermore, creaminess and greasiness both had an inverse relationship with drip-through rate while sensorial melt rate did not correlate with instrumental measured drip-through rate. In the controlled ice cream study, as emulsifiers (especially PS80), dasher speed, and overrun increased, partial coalescence increased. However, drip-through rate did not always correlate with partial coalescence, as hypothesized. In addition, as fat content increased, partial coalescence increased from 6% to 9% but not between 9% and 15%. Furthermore, no difference in drip-through rate was determined as fat increased.

Overall, there were various microstructure components that affected melt behavior of ice cream. The interaction of the size and number of air cells and partially-coalesced fat globules seemed to greatly affect drip-through rate. The amount of remnant foam corresponded with drip-through rates. With this knowledge, we were able to gain a better understanding of the effects on microstructure components and their interactions on drip-through rate.

DEDICATION

This dissertation is dedicated to my family, friends, and young scientists all around the world and is written in memory of my loving and hilarious Godfather, Mark Edward Collins.

ACKNOWLEDGEMENTS

Much gratitude and appreciation is given to my advisor, Professor Richard W. Hartel, for his willingness to allow me to complete my PhD in his lab and for his endless conversations and intriguing questions on ice cream. I am forever appreciative for the great mentorship you have provided and for always being a listening ear. You have helped me to truly follow my dreams and have always seen more in me than I have myself. Thank you for pushing me to be my best and for the unintentional countless laughs over the years! I look forward to more to come!

To my committee members, Dr. Shinya Ikeda, Dr. Scott Rankin, Dr. Mark Richards, and Dr. Hans Zoerb, thank you for time, encouragement, and dedication to the betterment and advancement in science.

Much gratitude it given to Dr. Eden Inoway-Ronni for the many chats over delicious meals and most of all, for connecting me to Professor Richard W. Hartel.

Thank you to the numerous undergraduate research assistants whom have worked under me during my time at Madison. Margaret, Becky, Michael, Peter, Caroline, Elli, Jacy, Alex, Katie Jones, Katie Moy, Nicole, Emma, Molly, Angie, Mack, Tassy (honorary) and Leah, for your work and dedication, I am forever grateful.

To my wonderful lab mates, it has been a great time in the basement of Babcock Hall. Truly a time that I will never forget. Thank you for putting up with the many Maya-isms! And a special thank you to my #SweetScientists partner in crime, Amy DeJong. Together, we experienced an adventure of a lifetime and inspired people all across the globe, including ourselves, showing what scientists and women can do and be.

And finally to all those who have encouraged me to not just reach for the stars, but leap

over the moon, I thank you. For listening to my countless stories on how much I love ice cream and for often being my taste testers, my appreciation goes to you! Thank you for believing in me and for helping my dreams become a reality. I hope this work inspires people to think outside the box and to do something that they've always wanted to do like this research has done for me.

TABLE OF CONTENTS

List of Tables

List of Figures

Introduction

Ice cream is a complex, partially frozen food composed of partially-crystalline individual fat globules, partially-coalesced fat globules (partially crystalline), ice crystals, and air cells, all dispersed in an unfrozen serum phase (Goff and Hartel, 2013). Each of these components are formed when ice cream mix enters into a barrel-shaped scraped surface heat exchanger, either a continuous or batch freezer, and the mix is frozen and whipped into ice cream (Cook and Hartel, 2010). Microstructural components (fat globules, partially-coalesced fat, ice, and air) are critical to the overall structure and properties of ice cream and differ greatly depending on the formulation and the processing conditions used to make ice cream. These microstructural components also affect meltdown/drip-through behavior (Hartel et al., 2003) and sensorial properties of ice cream products (Stampanoni Koeferli et al., 2004).

In the United States, roughly 1.53 billion gallons (5.79 billion liters) of ice cream and ice cream products were produced in 2011 (USDA, Natl. Agriculture Statistics Service). According to the Standard of Identity, in the United States, all products labeled ice cream must have at least 10% milk fat and 20% total milk solids and must weigh a minimum of 4.5 lb/gal (449 kg/m^3; Code of regulations, Title 2 Food and Drugs, Part 135 Frozen Desserts). Ice cream products include, but are not limited to, those labeled low fat, reduced fat, light, and nonfat ice cream.

Structural and compositional attributes are key to understanding the behavior of ice cream products. Both ingredients and processing conditions can greatly affect the structural attributes and therefore the rate of drip (the rate [g/min] at which ice cream drips through a mesh screen at ambient temperatures) of ice cream products. There are many key driving factors within the microstructure of ice cream products that influence the rate of drip (Muse and Hartel, 2004). An increase in the percentage of partially-coalesced fat (Berger and White, 1971; Berger

et al., 1972; Segall and Goff, 2002; Muse and Hartel, 2004), increase in overrun (Sakurai et al., 1996; Sofjan and Hartel, 2004), increase in total percent fat (Roland et al., 1999), and a decrease in mean ice crystal size (Muse and Hartel, 2004) have all been shown to decrease drip-through rate. However, there exist contradictions in the literature on the exact structural influences on the drip-through rate of ice cream products. Koxholt et al. (2001) did not find any influence of size of ice crystals on the rate of drip. In addition, overrun did not influence drip-through rate in the study by Muse and Hartel (2004). Koxholt et al. (2001) reported that slow drip-through rate could also be achieved with minimal extent of partial coalescence (critical fat globule size determined at $D_{50,3}$ approximately 1.15 μm resulted in a decrease in rate of drip). Thus, contradictory results relating the effects of structural attributes of ice cream on or to the drip-through rate have been observed. These inconsistencies most likely exist due to variations in the type of ingredients used and conditions of manufacturing.

Although there has been much research on the microstructure of ice cream, the impact on drip-through rate is not fully understood. The aim of this study was two fold. First, a better understanding of the microstructure, behavioral (melting), compositional, and sensorial properties of United States commercial ice cream products was sought. This was carried out via a survey of commercial ice cream samples. Based on the survey results, a second study was designed to control partial coalescence by varying processing conditions and formulation parameters and then to correlate the nature of fat clusters with drip-through rate.

2. Literature Review

Structural and compositional attributes are key to understanding the behavior of ice cream products. Both ingredients and processing conditions can greatly affect the structural attributes and, therefore, the melt rate (or drip-through rate - [g/min] at which ice cream drips through a mesh screen at ambient temperatures) of ice cream products. There are many key driving factors within the microstructure of ice cream products that influence the drip-through rate (Muse and Hartel, 2004). Partial coalescence is one aspect of the microstructure that is of particular importance. For this reason, controlling partial coalescence through both processing and formulation parameters is of interest. Understanding interaction parameters of the microstructure and their influences on the melt behavior of ice cream products will lead to the development of a structural model. This structural model for the melt behavior of ice cream products would have significant importance in better understanding the driving factors behind the drip-through rate of ice cream products.

2.1 Ice Cream Composition

Traditional ice cream mix is composed of milk fat, milk solids nonfat (MSNF), water, sweeteners, stabilizers, and emulsifiers. This mixture then becomes ice cream during the dynamic freezing process to create a complex, partially frozen food composed of partially-crystalline individual fat globules, partially-coalesced fat globules, ice crystals and air cells, all dispersed in the continuous serum phase (Goff and Hartel, 2013). **Figure 2.1** shows a schematic of ice cream mix and the structure of ice cream. In the United States, there is a standard identity for ice cream. To be labeled ice cream, it must consist of at least 10% milk fat and 20% total milk solids, contain1.6 lbs total solids per gallon, and must weigh a minimum of 4.5 lb/gal (449

kg/m^3) (21CFR135.110). Due to this standard of identity, there are numerous other categories of frozen dessert products that have different compositions (for example, lower in fat). The approximate compositions of ice cream and several other frozen dessert categories are listed in **Table 2.1**. As the level of fat increases and the overrun decreases, the premium level of ice cream tends to increase.

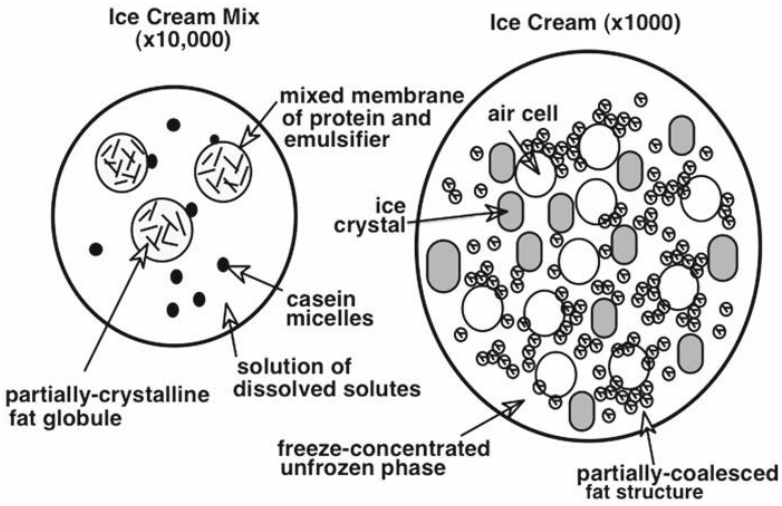

Figure 2.1: Schematic diagram of ice cream mix and ice cream (Goff and Hartel, 2013).

Table 2.1: Approximate composition (% weight) of various ice cream products (Adapted from Goff and Hartel, 2013).

Group	Milk fat	Milk solids-not-fat	Sweeteners[a]	Stabilizers[b] and emulsifiers	Total solids
Nonfat ice cream	<0.5	12–14	18–22	1.0	28–32
Low-fat ice cream	2–5	12–14	18–21	0.8	28–32
Light ice cream	5–7	11–12	18–20	0.5	30–35
Reduced-fat ice cream	7–9	10–12	18–19	0.4	32–36
Economy ice cream	10	10–11	15–17	0.4	35–36
Standard ice cream	10–12	9–10	14–17	0.2–0.4	36–38
Premium ice cream	12–14	8–10	13–16	0.2–0.4	38–40
Superpremium ice cream	14–18	5–8	14–17	0–0.2	40–42

2.1.1 Fat

Milk fat provides the lipid content to ice cream products. It can come from fresh, frozen, and or plastic cream, milk (minimal), butter, and or anhydrous milk fat (Goff and Hartel, 2013). By legal definition, ice cream must have 10% or more milk fat. It is an important ingredient in ice cream as it adds richness of flavor, helps to provide body and a smooth mouth feel, and assists in controlling melt behavior. Fat also assists in stabilizing air cells after freezing. Altering the total fat in ice cream products to produce low fat to nonfat ice cream products can greatly affect these properties.

2.1.2 Air

Air is incorporated into ice cream during the freezing process. It provides ice cream with a smooth and sometimes fluffy texture as well as assists with the scoopability of ice cream. Air often makes up the largest component of ice cream, on a volume basis. It can be injected and or directly entrapped into the ice cream during the freezing process.

The rotation of the dasher inside of the freezer provides a whipping action, which breaks up air cells and uniformly distributes them throughout the ice cream. Ice crystals must be present to assist with increasing the viscosity of the mix so that the air can be stabilized. The increase in the volume of the ice cream mix is referred to as the overrun, which is defined in **Equation 2.1**:

$$\%Overrun = \frac{weight\ of\ mix - weight\ of\ ice\ cream}{weight\ of\ ice\ cream} \times 100 \quad (2.1)$$

In the United States, the maximum overrun is governed by the standard of identity, which indicates that the finished product must not weigh less than 0.54 kg per liter (4.5lb/gal). Typical overruns based on the standard of identity are listed in **Table 2.2**.

Table 2.2: Approximate overruns for various categories of ice cream (Adapted from Goff and Hartel, 2013).

	Overrun(%)
Economy	Legal Maxium
Standard	100-120%
Premium	60-90%
Superpremium	25-50%

2.1.3 Water and Ice

Water is added to ice cream mix from cream, milk, and or added water. Ice cream mix typically ranges from 60 – 65% average total water (Goff and Hartel, 2013). After freezing, water is present as both a solid and a liquid. This is a result of the dissolved solutes (sweeteners, milk solids, salts), which affect the freezing point depression of the mix. For a typical ice cream, exiting the freezer between -5^{o}C to -6^{o}C, roughly 50% of the water is frozen (Berger et al., 1972). When hardened at -30^{o}C, approximately 95% of the water is frozen (Berger et al., 1972). Ice crystals in ice cream range in size from over a few to over 100 μm, with a mean size between 40 to 50 μm for commercially produced hard ice cream (Goff and Hartel, 2013). Generally, smooth ice cream requires the majority of ice crystals to be smaller than roughly 50 μm. The

presence of many crystals above 50 μm or extremely large ice crystals (over 100 μm) will give rise to coarse (icy) ice cream texture, which is a defect in ice cream (Russell et al., 1999).

2.1.4 Milk Solids Non Fat (MSNF)

Lactose, proteins (casein and whey), vitamins, and minerals make up the MSNF component of ice cream. MSNF are added to ice cream products to assist in improving body and texture, whippability, and overall resistance to heat shock (Goff and Hartel, 2013). MSNF can come from ingredients, such as nonfat dry milk, fresh or condensed skim milk as well as powdered sweet cream buttermilk (Arbuckle, 1986). Whey and modified whey products, which contain mostly lactose and minerals, can also be substituted for up to 25% of the MSNF (Goff, 1992; Code of regulations, 2014 [Title 2 Food and Drugs, Part 135 Frozen Desserts]). Although a higher amount of whey solids can assist in providing a softer ice cream by altering the freezing point depression, there is a greater likelihood of lactose crystallization, which can cause a sandy defect in ice cream during storage.

2.1.5 Sweeteners

Sweeteners in ice cream provide a desirable sensory appeal, assist in lowering the freezing point depression, add to the total solids in the product, and can contribute to the viscosity of the serum phase after freezing. Common sweeteners include corn sweeteners, lactose (added from MSNF source), and sucrose, with the most common being a blend of sucrose (10-12%) and corn sweeteners (e.g. corn syrup solids, 3-5%) (Goff and Hartel, 2013). If other sweeteners are used, they can be converted to an equivalent sucrose basis to keep the sweetness of the mix the same. Total amount of desired sweetness expressed as sucrose may vary from 13 to 16% in a system that has 36-38% total solids (Goff and Hartel, 2013).

2.1.6 Stabilizers

The stabilizer system, mainly consisting of polysaccharides, plays an important role in ice cream. Stabilizers are used in ice cream to enhance the viscosity of the unfrozen ice cream phase, promote smoothness in body and texture, retard and reduce growth of ice crystals during storage, create uniform product, and provide resistance to melting (Goff and Hartel, 2013). It is common to see stabilizers added at a concentration of 0.25 - 1% in an ice cream mix (Goff and Hartel, 2013). Common stabilizers used in ice cream are guar gum, xanthan gum, carboxymethyl cellulose, locust bean gum, and carrageenan. If the stabilizer is able to form a gel that is firm enough, it can assist in inhibiting ice crystal growth and alter the morphology of ice crystals (Muhr and Blanshard, 1986). Regand and Goff (2003) also suggested that stabilizers form a cryo-gel and entrap ice crystals within the gel, helping to inhibit ice crystal growth and or recrystallization.

2.1.7 Emulsifiers

Emulsifiers are amphiphilic molecules that stabilize an oil/water or air/water interface by their hydrophobic (resides in the fat phase) and hydrophilic (resides in the aqueous phase) regions. Due to their amphiphilic properties, they are able to lower the interfacial tension of the oil/water interface. Common emulsifiers in ice cream products are mono- and diglycerides (MDG) and polysorbate 80 (PS80), a common sorbitan ester. They are used at levels of 0.1-0.2% and 0.02-0.04%, respectively (Goff and Hartel, 2013).

The role of the emulsifier is critical throughout the ice cream process, from processing mix to freezing ice cream. During the homogenization process, emulsifiers are necessary to help

reduce the size of the fat globules. During freezing, emulsifiers assist in promoting fat destabilization, improve the whipping quality of the mix, decrease the melting rate, and provide a dry, stiff, and smooth desirable texture to the product upon exit (Goff and Hartel, 2013). Emulsifiers also help to promote stabilization of air cells (Berger, 1997).

2.2 Processing

Ice cream mix is made by combining and pasteurizing ingredients, followed by homogenizing, cooling, and ageing. Ice cream mix is made into ice cream by whipping and or injecting air into mix as it freezes. Ice cream is traditionally frozen in a batch or continuous freezer. The ice cream is then packaged and hardened.

2.2.1 Mixing and Pasteurizing

When making ice cream mix on a commercial scale, typically the liquid ingredients (cream, milk, water, liquid sweeteners, etc.) are agitated and heated in a vat. The dry ingredients (nonfat dry milk, dry sweeteners, stabilizers, emulsifiers, etc.) are added to the liquid mixture before the product reaches 50^{o}C (Goff and Hartel, 2013).

The blended ingredients are then either batch pasteurized or undergo high temperature short time (HTST) pasteurization. In batch pasteurization, the mix is heated to 69^{o}C for 30 minutes, whereas in HTST, it is held for 25 seconds at 80^{o}C (Goff and Hartel, 2013). Pasteurization is key in the mix making process as it helps to inactivate pathogenic and spoilage microorganisms.

2.2.2 Homogenization

Homogenization is also a critical step in the mix making process as it reduces the size of the fat globules to roughly less than 2 μm, allowing the fat to be stabilized and dispersed throughout the mix (Goff and Hartel, 2013). Homogenization occurs when mix (typically hot) passes through a very small narrow valve at a high pressure (Goff and Hartel, 2013). The liquid fat globules are distorted and then greatly reduced in size. During this time, proteins are also adsorbed to the newly formed fat interface. Mix is commonly processed between 60-80^{o}C at a pressure of 2500 psi (2000 psi (first stage) and 500 psi (second stage) (Goff and Hartel, 2013). As fat content increases, homogenization pressures in the first stage should be reduced to prevent excessive mix viscosity (Goff and Hartel, 2013).

2.2.3 Cooling and Ageing

After homogenization, mix is cooled to 4^{o}C and allowed to age for 4-24 hours. During the cooling and ageing time, the fat begins to crystallize, which in turn helps to promote partial coalescence during freezing. If emulsifiers are present in the mix, they will displace proteins at the fat globule interface, as their low molecular weight is more favorable at the fat globule interface than proteins (Gelin et al., 1994). During this time, stabilizers also undergo hydration and increase the viscosity of the mix (Goff and Hartel, 2013). If mix is not aged properly, there is risk of loss in shape retention and faster meltdown rates.

2.2.4 Freezing

Ice cream mix enters into a cylinder shaped barrel scraped-surface heat exchanger, in a continuous or batch freezer, and is frozen into ice cream. A refrigerant (-22 ^{o}C to -32^{o}C) surrounds the walls of the freezing chamber and cools the mix. A dasher, housed inside of the barrel, whips air into ice cream and also scrapes ice crystals off the inner surface of the barrel walls and incorporates them into the product. Partial coalescence of the fat globules also occurs during the freezing stage. These fat aggregates are advantageous as they assist in incorporating air and help to stabilize small air cells incorporated during whipping of the mix and ice cream.

The freezing process occurs the same in a batch versus continuous freezer; however, the incorporation of air is different. In a batch freezer, the dasher helps to whip in air from the chamber into the mix. In a continuous freezer, air is injected or drawn in via vacuum. Also, freezing on a continuous freezer is a continuous process of whipping, freezing and drawing of product, whereas in a batch freezer, this process occurs in stages for a given amount of product and the process of freezing takes a longer time to occur. Typically, ice cream exits the freezer between -5 ^{o}C and -6^{o}C (Goff and Hartel, 2013).

2.2.5 Hardening

After mix is processed into ice cream, it is drawn from the freezer at a semisolid consistency and packaged into containers. At this state, the product is not stiff and still contains much unfrozen water. Containers are placed into a hardening chamber, typically an air-blast freezer, set between -25 and -30^{o}C (Goff and Hartel, 2013). Product is usually kept at hardening temperature for 12-24 hours to ensure little unfrozen water remains. If hardened properly, a typical ice cream mix utilizing sucrose as a sweetener contains approximately 95% frozen water

(Berger et al., 1972). In the hardening chamber, forced air currents allow the ice cream to freeze at a faster rate than compared to a traditional freezer. The rate of freezing in the hardening chamber should occur quickly in order to minimize the growth of ice crystals and air cells (Goff and Hartel, 2013). In a still chamber, a 5 gallon (18.9 L) package could take up to 24 hours to harden while a 4 ounce (118.3 ml) package may only take 30 minutes (Goff and Hartel, 2013). After hardening, ice cream is commonly stored at -18 ^{o}C to -23^{o}C.

2.3 Physical Structure

Ice cream is a complex, partially frozen food composed of partially-crystalline individual fat globules, partially-coalesced fat globules, ice crystals and air cells, all dispersed in a serum phase (Goff and Hartel, 2013). Ice cream is comprised of three phases: solid (ice, crystalline fat), gas (air), and liquid (serum). The serum phase is located between the lamellae of the air cells, which also contains fat globules, ice crystals, milk proteins, sweeteners (sucrose, lactose), soluble and insoluble salts, and stabilizers (King, 1950). When the mix is whipped and frozen into ice cream, air cells are stabilized by partially-crystalline fat globules that also aggregate together to form a continuous fat and air network throughout the serum phase (Walstra and Jonkman, 1998). At this same time, ice is formed at the barrel wall, scraped off by the rotating dasher, and dispersed into the interior of the freezer where crystals form into disc-shaped blocks (Cook and Hartel, 2010). A schematic drawing of the structure of ice cream is depicted in **Figure 2.2**. The microstructure created during freezing greatly affects the texture and overall quality of ice cream.

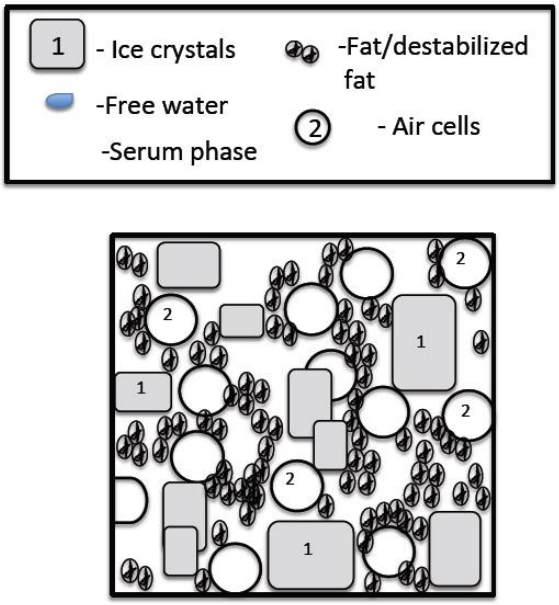

Figure 2.2: Cartoon depiction of the physical structure of ice cream.

2.3.1 Serum Phase

Ice crystals, air cells, fat globules, and partially-coalesced fat globules are dispersed in an unfrozen serum phase. The serum phase consist of sweeteners, milk salts, minerals, stabilizers, aqueous phase proteins, and any water that remains unfrozen. The serum forms the lamella between the other physical components in ice cream, assisting in holding all of the structures together (Goff and Hartel, 2013). This phase can vary greatly depending on mix composition and the temperature of the product.

2.3.2 Formation of Ice Crystals

The formation of ice occurs during the freezing process inside of the scraped surface heat exchanger. The liquid refrigerant (i.e., Freon or ammonia) surrounding the barrel vaporizes under pressure at -30^{o}C and allows for the ice cream mix to begin cooling. To begin freezing, the refrigerant removes heat to cause the mix to fall below its freezing point. This causes nucleation to occur at the barrel wall, where latent heat is released as ice begins to crystallize. An ice layer is scraped from the sides of the barrel wall by the blades of the dasher. As the ice crystals are removed, they are displaced to the middle of the product where the ice crystals ripen to form disc shapes. **Figure 2.3** from Cook and Hartel (2010) depicts the complex process of ice formation in the dynamic freezing process.

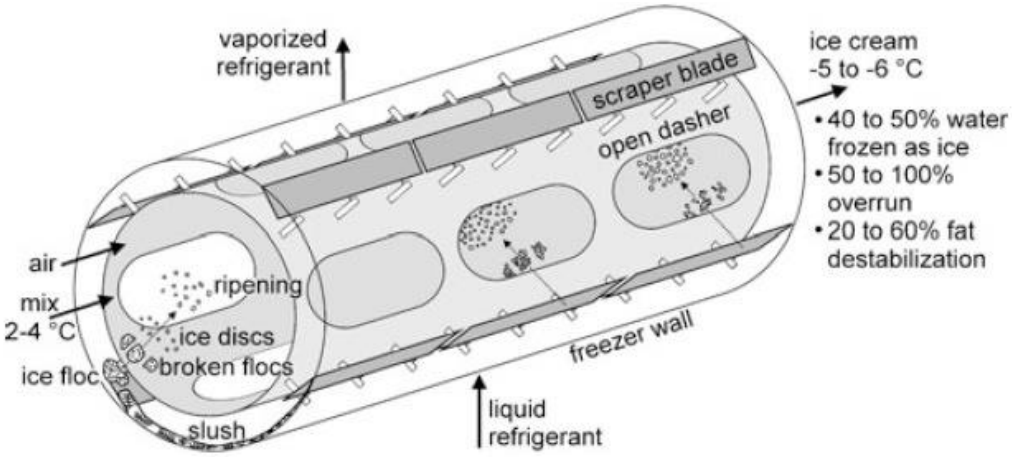

Figure 2.3: A 3-Dimensional diagram of ice formation during the dynamic freezing process. (Cook and Hartel, 2010).

The size of ice crystals can vary in ice cream due to the ingredients used and processing and storage conditions. For fresh ice cream exiting the freezer, the mean ice crystal size falls between 15 and 30 μm, although they typically grow to 35 to 45 μm for hardened ice cream (Goff and Hartel, 2013). Arbuckle (1986) and Sofjan and Hartel (2004) both indicated that the

incorporation of air during freezing governs the ice crystal size distribution, with larger ice crystals observed at lower overruns. Large ice crystals are known to lead to coarse ice cream while too much air can cause a fluffy and crumbly product, which are all defects in ice cream.

The amount of air in ice cream has also been noted to control ice crystal size. Flores and Goff (1999) indicated that at low overruns (below 50%) there was no effect on ice crystal size because lower overruns have less of an effect on the microstructure of the ice cream. At least 70% overrun was needed in order to have an effect on the microstructure and possibly act as a physical barrier during freezing. This has been attributed to well dispersed air cells being able to reduce the probability of collisions between ice crystals and disperse the unfrozen serum phase around them (Flores and Goff, 1999). Ice creams with higher amounts of air have a thinner serum phase dispersed around the air cells and as a result, the collision rate of ice crystals is decreased.

2.3.3 Formation of Air Cells

Aeration is an important part of making ice cream. Air is incorporated into ice cream via injection (continuous freezer) and or direct entrainment (batch freezer) during the dynamic freezing process. Large air cells are formed first and are then broken into smaller sizes the longer the product is in the freezer (Goff and Hartel, 2013). The sizes of air cells are greatly dependent on various mixing parameters. Kroezen (1998) indicated that in a rotor-stator type mixer, the sizes of the air cells are governed by rotor speed, residence time, gas-liquid ratio, and viscosity of the liquid phase. However, in ice cream, the incorporation and stabilization of air cells is greatly dependent on the freezing process (formation of ice crystals), which increases the viscosity of the product (Chang and Hartel, 2002b). In general, final mean air cell sizes are

determined by the balance between smaller air cells created by high shear stress on the fluid inside the freezer and the increased difference in Laplace pressure due to the formation of smaller bubbles, which in turn, led to coalescence (Chang and Hartel,2002a).

Goff and Hartel (2013) indicate that the sizes of air cells in ice cream are governed by the shear stress caused by the rotation of the dasher (whipping) and the development of ice crystals, which leads to increased viscosity of the mix. In a batch freezer study, Chang and Hartel (2002a) observed that neither fat content nor type and levels of emulsifier had an effect on air cell size distribution, even though differences were determined in levels of destabilized fat. On the other hand, rheological properties were attributed to influence air cell size as the addition of stabilizers (increase in apparent viscosity) led to smaller air cells. Caillet et al. (2003) also showed that decreasing draw temperature, which in turn increased ice crystal content, led to smaller air cells during continuous freezing. Sofjan and Hartel (2004) also noted a decrease in air cell size with an increase in overrun, which in turn, increases the apparent viscosity.

After air cells are formed, changes in their size distribution occur during both hardening and storage (Chang and Hartel, 2002c). Both Chang and Hartel (2002c) and Walstra (1996) have noted three mechanisms of instability of gas (air) in foam: disproportionation (Ostwald ripening – pressure difference between air cells that leads to the diffusion of air from small air cells to larger air cells), coalescence (amalgamation of air cells due to instability of network between them), and drainage (flowing of liquid through the foam layer due to warmer temperatures that leads to the rising of air cells). The rate at which these changes occur depend on the processing conditions (storage temperature) and formulation parameters (level and type of stabilizers and emulsifiers) (Chang and Hartel, 2002c). **Figure 2.4** displays the change in air cells during the hardening process (-28^{o}C) in ice creams produced from a continuous freezer for both natural and

forced convection freezing (Chang and Hartel, 2002c). Goff and Hartel (2013) also attributed a change in air cells due to distortion from growing ice crystals if a network of aggregated fat, protein, and or single fat globules inadequately stabilizes the membrane of the air cells. Partially-coalesced fat located in the serum phase has also been attributed to hinder disproportionation (Walstra and Jenness, 1984; Brooker et al., 1986; Walstra 1989; Chang and Hartel, 2002c).

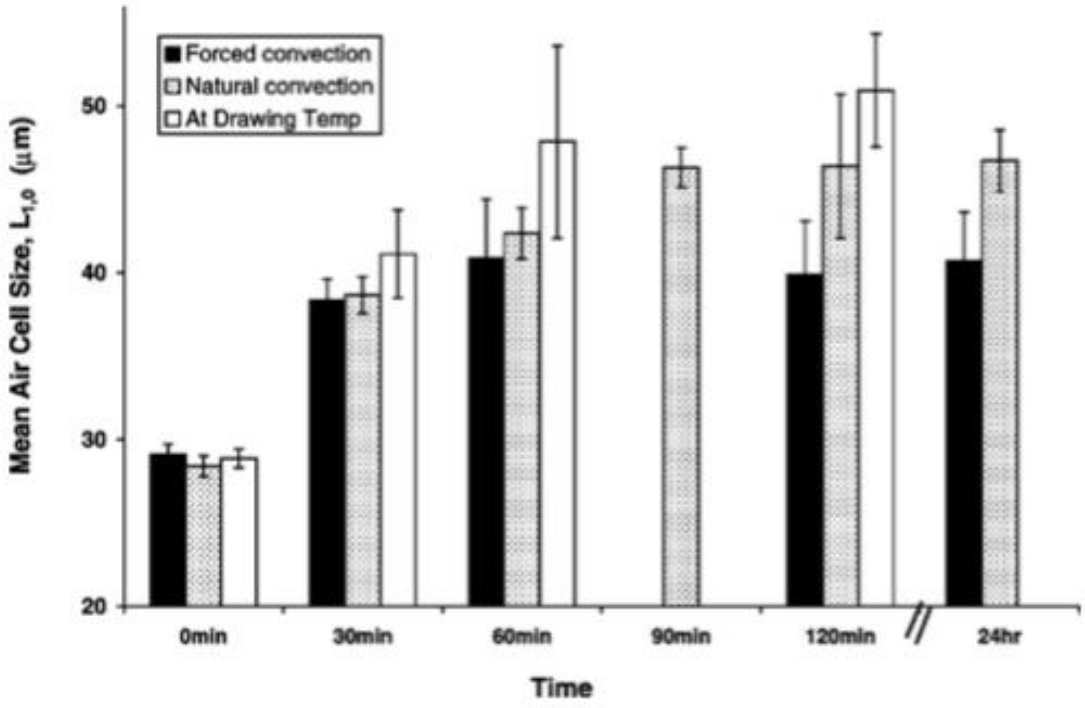

Figure 2.4: Comparison of mean air cell sizes of ice creams during the hardening process (-28^{o}C) for both natural and forced convection freezing and for ice creams kept at the -6^{o}C draw temperature. The error bars represent the standard deviations between measurements (Chang and Hartel, 2002c).

2.3.4 Partial Coalescence

Partial coalescence is the clustering of partially-crystalline fat globules and is often seen in dairy based emulsions, such as ice cream and whipped cream. In general, partial coalescence occurs when the surface area and interfacial tension is lowered between two or more globules under shear forces with a partially-crystalline network. There are, however, varying theories as to how partial coalescence actually occurs. One mechanism, as proposed by van Boekel and Walstra (1981), indicated that, under shear, crystalline fat is able to pierce through the fat globule, enter the water phase, and upon collision with another globule, pierce through the layer to create an oil-oil contact, resulting in partially-coalesced fat (**Figure 2.5**). Although widely accepted, more recent work refutes this theory.

According to Pawar et al. (2012), partial coalescence can be described as an energy balance between interfacial and elastic forces. In this study, emulsion droplets of hexadecane and wax in water were used. Full coalescence or partial (arrested) coalescence occurred under conditions of no shear when there was a reduction in surface energy between two globules coming into contact with each other. Upon contact, there is a reduction in their surface energy and a liquid oil neck was formed between them. Oil then flowed between the two droplets allowing them to come together, but were "arrested" from full coalescence due to formation of the crystalline wax network (**Figure 2.6**). This study showed that crystals do not have to be at the interface in order for partial coalescence to occur. Instead, partial coalescence and deformation of the shape of the globule depends on interfacial forces and the elastic energy of the internal crystalline matrix. Two droplets will coalesce until an energy balance is reached.

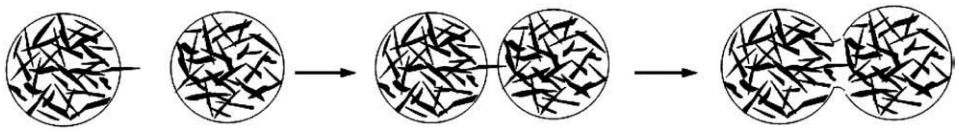

Figure 2.5: Illustration of partial coalescence where crystalline fat protruding from one fat globule pierces another to form partially-coalesced fat (Fredrick et al., 2010; Boode, 1992).

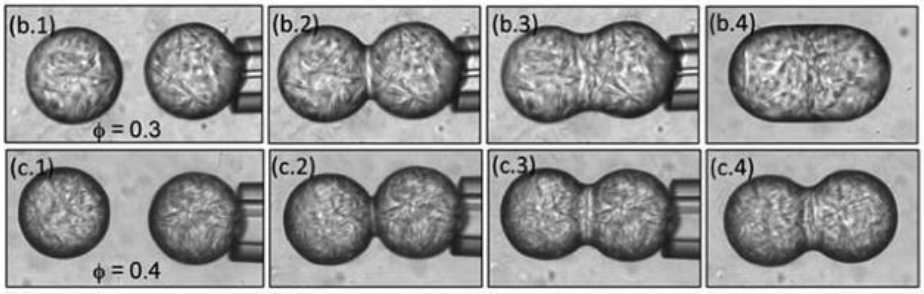

Figure 2.6: Illustration of partial coalescence where liquid oil flows from one droplet to another upon contact. Section **b** contains lower fat content than **c.** (Image adapted from Pawar et al., 2012).

Fat destabilization is influenced by both mix formulation and processing conditions for making ice cream. Key formulation parameters that affect the destabilization of fat globules are emulsifier types and levels, fat volume fraction, initial size of emulsion droplets, protein content, and solid fat content in the globules. Processing conditions, such as shear stress, temperature, and residence time also affect the destabilization of fat globules. Shear stresses during freezing are influenced by dasher design and rotation speed, mix viscosities, and formation of ice and air in the freezer within the freezer.

With an adequate level of fat destabilization, a dry ice cream with slower melting properties that resists shrinkage can be achieved (Berger et al., 1972). On the other hand, too

much fat destabilization can lead to buttering in ice cream, where visible fat granules are present and the ice cream has poor melting properties (Goff and Hartel, 2013).

There are many factors that affect partial coalescence. Emulsifier type and level, total fat content, solid fat content (including temperature effect), initial emulsion droplet size, the presence of proteins, and shear.

2.3.4.1 Emulsifiers

Low-molecular weight emulsifiers play an active role in helping to destabilize fat globules due to their ability to lower the interfacial tension between the fat and the water in the ice cream mix. Emulsifiers are added to ice cream to promote fat destabilization (Goff et al., 1987). Due to this lowering of interfacial tension, the fat globules then become less stable as the milk proteins are displaced from the fat globules by the emulsifiers during the ageing step. During freezing, the shear forces on the fat globules cause them to partially coalesce. PS80 and MDG are common emulsifiers used in ice cream. Typical concentrations used are 0.02 – 0.04% PS80 and 0.1 – 0.2% MDG (Goff and Hartel, 2013).

PS80 is more effective at the interface and therefore, plays a larger role in destabilizing the fat globules compared to MDG. The bulk concentration at which proteins saturate the oil-water interface is much lower than that of low molecular weight emulsifiers, like PS80 and MDG. When there is a substantial amount of low molecular weight emulsifiers in the system, competitive absorption occurs at the oil-water interface. The emulsifiers produce a lower interfacial tension than proteins and produce an efficiently packed monolayer at the oil-water interface, creating a fat globule with greater ability to partially coalesce (Dickinson, 1995). PS80 is more efficient at the competitive absorption process than MDG. The

hydrophilic/lipophilic nature of emulsifiers has been used to describe the competitive absorbance of emulsifiers (Hydrophilic Lipophilic Balance – HLB). PS80 is water soluble and has a high HLB value, whereas MDG is oil soluble and has a low HLB value. It was noted that the more water loving the emulsifier, the greater the amount of destabilization it would induce at the oil–water interface (Govin and Leeder, 1971; Lin and Leeder, 1974). This theory (HLB) has been refuted, indicating that the interfacial tension of the emulsion better explains the effectiveness of an emulsifier (Goff et al., 1989). These authors also indicated that the extent of destabilization that an emulsifier provides and the interfacial tension between the serum and lipid phase are inversely related. PS80 has a lower interfacial tension, whereas MDG results in a higher interfacial tension, making PS80 more effective at the oil-water interface. Numerous studies have shown that the addition of PS80 significantly increases the total amount of destabilized fat in ice cream (Gelin et al., 1994; Gelin, 1996a, b; Goff and Jordan, 1989; Pelan et al., 1997; Tharp et al., 1998; Thomsen and Holtsborg, 1998; Goff et al., 1999; Bolliger et al., 2000). Furthermore, Goff et al. (1989) noted that PS80 gave the lowest interfacial tension, indicating that PS80 promoted fat destabilization in ice cream better than the other emulsifiers.

2.3.4.2 Fat Volume Fraction

The fat volume fraction can play a major role in the extent of partial coalescence achieved in a system. However, although the relationship between fat volume fraction and partial coalescence has been studied in depth in various emulsion systems, it has not been thoroughly explored in ice cream. It is common to see ice cream products ranging in fat levels from < 0.5% - 18% milk fat, as noted in **Table 2.1**. As a result of the varying fat levels, it is expected that different amounts of partially-coalesced fat will be achieved, based on previous

research on emulsions. Hinrichs and Kessler (1997) showed that emulsions with higher fat volume fraction (φ) lead to higher amounts of partial coalescence than those with lower fat content. In this study, it was noted that cream with increasing fat content became more sensitive to shear strain during stirring and pumping. As the fat volume fraction increased, the shear thickening rate decreased, meaning that less shear was needed to destabilize the fat globules. Hinrichs and Kessler (1997) also observed a critical internal shear rate for fat destabilization, which was independent of the total fat content. At this maximum internal shear, any increase in fat content would result in fat destabilization. A maximum φ (φ_{max}) was also observed. This maximum concentration was the point at which the densest fat globule formation occurred under shear flow. This dense formation led to mechanical contact of the fat globules. If φ_{max} was reached for a given system, the globules would be so densely packed (mechanical contact) that slight agitation of the fat globules will lead to obstruction and the fat membrane material altered, leading to globules being able to coalesce or partially-coalesce, if enough crystalline fat present.

Walstra (2003) noted that with all other factors being equal, the encounter rate between two fat globules depends on φ, such that the aggregation rate of the fat globules is proportional to φ^2, as displayed in **Figure 2.7**. In addition, with $\varphi > 0.2$, there tends to be a greater increase in partial coalescence with added shear. Although there is not much evidence of this in ice cream, it is still assumed to hold true for emulsions, assuming all other factors are equal. Rossa et al. (2012) observed an increase in partial coalescence as fat increased from 4%, 6%, and 8% fat in ice creams made with 0.5% Emustab® emulsifier (distilled mono-and diglycerides). However, Gelin et al. (1996b) reported that at higher levels of PS80 (0.67 wt%), partial coalescence increased as total fat increased from 9 to 11 wt%. In contrast, at low levels of PS80, 0.17 wt%, an increase in partial coalescence was not seen as total fat increased from 9 to 11 wt%. This

might be related to an increase in protein and surface area as fat increases and not having enough low molecular weight emulsifier present to completely displace the proteins with constant PS80. Although in a different system, Dickinson (1995) showed that when increasing protein content (gelatin and β-lactoglobulin), the displacement of protein by Tween 20 became much more difficult. This study also indicated that when absorbed to the fat globule, proteins have a greater thermodynamic affinity if insufficient levels of low molecular weight surfactant are present. More work needs to be done to fully understand the impact of increased fat content and its role in partial coalescence in ice cream.

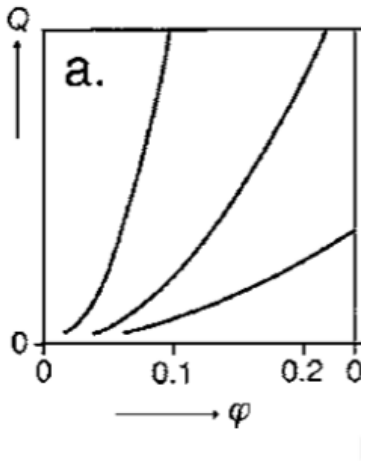

Figure 2.7: Illustrates the rate of partial coalescence (Q) in a protein stabilized O-W emulsions as volume fraction (φ) increases (Adapted from Walstra, 2003).

2.3.4.3 Solid Fat Content (SFC)

Partial coalescence is greatly influenced by the crystal content contained in the fat globules. In order to enhance aggregation and for partial coalescence to occur, there must be enough crystalline fat in the globule, but too much can also limit partial coalescence (Boode,

1992). In general, as the SFC increases, the degree of partial coalescence will decrease. With an increase in SFC, there is a more rigid structure present, which results in an increase in the elastic modulus (G') of the fat globule. The increase in G' increases the energy within the system, leading to a resistance in the system's drive to decrease the interfacial energy. **Figure 2.8** displays this occurrence through the use of hexadecane and wax (Pawar et al., 2012). In this study, it was noted that with an increase in SFC, G' of the fat globule would also increase. If the interfacial energy was greater than the elastic energy of the crystal network, the two globules relaxed and fully coalesced (**Figure 2.8 a.1 - a.4**). However, as the crystalline fat inside the globule increased, the extent of coalescence decreased because of the increase in elastic energy of the crystalline fat network increased (**Figure 2.8 b.1 – d.4**). However, if G' of the crystal network has become too high, no deformation or coalescence will occur and the globules stay as two individual droplets (**Figure 2.8 e.1 – e.4**).

For ice cream mix, the milk fat globules are partially crystalline due to the triglyceride composition. Adleman and Hartel (2001) observed that roughly two-thirds of milk fat is fully crystallized after 4-5 hours of ageing at 4^{o}C. The right amount of crystallized fat is important as too much crystallization can lead to insufficient partial coalescence while too little can lead to complete coalescence. In this study, Adleman and Hartel (2001) measured the rate of lipid crystallization during ice cream processing for products made with low-(LMF), middle-(MLF), high-(HMF) melting milk fat fractions and anhydrous milk fat (AMF). It was observed that HMF and MMF crystallized faster and more during ageing as compared to LMF and AMF. The higher the melting point, the faster the crystallization, due to the greater amount of long-chain, saturated fatty acids in higher melting milk fat fractions (Kaylegian and Lindsay, 1994).

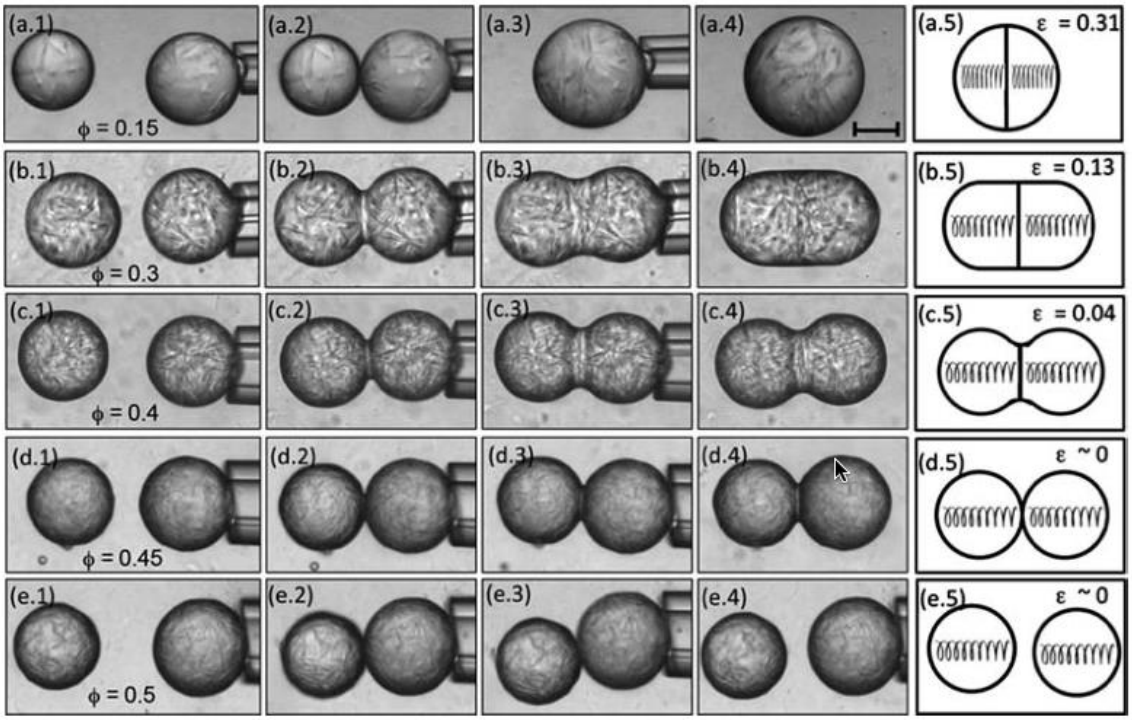

Figure 2.8: Illustration of the decrease in the extent of coalescence as solid fat content increases (top (a) to bottom (e)). Schematics of the final strain (ε) are shown (a.5, b.5, c.5, d.5, e.5) with decreasing strain as coalescence decreases. Scale bar = 50 μm (Pawar et al., 2012).

As a result, Adleman and Hartel (2001) noted that ice creams made with HMF and MMF had higher SFC and lower partial coalescence (measured via the turbidity method) than ice creams made with LMF or AMF. This can be attributed to fat globules with higher melting points having more crystalline fat (higher G' values) than globules with LMF or AMF. Hinrichs and Kessler (1997) further observed that with an increase in SFC (via a decrease in temperature), the amount of external shear force needed for partial coalescence to occur increased, further demonstrating the effect of SFC on partial coalescence.

2.3.4.4 Initial Emulsion Droplet Size

The initial emulsion droplet size is controlled by homogenization pressures. Size of fat globules has been shown to affect the level of destabilized fat (van Boekel, 1980). It was suggested that the larger the fat globule, the larger the crystalline fat (SFC) it can contain and therefore the larger the protruding crystals. This would result in an increase in the rate of partial coalescence as larger crystals protrude further into the interface, increasing the likelihood of protruding crystals at the interface, leading to a greater chance of the occurrence of partial coalescence with neighboring fat globules (Lopez et al., 2002; Thivilliers et al., 2008; Giermanska, 2007; Walstra, 1996).

However, recent work by Hendrickson (2013) disproved the theory that protruding crystals at the interface are needed to cause partial coalescence and confirmed the study by Pawar et al. (2012) by using fats (tristearin and triolein) in water. Hendrickson (2013) also found that a decrease in droplet size radius leads to an increase in strain. This was attributed to droplets with smaller radii having higher internal pressure and therefore having a greater tendency to coalesce. This study however did not determine surface tension to have a large impact on coalescence. In general, a decrease in surface tension results in a decrease in the overall energy in the system. Since coalescence leads to a reduced interfacial energy, if there is a low interfacial tension, there is less drive to coalesce. In turn, there would also be a decrease in strain as surface tension decreased, but the ease of coalescence is inversely proportional to surface tension. According to Walstra and van Vliet (2008), lower energy at the interface results in the thin film on the outside of the globule being more flexible and as a result, more likely to rupture.

2.3.4.5 Displacement of Proteins

In a traditional homogenized ice cream mix, proteins coat the newly formed globule surface. Emulsifiers, especially PS80, displace the proteins at the oil-water interface during the ageing process (Goff et al., 1987; Goff and Jordan 1989; Barfod et al., 1991). If no emulsifiers are present, the milk proteins, which are large and bulky in nature, stay at the surface of the fat globule, with a surface absorption level between 10-12 mg of protein per m^2 of fat (Bolliger et al., 2000). This creates a layer thick enough to stabilize the fat globules against partial coalescence. Under shear, fat globules with enough absorbed proteins can lead to colloidal repulsion instead of partial coalescence. However, if emulsifiers are present, the oil-water interfacial tension is lowered as proteins are desorbed so that only 3-6 mg protein per m^2 of fat is present (Bolliger et al., 2000). In a recent study on the effect of increased protein content in ice cream on partial coalescence (Daw and Hartel, 2015), it was noted that partial coalescence decreased as protein content increased. Partial coalescence was inhibited most in ice creams containing increased whey protein. This was attributed to the increased protein content present at the oil-water interface.

2.3.4.6 Shear

In general, in order for partial coalescence to occur, the fat globule network must undergo some type of physical disturbance. When an emulsion, like ice cream mix, undergoes shear, the partially crystalline fat droplets collide, overcoming the repulsive forces keeping the globules apart. The shear rate required to promote fat destabilization may be dictated by such factors as the composition of the adsorbed layer (proteins, emulsifiers, etc) in addition to the amount of solid fat in the fat globule. Minimal destabilization may occur until a certain critical shear rate is

reached, at which point the emulsion will destabilize extensively (Hinrichs and Kessler, 1997; Thivilliers-Arvis et al., 2010). As shear rate and number of collisions increases, the likelihood of coalescence increases.

The Weber number (We) is a dimensionless ratio between applied shear stress and the Laplace pressure that is used to determine the effect of an external force on droplet deformation and can be applied to partial coalescence (Walstra, 1983). We is the ratio between internal and external stress acting on a particle (Walstra, 2003). There are two types of shear under which droplets can be disrupted: laminar and turbulent flow. Globules are disrupted under laminar flow due to shear stress within the system and under turbulent flow due to pressure fluctuations (inertial effects), predominantly, and shear stress (Walstra, 1983). In laminar flow, We has been reported as 1 – critical Weber number (We_{cr}) (Walstra, 1983). There are cases where We_{cr} has been reported at slightly lower or at slightly higher values than 1 (Walstra, 1983). This was attributed to We_{cr} being dependent on the rate at which the velocity gradient, G, is obtained and the time that G lasts (Torsza et al., 1972). This indicates that the We_{cr} can be system dependent as change in velocity and shear can change the We_{cr}. If We is larger than 1, exceeding We_{cr}, the globules will be disrupted and break under pressure. Walstra (2003) indicated that coalescence tends to be much more rapid for high We than for low We, which was especially apparent in studies where interfacial tension varied. In turbulent flow, globule deformation is often attributed to the average velocity in the turbulent eddy (Walstra, 1983). The We_{cr} is reached when the pressure fluctuation across an eddy has a pressure greater than the Laplace pressure of a droplet of a set diameter.

The dynamic freezing process is dominated by turbulent flow. The shear forces caused by the rotation of the dasher, aeration, and the formation of ice crystals greatly influence the rate of

partial coalescence (Gelin et al., 1996a). The movement of the fat globules caused by the shear forces increases the encounter rate among the fat globules and thus, increases the rate of partial coalescence. Walstra (2003) noted that there exists a threshold value (structure and composition dependent) of shear for partial coalescence. Above that value, the partial coalescence rate is roughly proportional to the shear rate.

Residence time, the longer an emulsion is under shear, can also influence partial coalescence. Boode (1997) noted that under longer residence times at high shear, the breaking of partially-coalesced fat clusters must be considered. High shear forces over an extended period of time can disrupt the formed clusters. As a result, the total extent of partial coalescence is dependent on the rate of the formation and breaking up of partially-coalesced fat.

2.4 Melting of Ice Cream

Meltdown is an important aspect of ice cream quality. The physical structure of the ice cream influences its ability to collapse at ambient temperature (Muse and Hartel, 2004). The formulation parameters (total fat, initial emulsion size, emulsifier blend) and processing conditions (overrun, dasher speed, throughput rate, and draw temperature) under which the ice cream is made help to create specific physical structures. The air cells, ice crystals, and partially-coalesced fat globules formed during freezing are the primary structural components that affect the melt rate of ice cream products.

Typically, melt rate (the speed at which the ice cream melts, collapses, or does not collapse at ambient temperature) is determined by placing a sample of ice cream on a wire mesh screen at ambient temperature for up to two hours and recording the serum and/or ice cream that drips through the screen. There are many physical changes that occur as ice cream melts. As ice

cream is set out at ambient temperature, heat transfers from the outside to the inside of the ice cream, causing ice to melt. The latent heat must be removed as the ice cream melts. Water from the melted ice then begins to combine with the serum phase, diluting it and potentially causing it to drain from the remaining foam due to gravitational forces. If the structures (partially-coalesced fat globules) of the ice cream atop the screen are small enough, complete collapse takes place. In this instance, little to no blockage will occur, and the diluted serum, combined with the partially-coalesced fat, drips completely through the mesh screen, carrying all of the other components (air cells, fat globules, and diluted serum). This drainage can often lead to a fast drip-through rate, as shown schematically in **Figure 2.9**. However, if the structures (partially-coalesced fat globules, air cells) are large enough and or if there are enough small structures, blockage of the free diluted serum can occur, resulting in a slow drip-through rate and retention of most of the structures on top of the screen (remnant foam), as shown schematically in **Figure 2.10** (Goff and Hartel, 2013). The physical structure of the product governs how much shape is retained in each sample. Muse and Hartel (2004) determined that the extent of partially-coalesced fat and ice crystal size had the greatest effect on drip-through rate of ice cream products.

2.4.1 Factors that Affect Melting Rate

Microstructural and compositional parameters greatly influence the rate of drip in ice cream products. Outlined in the sections below are the factors (overrun, air cells, ice crystals, partially-coalesced fat, and the serum phase) that effect drip-through rate and the impact of each on this process.

2.4.1.1 Overrun and Air Cells

The amount of overrun has been noted to greatly affect the melting rate of ice cream products. Ice creams with higher overruns melted slower and had better resistance to melt than ice creams containing lower overruns (Sakuria et al., 1996). Sofjan and Hartel (2003) also noted the same effect between products with 80% and 100% overrun. The larger volume of air present in high overrun products caused a reduced rate of heat transfer, which resulted in slower melting rates. However, other studies have found no effect of overrun on meltdown rates of ice cream (Muse and Hartel, 2004). Since there are numerous interactions that occur during the melting of ice cream, it is sometimes difficult to determine the exact relationship between overrun and meltdown rate.

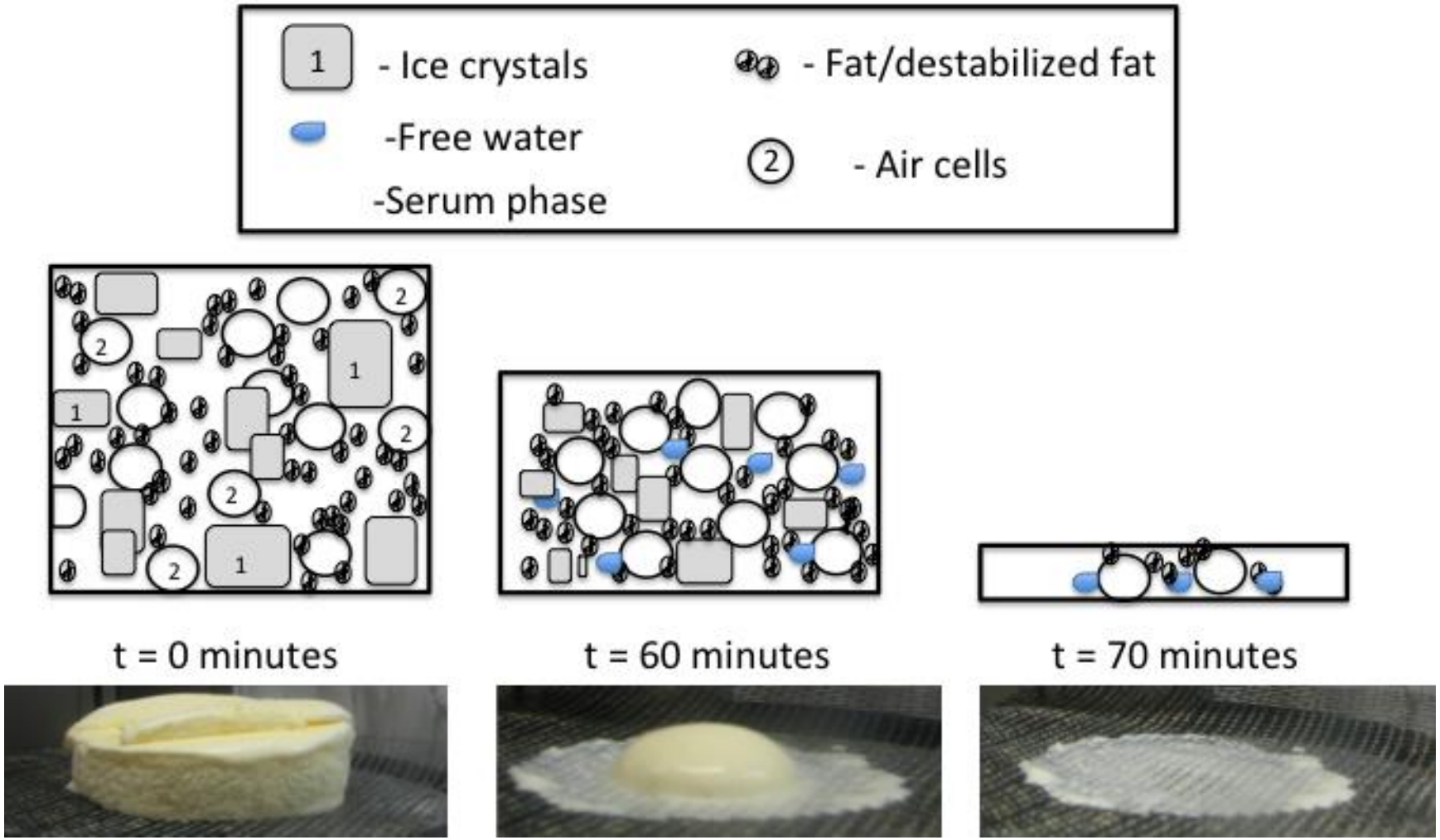

Figure 2.9: Cartoon depiction and actual ice cream sample during the meltdown test, representing ice cream with complete collapse and drainage, exhibiting a high drip-through rate during the meltdown test, up to 70 minutes.

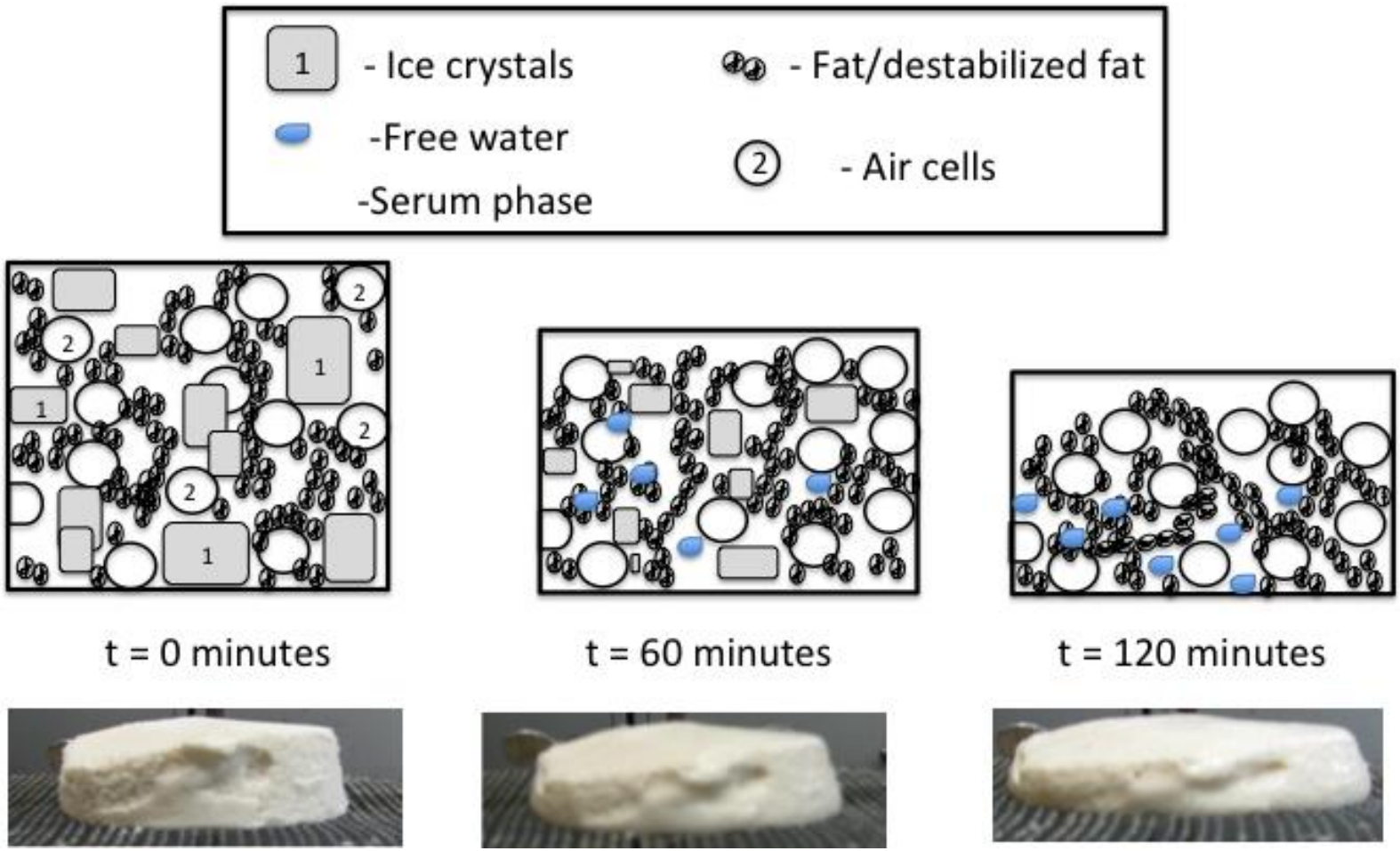

Figure 2.10: Cartoon depiction and actual ice cream sample during the meltdown test, representing ice cream resisting collapse during the meltdown test, up to 120 minutes.

The size of air cells has also been noted to affect the rate of melt. When air is injected into the ice cream during the freezing process, the rotation of the dasher increases the shear, which results in smaller ice crystals and air cells. Sofjan and Hartel (2003) observed that the smaller the air cells, the slower the meltdown rate. According to Pelan et al. (1997), resistance to melt increases as the stability of air cells increases. Air cells become more stable with an increase in destabilized fat absorbed to the air interface, hindering the coalescence of air cells during shear.

2.4.1.2 Ice Crystals

There are many influences on the size of ice crystals in ice cream. Ice phase volume, draw temperature, residence time, fluctuations in temperature during storage, and the use of stabilizers influence the size distribution of ice crystals (Russell et al., 1999; Drewett and Hartel, 2007; Goff and Hartel, 2013). However, the effect of ice crystals on drip-through rate of ice cream products is not fully understood. Muse and Hartel (2004) indicated that larger ice crystals resulted in a faster drip-through rate. This was attributed to water from the large melted ice crystals being able to migrate through the serum phase more easily than water from smaller ice crystals. With smaller ice crystals, limited space between them makes it more difficult for the diluted serum phase to flow. In contrast, Koxholt et al. (2001) and Daw and Hartel (2015) did not observe an influence of ice crystal size on the rate of drip. The effect of ice crystal size on drip-through rate needs to be further explored.

2.4.1.3 Fat and Partially-Coalesced Fat

Partially-coalesced fat plays a large role in the drip-through rate of ice cream products. The presence of emulsifiers, speed of the dasher, formation of ice crystals, and air cells helps to govern the extent of destabilized fat present in ice cream. Research has shown an inverse relationship between partial coalescence and drip-through rate (Berger and White, 1971; Berger et al.,1972; Segall and Goff, 2002; Muse and Hartel, 2004). On the other hand, Koxholt et al. (2001) noted that a low amount of partially-coalesced fat (critical fat globule size determined at $D_{50,3}$ approximately 1.5 μm) also led to slow drip-through rates. This was attributed to the gap between the lamellae not being large enough for the particles (air cells and partially-coalesced fat globules) to flow (**Figure 2.11**). This finding indicates that there may be other factors influencing the drip-through rate of ice cream products.

The relationships between emulsifiers, extent of partial coalescence, and meltdown rate have been studied widely (Gelin et al., 1994; Gelin, et al., 1996a, b; Goff et al., 1999; Goff and Jordan, 1989; Pelan et al., 1997; Tharp et al., 1998; and Thomsen and Holtsborg, 1998). Bolliger et al. (2000) further indicated that a level of 0.02% PS80 in ice cream decreased the drip-through rate but did not further observe an increased difference in drip-through rate when higher levels of PS80 were added (0.04% and 0.06%). In addition, PS80 helps with shape retention and decreases the amount of liquid that drips during the drip-through test (Tharp et al., 1998).

Decreasing total percent fat can also affect the rate of drip. Roland et al. (1999) found an inverse relationship between percent total fat and drip-through rate. As indicated by Hinrichs and Kessler (1997) and Walstra (2003), the extent of fat destabilization is dependent on the fat

volume fraction. The lower the total fat, the lower the amount of partially-coalesced fat formed and thus, the faster the drip-through rate. Resistance to melt has also been noted to occur because of a decrease in draw temperature, which in turn increased overrun and fat destabilization (Campbell and Pelan, 1998).

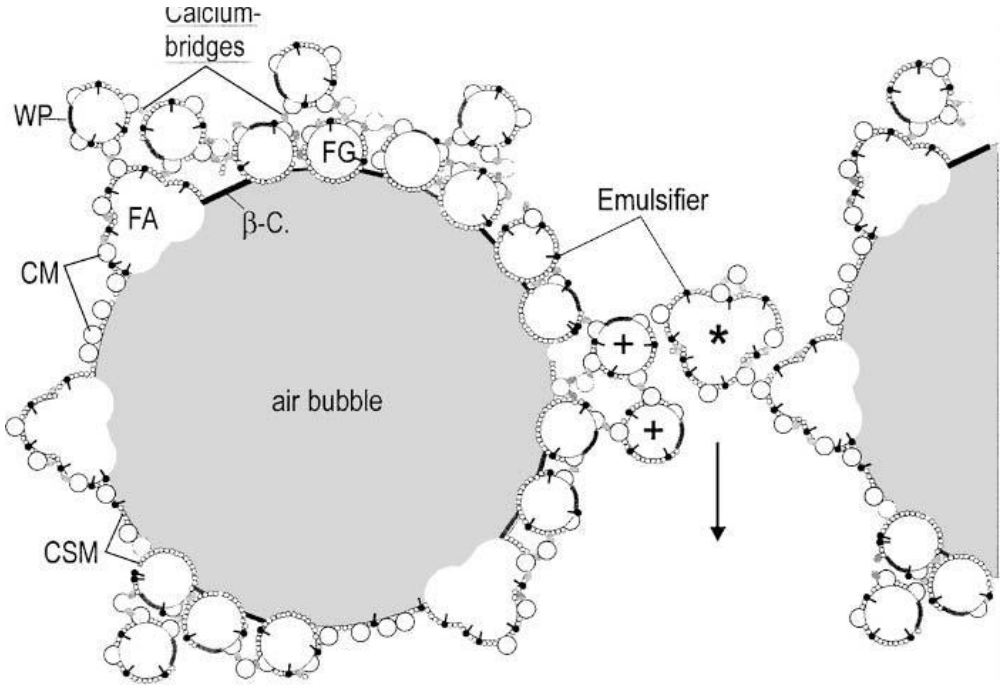

Figure 2.11: Model for a stabilized air bubble and the foam lamella during the meltdown of ice cream (FG: intact fat globule; +: intact fat globule attached to the air bubble via calcium bridges; FA: partial destabilized fat agglomerate; *fat agglomerate that blocks the foam lamella; CM: casein micelle; CSM: casein submicelle; B-C: B-casein; WP: whey protein) (Koxholt et al., 2001).

2.4.1.4 Serum Phase

The serum phase is composed of dissolved proteins, salts, sugars, minerals, and some stabilizers and helps to hold the entire structure of ice cream together (Goff and Hartel, 2013). The serum phase can vary greatly depending on mix composition and temperature of the product. One main variation that affects the drip-through rate is the viscosity of the serum phase (Muse

and Hartel, 2004. Ingredients, such as stabilizers, can greatly cause an increase in the viscosity of the serum phase. A more viscous serum phase will drain through the lamella more slowly than a less viscous serum phase which will result in a slower drip-through rate (Goff and Hartel, 2013).

2.4.2 Understanding and Predicting Melting Rate of Ice Cream

Muse and Hartel (2004) developed a structural model in which they determined the microstructure components that affected melt behavior of ice cream. Utilizing multiple linear regression, it was determined that fat destabilization (Turbidity method) ($p < 0.0001$), ice crystal size ($p < 0.0001$), and the consistency coefficient of the ice cream mix ($p = 0.0508$) affected melting rate according to **Equation 2.2**:

$$\text{Mean melting rate} = 2.006 - 0.046F - 0.004K + 0.039I \quad (2.2)$$

In **Equation 2.2**, an increase in extent of fat destabilization (F) (%), a decrease in the consistency coefficient (K) (Pa-s), and an increase in ice crystal size (I) (μm) led to an increase in melting rate (ml/min). Although a structural model was determined, this study utilized a batch freezer in which all physical properties were not controlled. Overrun, which has been noted to affect melt behavior in other studies, was difficult to control and measure in a batch freezer. As a result, overrun is not a factor in **Equation 2.2**. However, this author noted that with greater control and ranges of overrun, overrun could possibly influence the rate of melt. Overrun, in addition to microstructure components, could better be controlled and measured by utilizing a continuous freezer (Muse, 2003).

2.5 Sensory

Ice cream is such a desirable treat due to its sensory properties provided by the complex microstructure and ingredients. In general, ice cream is manufactured to produce a cold, creamy, sweet, and smooth texture that is enjoyed by consumers. Generally, sensory analyses are important to insure desirable products are produced.

2.5.1 Sensory Analysis

In order to properly evaluate the sensory profiles of food products, analysis by a trained panel should be carried out. It is important to choose proper methods that minimize variability and bias when attempting to qualitatively and quantitatively describe attributes. Controlling variables to allow the results of sensory analysis to measure the true differences between products is also extremely important. The sensorial qualities of frozen desserts are typically evaluated in three ways: 1. by experts, typically alone or in small groups, 2. by trained panelists using formal sensory evaluation methods, or 3. by a large number of untrained consumers (Goff and Hartel, 2013).

2.5.2 Sensorial Properties of Ice Cream Products

Compositional and microstructural aspects of ice cream not only affect the melt behavior of ice cream products at ambient temperature, but also greatly impact its sensorial properties (Conforti, 1994; Stampanoni Koeferli et al., 1996). Thus, the effect of microstructure and behavior attributes on sensory properties has also been studied.

2.5.2.1 Sensorial Melt Rate

Ingredients used and storage conditions impact the melt rate of ice cream both at ambient temperature (**Section 2.4**) and in the mouth. Total fat, ice crystal size and content, and overrun can all affect the rate of melt in the mouth. Through descriptive analysis studies, slower melt rates were perceived in higher fat ice creams when comparing 10% to 18% fat (Guinard, et al., 1997) and 3% to 12% fat (Stampanoni Koeferli et al., 1996). Conforti (1994) also reported a decrease in melt rate of ice cream as the percent fat increased; the difference in melt rate was also attributed to the sweetener system used. An increased perception of ice crystals has been reported to correlate with an increase rate of melt (Stampanoni Koeferli et al., 1996). This was attributed to the increase in fat content (lower melt rate) providing mechanical obscuration of ice crystals during freezing, which results in small ice crystals at higher fat content, as seen by Donhowe et al. (1990). As a result, lower fat ice creams (faster melt) will have larger ice crystals, as there is lower mechanical obscuration of the ice crystals during freezing. Therefore, trained panelists more easily perceived the ice crystals in lower fat ice creams than compared to higher fat ice creams (smaller ice crystals).

2.5.2.2 Impact of Fat and Fat Destabilization on Sensory

The presence of fat in ice cream is not only critical to its microstructure, but it is also important in providing desired sensorial qualities, such as creaminess perception. Too much destabilized fat can lead to a greasy mouth coating, which is often undesirable in ice cream. A decrease in fat content has been attributed to a decrease in the perception of creaminess in ice cream samples (Morris, 1992; Roland et al., 1999), whereas an increase in percent fat has resulted in an increase in perceived mouth coating during sensory analysis (Stampanoni Koeferli

et al., 2004; Aime et al., 2001). Prindiville et al. (1999) related an increase in creaminess perception to an increase in fat content.

Partially-coalesced fat globules larger than 30 μm caused a greasy mouth coating (Eisner et al., 2004). Such greasy mouth coating can be undesirable for consumers and can be noted as a defect in ice cream products. Stampanoni Koeferli et al. (1996) also indicated that an increase in total fat led to a decrease in the perception of ice crystals (coarse and icy feeling) noted by panelists.

2.6 Summary and Direction of Research

This dissertation represents an exploration of the impact of the microstructure on the melt behavior of ice cream. This study begins with a survey on the microstructure and sensorial properties of United States commercial ice cream products, resulting in an attempt to understand the impact of the microstructure parameters (air cells, ice crystals, fat globules, partially-coalesced fat globules, etc) and the interactions between such parameters on the melt behavior of ice cream. Following this survey, through the use of controlled formulation and process parameters, ice creams were made to control for partial coalescence and drip-through rate. The impact of controlled formulation and process parameters on the microstructure parameters and drip-through rate is further investigated. Understanding and controlling the effect of microstructure parameters can possibly lead to the control and prediction of melt behavior.

3. Materials and Methods

3.1 Materials for Survey on United States Commercial Ice Cream Products

Eighteen different vanilla ice cream products were analyzed for their microstructural properties. Three containers of each product, all containing the same lot/production code, were purchased from 2 local grocery stores in Madison, Wisconsin. Since samples were purchased, formulations, processing conditions, and storage prior to purchase were unknown. Samples analyzed included 11 full fat (samples with greater than 9.0 ± 0.5% total), 5 low/reduced fat or light, and 2 nonfat ice cream products. After purchase, products were placed in a −28.9 °C (−20 °F) hardening freezer until analysis (approximately 1 week). All analyses were carried out in triplicate.

3.1.1 Methods for Survey of United States Commercial Ice Cream Products

The focus of this study was to conduct a survey of United States commercial ice cream products. Commercial vanilla ice cream products from the United States (full fat, low fat, and nonfat) were analyzed for their structural, behavioral (i.e., melt rate and drip- through), compositional, and sensorial attributes. Mean size distributions of ice crystals and air cells, drip-through rates, percent partially coalesced fat, percent overrun and total fat, and density were determined. To determine relationships and interactions, principle component analysis and multivariate pairwise correlation were performed within and between the instrumental and sensorial data.

3.1.2 Analyses for Survey of United States Commercial Ice Cream Products

3.1.2.1 Fat Content

The Mojonnier Method (AOAC Method 989.05) was used to determine the percent total fat in each sample.

3.1.2.2 Total Solids and Mix Density

Total solids of each ice cream product were measured via a conventional microwave test utilizing the CEM SMART System 5 Microwave Moisture/Solids Analyzer (CEM Corporation, Matthews, N.C., U.S.A.). The CEM Ice Cream Mix Application was used to determine moisture/solids in each product. The density of the ice cream mix was then calculated from the total solids utilizing (**Equation 3.1**) (Hui, 2006).

$$\frac{\text{wt.}}{\text{L mix}} = \frac{\text{Weight per liter of water}}{\frac{\%\text{fat}}{100} \times 1.07527 + \left(\frac{\%\text{Total solids}}{100} - \frac{\%\text{fat}}{100}\right) \times 0.6329 + \frac{\%\text{water}}{100}} \quad (3.1)$$

3.1.2.3 Overrun

Volume displacement method (Archimede's Principle) was used to measure the overrun of ice cream as described by Clarke (2004). A 5000 mL beaker was filled with deionized water to approximately 3500 mL and stored in a refrigerator at a temperature of 3 to 5 °C for at least 24 h. The chilled water was placed on a scale and tared. Containers of

hardened ice cream (−28.9 °C) were cut into 90 to 120 g slabs. The slabs of ice cream were pierced with chilled tongs and submerged in the chilled water. The weight of the submerged ice cream, minus the tongs, was recorded. The weight of the displaced fluid is directly proportional to the volume of fluid displaced since the surrounding medium (water) is of uniform density. Readings were taken immediately prior to any change (melting of the product in the water) in the ice cream samples. Also, samples were not reused following the measurement. **Equation 3.2** was used to calculate the percent overrun in the ice cream, where V_{ic} is the volume of ice cream, m_1 the initial mass of ice cream slab, and ρ_{mix} is the density of ice cream mix (calculated from **Equation 3.1**).

$$\% \, Overrun = \left(\frac{V_{ic} \cdot \rho_{mix}}{m_1}\right) x \, 100 \tag{3.2}$$

3.1.2.4 Fat Globule Size Distribution/Partial Coalescence (PC)

Fat globule size distribution was measured via the Malvern Mastersizer 2000 (Malvern Instruments Ltd., Worcestershire, United Kingdom). This laser light diffraction and light scattering technique was used to measure the size of fat globules and globule clusters in melted ice cream products, including drip-through (refers to portion of the sample that drips through the screen during the drip-through test) and top (refers to portion of the sample that stays atop the screen after the drip-through test) samples from the drip-through test. The melted ice cream products were stored in the refrigerator at 4^{o}C until analysis. Of each tempered sample (4^{o}C), two to four drops were injected into the sampling unit to obtain the distributions. Water was used as the dispersant with a refractive index of 1.33. The particle refractive index was set at 1.47

(milk fat) with an absorbance set at 0.01. Measurements were performed at obscuration values between 13-15% for each sample measured. **Figure 3.1** displays the typical light scattering curve of a melted ice cream mix. Typically, ice cream mix was compared to melted ice cream to determine the total amount of destabilized fat that forms in ice cream (Bolliger et al., 2000). Since in this case only melted ice cream was available, several assumptions were made to determine extent of fat destabilization. From the melted ice cream distributions, the size of the initial emulsion was taken as the main peak (2^{nd} peak in **Figure 3.1**), usually between about 0.8 and 3.0 μm; in most cases, this peak was easily identifiable and separate from the peak of larger sizes (3^{rd} peak in **Figure 3.1**), which was taken to be the size distribution of clustered, or partially-coalesced, fat. The end of the initial emulsion peak in the melted ice cream was substituted for the baseline of the initial emulsion peak in the mix. It was assumed that where this baseline began (the end of the initial emulsion peak), the partially-coalesced fat peak began. The extent of destabilized fat in the ice cream was then determined by measuring the percent volume of clusters above the initial emulsion peak. This was calculated by taking the total percent volume of the destabilized fat clusters (total destabilized fat peak) divided by the total percent volume of fat globules and clusters, which is encompassed by the initial emulsion peak plus the destabilized fat peak.

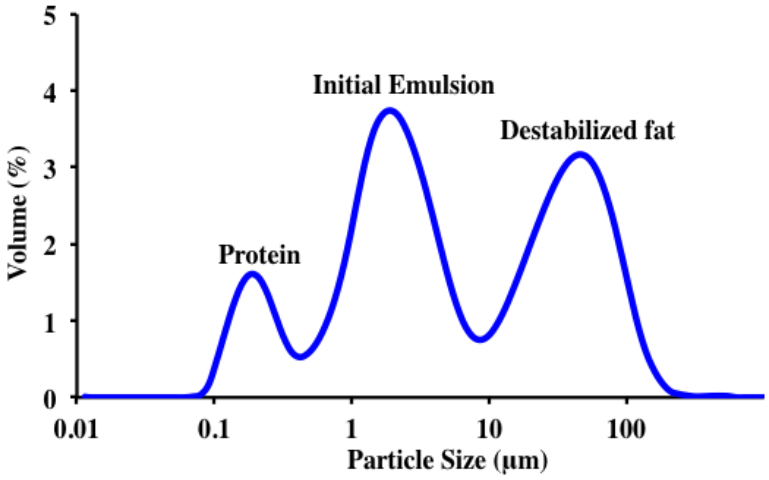

Figure 3.1: Example of a light scattering curve of melted ice cream (sample 880). Protein (casein micelles) peak around 0.15 µm, initial emulsion (fat globules) peak around 1.7µm, and destabilized fat (formed aggregates of fat globules) peak around 34.7 µm.

3.1.2.5 Ice Crystal Size Distribution

Ice crystals were analyzed using a light microscope (model FX-35DX, Nikon, Inc., Garden City, NY) housed in an insulated glove box system (Figure 3.2) (described by Donhowe et al., 1991) at a temperature of -15^{O}C. Samples were moved directly from the hardening freezer to the glove box (-15^{o}C) and allowed to equilibrate for 25-30minutes before sample preparation. For analysis, samples were taken from the middle of the container in the glove box, discarding the top layer of the product, and were transferred to the chilled microscope slides. Two to four drops of chilled 50% pentanol and 50% kerosene dispersing solution were added to aid in dispersing ice crystals and to assist in image quality. A chilled cover slip was placed on top of the sample and by applying a twisting motion and minimal pressure with chilled tweezers, the sample was gently spread thin for additional image clarity. Images of the ice crystals were obtained by optical light microscopy

at 40X magnification. Ice crystals were traced using Microsoft Windows Paint and analyzed via a custom ice crystal

macro in the OPTIMAS software program (OPTIMAS v6.1, Optimas Corp., Meyer Instruments Inc., Houston, Tex. U.S.A.). For each sample, approximately 300 to 400 ice crystals were measured.

3.1.2.6 Air Cell Size Distribution

Air cells were analyzed using the same arrangement and samples as used for ice crystals. After tempering the samples in the glove box (-15^{o}C) for roughly 5 minutes, a thin slice of hardened ice cream was taken from the middle of each container, discarding the top layer of the product, and transferred to a chilled microscope slide. Each sample was placed in a well depth of 100 to 200 μm that was created to allow a uniform flat plane for observation. The temperature was then raised to -6^{o}C for image acquisition (Chang & Hartel, 2002). Photos of the air cells were obtained by optical light microscopy at 40X magnification. Air cells were traced and analyzed for their size via a custom air cell macro in the OPTIMAS software program. For each sample, approximately 300 to 400 air cells were measured.

3.1.2.7 Optical Light Microscopy

The sizes of fat globules and fat globule clusters were confirmed via optical light microscopy. For each sample, two drops of product was diluted with 2 ml of chilled deionized water. Samples were gently mixed to a homogenous mixture of water and product. One drop of each sample was placed on a glass slide and covered with a cover slip. Samples were imaged at 400X magnification.

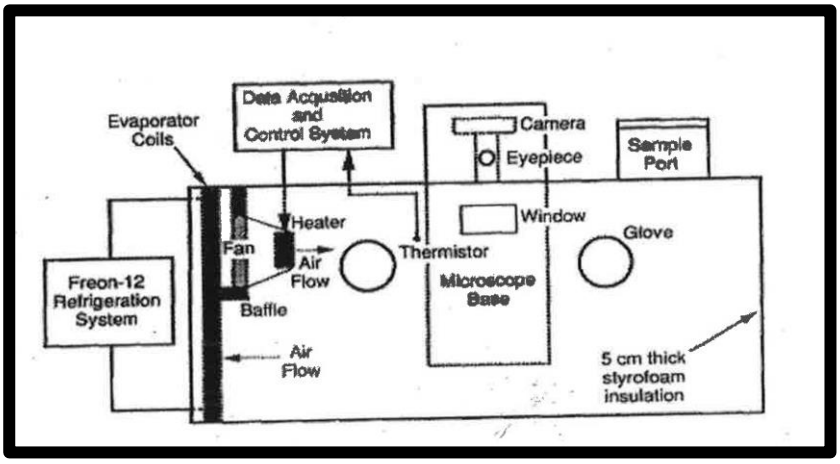

Figure 3.2: Diagram of refrigerated glove box for ice crystal and air cell analyses (Donhowe et al., 1991).

3.1.2.8 Drip-through Rate/Meltdown Rate

Drip-through rate (meltdown rate) was measured on each sample as described by Bolliger et al. (2000). Roughly 80g of ice cream was cut and placed on a wire mesh screen (3 holes/cm) in a 21±.3^{O}C temperature room. The mesh screen rested atop a ring stand with a 500 ml beaker placed underneath (roughly 20 cm underneath) to obtain the dripped portion of the sample as the ice cream melted. The beaker was placed on top of a scale to measure the weight of the dripped portion. Each sample was allowed to drip for up to 2 hours and the weight of the dripped portion was recorded every 5 minutes. Images of the ice cream were taken every 20 minutes. The weight of dripped portion was then plotted against time to obtain a drip-through curve. The slope of the linear portion of the curve was taken as the drip-through rate.

The percent weight of the drip-through portion was taken to calculate the drip-through rate by weight percent.

3.1.3 Sensory Analysis

A trained panel of 17 panelists, consisting of undergraduate and graduate students from University of Wisconsin-Madison, carried out the sensory analyses. Spectrum^{TM} descriptive analysis was used in order to determine correlations between ice cream microstructure attributes and sensory properties. Each panelist received approximately 20 hours of sensory training related to sensory evaluation techniques to assist with defining descriptors and references. The panelists learned and used 6 key sensorial attributes to describe the properties of ice cream (melt rate, breakdown, ice crystal size, denseness, greasiness [often undesirable], and overall creaminess). The panelists also assisted in defining the assessment of each of the descriptors. A 15-point numerical scale (0 = lowest intensity, 15 = highest intensity) was used to evaluate the ice cream according to the descriptors. **Table 3.1** shows the definitions, techniques, and references used in the Spectrum^{TM} descriptive analysis.

For sensory evaluation, each vanilla ice cream, differing by brand and or fat/calorie level, was purchased from 2 local grocery stores in Madison. Seventeen ice cream products were used for the sensory analysis (sample 824 was not available to use in the sensory analysis). Three samples of each ice cream from the same production lot were purchased for analysis roughly 1 week prior to evaluation. About 24 hours prior to evaluation, ice creams were taken from a −28.9 °C (−20 °F) freezer and samples were cut into 1 cm^3. The cubes were placed in Solo 4 oz (118.3 ml) plastic containers (4 cubes per container) and covered

with lids and stored at −19 °C (−2 °F) until analysis (approximately 20 to 24 h). Approximately 80 cubes were cut per sample.

During each sensory session, a maximum of 4 ice cream samples were evaluated. Each sample was identified with a random 3 digit numeric code. Panelists were provided with 3 to 4 cubes of ice cream products in 3 to 4 rounds to effectively evaluate the products. Panelists were provided with more cubes if requested. During the evaluation period, panelists were provided with references (**Table 3.1**) to assist in the evaluation. Samples were evaluated in duplicate.

3.1.4 Statistical Analysis for Survey

All data were analyzed with JMP statistical software (JMP Pro 10.0, SAS Inst., Cary, N.C., U.S.A. 2012). Multivariate pairwise correlation was used to determine correlations between microstructural and sensory attributes. Correlations with $p < 0.05$ were considered to be significant. Principle component analysis (PCA) was used to determine the interrelationships between and within the sensorial and microstructural data.

Table 3.1: Definitions, techniques, and references used in the spectrum descriptive analysis.

Descriptor	Definition	Technique	Reference
Melt Rate	Time required for the ice cream to melt in the mouth.	Place sample in mouth and continuously press lightly between tongue and upper pallet. Count the time it takes for sample to completely melt (1-1000 = 1 second). Time for sample to melt corresponds to the numerical score on the	1.5 = Popsicle brand popsicle (slow melt rate) 7 = Haagen-Dazs Vanilla Ice Cream (medium rate) 11 = Edy's Slow Churned Light Vanilla Ice Cream (fast melt rate)
Breakdown	Amount of force required to manipulate ice cream sample between tongue and palette.	Place sample in mouth and manipulate ice cream sample between tongue and palette 3- 5 times. Evaluate the amount of force required to manipulate the sample.	1 –ConAgra Foods Reddi-Wip Original (little to no force) 3.5 = Daisy Brand Sour Cream (very slight force) 7 = Original Philadelphia Cream Cheese (slight to definite force)
Size of Ice Particulate	Size of ice crystals in sample immediately detected by the tongue.	Place sample in mouth and manipulate using upper palette and tongue. Evaluate the initial size of ice crystals in sample (Note: Ice crystals melt so evaluation is done on the	1.5 = 100% Pure Argo Corn starch and tap water (small) 4.5 = Daisy Brand Sour cream and B&G Foods Cream of Wheat (medium) 10 = Daisy Sour Cream and Quaker Quick Grits (large)
Denseness	The compactness of the cross section.	Place sample between molars and compress once. Expectorate the sample	1 = ConAgra Foods Reddi-Wip Original (Airy) 4 = Nougat inside Mars 3 Musketeers Bar (very slight to slight) 6.5 = Orange Slice Starch Candy (slight to definite)
Greasiness	Degree of greasy/fatty/oily mouth coating or amount of oil left on the mouth surfaces.	Place sample in mouth. Allow to melt and warm in mouth. Expectorate the sample and evaluate greasy residual on mouth surfaces (tongue, lips,	2.5 = ConAgra Foods Reddi-Wip Original (very slight) 5 = Kraft Cool Wip Whipped Topping (slight) 9 = Filippo Berio Extra Virgin Olive Oil (Definite)
Overall Creaminess	Flavors and aromas associated with creamy, milky products.	Place sample in mouth and allow to melt and warm in mouth. Expectorate the sample.	0.5 = Babcock Hall Dairy Plant skim milk (Not creamy) 7 = Land O'Lakes Half and Half (Slight to Definite) 15 = Land O'Lakes Heavy Whipping Cream (Pronounced)

3.2 Materials and Methods for the Effect of Dasher Speed, Overrun, and Emulsifier Ratio, and Fat Content on Microstructure and Physical Properties of Ice Cream

3.2.1 Materials

Ice cream mix was made by combining cream, water, sugar, stabilizers, emulsifiers, and nonfat dry milk. Cream, sugar, and nonfat dry milk were obtained from the University of Wisconsin-Madison Dairy Plant (Madison, WI). Sugar was supplied by United Sugars (Edina, MN) and nonfat dry milk (NDFM) was supplied by Dairy America (Fresno, CA). Grinsted mono-and diglyceride (MDG) and the Germantown Premium I.C. Stabilizer Blend, consisting of locust bean gum, guar gum, and carrageenan, were supplied by Dansico USA (New Century, KS). Avapol™ 80K Sorbitan Ester (Polysorbate 80) (PS80) was supplied by Avatar® (University Park, IL).

3.2.2 Experimental Design

The focus of this study was on controlling partial coalescence and the melt behavior of ice cream through formulation and processing conditions. These parameters will lead to a greater understanding of the impact of the microstructure on the drip-through rate of ice cream and the development of a structure parameter that models the melt behavior of ice cream products. To carry out this research, a 3x3x2 factorial design on 12% fat ice cream was used to study the effects of processing conditions (dasher speed and overrun) and formulation parameters (emulsifier levels) on partial coalescence and melt behavior of ice cream products. Dasher speeds were set at 250, 500, and 750 RPM and overruns were set to 50%, 75%, and 100%. Emulsifier ratios (MDG:PS80) were set at 90:10 and 80:20 MDG:PS80 at 0.15%

emulsifier level. **Table 3.2** shows the 3x3x2 factorial design. All products were frozen in random order based on emulsifier ratio.

In addition to the 3x3x2 factorial design, three additional experiments were performed. To understand the effect of increased total fat content on partial coalescence and melt behavior at a constant fat to emulsifier ratio, an additional experiment with varied levels of fat was carried out (**Table 3.3**). This was taken out of the complete factorial in order to study the main effect of increased total fat with constant emulsifier ratio on partial coalescence and melt behavior. As a result, these mixes were manufactured under one set of processing conditions. Ice cream mixes were made with 6%, 9%, and 15% total fat, with constant emulsifier to fat ratios based on the 12% fat 80:20 ratio. Ice creams were processed at 500 RPM and 50% overrun. Ice cream was frozen in order of increasing fat content.

An additional 2x2 factorial design was carried out to better understand the impact of MDG on partial coalescence and melt behavior of ice cream and to control for the effect of PS80 on the responses studied. This factorial was taken out of the full factorial as the use of MDG alone does not significantly affect the extent of partially coalesced fat (Goff et al., 1989). However, it was still important to understand the effects of MDG alone as a control for the PS80 series of experiments. Ice creams contained 12% fat and were made with 100:0 (MDG:PS80) and processed at 500 and 750 RPM and 50% and 100% overrun (**Table 3.4**). Ice creams were frozen in random order.

Table 3.2: Experimental design for 12% fat ice creams consisting of 90:10 (mono- and diglyceride:polysorbate 80 - MDG:PS80) and 80:20 (MDG:PS80) emulsifier ratios. Ice creams were processed at three different dasher speeds and overruns to carry out the 3x3x2 factorial design.

Dasher Speed (RPM)	Overrun (%)	Emulsifier Ratio (0.15% level)
250	50	80:20
250	75	80:20
250	100	80:20
250	50	90:10
250	75	90:10
250	100	90:10
500	50	80:20
500	75	80:20
500	100	80:20
500	50	90:10
500	75	90:10
500	100	90:10
750	50	80:20
750	75	80:20
750	100	80:20
750	50	90:10
750	75	90:10
750	100	90:10

Table 3.3: Experimental design for ice creams with varied total fat at 500 RPM and 50% overrun and 80:20 (mono- and diglyceride:polysorbate 80 - MDG:PS80) emulsifier ratio. The emulsifier level changed according to the total fat in order to keep the same emulsifier ratio as used in the 12% fat 80:20 (MDG:PS80) emulsifier ratio formula, as described in **Table 3.2**.

% Fat	Emulsifier level (%)
6%	0.075
9%	0.113
12%	0.150
15%	0.188

Finally, a 3x3 factorial design was carried out to better understand the impact of no added emulsifier on partial coalescence and melt down rate. Ice creams contained 12% fat and were made with no added emulsifiers (0:0 - MDG:PS80) and processed at 250, 500, and 750 RPM and 50%, 75%, and 100% overrun (**Table 3.5**). Ice creams were frozen in random order.

All experiments were carried out in duplicate.

Table 3.4: Experimental design for ice cream made with 100:0 (mono- and diglyceride:polysorbate 80 - MDG:PS80) emulsifier ratio, at two different dasher speeds and overruns.

Dasher Speed	Overrun (%)
500	50
750	50
500	100
750	100

Table 3.5: Experimental design for ice creams made with no added emulsifiers. Ice creams were processed following the factorial design as described in **Table 3.2**.

Dasher Speed (RPM)	Overrun (%)
250	50
250	75
250	100
500	50
500	75
500	100
750	50
750	75
750	100

3.2.3 Ice Cream Mix Formulation and Making

Mix composition for the 3x3x2 factorial was 12% milkfat, 16.9% sucrose, 11.3% milk solids nonfat, 0.2% stabilizer, 0.135% MDG:0.015 PS80 (90:10 - MDG:PS80) and 0.12% MDG:0.03 PS80 (80:20 – MDG:PS80). This formulation resulted in approximately 41.0% total solids and a freezing point temperature of -2.52 ± 0.02^{o}C. For the experiment with increased fat content, 6%, 9%, and 15% fat ice cream mixes were made using the above composition with 12% fat 80:20 emulsifier level containing the same ratio of emulsifier to fat. The 2x2 factorial was made utilizing the 12% fat formula with 100:0 (MDG:PS80) at 0.15%. The 3x3 factorial was made utilizing the 12% fat formula with no added emulsifiers. Water was adjusted according to each formula to provide the -2.52 ± 0.02^{o}C freezing point temperature.

Ice cream mix was prepared by combining all of the dry and liquid ingredients into the Stephan Mixer, a batch-jacketed pasteurization system, and stirred and heated until the mixture reached 85^{o}C, roughly 10 to 12 minutes. For each batch, up to 34.07 kg of mix was processed at one time.

3.2.3.1 Homogenization, Cooling, and Ageing

The pasteurized samples were homogenized via a two-stage homogenizer (The Manton-Gaulin MFG,Co. Inc., Everett, Mass., USA) at 2500 psi (500 psi second stage and 2000 psi first stage). After homogenization, the mix was then transferred and chilled to roughly 10^{o}C via the Stephan Mixer, collected into containers, and placed in the refrigerator at 4^{o}C for roughly 24 hours for the aging process to take place.

3.2.3.2 Freezing and Hardening

All ice cream was frozen on the Hoyer Frigus KF 80 F continuous freezer (Tetra Pak Hoyer Inc., Aarhus, Denmark) at University of Wisconsin-Madison Food Science Department. This freezer utilizes a solid dasher with a volume displacement of roughly 40%. The freezer was operated in manual mode in order to properly control the desired parameters in the experimental design. Under the manual mode operation, parameters could be controlled and or held constant while other variables were manipulated. The amount of ice cream produced varied depending on the time to reach equilibrium between change in overrun and dasher speed settings. For all samples, the draw temperature was $-6.1 \pm 0.1^{o}C$. This temperature was taken via an internal thermometer on the Hoyer continuous freezer. Overrun was generated by the injection of high-pressure air during the continuous freezing process. The amount of air injected was set and adjusted for each desired overrun. When necessary, the cylinder pressure was also adjusted to assist in achieving the desired overrun. Once steady state operation was achieved, including proper draw temperature and overrun, ice cream was collected into 473.2 ml containers (6 containers for each variable), which were sealed, and placed directly into a hardening cabinet ($-29^{o}C$). Samples were transferred into a $-29^{o}C$ walk-in freezer roughly 1 hour after production for further analysis. Samples were produced and collected in duplicate.

3.2.4 Analyses

Fat globule size distribution was measured on ice cream mixes before and after homogenization. During freezing, the ice creams were measured for draw temperature and overrun. After hardening, fat globule size distribution, ice crystal size, air cell size, and drip-through rate were measured. All analyses were completed in triplicate.

3.2.4.1 Draw Temperature

Draw temperature was measured for all ice creams upon exit of the scraped-surface heat exchanger via an internal thermometer in the Hoyer continuous freezer.

3.2.4.2 Overrun

Overrun, the amount of air whipped/injected into the ice cream, was calculated during the freezing process using equation 3.3.

$$\%\ Overrun = \frac{Ice\ cream\ mix\ (g) - Ice\ cream\ (g)}{Ice\ cream\ (g)} \times 100 \tag{3.3}$$

Overrun measurements were taken utilizing the weight of the mix in a fixed volume container (177.4 ml cup) and the weight of the fixed volume of ice cream (177.4 ml cup). Overrun measurements were taken at the beginning, middle, and end of each collection point, providing three overrun measurements per collection point.

3.2.4.3 Fat Globule Size Distribution/Partial Coalescence (PC)

Fat globule size distribution was measured as described in **Section 3.1.2.4**. In this set of experiments, the size of fat globules and clusters were measured in ice cream mix before and after homogenization and in melted ice cream products, including drip- through and top samples from the drip-through test. The mix and melted ice cream products were stored in the refrigerator at 4^{O}C until analysis. **Figure 3.3** displays a typical light scattering curve of homogenized ice cream mix and ice cream. The extent of destabilized fat in the ice cream was determined by measuring the percent volume of clusters above the end of the homogenized mix curve.

3.2.4.4 Ice Crystal Size Distribution

Ice crystal size analysis was carried out as outlined in **Section 3.1.2.5**. For this portion of work, ice crystals were traced using Microsoft Softonic Paintbrush for Mac and analyzed via a custom ice crystal macro in the Image Pro Plus software program (Image Pro Plus 7.0, Media Cybernetics, Inc, Rockville, MD, USA). For each sample, approximately 300 to 400 ice crystals were measured.

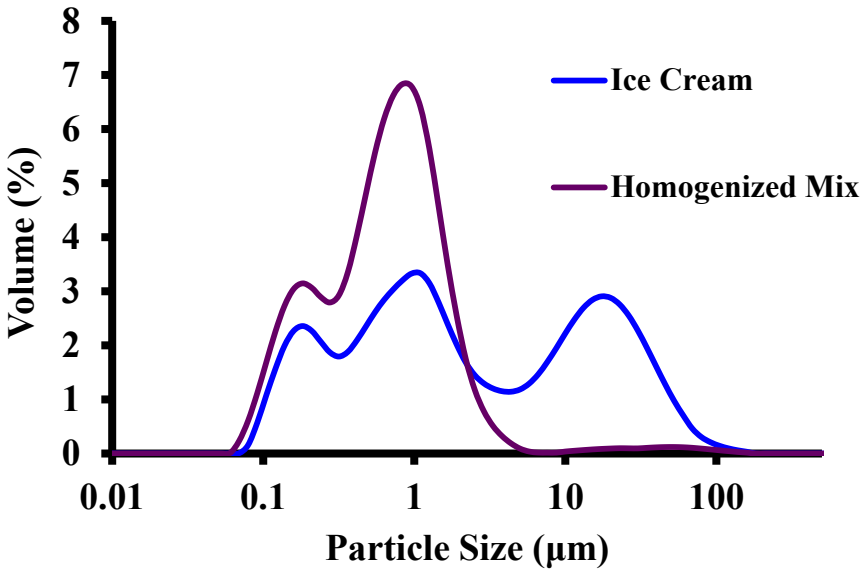

Figure 3.3: Example of a light scattering curve of homogenized mix and ice cream. Protein (casein micelles) peak around 0.15 µm, initial emulsion (fat globules) peak around .83 µm, and destabilized fat (formed aggregates of fat globules only in ice cream) peak around 15.1 µm in this example.

3.2.4.5 Air Cell Size Distribution

Air cell size distribution was carried out as outlined in **Section 3.1.2.6**. For this portion of work, air cells were traced and analyzed for their size via the Image Pro Plus software program. For each sample, approximately 300 to 400 air cells were measured.

3.2.4.6 Optical Light Microscopy

The sizes of fat globules and fat globule clusters were confirmed via optical light microscopy as described in **Section 3.1.2.7**. In this study, three drops of product were diluted with 2 ml of chilled deionized water to improve image quality. Samples were imaged at 400X magnification.

3.2.4.7 Drip-through Rate/Meltdown Rate

Analysis and calculation carried out as described in **Section 3.1.2.8**. Images of the ice cream were taken every 1-minute during this test.

3.2.5 Statistical Analyses

The data was analyzed utilizing various statistical methods. Analyses were carried out using JMP statistical software JMP Pro 11.0 (SAS Inst., Cary, N.C., U.S.A. 2014). Analysis of variance (ANOVA) and Tukey's Honest Significant Difference (HSD) test were applied to all data (ice crystal size, air cell size, calculated partial coalescence, and drip-through rate). One-way ANOVA ($\alpha < 0.05$) was used to individually assess the impact of emulsifier ratios, dasher speed, and overrun, on the measured responses. Tukey's HSD was used to determine statistical differences between the different processing conditions, emulsifier ratios, and fat content on the measured responses. A two-way ANOVA ($\alpha < 0.05$) was used to analyze the effect of dasher speed and overrun on ice cream products with PS80. Multivariate analysis was used to determine significant correlations ($p < 0.05$) between measured responses.

The significant factors in the melt behavior were determined for each emulsifier ratio via regression and factors with $p > 0.05$ (95% confidence) were removed. The regression was then re-ran, excluding factors with $p > 0.05$, until all remaining factors were within a 95% confidence interval. The remaining factors were then considered significant factors that impact the melt behavior of ice cream at a particular emulsifier ratio.

Ice creams made with different fat contents were analyzed separately. A one-way ANOVA was used to determine the effects of percent change in fat on all measured responses.

A Tukey's HSD was used to determine the statistical differences between the responses for the various fat levels tested. Multivariate analysis was used to determine significant correlations ($p < 0.05$) between responses.

4. Results and Discussion

4.1 Survey of United States Commercial Ice Cream Products

Commercial vanilla ice cream products from the United States (full fat, low fat, and nonfat) were analyzed for their structural, behavioral, compositional and sensorial attributes. Mean size distributions of ice crystals and air cells, drip-through rates, percent partially-coalesced fat, percent overrun and total fat, and density were determined. Sensory analyses were carried out by a trained panel in order to determine correlations between ice cream microstructure attributes and sensory properties using a Spectrum^{TM} Descriptive Analysis. Analyses included melt rate, breakdown, size of ice particulates (iciness), denseness, greasiness, and overall creaminess. To determine relationships and interactions, principle component analysis (PCA) and multivariate pairwise correlation were performed within and between the instrumental and sensorial data.

4.1.1 Structural, Behavioral, and Compositional Attributes

The mean values and ranges of the compositional and structural attributes of 18 United States commercial vanilla ice cream products are listed in **Table 4.1**. The wide range in the attributes is due to the varying formulations of each ice cream, along with differences in processing conditions, which were both unknown. Freezer type, dasher speeds, ingredients, and storage conditions all contribute to the wide range of attributes in the ice cream products.

Table 4.1: Ranges, averages, and standard errors of compositional and structural attributes of commercial ice cream samples.

Components	Average and Standard Error	Range
Mean ice crystal size (μm)	48.1 ± 2.3	26.3 – 67.1
Mean air cell size (μm)	29.9 ± 1.5	17.1 – 39.5
Percent total fat (%)	8.6 ± 1.0	0.01 – 14.3
Percent fat destabilization (%)	21.9 ± 3.88	2.60 – 55.3
Overrun (%)	75.0 ± 6.5	21.7 – 119
Density of ice cream (g/L)	649 ± .03	509 – 904
Density of ice cream mix (kg/L)	1.10 ± .01	1.07 – 1.16
Drip-through rate (g/min)	1.07 ± 0.15	0.13 – 1.88
Total solids (%)	38.3± 0.67	31.1 – 42.6

The mean values also provide a basic overview of the average microstructure and compositional make-up of ice cream products sold in the current national and regional (Wisconsin) markets. **Table 4.2** lists the mean values for the compositional and structural analyses and the corresponding Student's *t*-test (paired samples) of significant differences at $p < 0.05$ for the 18 independent samples analyzed.

Figure 4.1 displays physical attributes and compositional parameters via a biplot. The independent principle component (PC)1 accounts for the maximum amount of variance in the variables observed while PC2 accounts for the maximum amount of total variance not accounted for by PC1. Combined, PC1 and PC2 explain 62.7% of the variance of the data. Nonfat samples were distinguishable in their percent fat (low) and drip-through rate (high). Three full fat samples 293, 559, and 880 were separated from the other full fat samples based on the combination of their high percent total fat, slow drip through rate, and high total solids.

Table 4.2: Mean values of compositional and structural analyses and the corresponding Student t-Test of significant differences at $p < 0.05$ for the 18 commercial ice creams analyzed.

Sample Code	Mean ice crystal size (µm)	Mean air cell size (µm)	Total fat (%)	Fat Destabilization (%)	Overrun (%)	Ice Cream Mix density (kg/L)*	Drip-through rate (g/min)	Total Solids (%)
106	46.3 ± 5.0^{cde}	30.4 ± 2.0^{bcde}	10.3 ± 0.1^{def}	15.1 ± 1.7^{gh}	95.1 ± 1.1^{bc}	1.10^{ef}	1.20 ± 0.14^{d}	40.2 ± 0.6^{bc}
159	26.3 ± 1.6^{h}	22.2 ± 1.1^{fgh}	0.1 ± 0.1^{J}	11.0 ± 4.1^{hi}	96.0 ± 2.9^{b}	1.16^{a}	1.85 ± 0.11^{a}	36.9 ± 0.2^{fg}
171	53.0 ± 2.3^{b}	30.1 ± 4.1^{cde}	13.1 ± 0.3^{b}	20.4 ± 1.6^{fg}	67.0 ± 2.4^{g}	1.09^{g}	0.33 ± 0.05^{gh}	39.1 ± 0.3^{cd}
215	53.5 ± 1.3^{b}	24.6 ± 0.5^{defg}	9.0 ± 0.5^{g}	7.8 ± 1.0^{ijk}	91.8 ± 2.6^{cd}	1.09^{g}	0.67 ± 0.06^{e}	36.4 ± 0.1^{g}
286	40.0 ± 5.1^{fg}	28.0 ± 5.2^{defg}	0.2 ± 0.1^{J}	26.0 ± 2.7^{ef}	68.4 ± 2.7^{g}	1.16^{a}	1.72 ± 0.13^{ab}	34.6 ± 0.1^{h}
293	50.8 ± 1.4^{bcd}	26.4 ± 1.3^{efg}	9.4 ± 0.4^{fg}	55.3 ± 5.9^{a}	83.4 ± 4.3^{ef}	1.13^{b}	0.24 ± 0.04^{gh}	42.6 ± 3.2^{a}
313	61.9 ± 4.9^{a}	27.1 ± 2.8^{efg}	14.3 ± 0.6^{a}	6.0 ± 1.6^{ijk}	26.9 ± 1.1^{i}	1.09^{g}	1.40 ± 0.32^{cd}	40.9 ± 0.4^{b}
423	51.7 ± 1.9^{bc}	36.5 ± 1.7^{abc}	7.6 ± 1.0^{h}	2.6 ± 0.2^{k}	51.0 ± 1.5^{h}	1.09^{g}	1.69 ± 0.08^{ab}	35.9 ± 0.2^{gh}
472	41.3 ± 1.1^{efg}	38.2 ± 1.7^{a}	5.7 ± 0.4^{i}	30.6 ± 1.0^{de}	119 ± 4.0^{a}	1.12^{c}	1.26 ± 0.09^{d}	35.8 ± 0.3^{gh}
559	42.8 ± 0.6^{efg}	37.4 ± 3.7^{a}	$*11.5^{c}$	45.0 ± 3.4^{bc}	21.7 ± 1.1^{J}	1.10^{e}	0.20 ± 0.20^{h}	40.7 ± 0.6^{b}
603	53.6 ± 1.2^{b}	26.0 ± 1.2^{efg}	11.0 ± 0.1^{cd}	21.9 ± 7.5^{f}	80.3 ± 1.9^{f}	1.11^{ef}	0.26 ± 0.03^{gh}	38.6 ± 0.2^{de}
638	40.9 ± 2.6^{egh}	36.6 ± 2.3^{ab}	9.9 ± 0.2^{efg}	5.0 ± 0.8^{jk}	97.5 ± 1.7^{b}	1.11^{d}	1.72 ± 0.07^{ab}	40.9 ± 0.4^{b}
652	45.8 ± 3.2^{de}	21.9 ± 1.8^{gh}	10.8 ± 1.7^{cde}	7.9 ± 2.3^{ijk}	72.2 ± 2.2^{g}	1.10^{e}	0.44 ± 0.05^{fg}	39.2 ± 0.1^{cd}
727	43.9 ± 2.6^{ef}	28.5 ± 1.6^{def}	5.5 ± 0.2^{i}	32.3 ± 2.8^{d}	89.6 ± 3.2^{d}	1.11^{c}	0.64 ± 0.07^{ef}	37.8 ± 0.3^{ef}
824	45.7 ± 2.9^{de}	34.2 ± 4.9^{abcd}	5.9 ± 0.2^{i}	47.0 ± 1.7^{b}	95.4 ± 0.7^{bc}	1.09^{f}	0.89 ± 0.16^{e}	$*38.0^{def}$
880	67.1 ± 3.9^{a}	39.5 ± 1.8^{a}	14.0 ± 0.6^{ab}	40.4 ± 7.3^{c}	23.7 ± 0.6^{ij}	1.10^{ef}	0.13 ± 0.02^{h}	40.6 ± 0.2^{b}
913	66.3 ± 3.1^{a}	30.1 ± 3.6^{cde}	5.2 ± 0.6^{i}	10.0 ± 0.6^{hij}	85.7 ± 2.1^{e}	1.07^{h}	1.53 ± 0.07^{bc}	31.1 ± 0.1^{i}
957	37.9 ± 2.5^{g}	17.1 ± 1.6^{h}	11.5 ± 0.5^{c}	9.0 ± 3.6^{ij}	83.3 ± 1.6^{ef}	1.11^{d}	1.86 ± 0.31^{a}	41.0 ± 0.3^{b}

*Denotes significant differences within ± 0.04

^{a,b,c,d,e,f,g,h,i,j,k} Means not sharing the same letter are significantly different ($\alpha = 0.05$).

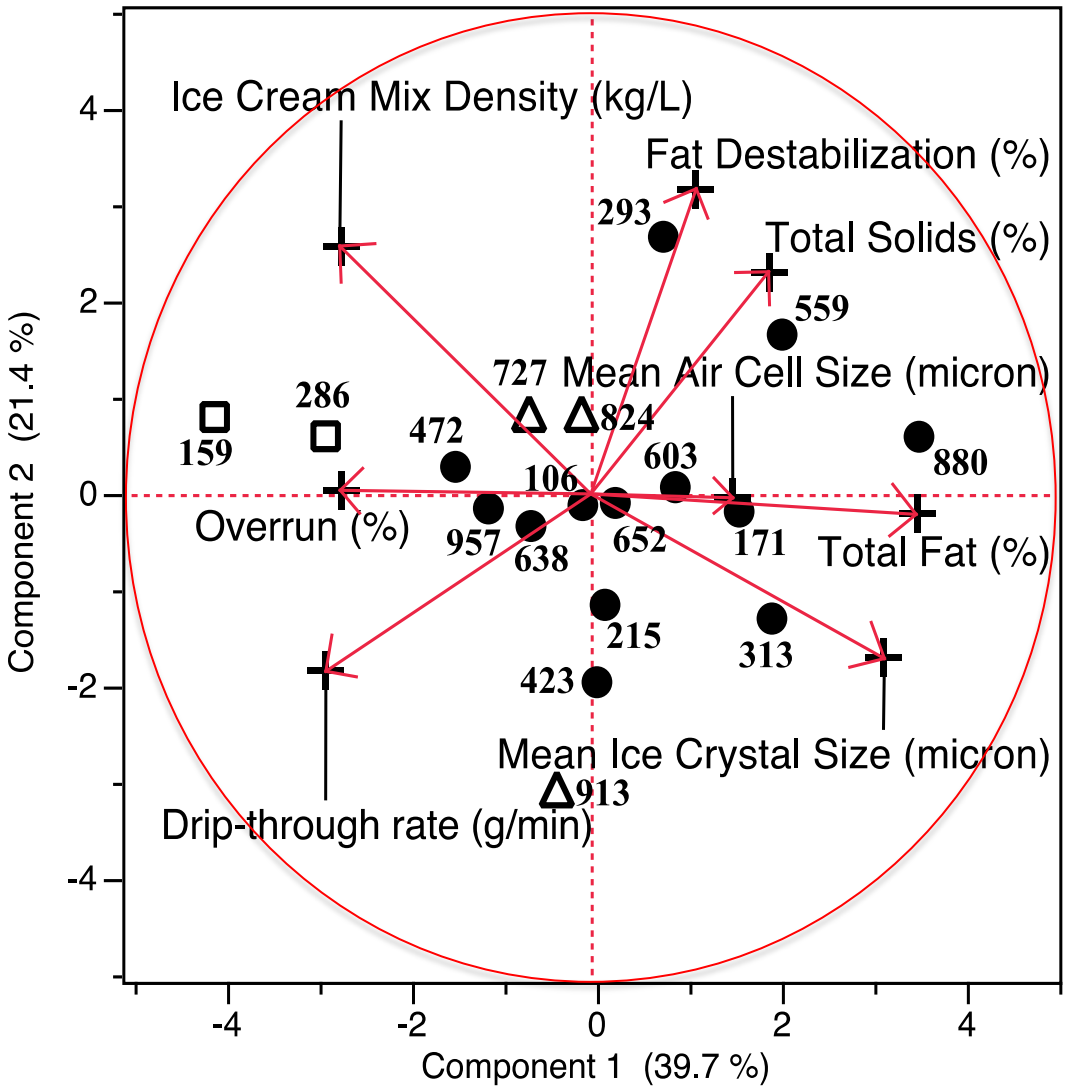

Figure 4.1: Principle component analysis biplot of the microstructure parameters/instrumental measurements of commercial ice creams. Ice cream product samples are represented by a three-digit code and the vectors represent the microstructure parameters tested. The following shapes represent the levels of fat present in the ice cream products:

●=full fat products; △= reduced fat/light products; □= nonfat products.

4.1.1.1 Drip-through Rate

Microstructure components greatly affect drip-through rates of ice cream products (Muse and Hartel, 2004). In this study, drip-through rate ranged from 0.13 to 1.88 g/min. The ranges of drip-through (% weight) curves and the images of the structure left atop the screen at the end of the drip-through test can be found in **Figure 4.2** (**a-b**). A comparison of the structures left atop the screen at the end of the drip-through test and drip-through curves can be found in **Appendix A1-2**. The effect of microstructure and composition on drip-through/behavior of ice cream products and their effect on each other are outlined in the following sections.

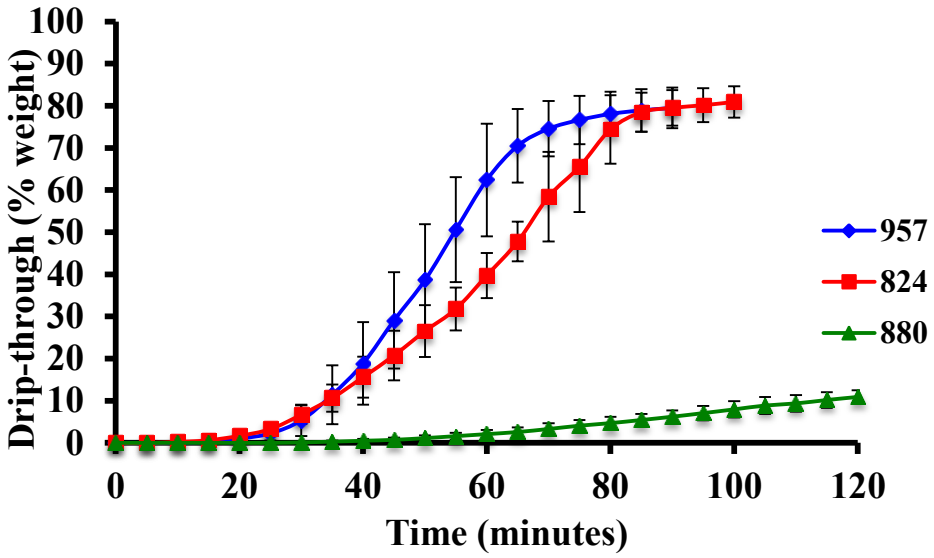

Figure 4.2a: Drip-through (% weight) curves of commercial ice creams representing the wide range of drip-through (% weight) in ice creams from samples 957 (1.86 g/min), 824 (0.89 g/min), and 880 (0.13 g/min) Error bars represent the standard deviation between replicates for each sample.

Sample 957 (90 min) Sample 824 Sample 880

Figure 4.2b: Images of the range of commercial ice cream structures left atop the screen at the end of the drip-through test (120 minutes unless otherwise indicated). Sample 957 had minimal structure, sample 824 had mid-range structure, and sample 880 had large amounts of structure left atop the screen at the end of the drip-through test.

4.1.1.2 Ice Crystal Size

Mean ice crystal size ranged between 26.3 and 67.1 μm, displaying a large range of ice crystals found in commercial ice cream products. **Figure 4.3 (a-b)** displays the wide range of ice crystal size distributions and the microscopy images across the ice creams analyzed. This large range in ice crystal size can be attributed to the ice phase volume, draw temperature, residence time, fluctuations in temperature during storage, and the use of stabilizers to influence the size distribution of ice crystals (Russell et al., 1999; Drewett and Hartel, 2007; Goff and Hartel, 2013). The complete set of microscopy images of ice crystals can be found in **Appendix B**.

Ingredients such as stabilizers, sweetener systems, and bulking agents can influence the broad range of ice crystal sizes. Although the amount of stabilizers used in these ice cream products was not known, the type of stabilizers (i.e., guar gum, locust bean gum, carrageenan), whether used singly or combined, most likely influenced the overall size of ice crystals. Sample 159 contained ice-structuring proteins and had the smallest ice crystals across all samples. Ice-structuring proteins were used to create small ice crystals and provide body and stability to reduced and nonfat ice cream products similar to that of full-fat ice cream. More information

regarding the levels of stabilizers in combination with sweetener systems and bulking agents used in ice cream needs to be known in order to determine the exact relationship with ice crystal size.

The hardening process can also affect the overall mean ice crystal size. Ice cream can undergo many physical changes during the hardening process (Chang and Hartel, 2002a). During this process, as the temperature of the product decreases, the ice phase volume increases. As a result, ice crystals increase in size. If this process is slow and not efficient, this will cause some ice crystals to melt and others increase in size (Goff and Hartel, 2013). Although the storage conditions prior to purchase were not known for the ice creams studied, it can be assumed that both hardening and storage conditions most likely affected the overall mean ice crystal size.

Mean ice crystal size inversely correlated with drip-through rate ($p < 0.01$). This finding does not align with the study done by Muse and Hartel (2004). A decrease in mean ice crystal size was identified as one of the greatest influences on the decrease in drip-through rate. In contrast, Koxholt et al. (2001) did not observe an influence of ice crystal size on the rate of drip. More work is needed in order to understand the influence of ice crystal size on the melting behavior of ice cream. Mean ice crystal size also had other significant interactions with physical and structural components of ice cream products, as outlined in the sections below.

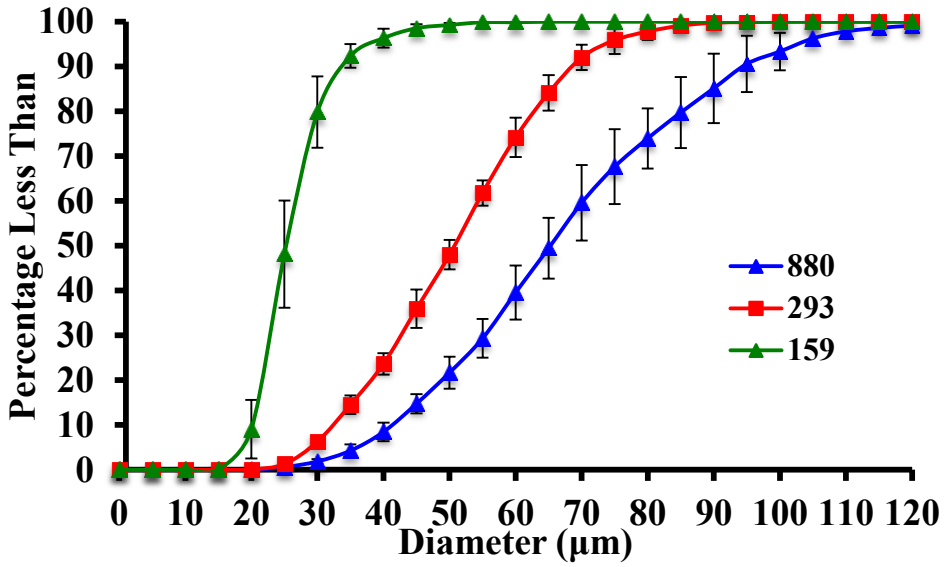

Figure 4.3a: Range of ice crystal size distributions of commercial ice creams from samples 880 (mean size: 67.1 µm), 293 (mean size: 50.8 µm), and 159 (mean size: 26.3 µm). The error bars represent the standard deviations of the mean ice crystal sizes for the sample measured.

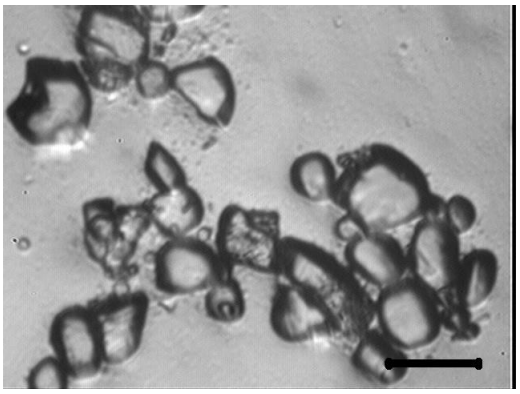

Sample 880

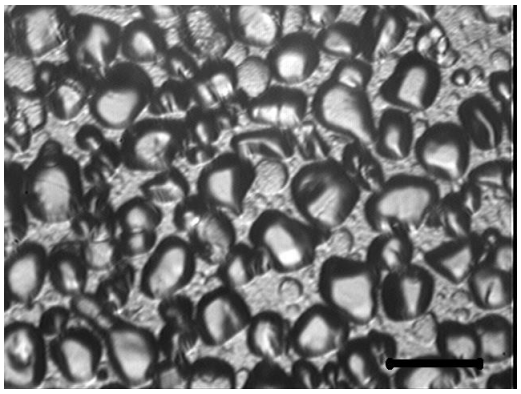

Sample 293

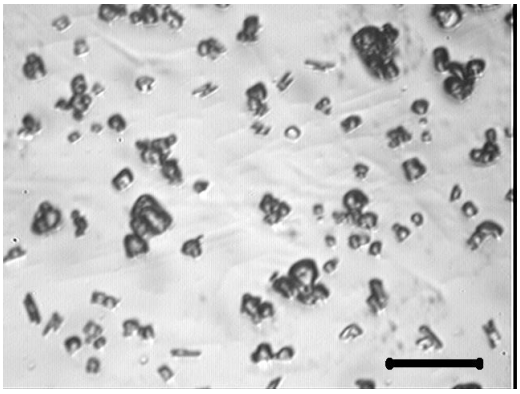

Sample 159

Figure 4.3b: Microscope images of the wide range of ice crystals in commercial ice creams from samples 880 (mean size: 67.1 μm), 293 (mean size: 50.8 μm), and 159 (mean size: 26.3 μm) (40x magnification, 100 μm scale bar).

4.1.1.3 Percent Fat Destabilization

The percent of destabilized fat ranged from 2.60 to 55.3%, displaying a large range of destabilized fat in the commercial ice cream products. **Figure 4.4** (**a-b**) displays the wide range of particle size distribution curves and the corresponding microscopy images. Percent fat destabilization inversely correlated with drip-through rate ($p < 0.0001$). This finding aligns with previous research that has indicated that an increase in partially- coalesced fat led to a decrease in drip-through rate (Berger and White, 1971; Berger et al., 1972; Segall and Goff, 2002; Muse and Hartel, 2004). On the other hand,

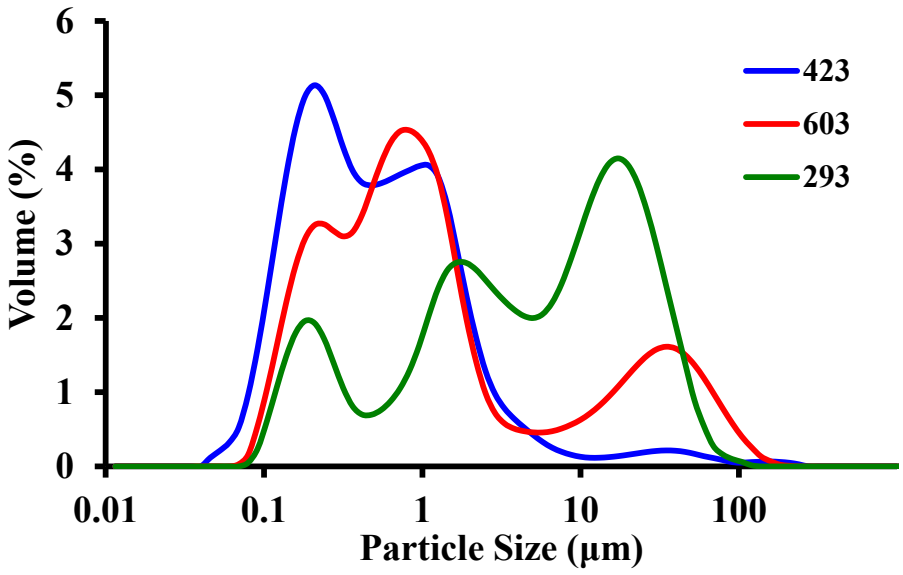

Figure 4.4a Particle size distribution curves representing the wide range in particle size of the 18 commercial ice creams surveyed. Sample 423 represents low partial coalescence (2.6%), sample 603 represents the middle range of partial coalescence (21.9%), and sample 293 represents the high range of partial coalescence (55.3%).

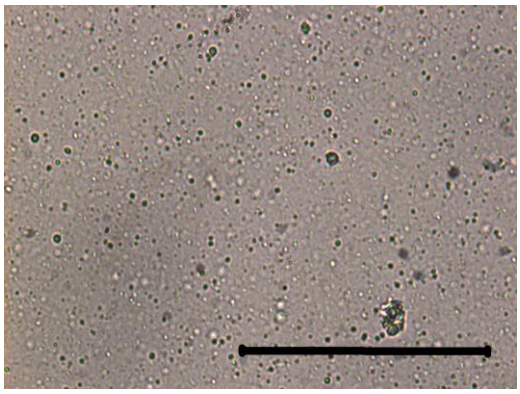

Sample 423

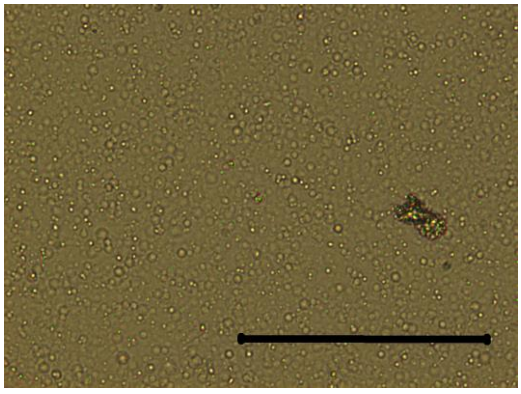

Sample 603

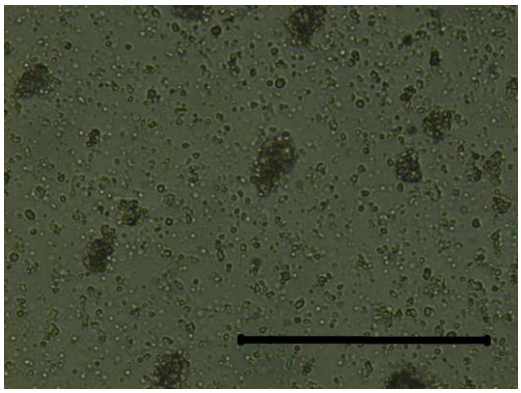

Sample 293

Figure 4.4b Microscope images of melted ice creams representing the range of partially-coalesced fat in the 18 commercial ice creams (400x magnification, 100 μm scale bar).

Koxholt et al. (2001) noted that a low amount of partially-coalesced fat (critical fat globule size determined at $D_{50,3}$ of approximately 1.15 μm) also led to slow meltdown rates. Although the general trend displayed an inverse relationship for drip-through rate and percent fat destabilization, a few products in the survey did not fit the model very well. For instance, sample 652 had 7.9 ± 2.3% destabilized fat with a drip-through rate of 0.44 ± 0.05 g/min and sample 293 contained 55.3 ± 5.9% destabilized fat with a drip-through rate of 0.24 ± 0.04 g/min. These products differed greatly in their percentage of partially-coalesced fat but both had a slow drip-through rate (**Figure 4.5(a-c)**). Although the impact of partially-coalesced fat on drip-

through rate was statistically significant ($p < 0.0001$), **Figure 4.6** displays the lack of trend in drip-through rate versus percent destabilized fat of the 18 samples analyzed. Most likely, there are other factors than percent of destabilized fat that influence rate of drip, including size and number of clusters as well as other interaction parameters. The complete set of particle size curves and microscopy images can be found in **Appendix C1-C2**.

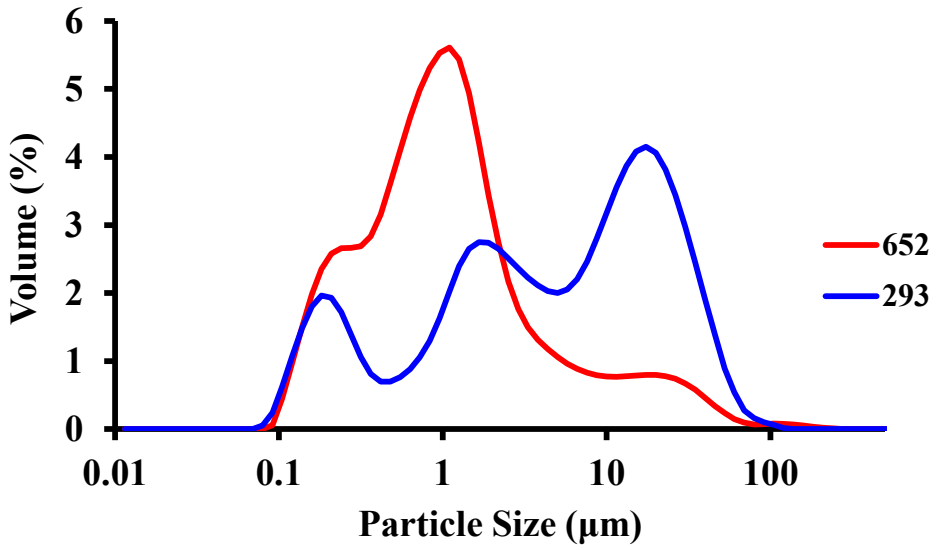

Figure 4.5a: Particle size distribution curves of samples 652 (mean size: 7.9%) and 293 (mean size: 55.3%).

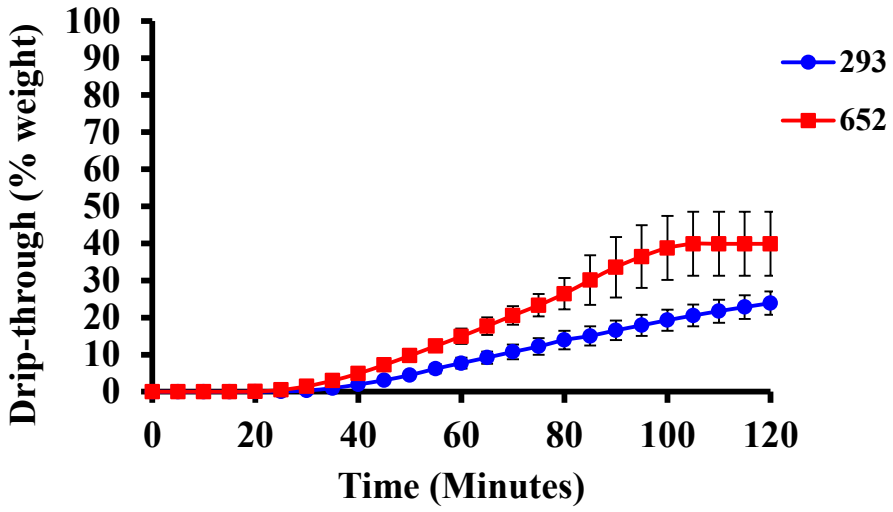

Figure 4.5b: Drip-through curves (% weight) of commercial samples 652 (drip-through rate: 0.44 g/min) and 293 (drip-through rate: 0.24 g/min). Error bars represent the standard deviation between replicates of drip-through rate for each sample.

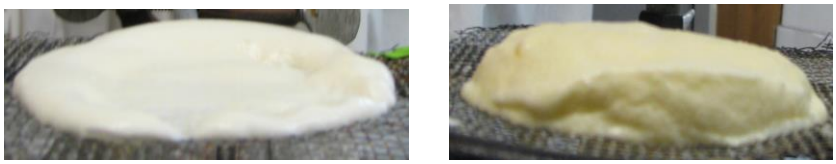

Sample 652 Sample 293

Figure 4.5c: Images of ice cream structure left on top of screen at the end of a drip-through test of commercial ice cream samples 652 and 293.

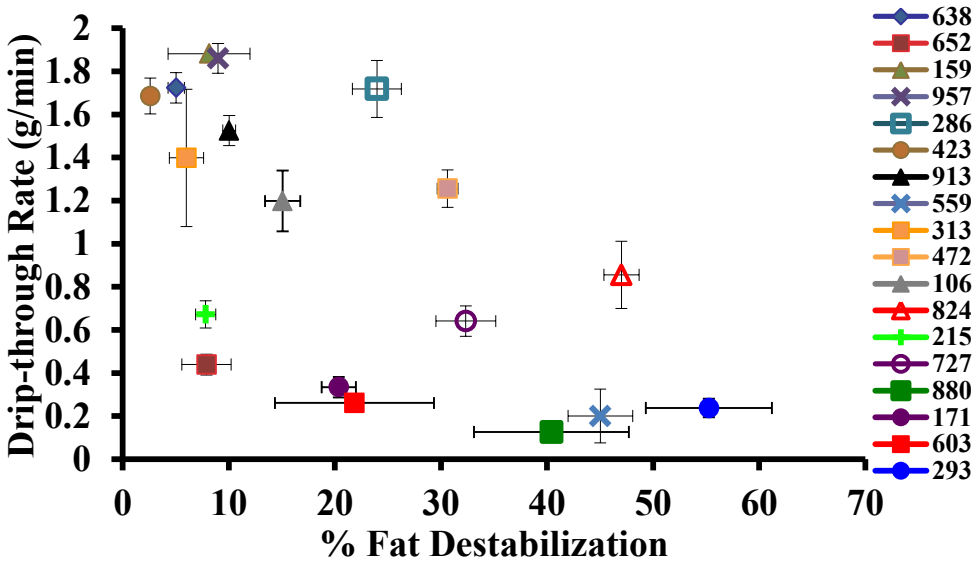

Figure 4.6: Comparison of drip-through rate versus percent fat destabilization of the commercial ice cream samples surveyed. The horizontal error bars represent the standard deviations of the mean percent fat destabilization measured for a specific sample. The vertical error bars represent the standard deviations of the mean drip-through rates measured for a specific sample.

Previous research noted relationships between emulsifier type and levels present in ice cream products to the amount of partially-coalesced fat and the rate of drip (Tharp et al., 1998; Goff et al., 1987). Products surveyed here contained a wide range of emulsifiers, from no added emulsifiers, egg yolk, mono-and diglycerides (MDG), polysorbate 80 (PS80), or a combination of the above. However, no relationship was found between the presence and or type of emulsifier used to the amount of partial coalescence or rate of drip. Other factors must also influence the extent of partial coalescence and rate of melt, such as freezer type, dasher speed, residence time, overrun, and ice content.

4.1.1.4 Overrun

Overrun, which spanned from a low of 21.7% to a high of 119%, was not found to have a correlation with drip-through rate ($p = 0.5757$). This finding does not support that of Sofjan and Hartel (2004) who found that ice creams with high overrun resulted in slow drip-through rates due to the decrease in thermal diffusivity during the melting process. Barring the effect of thermal diffusivity and amount of melted ice, if air cells are not able to collapse the product will resist the natural force of gravity, resulting in a slow drip-through rate (Goff and Hartel, 2013). Our finding also does not support that of Sakurai et al. (1996), who noted that ice creams with low overrun have a fast meltdown rate and ice creams with higher overrun displayed greater resistance to melt. Muse and Hartel (2004) did not notice an influence of overrun on drip-through rate. This was most likely due to the narrow range of overrun in the ice creams produced. On the other hand, Koxholt et al. (2001) determined that drip-through rate depended greatly on overrun and the size of air cells, but they could not draw significant conclusions of their true impact on drip-through rate. Similar to mean ice crystal size, more work is needed to understand the influence of overrun on the rate of drip for ice cream products.

The size of air cells, in addition to the overall stability of the foam, influenced by the network of the fat globules and destabilized fat globules, can affect how the product holds its shape. Sofjan and Hartel (2004) and Koxholt et al. (2001) also found a relationship between overrun and air cell size distribution; an increase in overrun resulted in the break up of larger air cells into smaller air cells. This finding was not supported by the present work ($p = 0.1950$), which could possibly be attributed to air cells changing over time during storage, as noted by Chang and Hartel (2002).

An inverse relationship was found between overrun and mean ice crystal size ($p < 0.001$), as indicated by the direction of the arrows (**Figure 4.1**). This supports the observations made by Arbuckle (1977) and Flores and Goff (1999). Overrun was also inversely correlated to percent total fat ($p < 0.05$). In the market, ice creams with higher amounts of fat generally have less overrun in order to achieve the desired quality.

4.1.1.5 Mean Air Cell Size

Sofjan and Hartel (2004) found that smaller air cells correlated with an increase in overrun, potentially due to an increase in shear stress caused by higher injected air contents. However, in this study, the size of air cells did not have a significant effect on any microstructural, compositional, or behavioral (melt) attributes. Although no significant relationships between air cells and other aspects of ice cream was noted in this study, air cells are important as they help to prevent shrinkage and provide "scoopability" to ice cream products. Here, mean air cell size ranged from a low of 17.1 to as high as 39.5 μm. **Figure 4.7** (**a-b**) displays the size range (large, medium, small) of the air cell size distributions and the microscopy images that coincide with the distributions. This wide range of air cell size is attributed to the freezing conditions, such as pre-aeration, shearing, residence time, and the formation of ice in the freezer. Since air cells can coalesce, leading to larger air cells, in various storage conditions above −28.9 °C, as noted by Chang and Hartel (2002), it is possible that air cells in the ice cream products surveyed changed over time. This change may make it difficult to determine any correlations and influences of air cells on other components of the ice cream products. Analyzing fresh ice cream products with unchanged air cells may provide different relationships and influences on product attributes. The complete set of microscopy images can be found in **Appendix D**.

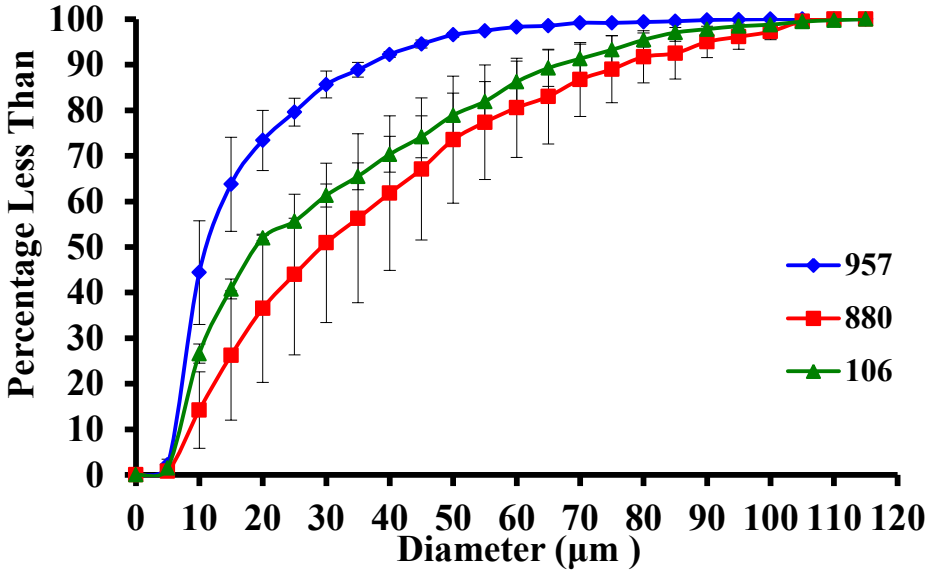

Figure 4.7a: The wide range of mean air cell size distributions of commercial ice creams from samples 880 (mean size: 39.5 µm), 106 (mean size: 30.4 µm), and 957 (mean size: 17.1 µm). The error bars represent the standard deviations of the mean air cell sizes measured.

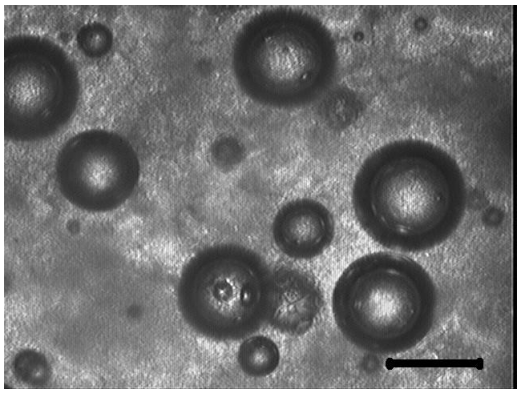

Sample 880

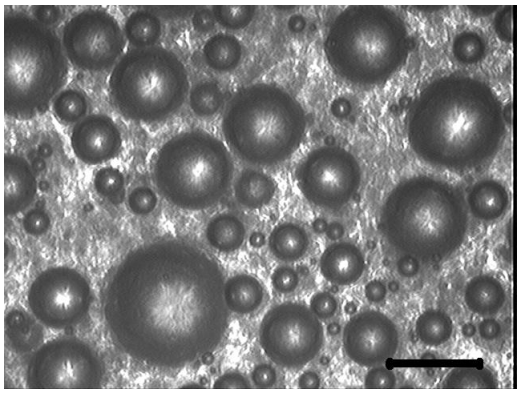

Sample 913

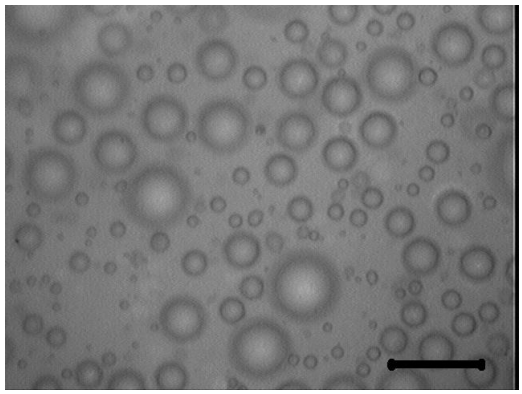

Sample 957

Figure 4.7b: Microscope images of ranges of air cells in commercial ice creams from samples 880 (mean size: 39.5 μm), 913 (mean size: 30.1 μm), and 957 (mean size: 17.1 μm) (40x magnification, 100 μm scale bar).

4.1.1.6 Total Fat

Percent fat, which ranged from as low as 0.01% to a high of 14.3%, negatively correlated with drip-through rate ($p < 0.0001$), which aligns with results of Roland et al. (1999). Percent total fat also had a positive relationship with mean ice crystal size ($p < 0.0001$). This finding does not align with that of Donhowe et al. (1991) and Stampanoni Koeferli et al. (2004). Both indicated that increased fat leads to the formation of smaller ice crystals due to the mechanical

obstruction provided by fat. In these commercial products, nonfat ice cream products tended to have smaller ice crystals as they most likely contained increased amount and types of stabilizers.

4.1.1.7 Total Solids

Total solids (measured between 31.1% and 42.6%) inversely correlated with drip-through rate ($p < 0.01$) and positively correlated with percent fat ($p < 0.0001$). As percent fat increased, it contributed to more total solids present in the mix. Total solids were reported to have an inverse relationship with mean ice crystal size (Donhowe et al., 1991), although no relationship was noted in this study ($p = 0.81$).

4.1.1.8 Density of Mix

Density of the ice cream mix, which is influenced by percent total water, fat, and nonfat solids, was measured (Steinberg, 1963). In general, ice cream mixes have been noted to have a density near 1.1 kg/L, with higher fat attributing to lower densities (Goff and Hartel, 2013). Here, density of ice cream mix ranged between 1.07 and 1.16 kg/L. From the survey, total percent fat and the density of ice cream mix were negatively correlated ($p < 0.0001$), with the 2 nonfat ice creams having the highest densities (1.16 kg/L). As fat content decreases, density of the mix increases as fat is less dense than water and bulking agents/fat replacers.

4.1.2 Sensory Attributes of Ice Cream

Seventeen vanilla ice cream samples were evaluated for 6 key sensory attributes: creaminess, greasiness, melt rate, breakdown (deformation under the manipulation, force, and stresses caused in the mouth), denseness, and particle size (iciness). The sensory lexicon and

ballot used for the evaluation of the ice cream samples can be found in **Appendix E1-E2**. The mean values and the ranges for each sensory attribute are listed in **Table 4.3**. The range for greasiness score is not very wide due to the limitations in the scale used in the study (Appendix A4). **Table 4.4** lists the descriptive analysis ratings on the 15-point numeric scale and the corresponding Student's *t*-test of significant differences at $p < 0.05$ for the 17 samples analyzed.

Table 4.3: Ranges, averages, and standard errors of sensory attributes of commercial ice cream samples.

Attribute	Mean and Standard Error	Range
Breakdown	4.63 ± 0.20	2.79 – 6.67
Creaminess	5.71 ± 0.31	2.42 – 7.32
Denseness	3.46 ± 0.13	2.24 – 4.59
Greasiness	2.95 ± 0.71	2.46 – 3.73
Melt Rate	10.82 ± 0.27	7.17 – 12.40
Particle Size/Iciness	1.11 ± 0.08	0.59 – 2.12

Figure 4.8 displays a biplot of the differences and similarities among samples (numeric points) in relation to the sensory parameters measured (vectors). PC1 and PC2 accounted for 79.7% of the variance in the data. As indicated by the direction of the vectors, melt rate had an inverse relationship with both breakdown ($p < 0.0001$) and denseness ($p < 0.0001$). Since products with higher overrun tend to have a weak body and poor structure, they tended to melt and collapse more quickly in panelists' mouths. Ice cream samples that were perceived as creamy were also noted to be greasy ($p < 0.0001$). Full fat samples also span the range of the sensorial map, providing a broad range of sensory experiences, similar to those of nonfat and low fat. However, full fat samples were noted to be more creamy and greasy than reduced fat and

nonfat samples, as expected (Morris, 1992; Roland et al., 1999). Melt rate was not distinguishable by percent total fat alone as seen by the wide scatter of full fat samples across the biplot. However, in a study by Hyvönen et al. (2003), it was observed that an increase in fat content led to a slight retard of melt in the mouth. This was based on the melting of ice cream in the mouth being attributed to the liquefying of both fat crystals and ice crystals and ice crystals melting at lower temperatures than fat crystals.

Other interactions, such as the breakdown and denseness, can also contribute to the rate of melt as noted above. Products that were perceived as greasy were also noted to have a slower melt rate ($p < 0.01$). The size of ice particulates had no relationship to melting rate of ice cream ($p = 0.34$). This finding is contrary to the findings by Stampanoni Koeferli et al. (2004). This may be attributed to other interactions such as the warmth of the panelists' mouths, enzymatic interactions from saliva, as well as the breakdown and denseness. No relationship was obtained between percent fat and iciness as seen by the large span of samples across the biplot (**Figure 4.8**), again in contrast to that of Stampanoni Koeferli et al. (2004). Creaminess did not affect the melt rate of ice cream ($p = 0.07$). This too can be attributed to the complex interactions that occurred between the panelists' mouths and the ice cream samples.

Table 4.4: Mean descriptive analysis ratings on the 15-point numeric scale and the corresponding Student t-Test of significant differences at $p < 0.05$ for the 17 samples analyzed.

Sample Code	Melt rate	Breakdown	Size of ice particulate	Denseness	Greasiness	Overall creaminess
106	12.4 ± 1.3^{a}	2.8 ± 1.1^{h}	2.1 ± 1.6^{a}	2.2 ± 0.7^{e}	2.8 ± 1.4^{bcdef}	5.8 ± 2.4^{bcd}
159	11.9 ± 1.7^{ab}	3.9 ± 1.9^{fgh}	0.7 ± 0.8^{f}	3.1 ± 0.8^{cd}	2.9 ± 1.3^{bcdef}	5.1 ± 2.5^{de}
171	11.3 ± 2.2^{bcd}	4.0 ± 2.0^{defg}	1.2 ± 0.9^{bcde}	3.0 ± 1.2^{cd}	3.2 ± 1.5^{abc}	6.4 ± 2.1^{abc}
215	12.2 ± 1.3^{ab}	3.6 ± 1.7^{gh}	1.4 ± 1.0^{bc}	2.8 ± 0.9^{de}	2.6 ± 0.9^{def}	4.6 ± 1.9^{ef}
286	10.9 ± 1.9^{cde}	5.2 ± 2.2^{abc}	0.8 ± 0.9^{ef}	3.3 ± 1.1^{bcd}	3.2 ± 1.4^{abcd}	4.1 ± 2.0^{f}
293	11.2 ± 2.9^{bcde}	3.9 ± 1.6^{efg}	1.7 ± 1.5^{ab}	3.2 ± 0.9^{cd}	3.1 ± 1.3^{abcde}	6.1 ± 2.2^{bcd}
313	11.1 ± 2.6^{bcde}	4.5 ± 1.9^{bcdefg}	0.7 ± 0.5^{f}	3.3 ± 1.0^{bcd}	3.2 ± 1.5^{abcd}	6.5 ± 1.9^{abc}
423	11.6 ± 2.1^{abc}	4.4 ± 1.9^{cdefg}	0.9 ± 1.0^{def}	3.3 ± 1.0^{bcd}	2.9 ± 1.8^{bcdef}	3.7 ± 2.8^{f}
472	10.9 ± 1.6^{cde}	4.7 ± 1.9^{abcdef}	1.0 ± 0.6^{cdef}	3.8 ± 1.1^{ab}	2.7 ± 1.1^{bcdef}	4.6 ± 1.7^{ef}
559	9.08 ± 2.1^{f}	5.5 ± 3.1^{ab}	1.4 ± 1.3^{bcd}	4.2 ± 2.1^{a}	3.3 ± 1.5^{ab}	6.8 ± 2.1^{ab}
603	11.5 ± 2.4^{abcd}	4.7 ± 1.6^{bcdef}	0.8 ± 0.7^{ef}	3.4 ± 0.7^{bc}	3.0 ± 1.1^{bcde}	5.8 ± 1.5^{bcd}
638	10.8 ± 1.5^{cde}	5.1 ± 2.1^{abc}	1.1 ± 0.8^{cdef}	3.8 ± 1.3^{ab}	2.4 ± 1.0^{f}	4.2 ± 1.7^{ef}
652	10.9 ± 2.5^{cde}	3.5 ± 1.4^{gh}	1.4 ± 1.2^{bc}	2.8 ± 1.0^{de}	3.0 ± 1.0^{bcdef}	5.7 ± 2.4^{cd}
727	11.6 ± 1.7^{abc}	4.0 ± 1.9^{defg}	1.2 ± 1.2^{bcde}	3.1 ± 1.2^{cd}	2.7 ± 1.1^{cdef}	5.2 ± 1.6^{de}
880	10.2 ± 2.6^{e}	5.7 ± 3.1^{a}	0.6 ± 0.6^{f}	4.1 ± 1.8^{a}	3.7 ± 1.5^{a}	7.3 ± 1.9^{a}
913	$10.3\pm2.2d^{e}$	4.9 ± 2.1^{abcd}	1.1 ± 1.0^{cdef}	3.8 ± 1.1^{ab}	2.5 ± 1.0^{ef}	3.9 ± 1.8^{f}
957	11.3 ± 2.0^{bcd}	4.9 ± 2.0^{abcde}	1.1 ± 1.1^{cdef}	3.2 ± 1.2^{bcd}	2.8 ± 1.2^{bcdef}	6.2 ± 2.8^{bcd}

^{a,b,c,d,e,f,g,h,i,j,k} Means not sharing the same letter are significantly different ($\alpha = 0.05$).

4.1.3 Correlations Between Sensory and Structural Parameters of Ice Cream

Sensorial characteristics are very important for analyzing ice cream products. Determining relationships between sensorial and microstructural components can assist in understanding how microstructure components possibly predict sensorial behaviors. **Figure 4.9** represents the combined biplot of microstructure and sensorial attributes of ice cream products. Here, PC1 and PC2 accounted for 56.8% of the variance of the data. A lower degree of variance of PC1 and PC2 occurred when combining sensorial and structural attributes.

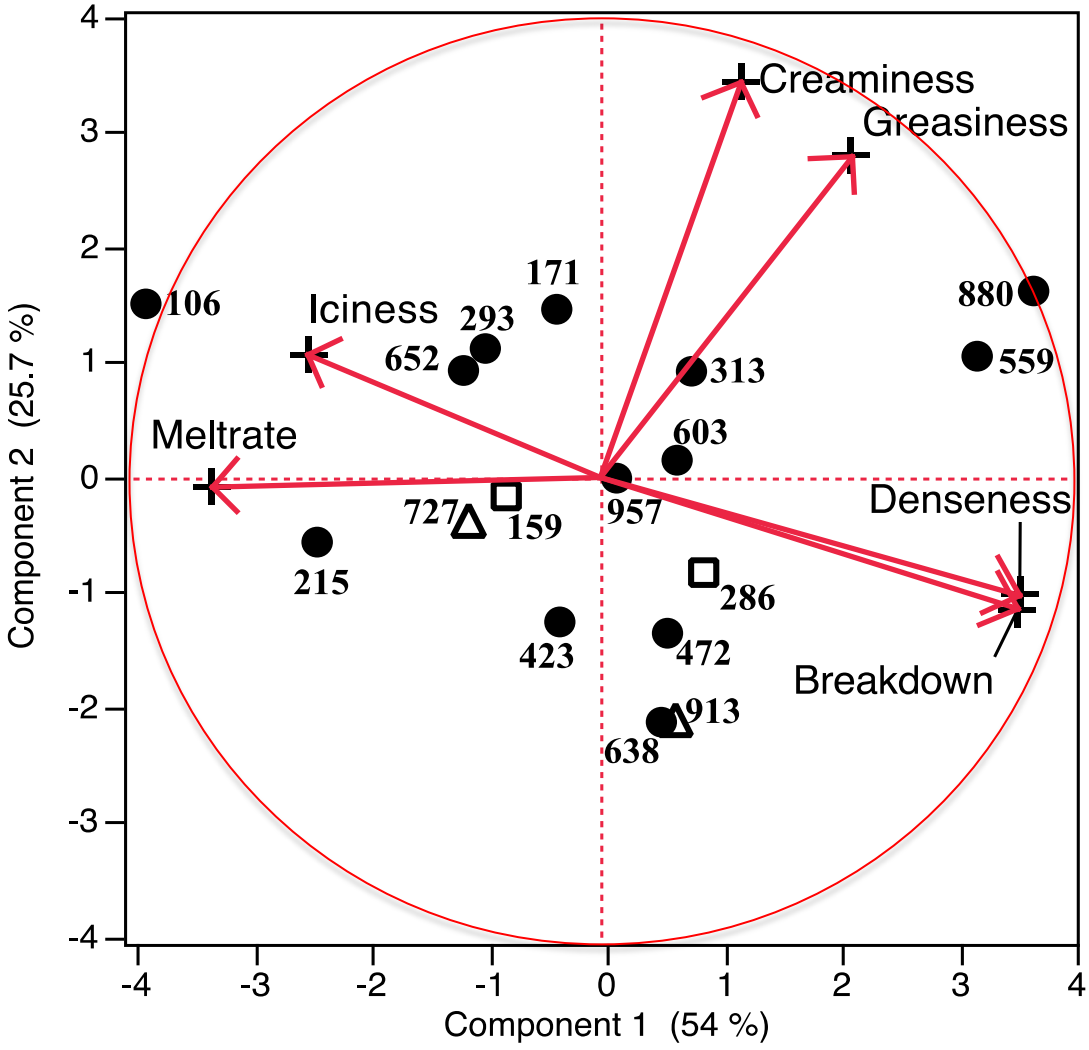

Figure 4.8: Principle component analysis biplot of the sensory parameters of commercial ice cream samples. Ice cream product samples are represented by a three-digit code and the vectors represent the microstructure parameters tested. The following shapes represent the levels of fat present in the ice cream products:

●=full fat products; △= reduced fat/light products; □= nonfat products.

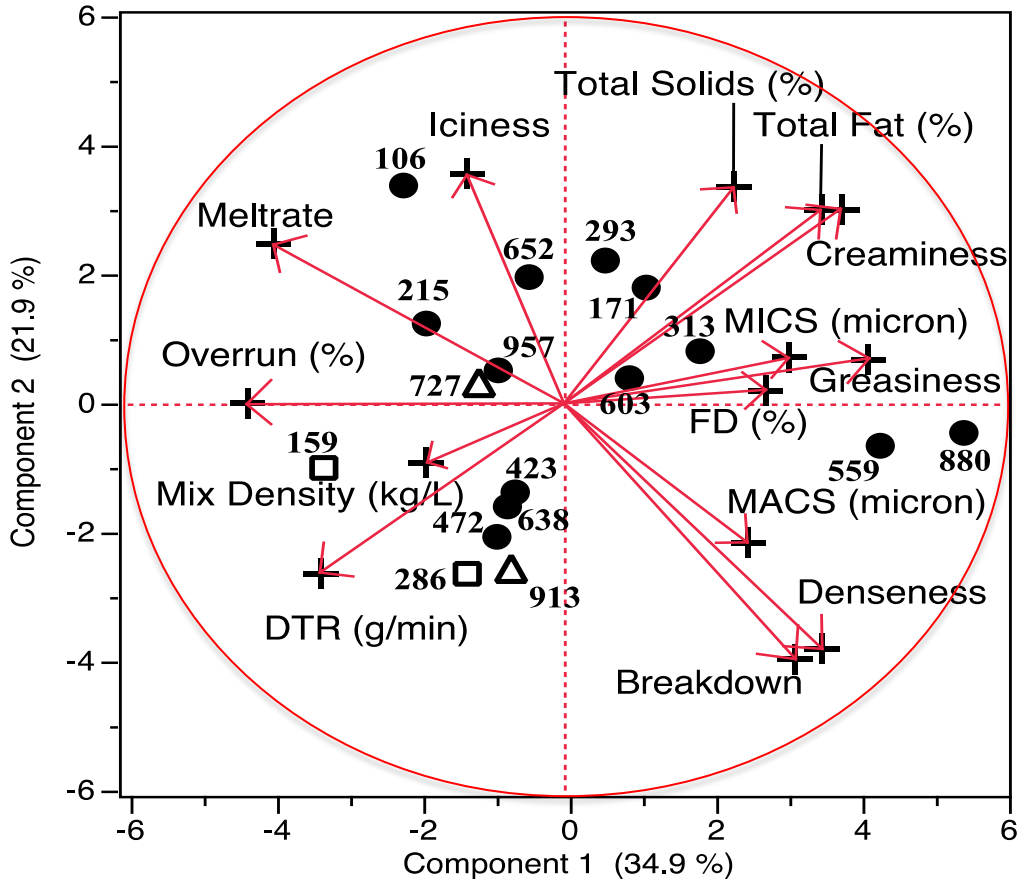

Figure 4.9: Biplot of sensorial and microstructural parameters/instrumental measurements of commercial ice cream products. Ice cream product samples are represented by a three-digit code and the vectors represent the microstructure parameters tested. The meaning of the abbreviations above are as follows: **MACS** = Mean Air Cell Size; **MICS** = Mean Ice Crystal Size, **FD** = Fat Destabilization; **DTR** = Drip-through Rate. The following shapes represent the levels of fat present in the ice cream products:

●=full fat products; △= reduced fat/light products; □= nonfat products.

Percent fat destabilization ($p < 0.01$) and mean air cell size distribution ($p < 0.01$) had an inverse relationship with sensory melt rate. Mean air cell size had a stronger correlation with denseness ($p < 0.001$) and breakdown ($p < 0.01$) than overrun (dense- ness and breakdown—$p < 0.05$). Overrun did not have a significant correlation with mean air cell size distribution ($p = 0.19$) as seen in the direction of the corresponding arrows in **Figure 4.9**. Greasiness ($p < 0.01$) and creaminess ($p < 0.0001$) both had an inverse relationship with drip-through rate. In general,

nonfat and low fat ice cream samples were perceived as less creamy and greasy than the majority of the full fat ice cream samples. Creaminess corresponded with percent total fat ($p < 0.0001$) and percent fat destabilization ($p < 0.01$), whereas greasiness only corresponded with percent fat destabilization ($p < 0.01$). Samples 559 and 880 were perceived to have maximum greasiness and creaminess as they had high percentages of destabilized fat and total fat. This reaffirms that destabilized fat contributes to the increased perception of creaminess and greasiness in ice cream products. Greasiness and overall creaminess had a strong inverse relationship with overrun (greasiness—$p <0.0001$, creaminess—$p < 0.0001$). This could be attributed to the perception of both greasiness and creaminess being sensed more readily by the panelists in ice cream products with less overrun. Also, products with lower overrun tend to have larger amounts of total fat and destabilized fat, which leads to the creamy and greasy mouth feel. Those ice creams with high percent total solids were perceived to have a high overall creaminess score ($p < 0.0001$) as well as greasiness ($p < 0.05$).

However, not all sensorial and microstructural components of ice cream products correlated with one another, as there were other interactions that impacted the behavior at both ambient and mouth temperatures. Surprisingly, no significant relationship was found between iciness and mean ice crystal size ($p = 0.59$), in contrast to the results of Russell et al. (1999). Perhaps the naturally warm temperature of the panelists' mouths could have influenced the lack of detection of ice crystals in the samples. Other interactions and components that influence sensorial properties, like creaminess due to percent fat and percent fat destabilization, also might hinder the detection of ice crystals in ones mouth. Also, no correlation was observed between mean ice crystal size and overall creaminess ($p = 0.12$), as samples with the highest creaminess factor also had the largest mean ice crystal size (e.g., sample 880). For these samples, the

panelists noted a small size of ice particulates despite the large ice crystals (measured at 67.1 μm). It is generally assumed that ice crystals above 50 μm are detectable by the tongue. This lack of correlation with ice crystal size in this particular sample could be attributed to the high percentage of fat destabilization, which may be a factor in limiting the detection of large ice crystals and increasing the perception of overall creaminess. Sample 106 was perceived to be the iciest although sample 880 had the largest mean ice crystal mean size.

Melt rate and drip-through rate were not found to have a significant correlation ($p = 0.14$), which supports findings of Guinard et al. (1997). Since the temperature of the inside of the mouth is warmer than that of ambient temperatures, the condition under which ice cream melts in the mouth may not be comparable to that of ambient temperatures. This lack of correlation might also be due to the shear forces that are created during consumption. As a result, the current drip-through test, although significant in analysis of production and compositional parameters, may not be the best approach to understanding the sensorial relationship between drip-through and melt rate. Further research is needed to determine an instrumental method of analysis that best correlates with sensory melt rate.

4.2 Effect of Dasher Speed, Overrun, and Emulsifier Ratio on Microstructure and Physical Properties of Ice Cream

The effect of processing conditions (dasher speed and overrun) and ingredients (emulsifier ratio and fat content) on partial coalescence and drip-through rate were studied. Various responses and their interactions were measured, including actual overrun, draw temperature, mean ice and air cell size, partial coalescence, and drip-through rate.

Across all conditions, the average draw temperature was -6.1±0.1^{o}C, which was close to the target draw temperature of -6.0^{o}C. Actual overrun was also very similar to the target overrun (50% = 52.5 ± 3.7% overrun, 75% = 74.8 ± 2.7% overrun, and 100% = 99.5 ± 5.6% overrun) for all conditions.

4.2.1 Mean Ice Crystal Size

The mean ice crystal sizes ranged from 28.7 to 37.2 μm for all ice creams. Goff and Hartel (2013) indicated that ice crystals typically range between 35 to 45 μm. The majority of the ice crystals from this study fell within this range. The differences in average size of ice crystals in this study were very small as all ice creams were frozen to -6.1±0.1^{o}C. **Table 4.5** displays the mean ice crystal size distributions, values, and standard deviations for all ice crystals. All microscopy images and graphs of ice crystal size distributions for constant overrun, dasher speed, and emulsifier ratio can be found in **Appendix F.1-F.18**.

As dasher speed increased, it was expected that mean ice crystal size would increase as the temperature inside the freezer increased due to greater frictional heat released, resulting in dissolution and recrystallization (Donhowe and Hartel, 1996). A Tukey's HSD test determined statistical differences ($\alpha = 0.05$) in ice crystals sizes for ice creams made with 80:20 (MDG:PS80) at 75% and 100% overrun as dasher speed increased. However, the freezer was controlled to produce ice creams at the same draw temperature by lowering the evaporator pressure to counter heat generated by the increase in dasher speed. Generally, the differences between the mean sizes at different dasher speeds were small and not significant for this reason.

Table 4.5: Means and standard deviations of ice crystal size for ice creams based on emulsifier ratio (mono- and diglyceride:polysorbate 80 (MDG:PS80)), dasher speed (RPM), and overrun (%). The standard deviation (±) represents the variation between replicate means of ice crystal size measurements determined at a set overrun, dasher speed, and emulsifier ratio.

		Mean Ice Crystal Size (µm)		
MDG:PS80	**RPM**	**50%**	**75%**	**100%**
[1]0:0	250	$35.7\pm2.7^{ab,A,x}$	$33.6 \pm 3.3^{a,A,x}$	$34.3 \pm 0.8^{a,A,x}$
	500	$37.2 \pm 1.5^{a,A,x}$	$32.2\pm 1.0^{a,B,xy}$	$30.2 \pm 0.7^{b,C,x}$
	750	$33.7 \pm 1.6^{b,A,x}$	$33.8\pm 2.0^{a,A,x}$	$32.4 \pm 2.7^{ab,A,x}$
[2]100:0	250	N/A*	N/A*	N/A*
	500	$29.4\pm1.4^{a,A,z}$	N/A*	$30.6\pm2.0^{a,A,x}$
	750	$28.9\pm1.8^{a,A,y}$	N/A*	$32.4\pm2.6^{a,B.x}$
[3]90:10	250	$35.3 \pm 1.1^{a,A,x}$	$32.3 \pm 2.1^{a,AB,x}$	$32.0 \pm 2.9^{a,A,xy}$
	500	$34.4 \pm 0.8^{a,A,y}$	$34.3\pm 3.1^{a,A,x}$	$34.1 \pm 0.7^{a,A,y}$
	750	$34.6 \pm 1.2^{a,A,x}$	$33.9 \pm 2.5^{a,A,x}$	$32.4 \pm 3.0^{a,A,x}$
[4]80:20	250	$34.3 \pm 1.8^{a,A,x}$	$28.7 \pm 1.5^{a,B,y}$	$31.3 \pm 0.9^{a,C,y}$
	500	$30.0 \pm 1.6^{a,A,z}$	$29.6\pm 1.8^{a,A,y}$	$30.7 \pm 1.7^{a,A,x}$
	750	$34.0 \pm 2.2^{a,A,x}$	$34.4 \pm 1.4^{b,A,x}$	$34.5 \pm 2.1^{b,A,x}$

[a,b,c] denote significant differences among ice creams based on constant overrun (columns)
[A,B,C] denote significant differences among ice creams based on constant dasher speed (rows)
[x,y,z] denote significant differences among ice creams based on emulsifier ratio, constant dasher speed, and constant overrun (columns)
*Samples not included in experimental design
[1]no added emulsifiers in the formula
[2]total emulsifiers added consisted of 100% MDG at 0.15% in the formula
[3]total emulsifiers added consisted of 90:10 MDG:PS80 at 0.15% in the formula
[4]total emulsifiers added consisted of 80:20 MDG:PS80 at 0.15% in the formula

Overrun has also been known to affect the size of ice crystals. Arbuckle (1977), Thomas (1981), and Flores and Goff (1999) found that larger ice crystals were produced at lower overrun. These studies attributed this occurrence to an increase in overrun resulting in a thinner serum phase, which in turn increased the collision rate of ice crystals (secondary effect). Although not a large effect, Sofjan and Hartel (2003) too found that mean ice crystal size

generally decreased with increasing overrun. Utilizing one-way ANOVA and Tukey's HSD test, statistical differences ($\alpha = 0.05$) were found as overrun increased for ice creams made with no added emulsifiers at 500 RPM and at 250 RPM for ice creams made with 80:20 (MDG:PS80). These differences, although statistically significant, were very small. Again, controlling the draw temperature during freezing allowed for the control of ice crystal sizes, despite the increase in overrun.

For ice creams made with PS80, (90:10 (MDG:PS80) and 80:20 (MDG:PS80)) a two-way ANOVA determined that the interaction of both dasher speed and overrun had a marginal effect on ice crystal size ($p = 0.0117$). Although the probability was not high, dasher speed ($p = 0.0032$) was found to have a more significant effect than overrun ($p = 0.0155$). Statistically significant differences were determined between 750 RPM and both 250 RPM and 500 RPM and for 50% and 75% overrun. Although these effects were determined to be statistically significant, the differences between mean sizes were very small (**Table 4.1**). All ice crystal size distributions and microscopy images for mean ice crystal size distributions processed at 50% overrun (constant dasher speed), 500 RPM (constant overrun), and across emulsifier ratio (500 RPM, 50% overrun) can be found in **Appendix F.1-F.18**. Ice crystal size distributions for 750 RPM and 250 RPM (constant dasher speed) and 100% and 75% (constant overrun) were very similar to 500 RPM (constant dasher speed) and 50% (constant overrun) and are not displayed.

4.2.2 Partial Coalescence (PC)

The amount of partially-coalesced fat in ice creams varied with the emulsifier ratio, dasher speed, and overrun. **Table 4.6** shows the mean values and standard deviations for PC across all ice creams. PC values ranged from 5.5 to 84.4 %. The ice creams made with 80:20 (MDG:PS80) had the highest levels of PC, whereas the ice creams made with no added emulsifiers had the lowest levels. In general, as dasher speed increased, PC increased. In addition, an increase in overrun increased the level of PC. These trends are generally seen throughout each emulsifier ratio. The level of PC increased with added emulsifiers and further increased as PS80 increased.

An increase in dasher speed increased the level of PC by increasing the shear stress on the ice cream across all emulsifier ratios ($p < 0.0001$ for all emulsifier ratios except 100:0 (MDG:PS80) – $p = 0.2792$)). The ice creams made at 750 RPM had the highest levels of PC due to the high shear forces on the ice cream across all emulsifier levels, except 100:0 (MDG:PS80) at 50% overrun. No significant difference was determined as dasher speed increased from 500 RPM to 750 RPM at 50% overrun for ice creams made with 100:0 (MDG:PS80). **Figure 4.10 (a-d)** shows the particle size distributions for ice creams at 50% overrun across all emulsifier ratios. With an increase in shear rate, there was an increase in the encounter rate among the fat globules, which resulted in an increase in partial coalescence (Walstra, 2003). For all emulsifier ratios, ice creams processed at 250 RPM had the lowest levels of PC, following previous findings in literature (Goff, 1997, 2002; Goff and Hartel, 2013). Particle size distributions for 75% and 100% overrun can be found in **Appendix G** (**Figure G.1 –G.6**). **Figure 4.11 (a-d)** displays the microscopy images of fat clusters as dasher speed increased for ice creams processed at 50%

overrun across all emulsifier ratios. Additional microscopy images for 75% and 100% overrun can be found in **Appendix G** (**Figure G.8-G.11**).

Table 4.6: Means and standard deviations of partial coalescence for ice creams based on emulsifier ratio (mono- and diglyceride:polysorbate 80 (MDG:PS80)), dasher speed (RPM), and overrun (%). The standard deviation (±) represents the variation between replicate means of calculated partial coalescence measurements determined at a set overrun, dasher speed, and emulsifier ratio.

		Partial Coalescence (%)		
MDG:PS80	**RPM**	**50%**	**75%**	**100%**
[1]0:0	250	$5.5\pm 1.5^{a,A,w}$	$8.2 \pm 1.5^{a,B,w}$	$9.5\pm 1.7^{a,B,w}$
	500	$5.9\pm 1.9^{a,A,w}$	$9.3\pm 1.8^{a,B,w}$	$16.5\pm4.0^{b,C,w}$
	750	$10.8 \pm 2.6^{b,A,w}$	$15.9\pm 2.6^{b,B,w}$	$18.8\pm 1.7^{b,B,w}$
[2]100:0	250	N/A*	N/A*	N/A*
	500	$19.6\pm3.2^{a,A,x}$	N/A*	$56.0\pm6.0^{a,B,x}$
	750	$24.9\pm3.8^{a,A,x}$	N/A*	$70.9\pm8.1^{b,B,x}$
[3]90:10	250	$18.5 \pm 7.3^{a,A,x}$	$27.4 \pm 5.0^{a,B,x}$	$37.9\pm 3.0^{a,C,x}$
	500	$28.3 \pm 2.6^{b,A,y}$	$44.1 \pm 4.2^{b,B,x}$	$60.3 \pm 2.8^{b,C,x}$
	750	$35.0 \pm 3.4^{b,A,y}$	$58.1 \pm 5.6^{c,B,x}$	$73.7 \pm 1.6^{c,C,x}$
[4]80:20	250	$43.9 \pm 6.0^{a,A,y}$	$56.1 \pm 3.4^{a,B,y}$	$68.8 \pm 6.7^{a,C,y}$
	500	$56.2 \pm 9.1^{b,A,z}$	$65.9 \pm 12.3^{ab,AB,y}$	$73.8 \pm 2.1^{a,B,y}$
	750	$66.5 \pm 3.4^{c,A,z}$	$70.3 \pm 3.2^{b,A,y}$	$84.4 \pm 3.5^{b,B,y}$

^{a,b,c} denote significant differences among ice creams based on constant overrun (columns)
^{A,B,C} denote significant differences among ice creams based on constant dasher speed (rows)
^{w,x,y,z} denote significant differences among ice creams based on emulsifier ratio, constant dasher speed, and constant overrun (columns)
*Samples not included in experimental design
[1]no added emulsifiers in the formula
[2]total emulsifiers added consisted of 100% MDG at 0.15% in the formula
[3]total emulsifiers added consisted of 90:10 MDG:PS80 at 0.15% in the formula
[4]total emulsifiers added consisted of 80:20 MDG:PS80 at 0.15% in the formula

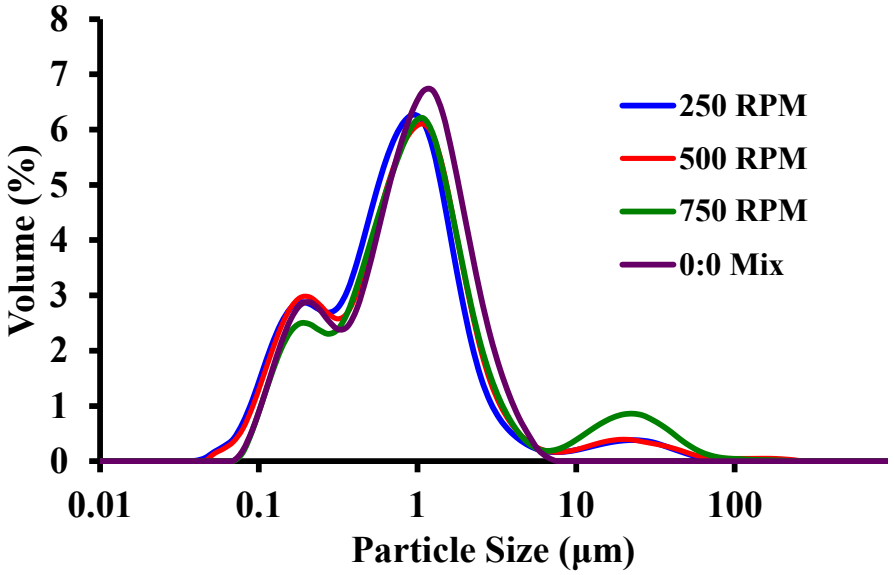

Figure 4.10a: Particle size distributions for ice cream mix made with no added emulsifiers and ice creams processed at 50% overrun and at set dasher speeds of 250 RPM, 500 RPM, and 750 RPM. Similar results were seen for 250 RPM and 750 RPM and 75% and 100% overrun (**Appendix G**).

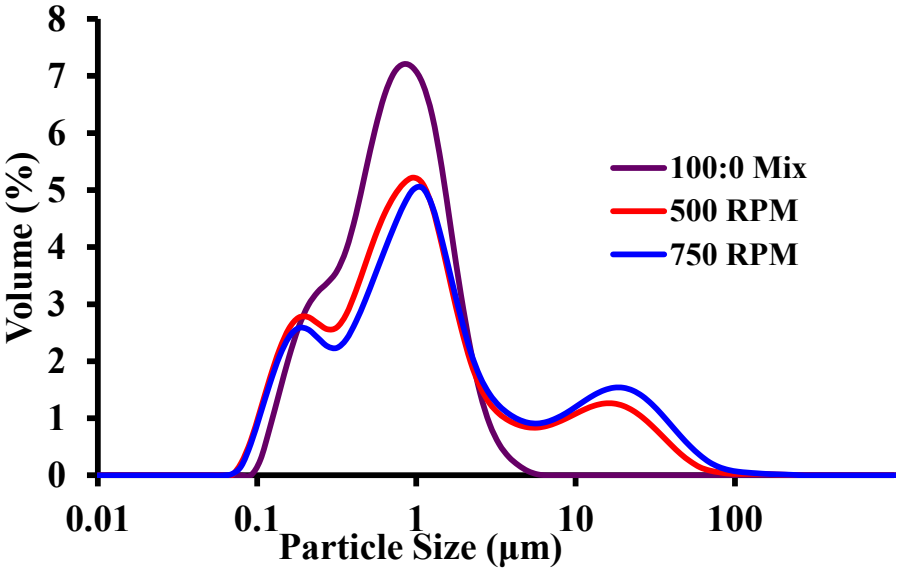

Figure 4.10b: Particle size distributions for ice cream mix made 100:0 (mono- and diglyceride:polysorbate 80 - MDG:PS80) and ice creams processed at 50% overrun and at set dasher speeds of 500 RPM and 750 RPM. Similar results were seen for 750 RPM and 100% overrun (**Appendix G**).

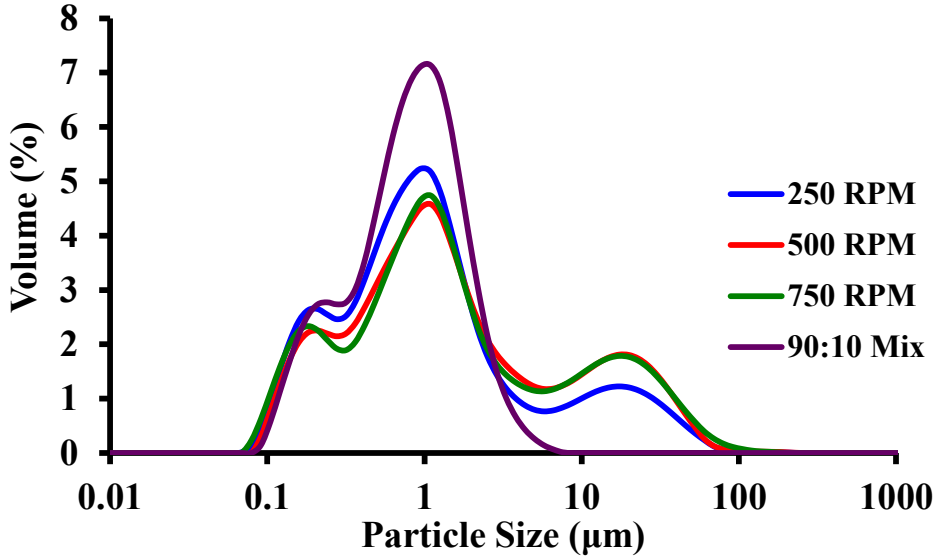

Figure 4.10c: Particle size distributions for ice cream mix made with 90:10 (mono- and diglyceride:polysorbate 80 - MDG:PS80) and ice creams processed at 50% overrun at dasher speeds of 205 RPM, 500 RPM, and 750 RPM. Similar results were seen for 250 RPM and 750 RPM and 75% and 100% overrun (**Appendix G**).

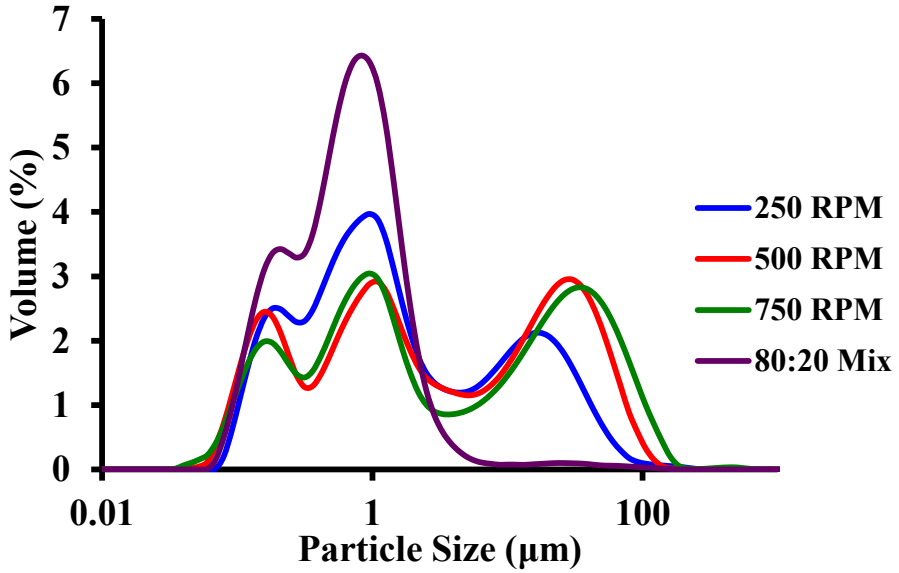

Figure 4.10d: Particle size distributions for ice cream mix made with 80:20 (mono- and diglyceride:polysorbate 80 - MDG:PS80) and ice creams processed at 50% overrun and at set dasher speeds of 250 RPM, 500 RPM, and 750 RPM. Similar results were seen for 250 RPM and 750 RPM and 75% and 100% overrun (**Appendix G**).

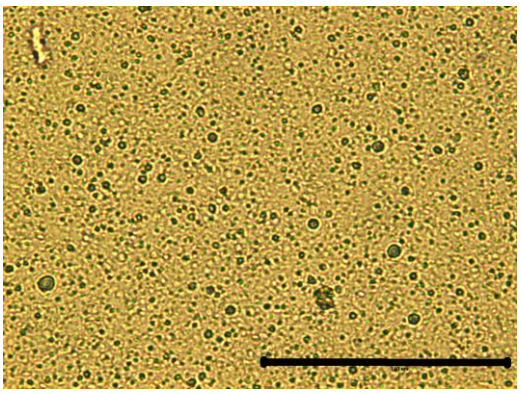

250 RPM

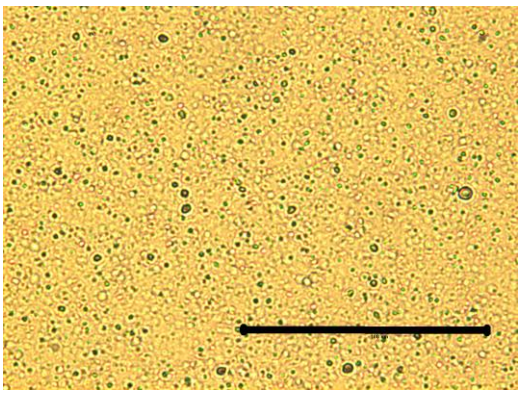

500 RPM

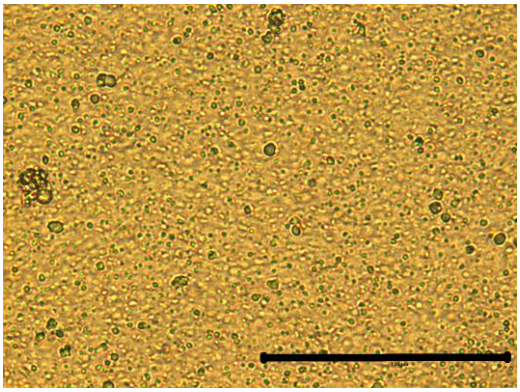

750 RPM

Figure 4.11a: Microscope images of melted ice creams made with no added emulsifiers at 50% overrun and dasher speeds of 250 RPM, 500 RPM, and 750 RPM (400x magnification, 100 μm scale bar).

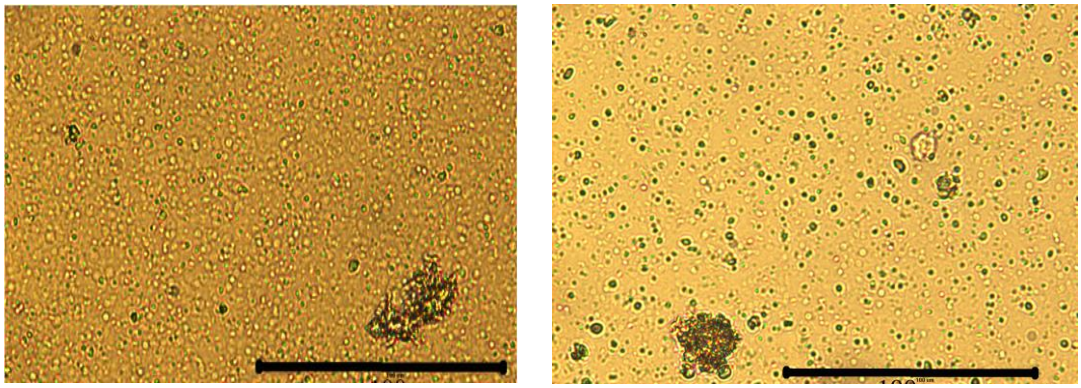

500 RPM 750 RPM

Figure 4.11b: Microscope images of melted ice creams made 100:0 (mono- and diglyceride:polysorbate 80 - MDG:PS80) at 50% overrun and dasher speeds of 500 RPM and 750 RPM (400x magnification, 100 μm scale bar).

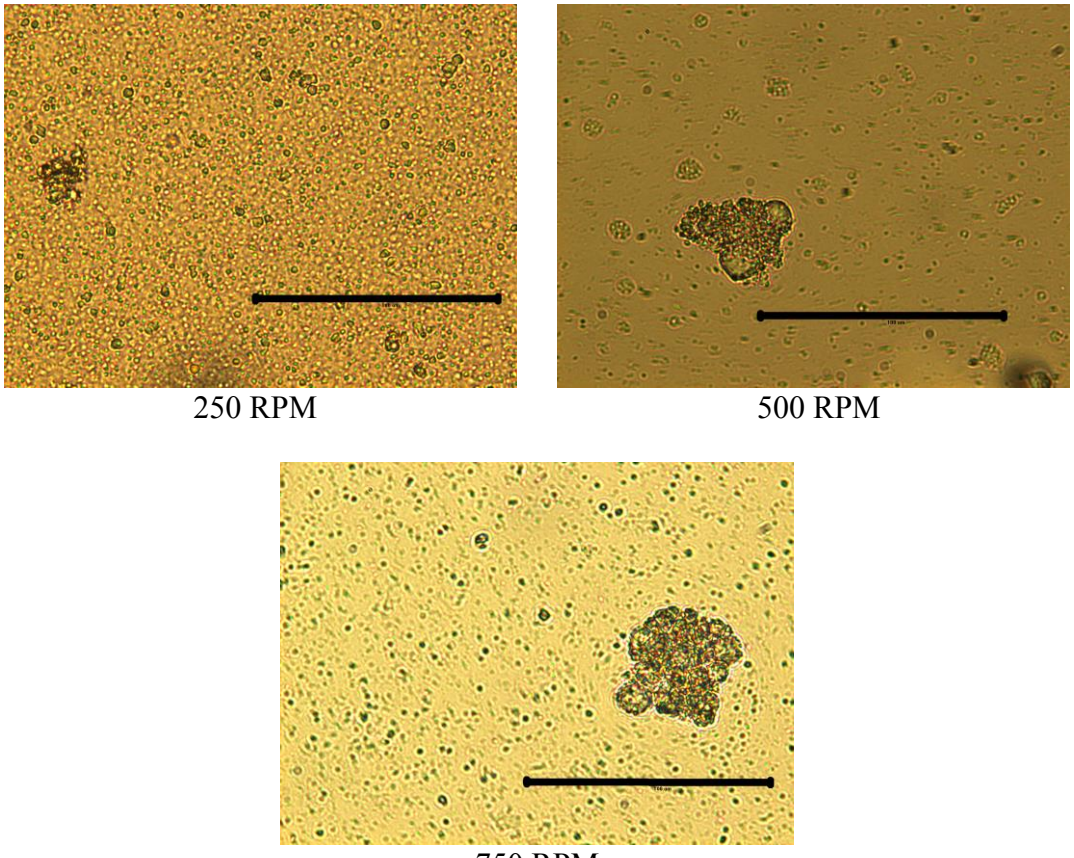

250 RPM 500 RPM

750 RPM

Figure 4.11c: Microscope images of melted ice creams made with 90:10 (mono- and diglyceride:polysorbate 80 - MDG:PS80) at 50% overrun and 250 RPM, 500 RPM, and 750 RPM (400x magnification, 100 μm scale bar).

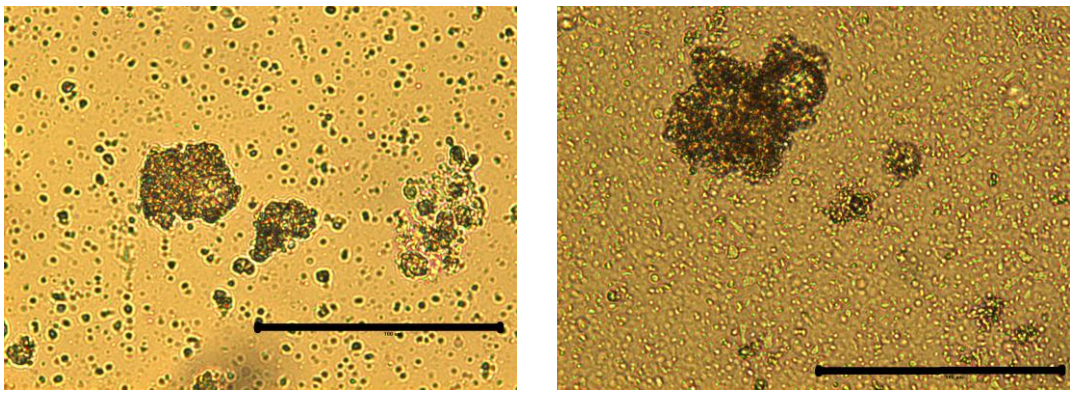

250 RPM 500 RPM

750 RPM

Figure 4.11d: Microscope images of melted ice creams made with 80:20 (mono- and diglyceride:polysorbate 80 - MDG:PS80) at 50% overrun and dasher speeds of 250 RPM, 500 RPM, and 750 RPM (400x magnification, 100 μm scale bar).

PC increased as overrun increased, a trend also observed by Goff and Vega (2007) (**Figure 4.12(a-d)**). An increase in air content causes the repeated adsorption/desorption of fat to the air interface, which in turn increases the collision rate of the fat globules. As a result, the introduction of more air along with shear causes an increase in PC. Similar, in this study, ice creams with 100% overrun had the highest level of PC while ice creams with 50% overrun had the lowest levels of PC. This trend was seen across all emulsifier levels and dasher speeds. Microscopy images of fat clusters as overrun changed are displayed in **Figure 4.13(a-d)** for all

emulsifier levels at 500 RPM. Additional particle size distribution curves and microscopy images of fat clusters across all emulsifier levels for 250 RPM and 750 RPM are located in **Appendix G (Figure G.8 – G.18)**.

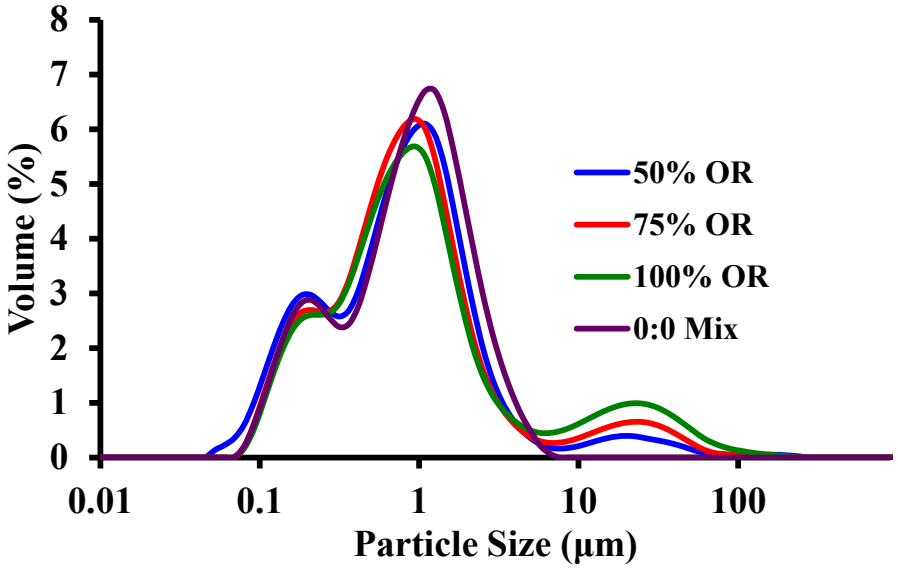

Figure 4.12a: Particle size distributions for ice cream mix made with no added emulsifiers and ice creams processed at dasher speed of 500 RPM with overruns (OR) of 50%, 75%, and 100%.

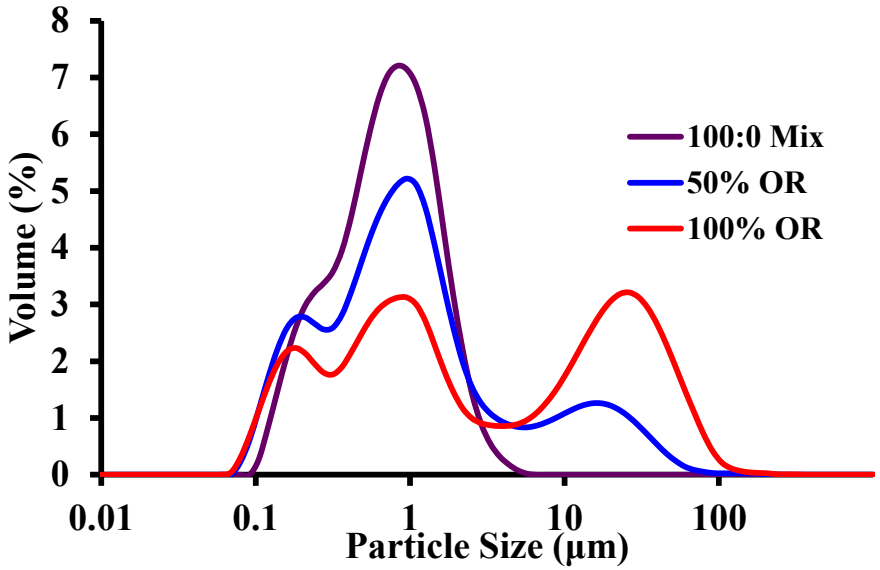

Figure 4.12b: Particle size distributions for ice cream mix made with 100:0 (mono- and diglyceride:polysorbate 80 - MDG:PS80) and ice creams processed at dasher speed of 500 RPM and overruns (OR) of 50% and 100%.

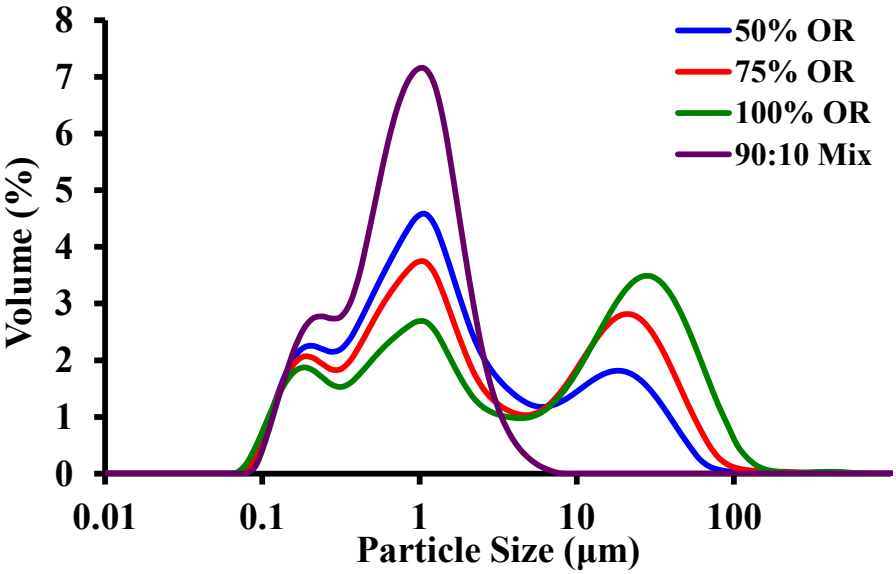

Figure 4.12c: Particle size distributions for ice cream mix made with 90:10 (mono- and diglyceride:polysorbate 80 - MDG:PS80) and ice creams processed at dasher speed of 500 RPM and overruns (OR) of 50%,75%, and 100%.

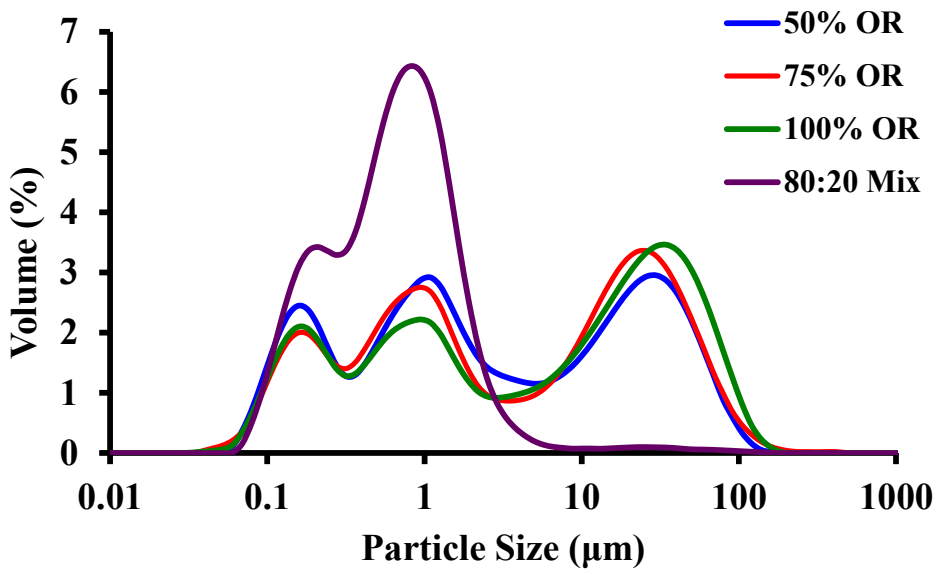

Figure 4.12d: Particle size distributions for ice cream mix made with 80:20 (mono- and diglyceride:polysorbate 80 - MDG:PS80) and ice creams processed at dasher speed of 500 RPM and overruns (OR) of 50%,75%, and 100%.

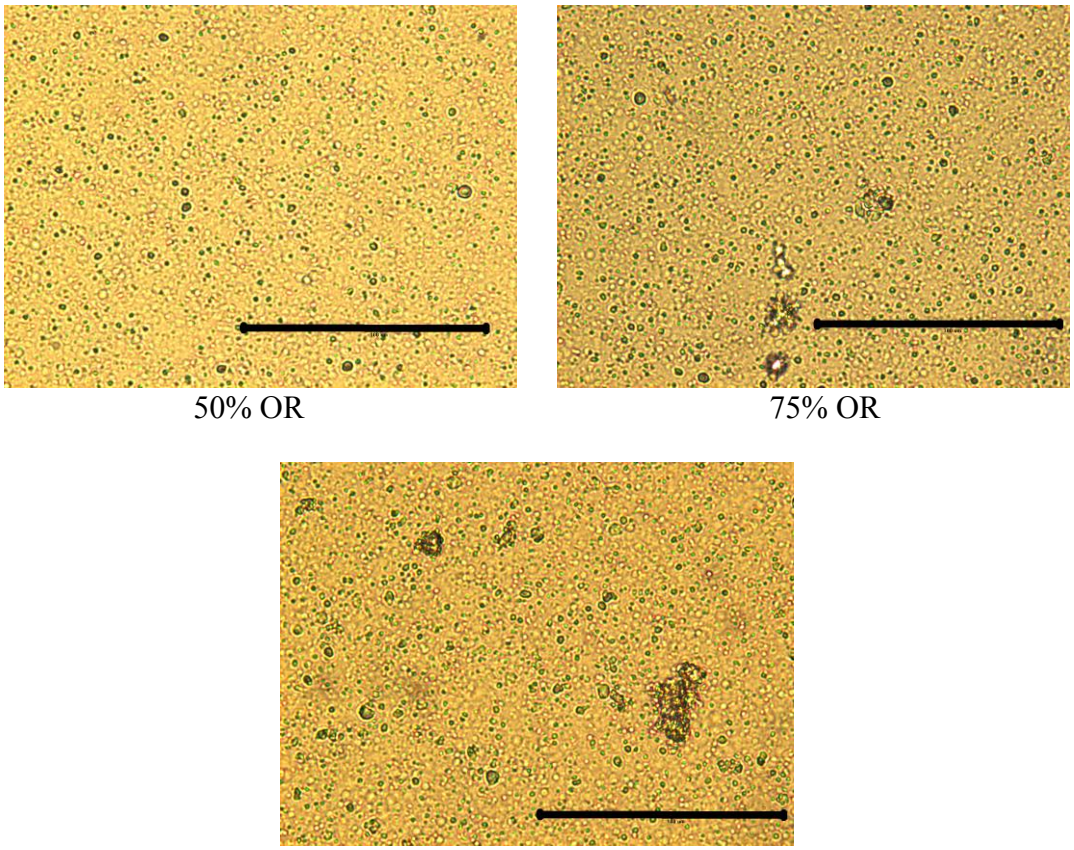

Figure 4.13a: Microscope images of melted ice creams made with no added emulsifier at 500 RPM and 50%, 75%, and 100% overrun (OR) (400x magnification, 100 µm scale bar)

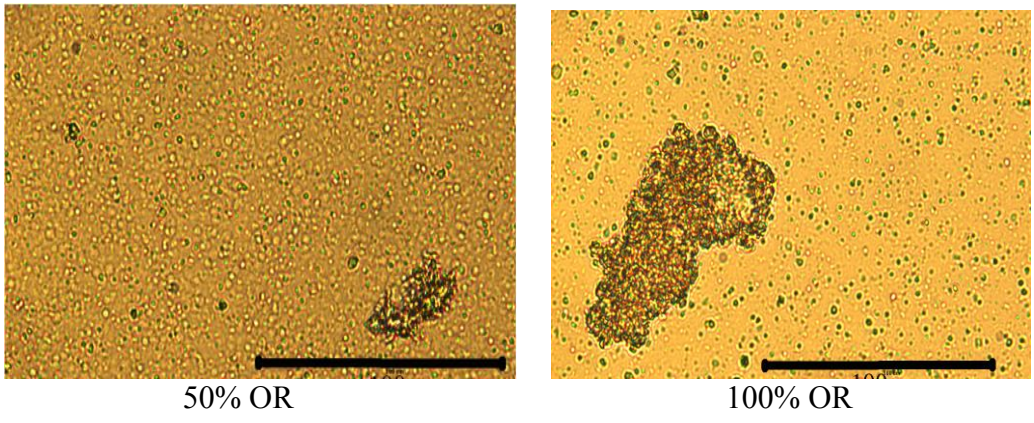

Figure 4.13b: Microscope images of melted ice creams made with 100:0 (mono- and diglyceride:polysorbate 80 - MDG:PS80) at 500 RPM and 50% and 100% overrun (OR) (400x magnification, 100 µm scale bar).

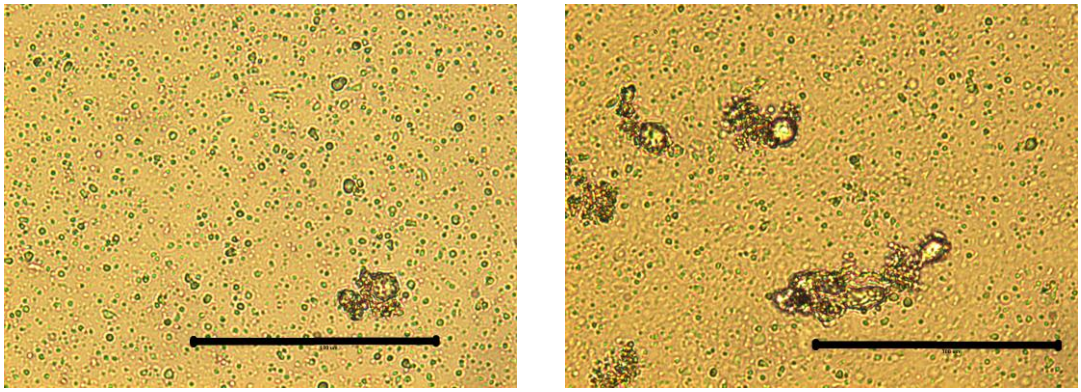

50% OR 75% OR

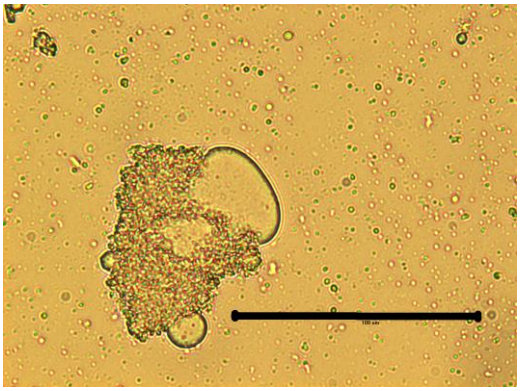

100% OR

Figure 4.13c: Microscope images of melted ice creams made with 90:10 (mono- and diglyceride:polysorbate 80 - MDG:PS80) at 500 RPM and 50%, 75%, and 100% overrun (400x magnification, 100 μm scale bar).

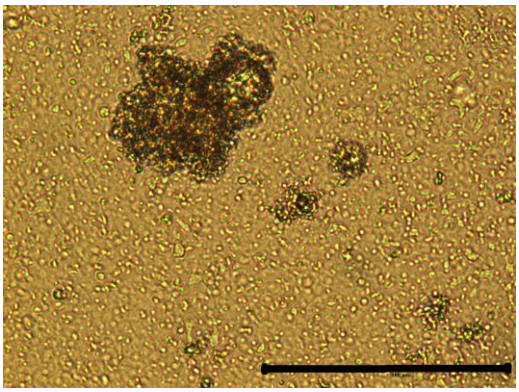

50% OR

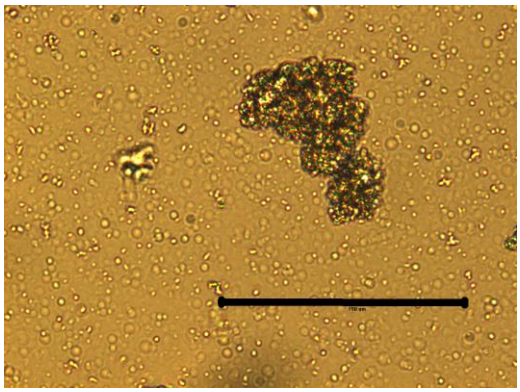

75% OR

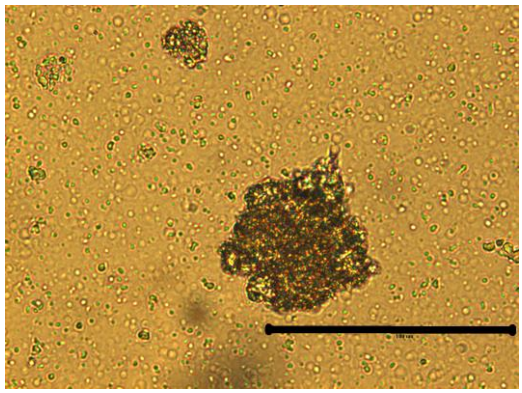

100% OR

Figure 4.13d: Microscope images of melted ice creams made with 80:20 (mono- and diglyceride:polysorbate 80 - MDG:PS80) at 500 RPM and 50%, 75%, and 100% overrun (400x magnification, 100 μm scale bar).

The amount of PC increased with the addition of emulsifiers in general, but specifically with the increase in PS80 (**Table 4.6** and **Figure 4.14**). This observation follows trends previously observed by Goff et al. (1987), Gelin et al. (1994), Gelin (1996a, b), Goff and Jordan (1989), Pelan et al. (1997), Tharp et al. (1998), Thomsen and Holtsborg (1998), Goff et al. (1999), and Bolliger et al. (2000). Although PS80 is more effective at the interface, an increase in PC was also seen with the addition of MDG, but at a reduced level. The addition of PS80 significantly increased the amount of fat clusters for all ice creams. Microscopy images of PC at

various emulsifier ratios are shown in **Figure 4.15**. At 100% overrun and 750 RPM, the partial coalescence increased with the addition of emulsifiers but did not vary greatly once emulsifiers were present. This trend can be seen in **Appendix G**.

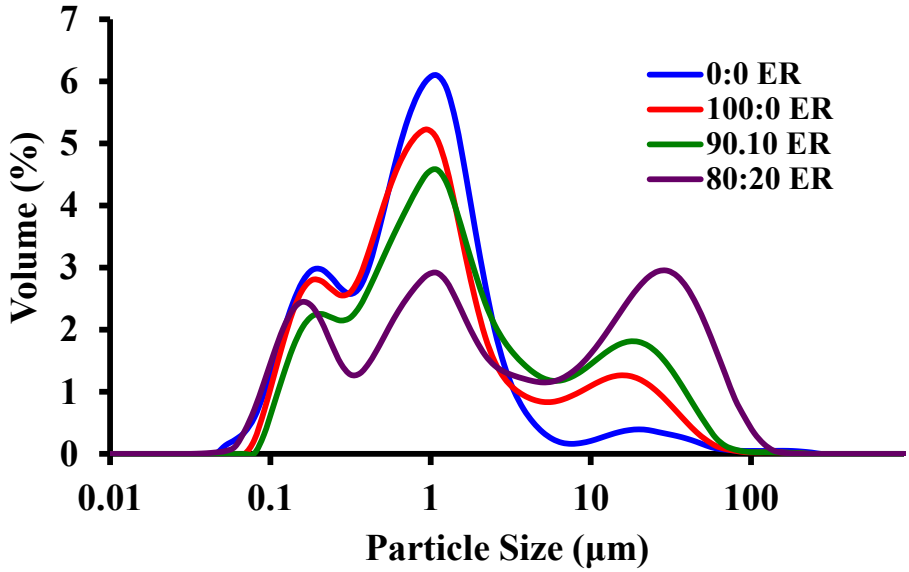

Figure 4.14: Particle size distributions for ice creams processed at 500 RPM, 50% overrun, and with no added emulsifiers (0:0 ((mono- and diglyceride:polysorbate 80 - MDG:PS80)), 100:0 (MDG:PS80), 90:10 (MDG:PS80), and 80:20 (MDG:PS80) emulsifier ratio (ER).

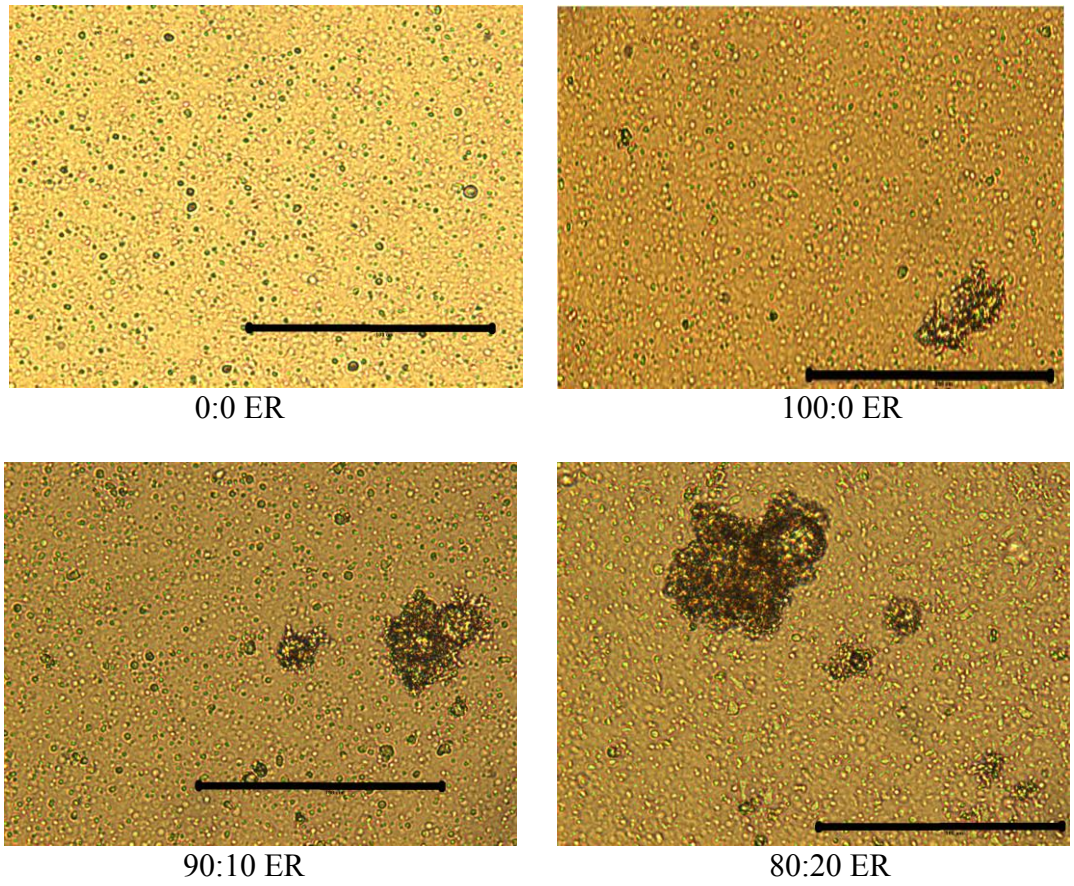

Figure 4.15: Microscope images of melted ice creams processed at 500 RPM, 50% overrun, and with no added emulsifiers (0:0 (mono- and diglyceride:polysorbate 80) (MDG:PS80)), 100:0 (MDG:PS80), 90:10 (MDG:PS80), and 80:20 (MDG:PS80) emulsifier ratios (ER) (400x magnification, 100 μm scale bar).

From the two-way ANOVA utilizing data from ice creams with PS80 (90:10 (MDG:PS80) and 80:20 (MDG:PS80)), both dasher speed ($p < 0.0001$) and overrun ($p < 0.0001$) were determined to have a significant effect on PC. Statistically significant differences were determined between all dasher speeds and overruns. However, the interaction between the two parameters was not determined to be significant ($p = 0.9577$).

4.2.3 Mean Air Cell Size

Mean air cell size distributions varied across change in dasher speed, overrun, and emulsifier ratio (**Table 4.7)**. Mean air cell size ranged from 16.8 to 28.9 μm. The impacts of dasher speed, overrun, and emulsifier ratio on air cells from hardened ice creams are outlined below.

As dasher speed increased, it was expected that air cell size would decrease (Kroezen, 1998; Goff and Hartel, 2013). This occurrence greatly depended on the viscosity of the slurry phase and the applied force in the system during freezing (Chang and Hartel, 2002a). If the slurry phase has the same viscosity across dasher speeds, air cells produced should be similar in size (Chang and Hartel, 2002a). In this study, it can be assumed that all samples had similar viscosities as all samples were frozen to the same draw temperature (similar mean ice crystal sizes) at constant overrun and had the same freezing point depression and mix flow rate. As the dasher speed increased, however, the shear stress increased, which in turn, should have decreased the air cell size. Although the size of air cells immediately exiting the freezer was not known, it is likely that higher dasher speeds resulted in smaller air cells.

However, as ice cream hardens, changes in the microstructure occur (Chang and Hartel, 2002c). Once filled, containers were sealed and placed into the hardening freezer. Ice crystals and air cells undoubtedly increased in size during the hardening phase. If air cells were not stabilized by partially-coalesced fat globules (addition of emulsifiers), a high viscosity continuous phase (addition of stabilizers), or the ice crystals, small air cells could easily ripen into larger air cells due to differences in Laplace pressure (Goff and Hartel, 2013). In a forced convection-hardening freezer, Chang and Hartel (2002c) determined that air cells

Table 4.7: Means and standard deviations of air cell size for ice creams based on emulsifier ratio (mono- and diglyceride:polysorbate 80 (MDG:PS80)), dasher speed (RPM), and overrun (%). The standard deviation (±) represents the variation between replicate means of air cell size measurements determined at a set overrun, dasher speed, and emulsifier ratio.

		Mean Air Cell Size (µm)		
MDG:PS80	**RPM**	**50%**	**75%**	**100%**
[1]0:0	250	29.1 ±3.1^{a,A,x}	23.3 ±1.8^{a,B,x}	24.7 ±2.0^{a,B,x}
	500	28.9 ±3.0^{a,A,x}	26.3 ±1.1^{a,AB,x}	23.2 ±1.2^{a,B,x}
	750	26.1±1.0^{a,A,x}	24.6 ±3.9^{a,A,x}	26.0 ±2.3^{a,A,x}
[2]100:0	250	N/A*	N/A*	N/A*
	500	26.2±0.8^{a,A,y}	N/A*	17.1±2.4^{a,B,y}
	750	24.2±2.0^{a,A,x}	N/A*	17.1±2.1^{a,B,y}
[3]90:10	250	28.8 ±1.2^{a,A,xy}	23.7 ±1.4^{a,B,x}	24.2 ±1.9^{a,B,x}
	500	26.5 ± 1.0^{b,A,xy}	21.9 ± 2.7^{a,B,y}	22.1 ± 1.0^{b,B,x}
	750	20.4 ±2.0^{c,A,y}	17.0 ±3.1^{b,B,y}	17.8 ±0.8^{c,AB,y}
[4]80:20	250	25.9 ±1.7^{ab,AB,y}	27.7 ±2.6^{a,A,y}	24.6 ±0.7^{a,B,x}
	500	20.5 ± 1.4^{b,AB,z}	19.4 ± 0.6^{b,A,y}	21.6 ± 1.0^{b,B,x}
	750	18.5 ±1.5^{b,A,y}	17.1 ±2.4^{b,A,y}	16.8 ±1.7^{c,A,y}

^{a,b,c} denote significant differences among ice creams based on constant overrun (columns)
^{A,B,C} denote significant differences among ice creams based on constant dasher speed (rows)
^{x,y,z} denote significant differences among ice creams based on emulsifier ratio, constant dasher speed, and constant overrun (columns)
*Samples not included in experimental design
[1]no added emulsifiers in the formula
[2]total emulsifiers added consisted of 100% MDG at 0.15% in the formula
[3]total emulsifiers added consisted of 90:10 MDG:PS80 at 0.15% in the formula
[4]total emulsifiers added consisted of 80:20 MDG:PS80 at 0.15% in the formula

increased by 11 µm in 60 minutes (no changes occurred after this time) and for ice creams cooled in a natural convection hardening freezer, air cells increased by 17 µm in 90 minutes (no changes occurred after this time).

In this current study, a one-way ANOVA and Tukey's HSD test determined no statistical difference ($\alpha = 0.05$) in mean air cell sizes in hardened ice creams as dasher speed increased for

ice creams processed with no added emulsifiers (p = 0.7786) (**Figure 4.16 (a-c)**. **Figure 4.17 (a-c)** displays the microscopy images of these air cells as dasher speed increased for a set overrun. The size of the air cells (all above 23 μm) is most likely attributed to air cells being measured from hardened ice creams and not fresh from the freezer. The results are similar for ice creams made with 100:0 (MDG:PS80) (p = 0.6139) (**Figure 4.18 (a-b)** and **Figure 4.19 (a-b)**).

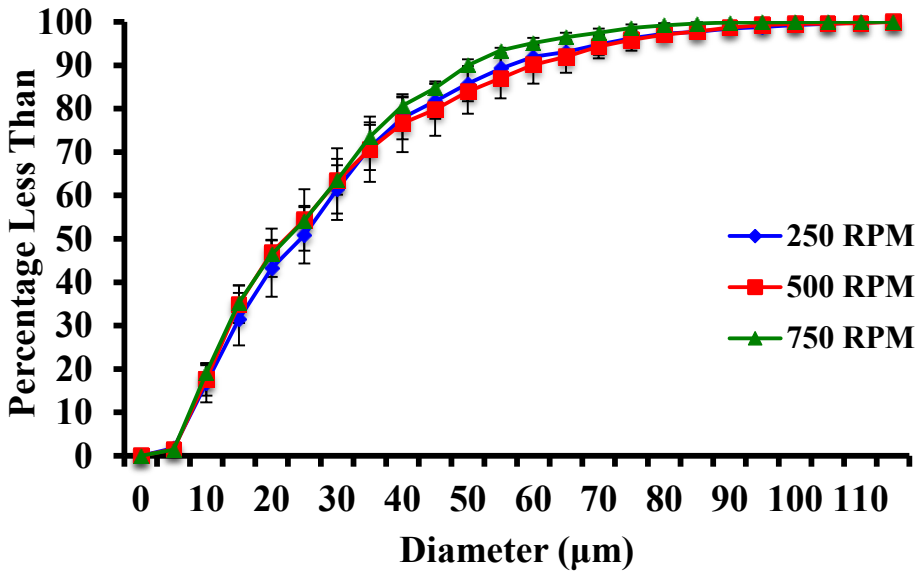

Figure 4.16a: Air cell size distributions of ice creams made with no added emulsifiers at dasher speeds of 250 RPM, 500 RPM, and 750 RPM and 50% overrun. The error bars represent the standard deviations of the mean air cell sizes measured.

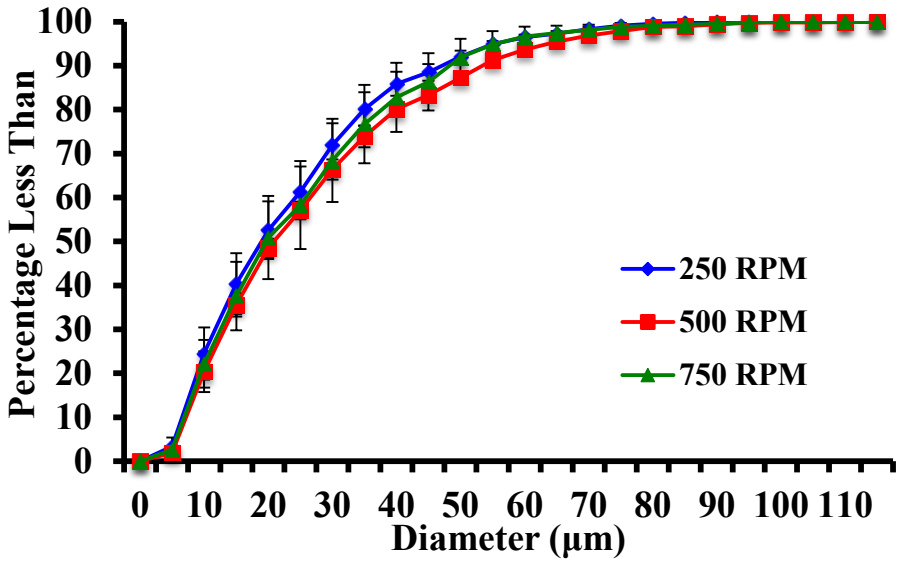

Figure 4.16b: Air cell size distributions of ice creams made with no added emulsifiers at dasher speeds of 250 RPM, 500 RPM, and 750 RPM and 75% overrun. The error bars represent the standard deviations of the mean air cell sizes measured.

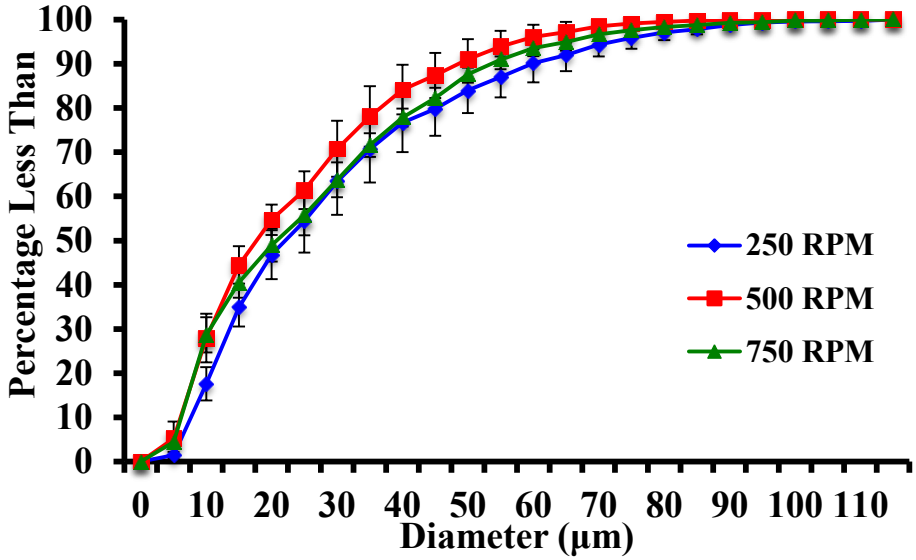

Figure 4.16c: Air cell size distributions of ice creams made with no added emulsifiers at dasher speeds of 250 RPM, 500 RPM, and 750 RPM and 100% overrun. The error bars represent the standard deviations of the mean air cell sizes measured.

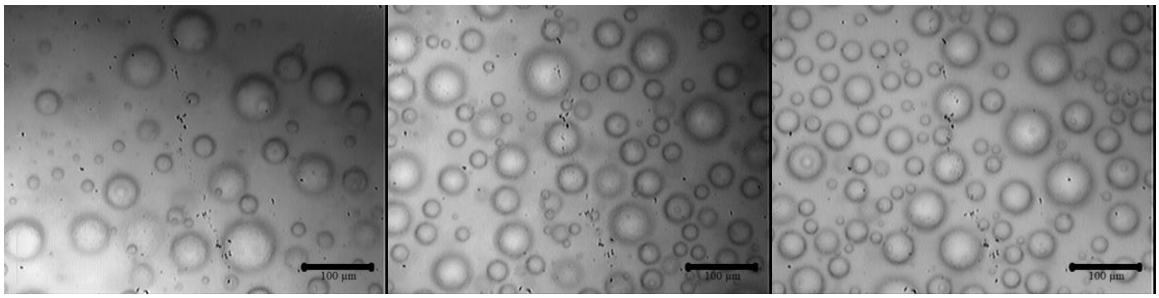

a.1: 250 RPM, 50% OR **a.2:** 250 RPM, 75% OR **a.3:** 250 RPM, 100% OR

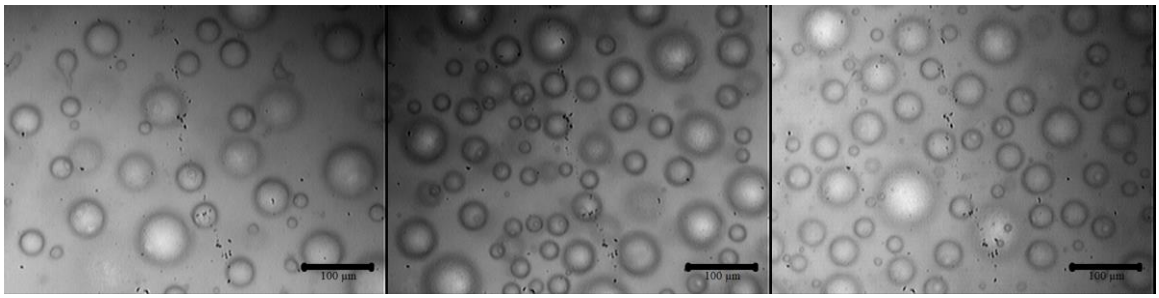

b.1: 500 RPM, 50% OR **b.2:** 500 RPM, 75% OR **b.3:** 500 RPM, 100% OR

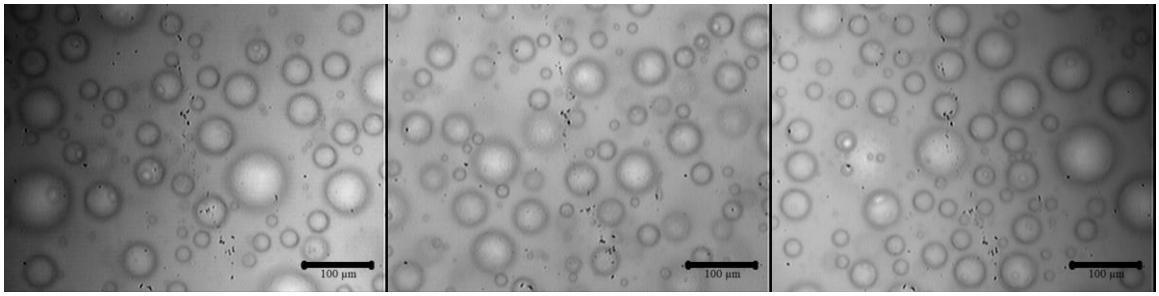

c.1: 750 RPM, 50% OR **c.2:** 750 RPM, 75% OR **c.3:** 750 RPM, 100% OR

Figure 4.17: Microscope images of air cells for ice creams made with no added emulsifiers at dasher speeds of 250 RPM (**a**), 500 RPM (**b**), and 750 RPM (**c**) and at 50% (**1**), 75% (**2**), and 100% (**3**) overrun (OR) (40x magnification, 100 µm scale bar).

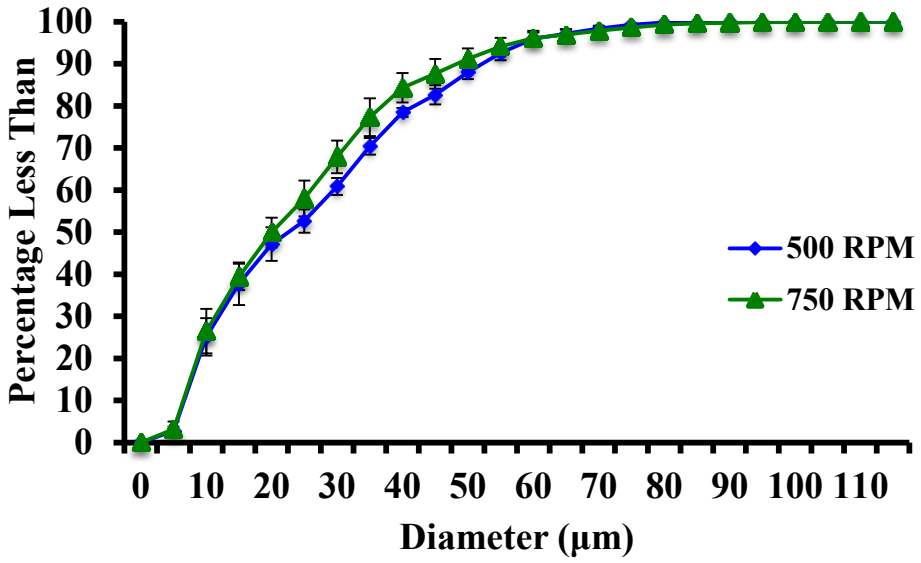

Figure 4.18a: Air cell size distributions of ice creams made with 100:0 (mono- and diglyceride:polysorbate 80 - MDG:PS80) at dasher speeds of 500 RPM and 750 RPM and 50% overrun. The error bars represent the standard deviations of the mean air cell sizes measured.

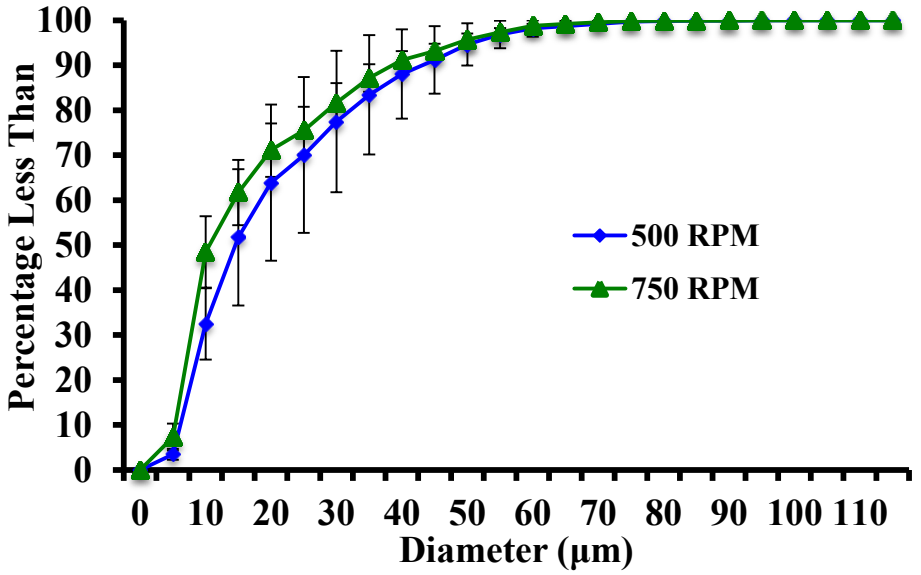

Figure 4.18b: Air cell size distributions of ice creams made with 100:0 (mono- and diglyceride:polysorbate 80 - MDG:PS80)at dasher speeds of 500 RPM and 750 RPM and 100% overrun. The error bars represent the standard deviations of the mean air cell sizes measured.

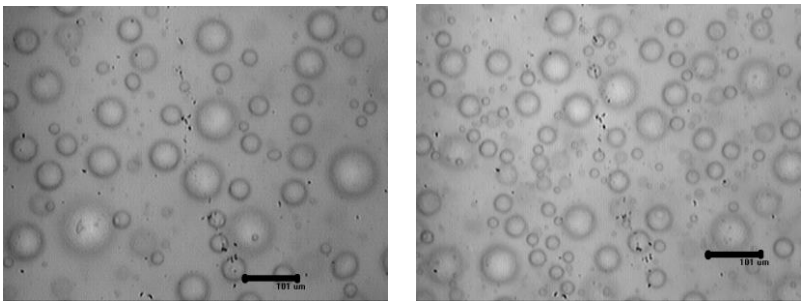

a.1: 500 RPM, 50% OR **b.2:** 500 RPM, 100% OR

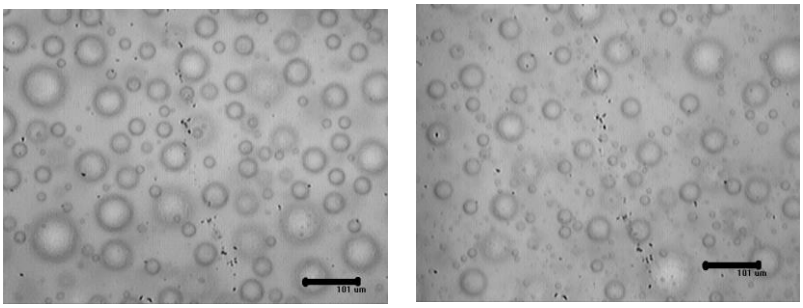

a.1: 750 RPM, 50% OR **b.2:** 750 RPM, 100% OR

Figure 4.19: Microscope images of air cells for ice creams made with 100:0 (mono- and diglyceride:polysorbate 80 - MDG:PS80) and processed at 500 RPM (**a**) and 750 RPM (**b**) at 50% (**1**) and 100% (**2**) overrun (OR) (40x magnification, 100 μm scale bar).

According to Walstra and Jenness (1984), Brooker et al. (1986), Walstra (1989) and Chang and Hartel (2002c), during storage, air cells were stabilized and hindered from recombining by the destabilized fat in the serum phase. If there was little to no partially-coalesced fat present in the system, air cells were more prone to coalescence during hardening, assuming viscosity and ice crystals were constant. In this study, ice creams made with no added emulsifiers contained low levels of partially-coalesced fat, as seen in **Section 4.2.2**, and had the largest mean air cell size. With the addition of PS80, dasher speed had a greater effect (90:10 – $p < 0.0001$, 80:20 – $p < 0.0001$) on mean air cell size than ice creams made with no added emulsifiers ($p = 0.7786$) and 100:0 ($p = 0.6139$). This is a secondary effect and is attributed to an increase in partially-coalesced fat during freezing with the addition of PS80. Although

emulsifiers are not thought to affect air cell sizes during the freezing process, in this study, air cell sizes significantly decreased in hardened ice creams with the addition of PS80 (**Table 4.7**) (Chang and Hartel, 2002a). Unlike air cells in ice creams with no added emulsifiers and 100:0 (MDG:PS80), air cells were not able to coalesce during the hardening process due to the increase in PS80 (higher amounts of destabilized fat). Air cell size distributions and microscopy images for air cells from ice creams made with 90:10 (MDG:PS80) can be found in **Figure 4.20 (a-c)** and **Figure 4.21 (a-c)**, respectively. The same distributions and images for ice creams made with 80:20 (MDG:PS80) are shown in **Figure 4.22 (a-c)** and **Figure 4.23 (a-c)**. In order to determine the true effect of dasher speed on air cell size, samples would have to be analyzed inline and/or directly from the freezer, prior to hardening.

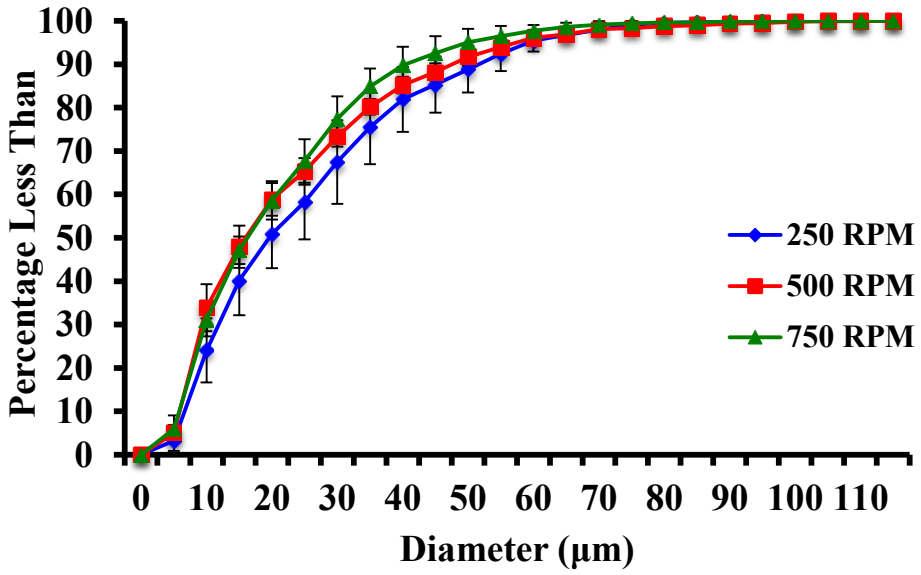

Figure 4.20a: Air cell size distributions of ice creams made with 90:10 (mono- and diglyceride:polysorbate 80 - MDG:PS80) emulsifier ratio at dasher speeds of 250 RPM, 500 RPM, and 750 RPM and 50% overrun. The error bars represent the standard deviations of the mean air cell sizes measured.

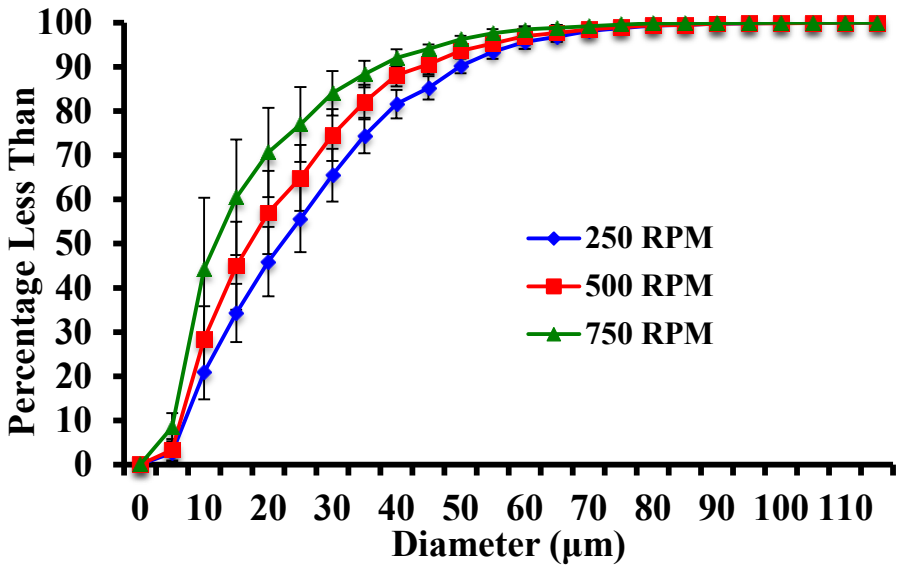

Figure 4.20b: Air cell size distributions of ice creams made with 90:10 (mono- and diglyceride:polysorbate 80 - MDG:PS80) emulsifier ratio at dasher speeds of 250 RPM, 500 RPM, and 750 RPM and 75% overrun. The error bars represent the standard deviations of the mean air cell sizes measured.

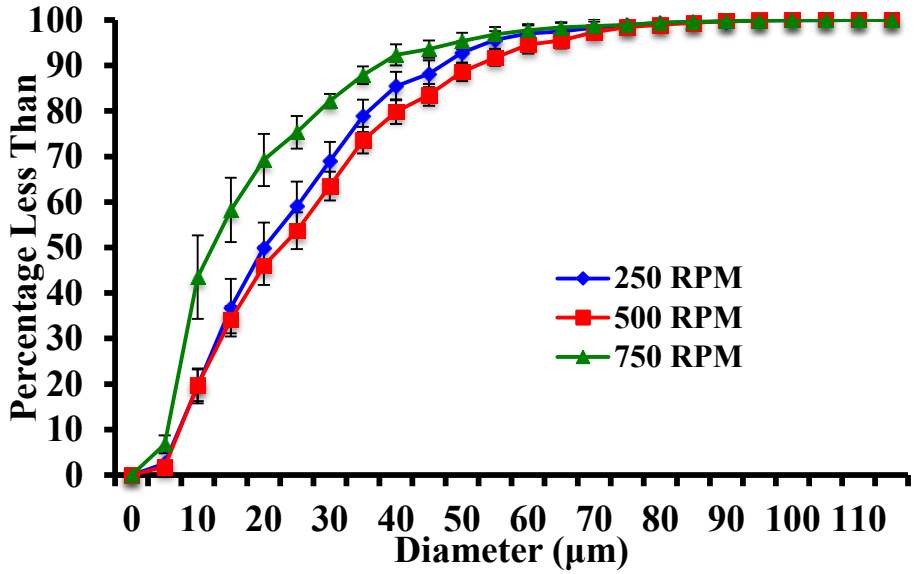

Figure 4.20c: Air cell size distributions of ice creams made with 90:10 (mono- and diglyceride:polysorbate 80 - MDG:PS80) emulsifier ratio at dasher speeds of 250 RPM, 500 RPM, and 750 RPM and 100% overrun. The error bars represent the standard deviations of the mean air cell sizes measured.

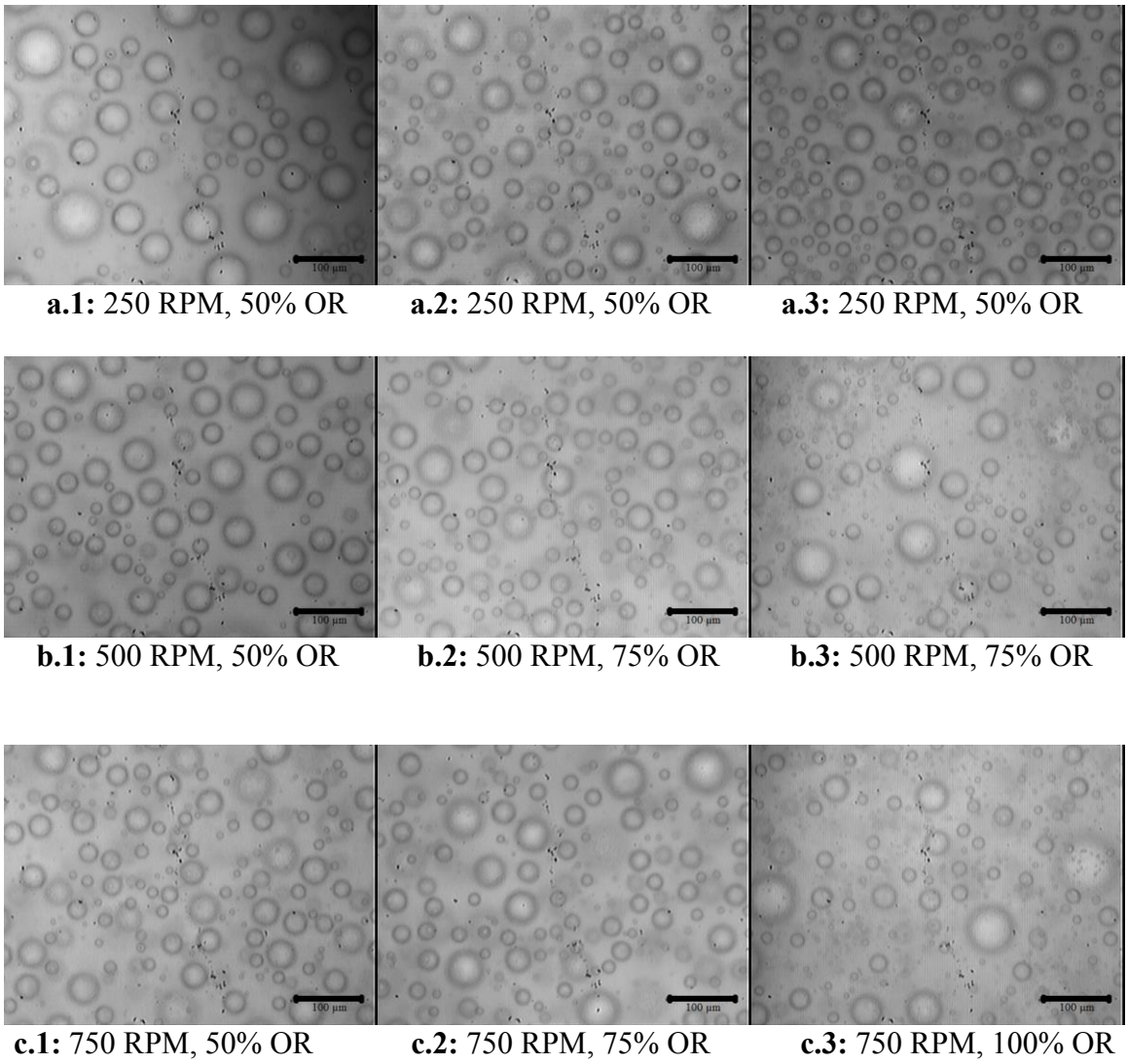

a.1: 250 RPM, 50% OR **a.2:** 250 RPM, 50% OR **a.3:** 250 RPM, 50% OR

b.1: 500 RPM, 50% OR **b.2:** 500 RPM, 75% OR **b.3:** 500 RPM, 75% OR

c.1: 750 RPM, 50% OR **c.2:** 750 RPM, 75% OR **c.3:** 750 RPM, 100% OR

Figure 4.21: Microscope images of air cells for ice creams made with 90:10 (mono- and diglyceride:polysorbate 80 - MDG:PS80) emulsifier ratio at dasher speeds of 250 RPM (**a**), 500 RPM (**b**), and 750 RPM (**c**) and at 50% (**1**), 75% (**2**), and 100% (**3**) overrun (OR) (40x magnification, 100 µm scale bar).

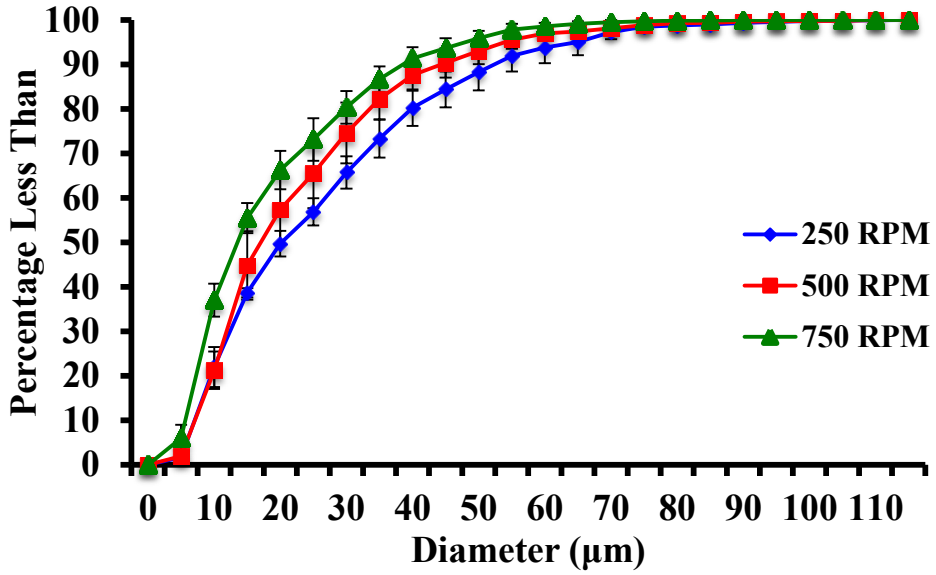

Figure 4.22a: Air cell size distributions of ice creams made with 80:20 (mono- and diglyceride:polysorbate 80 - MDG:PS80) emulsifier ratio at dasher speeds of 250 RPM, 500 RPM, and 750 RPM and 50% overrun. The error bars represent the standard deviations of the mean air cell sizes measured.

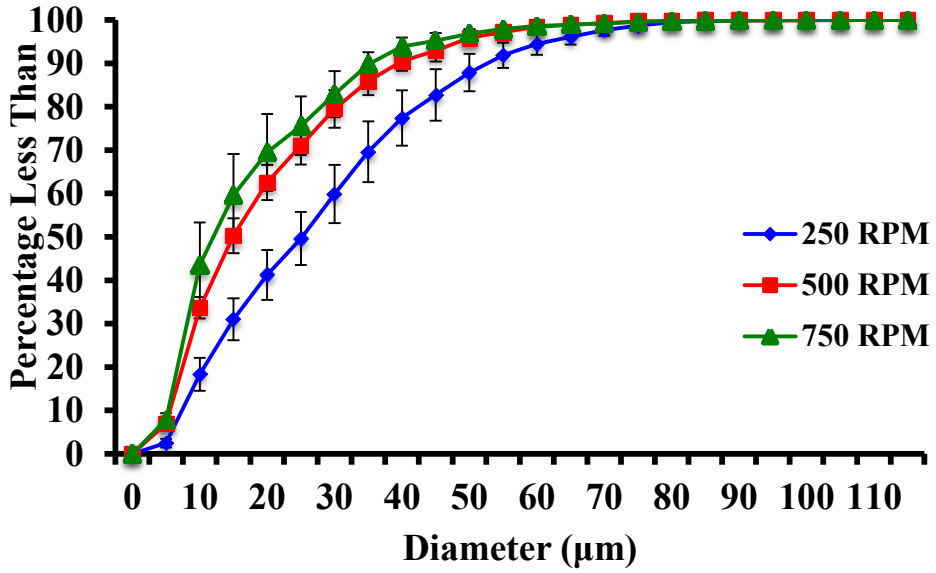

Figure 4.22b: Air cell size distributions of ice creams made with 80:20 (mono- and diglyceride:polysorbate 80 - MDG:PS80) at 75% overrun across 250 RPM, 500 RPM, and 750 RPM dasher speeds. The error bars represent the standard deviations of the mean air cell sizes measured.

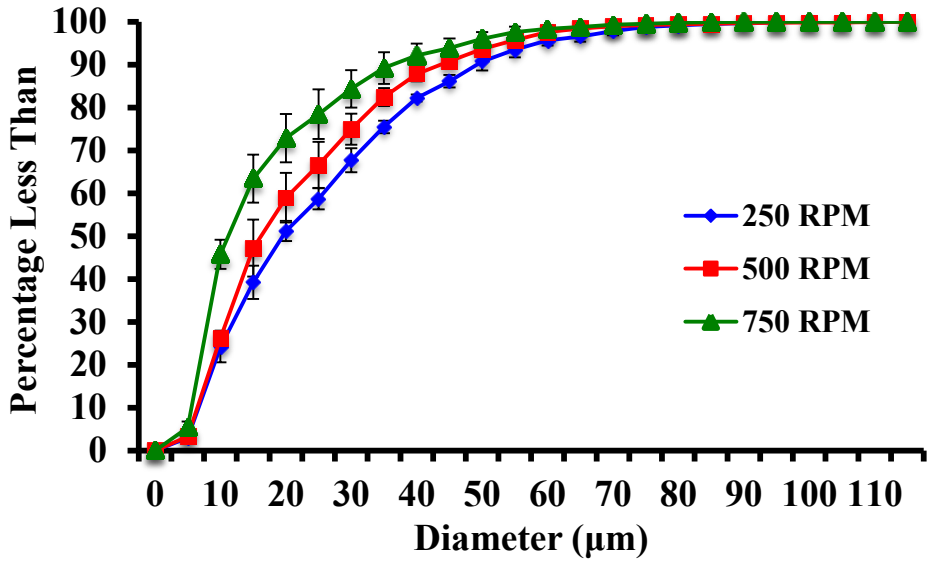

Figure 4.22c: Air cell size distributions of ice creams made with 80:20 (mono- and diglyceride:polysorbate 80 - MDG:PS80) at 100% overrun across 250 RPM, 500 RPM, and 750 RPM dasher speeds. The error bars represent the standard deviations of the mean air cell sizes measured.

Overrun has also been known to affect mean air cell size during freezing and storage. Sofjan and Hartel (2004) determined that with an increase in overrun, air cell sizes decreased at draw. This was attributed to the increase in the apparent viscosity of the slurry as overrun increased (Chang and Hartel, 2002c). Although not measured, it can be assumed that the same occurred in this study; as overrun increased, apparent viscosity also increased. In general, final mean air cell sizes were determined by the balance between smaller air cells created by high shear stress on the fluid inside the freezer and the increased difference in Laplace pressure due to the formation of smaller bubbles, which in turn, led to coalescence (Chang and Hartel,2002a). At constant dasher speed, the breakage of air cells was influenced by the percentage of overrun as an increase in overrun lead to an increase in viscosity.

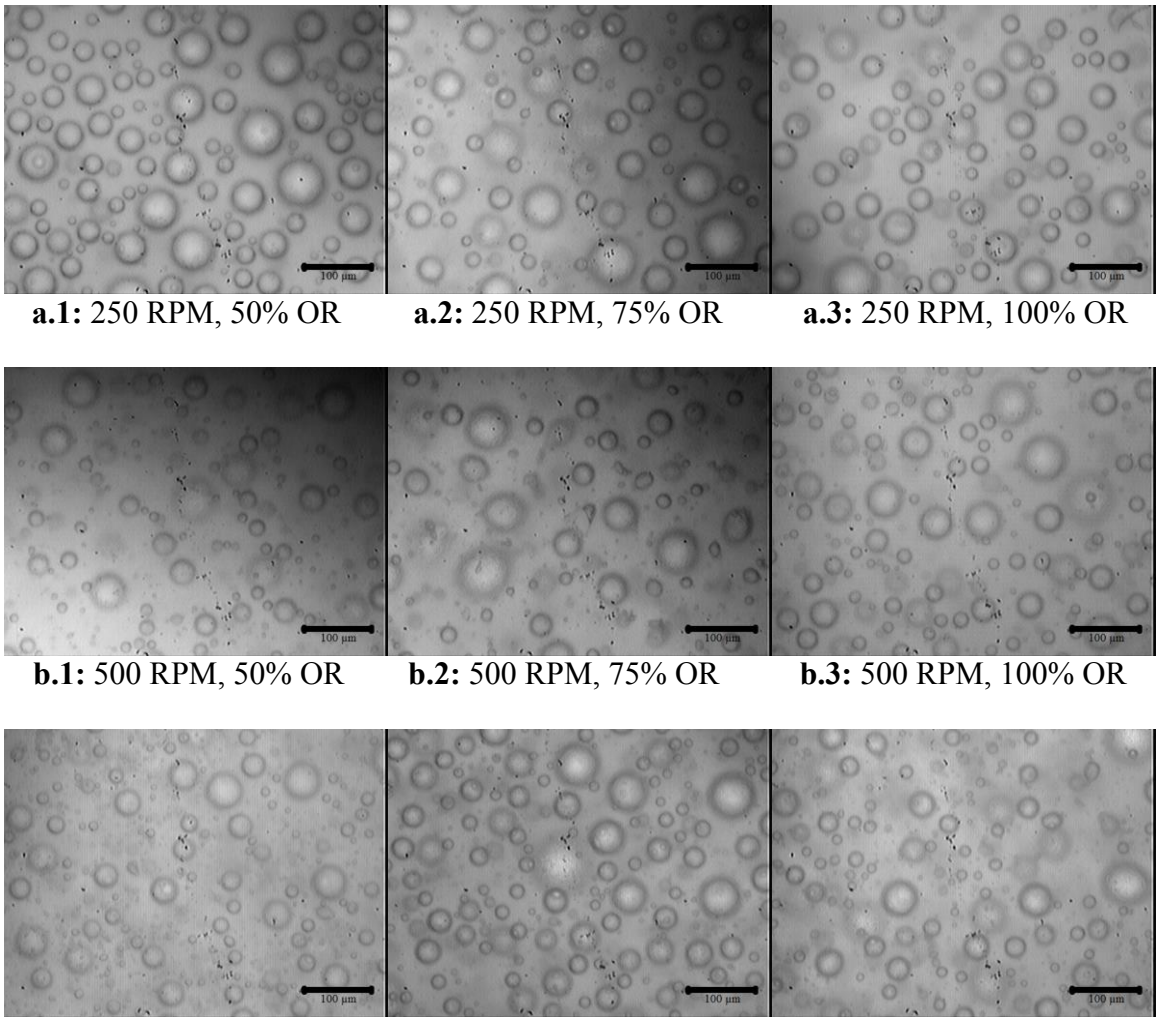

a.1: 250 RPM, 50% OR **a.2:** 250 RPM, 75% OR **a.3:** 250 RPM, 100% OR

b.1: 500 RPM, 50% OR **b.2:** 500 RPM, 75% OR **b.3:** 500 RPM, 100% OR

c.1: 750 RPM, 50% OR **c.2:** 750 RPM, 75% OR **c.3:** 750 RPM, 100% OR

Figure 4.23: Microscope images of air cells for ice creams made with 80:20 (mono- and diglyceride:polysorbate 80 - MDG:PS80) emulsifier ratio at dasher speeds of 250 RPM (**a**), 500 RPM (**b**), and 750 RPM (**c**) and at 50% (**1**), 75% (**2**), and 100% (**3**) overrun (OR) (40x magnification, 100 µm scale bar).

Sofjan and Hartel (2004) also noted a decrease in air cell sizes with an increase in overrun for ice creams measured after hardening. This study determined that air cells in ice cream with lower overrun (80%) increased in size more than air cells produced at higher overrun (120%) during storage. This too could be attributed to the partially-coalesced fat acting as a barrier to air cell coalescence during the hardening process since an increased overrun also increased PC (**Section 4.2.2**).

Tukey's HSD tests determined significant differences between mean air cell size as overrun increased, mostly between the 50% overrun when compared to 75% and 100% overrun settings. This trend was generally seen across emulsifier ratios and dasher speeds (**Table 4.7)**. **Figure 4.24 (a-c)** and **Figure 4.17 (1-3)** display the air cell size distributions and microscopy images for ice creams made with no added emulsifiers at constant dasher speed. One-way ANOVA determined that change in overrun had statistical significance on mean air cell size for ice creams made with no added emulsifiers ($p < 0.0001$). Since air cells were measured from hardened containers, it can be assumed that air cells changed during the hardening process and since low percentages of PC were formed in ice creams with no added emulsifiers, minimal fat clusters were available to keep air cells from coalescing.

Mean air cell sizes ($p < 0.0001$) were noted to be statistically significant as overrun changed for ice creams made with 100:0 (MDG:PS80). It is not clear why air cell sizes for 100:0 (MDG:PS80) at 100% overrun were so small when compared to air cells of ice creams made with PS80 (**Table 4.7**). However, since MDG is more functional at the air interface and can

stabilize air more efficiently than PS80, smaller air cell size distributions are able to be produced (Goff and Hartel, 2013) (**Figure 4.25 (a-b)** and **Figure 4.19 (1-2)**). This could also be attributed to the amount of partially-coalesced fat formed at 100% overrun as seen in **Table 4.6**.

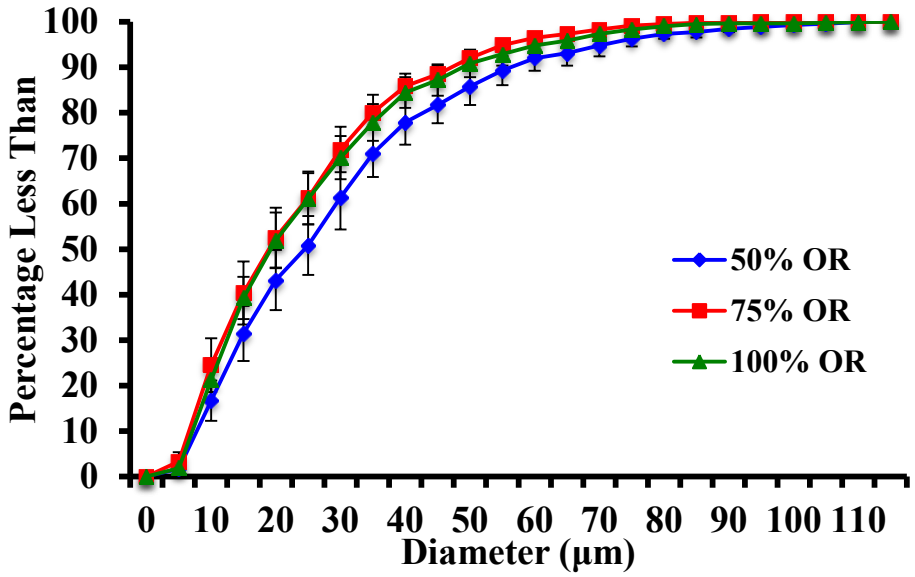

Figure 4.24a: Air cell size distributions of ice creams made with no added emulsifiers and processed at 50%, 75%, and 100% overrun (OR) overrun and 250 RPM. The error bars represent the standard deviations of the mean air cell sizes measured.

.

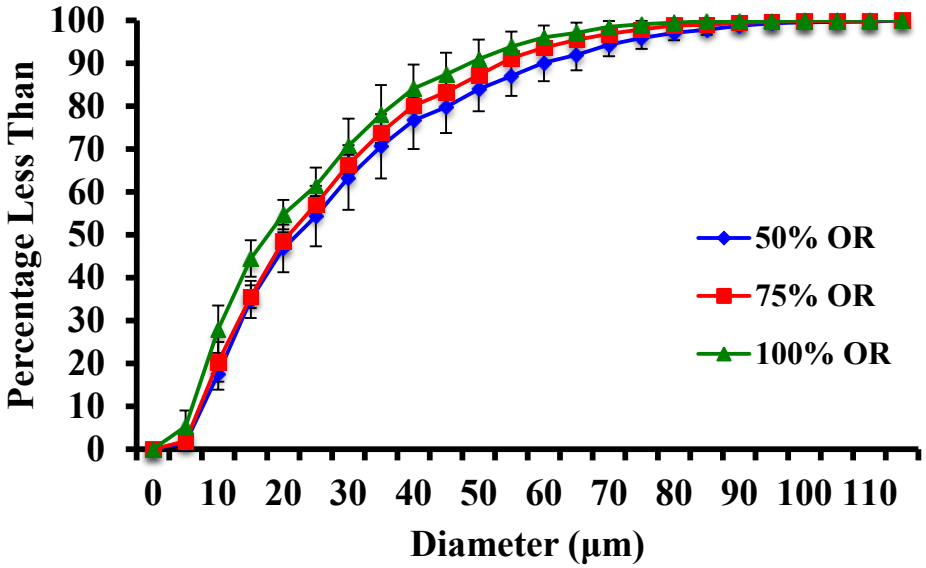

Figure 4.24b: Air cell size distributions of ice creams made with no added emulsifiers and processed at 50%, 75%, and 100% overrun (OR) and 500 RPM. The error bars represent the standard deviations of the mean air cell sizes measured.

.

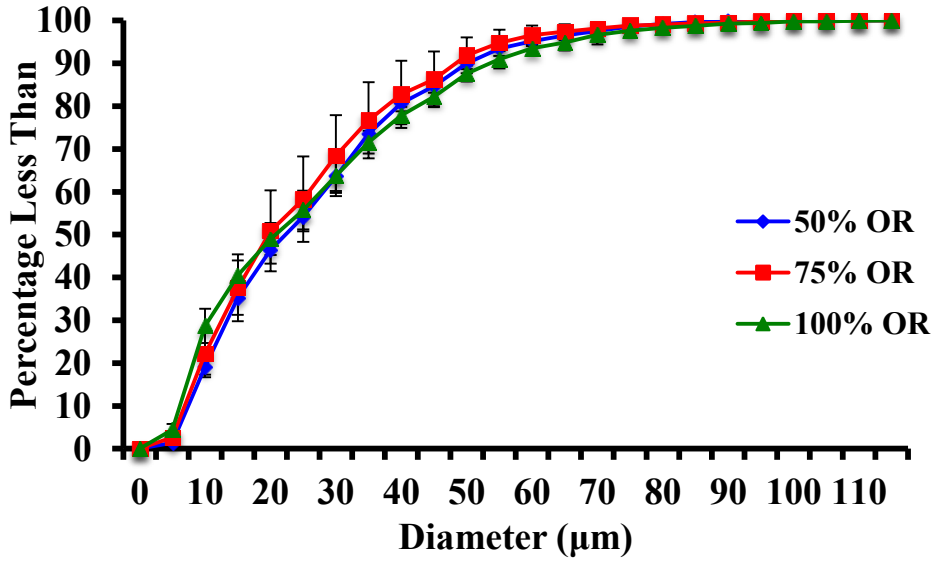

Figure 4.24c: Air cell size distributions of ice creams made with no added emulsifiers and processed at 50%, 75%, and 100% overrun (OR) and 750 RPM. The error bars represent the standard deviations of the mean air cell sizes measured.

.

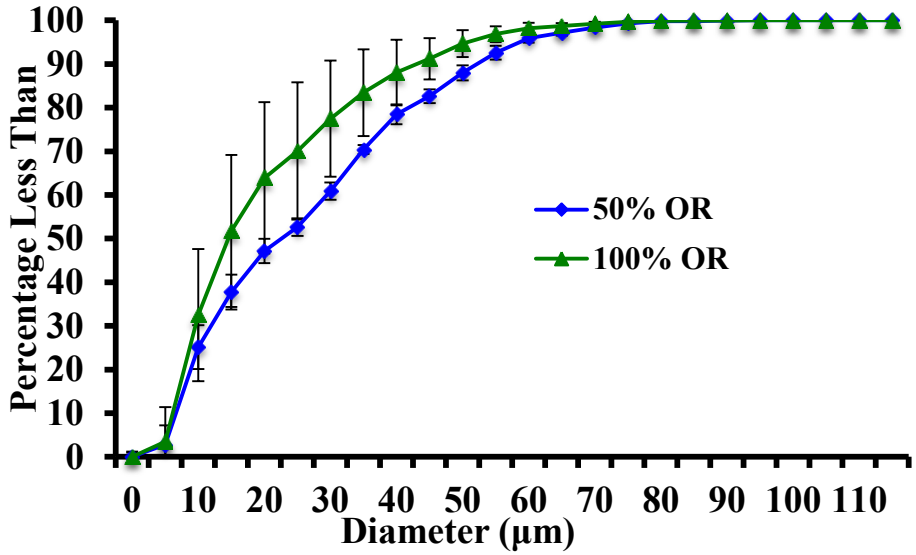

Figure 4.25a: Air cell size distributions of ice creams made with 100:0 (mono- and diglyceride:polysorbate 80 - MDG:PS80) at 500 RPM and 50% and 100% overrun. The error bars represent the standard deviations of the mean air cell sizes measured.

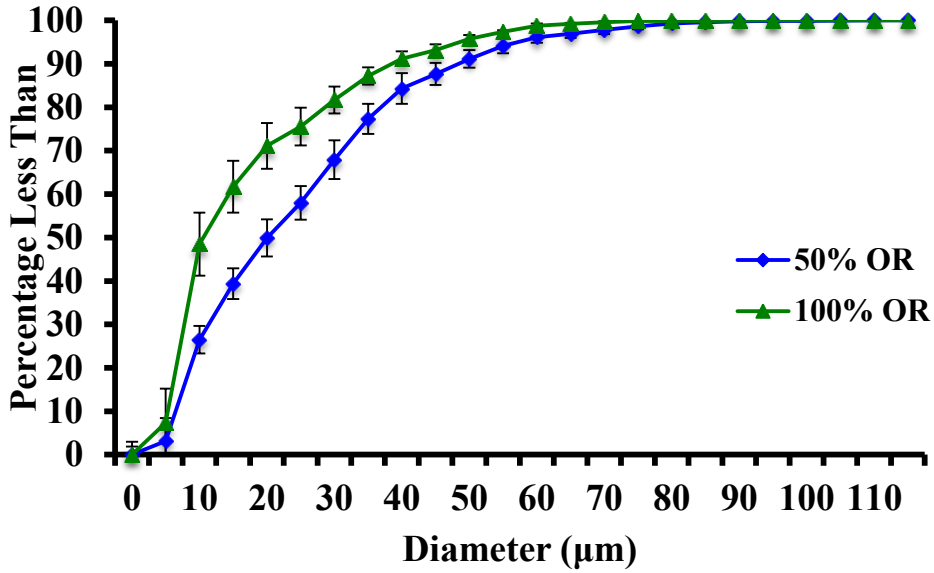

Figure 4.25b: Mean air cell size distributions of ice creams made with 100:0 (mono- and diglyceride:polysorbate 80 - MDG:PS80) at 750 RPM and 50% and 100% overrun. The error bars represent the standard deviations of the mean air cell sizes measured.

With the addition of PS80, the effect of overrun on mean air cell size became less significant. One-way ANOVA showed that overrun had a significant statistical ($p = 0.0016$) impact on mean air cell size for ice creams made with 90:10 (PDG:PS80) but not for 80:20 (MDG:PS80) ice creams ($p = 0.8907$). This can be attributed to little to no coalescence of air cells during the hardening process due to the high amounts of partially-coalesced fat in ice cream made with 80:20 (MDG:PS80) (**Table 4.6**). As a result, it can be assumed that air cells stayed closer to their initial draw size. These findings indicate that mean air cell size distributions in hardened ice creams are a secondary effect to the amount of formed PC in the system. A multivariate pairwise comparison test also showed an indirect relationship between mean air cell size and PC for all emulsifier ratios ($p < 0.0001$) (no emulsifier added – $p = 0.138$, 100:0 (MDG:PS80) – $p < 0.0001$, 90:10 (MDG:PS80) – $p < 0.0001$, 80:20 (MDS:PS80) – $p = 0.0031$). **Figure 4.26 (a-c)** displays the air cell size distributions for ice creams made at 90:10 (MDG:PS80) as overrun changes and **Figure 4.27** (**a-c**) displays this same data for ice creams made with 80:20 (MDG:PS80).

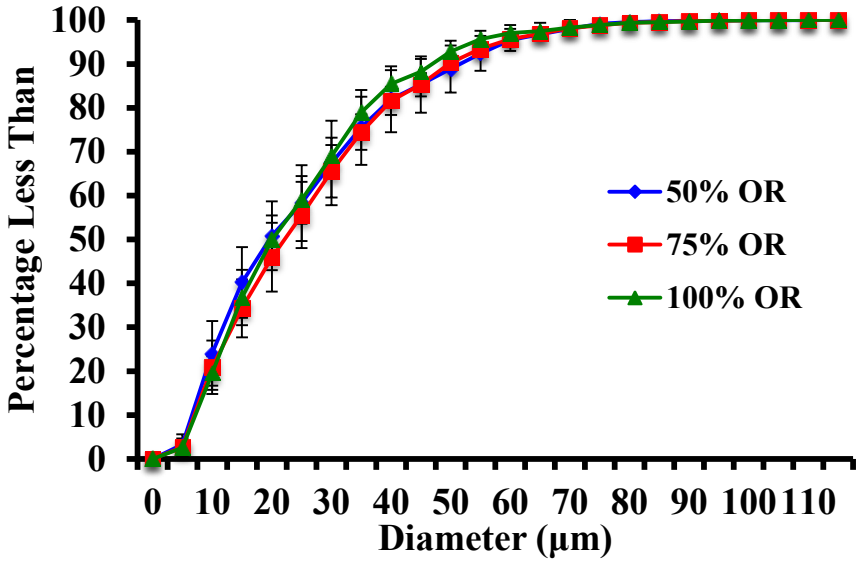

Figure 4.26a: Air cell size distributions of ice creams made with 90:10 (mono- and diglyceride:polysorbate 80 - MDG:PS80) emulsifier ratio at 50%, 75%, and 100% overrun and 250 RPM. The error bars represent the standard deviations of the mean air cell sizes measured.

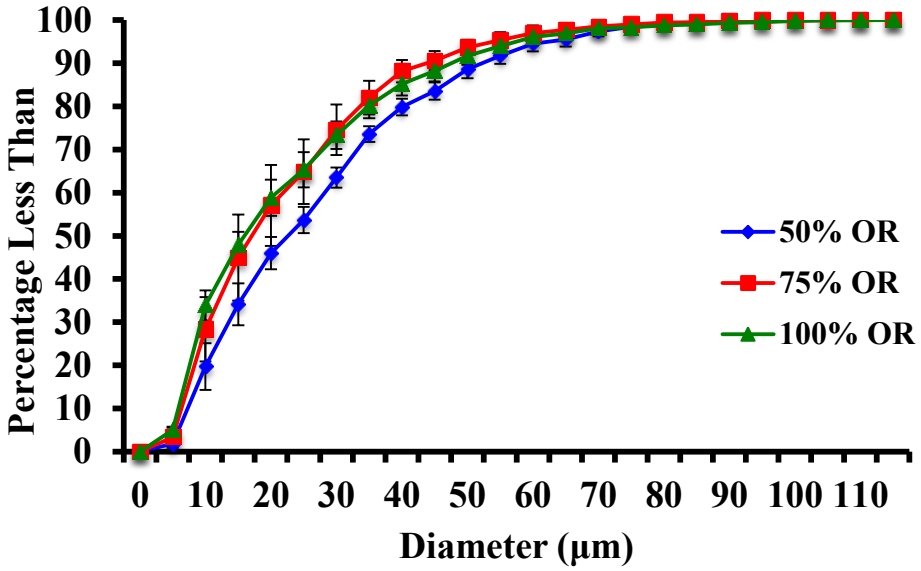

Figure 4.26b: Air cell size distributions of ice creams made with 90:10 (mono- and diglyceride:polysorbate 80 - MDG:PS80) emulsifier ratio at 50%, 75%, and 100% overrun and 500 RPM. The error bars represent the standard deviations of the mean air cell sizes measured.

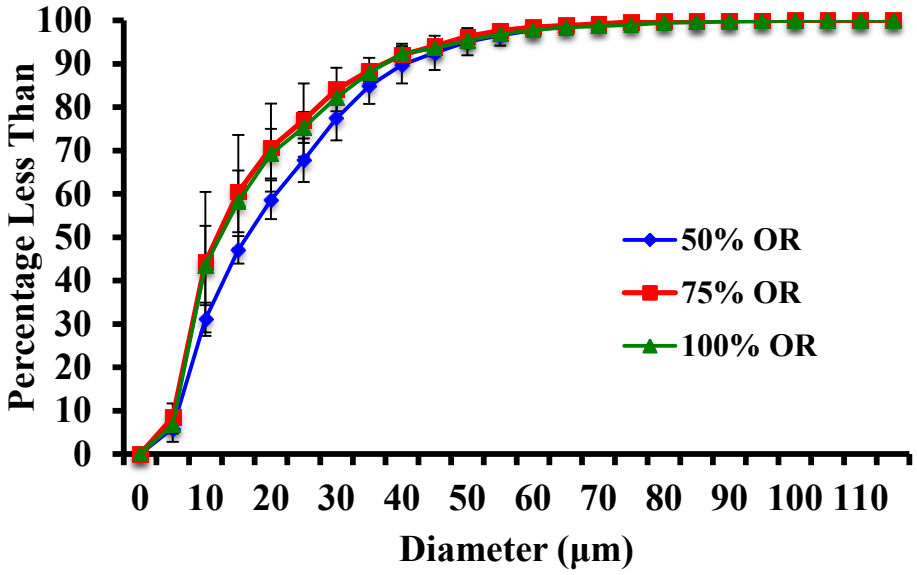

Figure 4.26c: Air cell size distributions of ice creams made with 90:10 (mono- and diglyceride:polysorbate 80 - MDG:PS80) emulsifier ratio at 50%, 75%, and 100% overrun and750 RPM. The error bars represent the standard deviations of the mean air cell sizes measured.

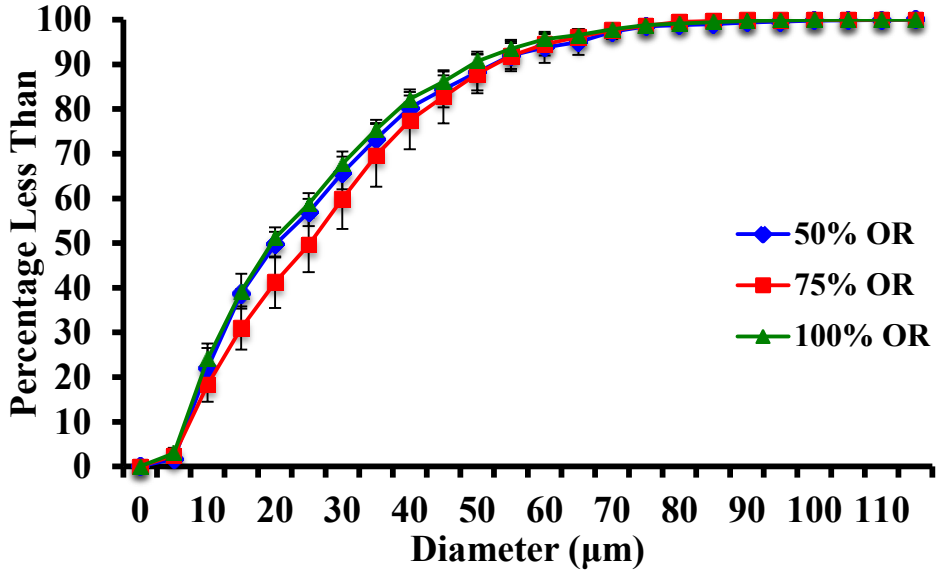

Figure 4.27a: Air cell size distributions of ice creams made with 80:20 (mono- and diglyceride:polysorbate 80 - MDG:PS80) emulsifier ratio at 50%, 75%, and 100% overrun (OR) and 250 RPM. The error bars represent the standard deviations of the mean air cell sizes measured.

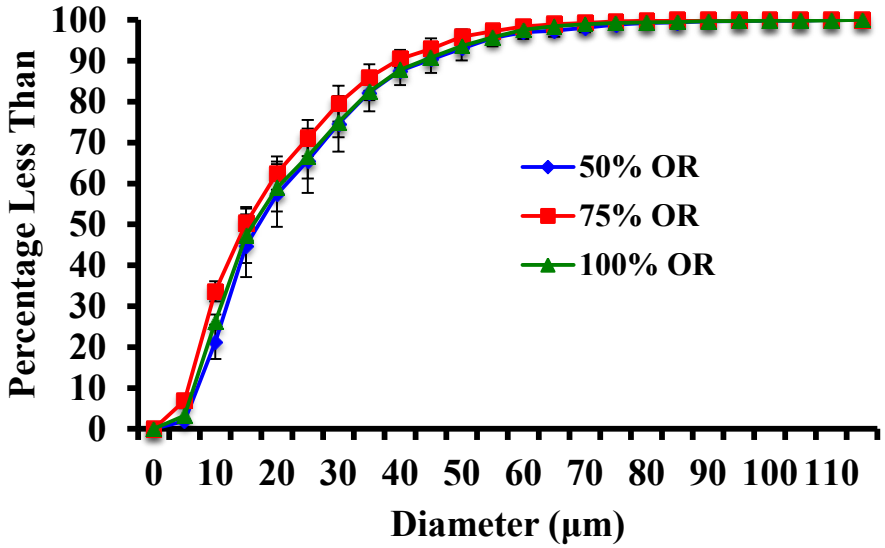

Figure 4.27b: Air cell size distributions of ice creams made with 80:20 (mono- and diglyceride:polysorbate 80 - MDG:PS80) emulsifier ratio at 50%, 75%, and 100% overrun (OR) and 500 RPM. The error bars represent the standard deviations of the mean air cell sizes measured.

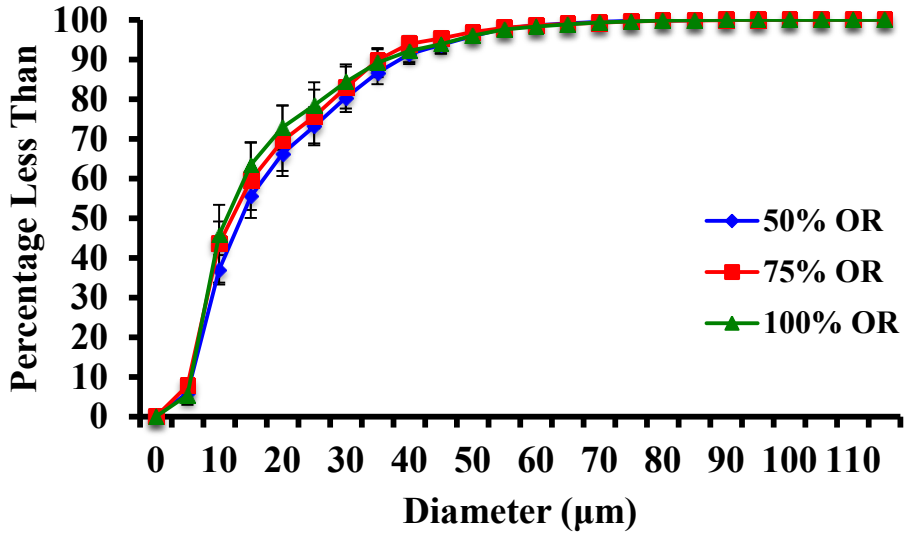

Figure 4.27c: Air cell size distributions of ice creams made with 80:20 (mono- and diglyceride:polysorbate 80 - MDG:PS80) emulsifier ratio at 50%, 75%, and 100% overrun (OR) and 750 RPM. The error bars represent the standard deviations of the mean air cell sizes measured.

In general, at constant overrun and dasher speed, mean air cell sizes for hardened ice creams decreased as emulsifier ratio and PS80 levels increased ($p = 0.0007$ for 50% overrun and 500 RPM; $p = 0.0004$ for 100% overrun and 750 RPM**).** The largest differences in mean air cell sizes were seen between ice creams made with no added emulsifier and 80:20 (MDG:PS80) **(Table 4.7**). **Figure 4.28** (**a-b**) and **Figure 4.29** show the air cell distributions and microscopy images of air cells associated with change in emulsifier ratios at constant dasher speed and overrun. At 750 RPM, air cell size distributions for 100% overrun with no added emulsifiers differed greatly from those with added emulsifiers (**Table 4.7** and **Figure 4.28** (**b**)). This trend was not observed at 750 RPM/50% overrun implying that air cells must be governed more by overrun than dasher speed as a similar trend was seen at 50% overrun for 500 RPM and 750 RPM.

Two-way ANOVA, using only 90:10 (MDG:PS80) and 80:20 (MDG:PS80), showed that both dasher speed ($p < 0.0001$) and overrun ($p < 0.0001$) had a significant effect on air cell sizes for hardened ice creams. This follows what previous literature has determined as outlined above. Statistically significant differences were determined between all dasher speeds and between 50% and 75% overrun and 50% and 100% overrun. However, the interaction between the two parameters was not found to the significant ($p = 0.4515$).

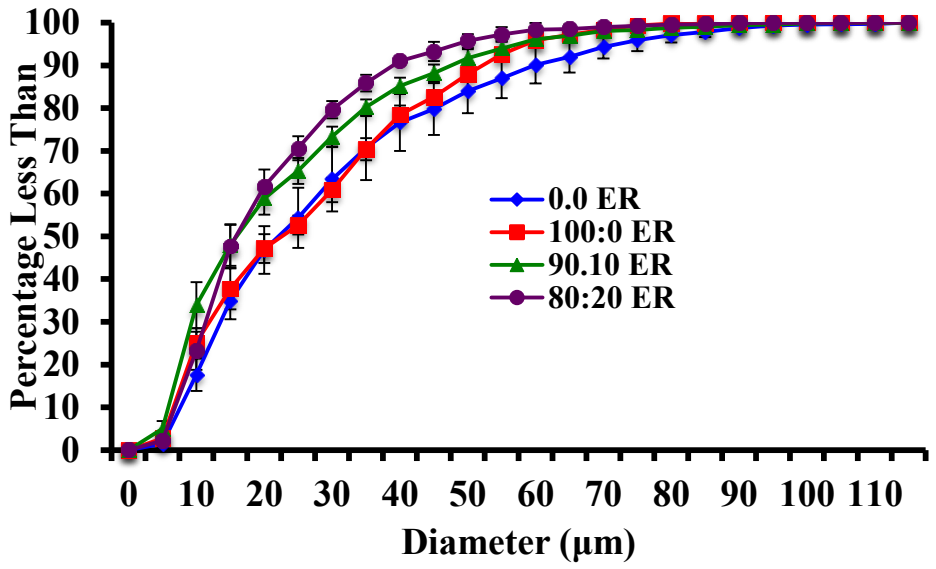

Figure 4.28a: Air cell size distributions of ice cream made with no added emulsifiers (0:0 (mono- and diglyceride:polysorbate 80 - MDG:PS80)), 100:0 (MDG:PS80), 90:10 (MDG:PS80), and 80:20 (MDG:PS80) emulsifier ratios (ER) at 50% overrun and 500 RPM. The error bars represent the standard deviations of the mean air cell sizes measured.

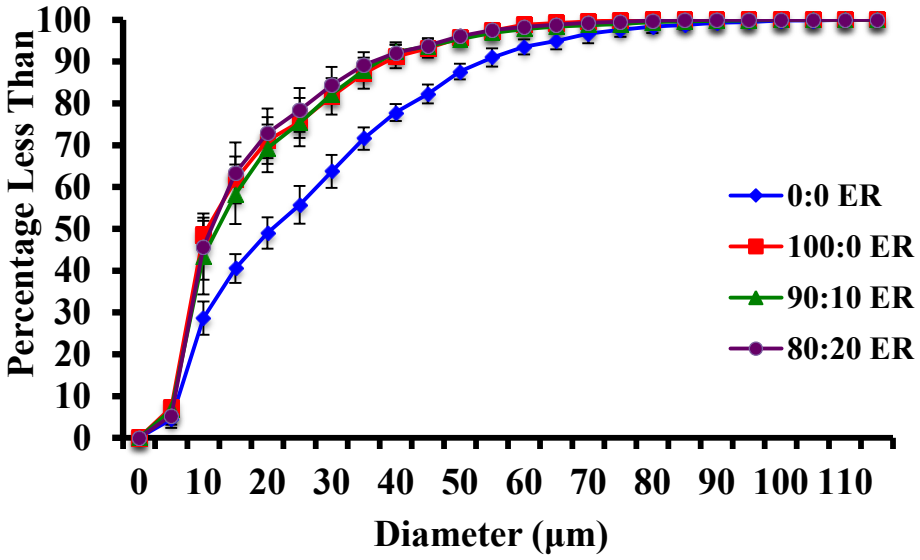

Figure 4.28b: Air cell size distributions of ice cream made with no added emulsifiers (0:0 (mono- and diglyceride:polysorbate 80 - MDG:PS80)), 100:0 (MDG:PS80), 90:10 (MDG:PS80), and 80:20 (MDG:PS80) emulsifier ratios (ER) at 100% overrun and 750 RPM. The error bars represent the standard deviations of the mean air cell sizes measured.

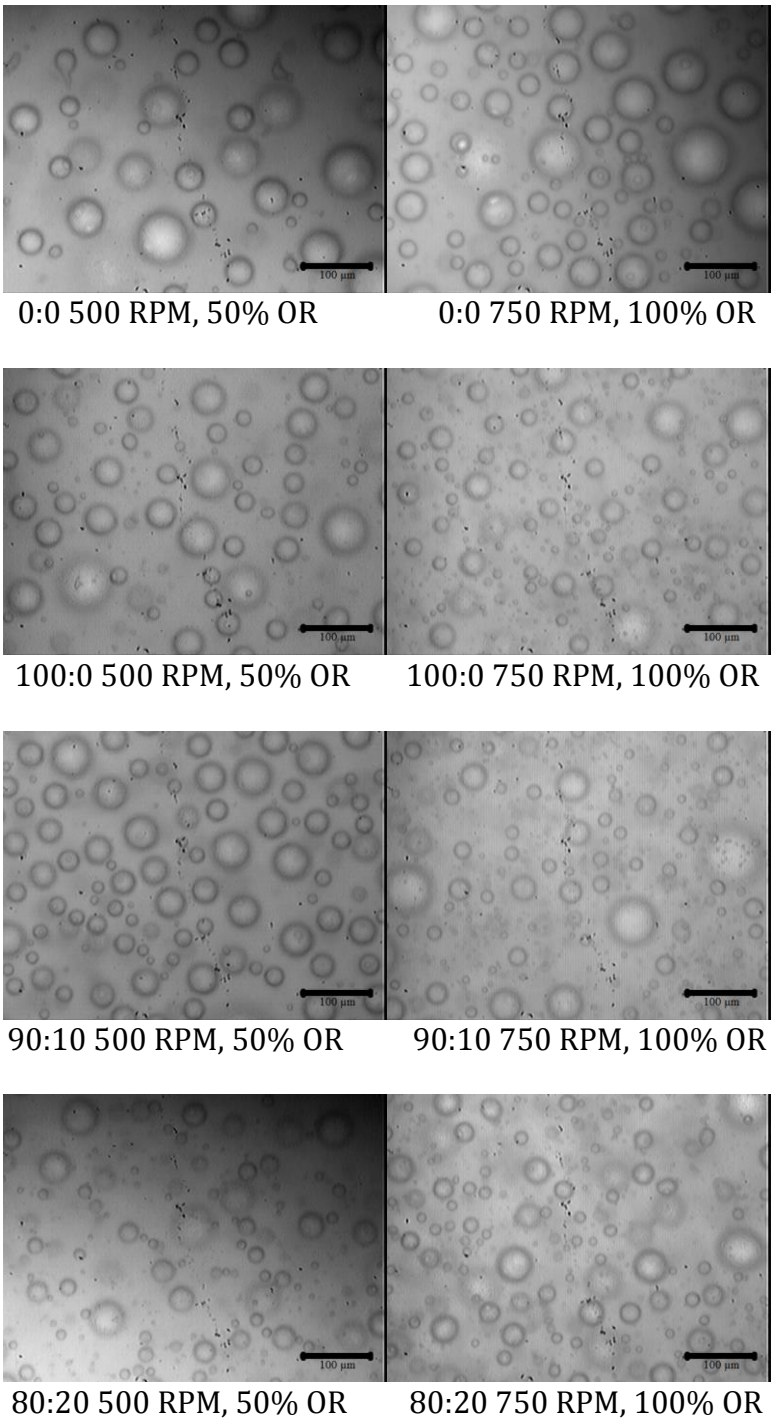

Figure 4.29: Microscope images of air cells from ice cream made with no added emulsifiers (0:0 (mono- and diglyceride:polysorbate 80 - MDG:PS80)) 100:0 (MDG:PS80), 90:10 (MDG:PS80), and 80:20 (MDG:PS80) emulsifier ratios (ER) at 500 RPM and 50% overrun and 750 RPM and 100% overrun (OR).

4.2.4 Drip-through Rate

Drip-through rate (g/min) was determined by allowing ice cream to drip-through a wire mesh screen at ambient temperature and measuring the dripped weight every 5 minutes. The weight of the dripped portion was then plotted versus time and the slope of the drip-through curve was determined as the drip-through rate. Means and standard deviations of drip-through rates for ice creams across dasher speeds, overrun, and emulsifier ratios are shown in **Table 4.8**. The drip-through rates ranged from 1.42 to 0.18 g/min and differed among overrun and emulsifier ratio but not by dasher speed. In general, ice creams made without PS80 (no added emulsifiers and 100:0 (MDG:PS80)) had the fastest drip-through rates at 50% overrun. Ice creams made with 75% and 100% overrun had the slowest drip-through rates, regardless of dasher speed and emulsifier ratio. For 50% overrun, the addition of PS80 resulted in slower melting rates, although, at 75% and 100% overrun, this effect was not seen. Ice creams with faster drip-through rates also had less remnant foams left atop the screen at the end of the drip-through test. More remnant foam was seen in ice creams with slower drip-through rates.
In general, the effect of dasher speed on drip-though rate was not significant across emulsifier ratios and overrun. **Figure 4.30(a-d)** and **Figure 4.31 (a-d)** shows the observation for ice creams made with 50% overrun across all emulsifier ratios. With an increase in dasher speed, no effect was determined on drip-through rate for ice creams made with no added emulsifiers ($p = 0.0875$), 100:0 (MDG:PS80) ($p = 0.8056$), and 90:10 (MDG:PS80) ($p = 0.1133$). For ice creams processed with 80:20 (MDG:PS80), dasher speed had a statistically significant effect on drip-through rate ($p = 0.0004$). Despite being statistically significant, these differences were very small (0.32 to 0.25 g/min).

Table 4.8: Means and standard deviations of drip-through rates for ice creams based on emulsifier ratio (mono- and diglyceride:polysorbate 80 (MDG:PS80)), dasher speed (RPM), and overrun (%). The standard deviation (±) represents the variation between replicate means of drip-through rates determined at a set overrun, dasher speed, and emulsifier ratio.

		Drip-through Rate (g/min)		
MDG:PS80	**RPM**	**50%**	**75%**	**100%**
0:0	250	$1.42 \pm 0.23^{a,A,x}$	$0.26 \pm 0.02^{a,B,xy}$	$0.33 \pm 0.03^{a,B,x}$
	500	$1.14 \pm 0.05^{b,A,y}$	$0.28 \pm 0.04^{a,B,x}$	$0.23 \pm 0.02^{b,B,y}$
	750	$1.13 \pm 0.04^{b,A,x}$	$0.28 \pm 0.02^{a,B,x}$	$0.29 \pm 0.02^{c,B,x}$
100:0	250	N/A*	N/A*	N/A*
	500	$1.23 \pm 0.08^{a,A,x}$	N/A*	$0.30 \pm 0.02^{a,B,x}$
	750	$1.18 \pm 0.07^{a,A,x}$	N/A*	$0.26 \pm 0.04^{a,B,x}$
90:10	250	$0.26 \pm 0.04^{a,A,y}$	$0.25 \pm 0.05^{a,A,x}$	$0.24 \pm 0.01^{a,A,y}$
	500	$0.29 \pm 0.03^{a,A,z}$	$0.29 \pm 0.05^{a,A,x}$	$0.21 \pm 0.02^{b.B,y}$
	750	$0.28 \pm 0.04^{a,A,y}$	$0.23 \pm 0.04^{b,A,x}$	$0.18 \pm 0.02^{c,B,y}$
80:20	250	$0.31 \pm 0.02^{a,A,y}$	$0.31 \pm 0.03^{a,A,x}$	$0.32 \pm 0.02^{a,A,x}$
	500	$0.26 \pm 0.04^{b,A,z}$	$0.29 \pm 0.08^{a,A,x}$	$0.25 \pm 0.05^{b,A,y}$
	750	$0.28 \pm 0.03^{ab,A,y}$	$0.26 \pm 0.02^{a,A,x}$	$0.26 \pm 0.07^{b,A,x}$

^{a,b,c} denote significant differences among ice creams based on constant overrun (columns)
^{A,B,C} denote significant differences among ice creams based on constant dasher speed (rows)
^{x,y,z} denote significant differences among ice creams based on emulsifier ratio, constant dasher speed, and constant overrun (columns)
*Samples not included in experimental design
[1]no added emulsifiers in the formula
[2]total emulsifiers added consisted of 100% MDG at 0.15% in the formula
[3]total emulsifiers added consisted of 90:10 MDG:PS80 at 0.15% in the formula
[4]total emulsifiers added consisted of 80:20 MDG:PS80 at 0.15% in the formula

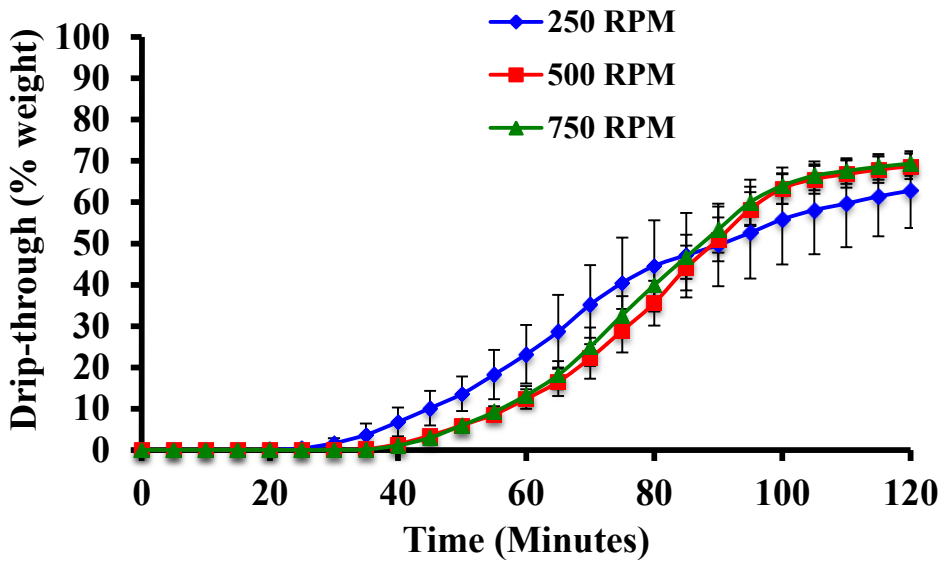

Figure 4.30a: Drip-through (% weight) curves for ice creams made with no added emulsifiers at 50% overrun and 250 RPM, 500 RPM, and 750 RPM. The error bars represent the standard deviations of the mean drip-through (%weight) measured.

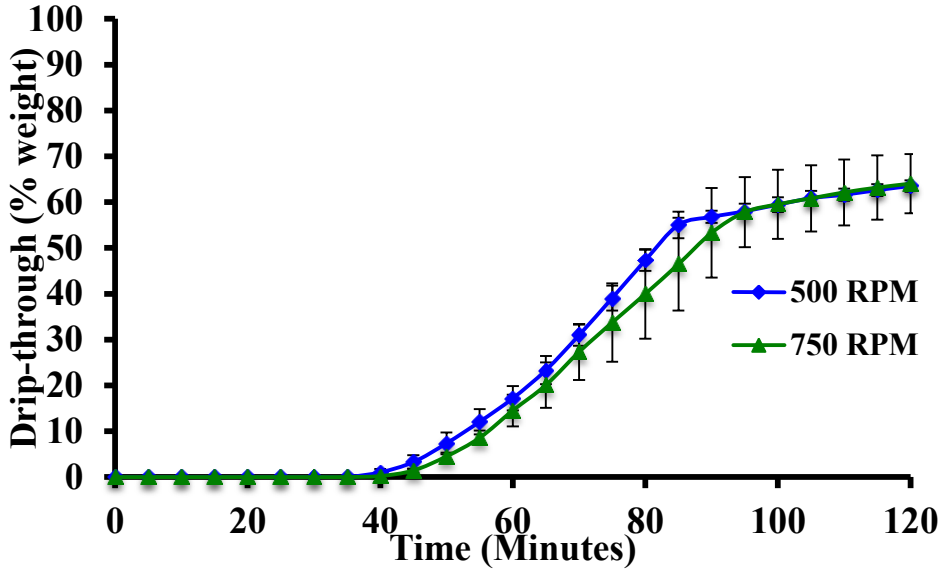

Figure 4.30b: Drip-through (% weight) curves for ice creams made with 100:0 (mono- and diglyceride:polysorbate 80 - MDG:PS80) emulsifiers at 50% overrun and 500 RPM and 750 RPM. The error bars represent the standard deviations of the mean drip-through (%weight) measured.

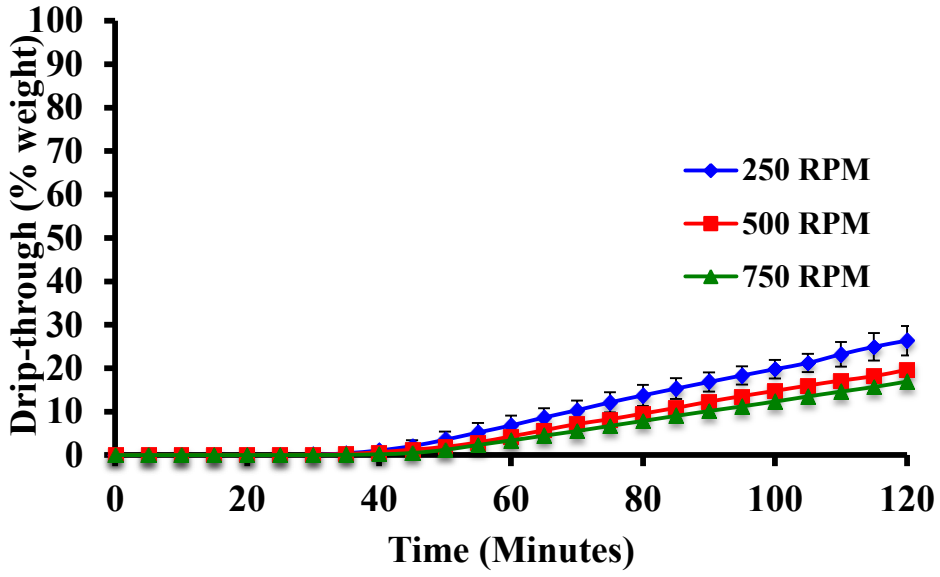

Figure 4.30c: Drip-through (% weight) curves for ice creams made with 90:10 (mono- and diglyceride:polysorbate 80 - MDG:PS80) emulsifiers at 50% overrun and 250 RPM, 500 RPM, and 750 RPM. The error bars represent the standard deviations of the mean drip-through (%weight) measured.

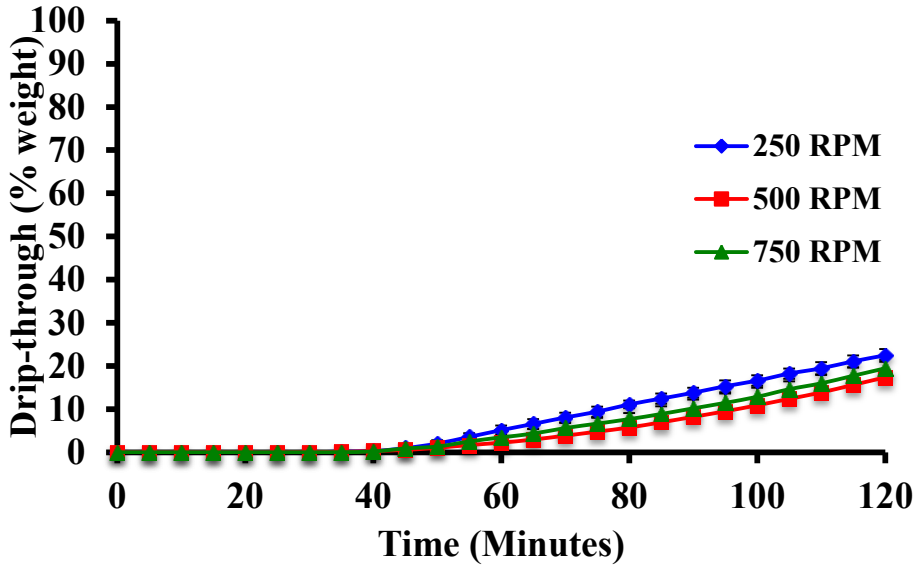

Figure 4.30d: Drip-through (% weight) curves for ice creams made with 80:20 (mono- and diglyceride:polysorbate 80 - MDG:PS80) emulsifiers at 50% overrun and 250 RPM, 500 RPM, and 750 RPM. The error bars represent the standard deviations of the mean drip-through (%weight) measured.

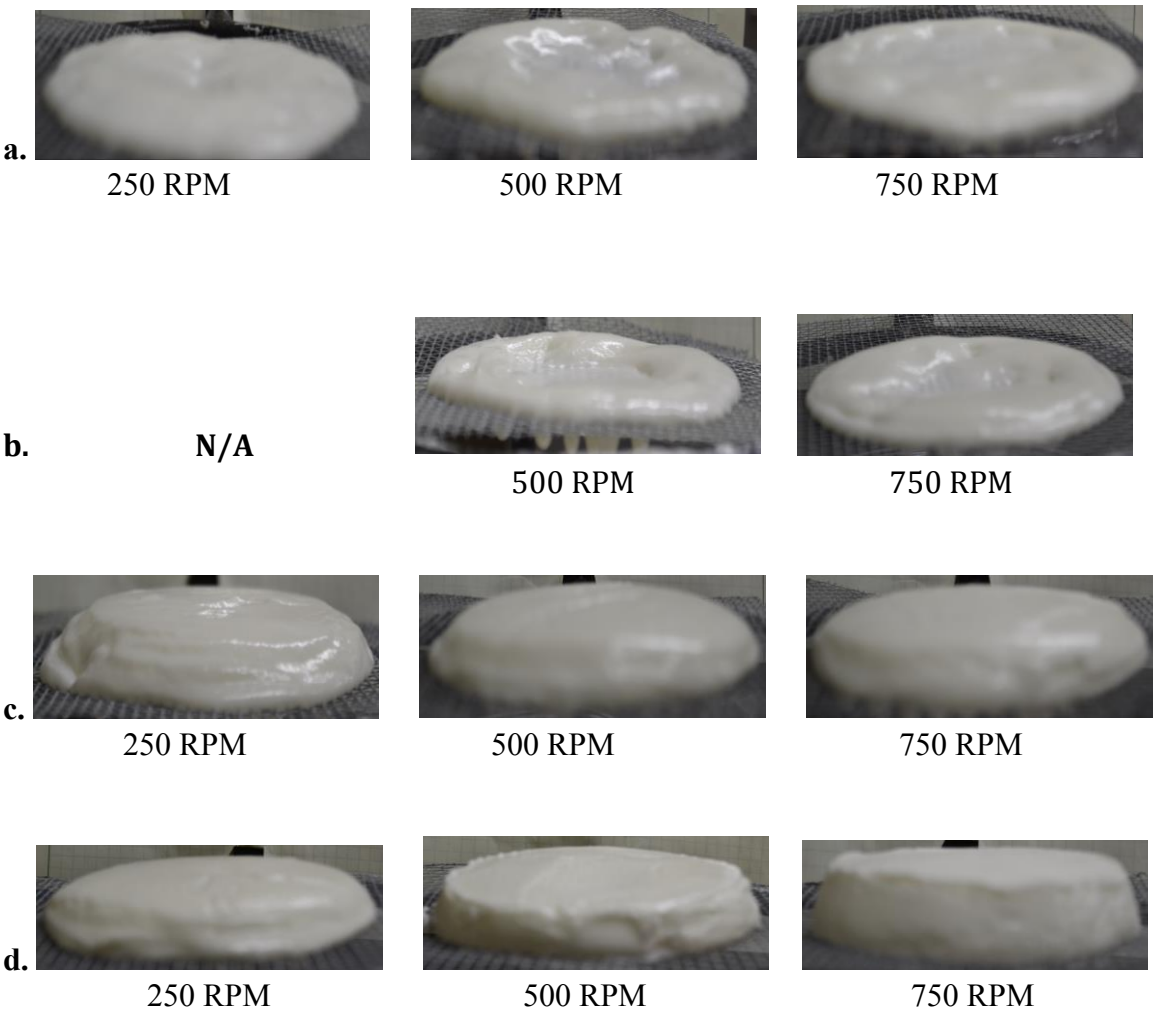

Figure 4.31: Images of ice cream structure left on top of screen at the end of a drip-through test of ice creams made with no added emulsifiers (**a**), 100:0 (mono- and diglyceride:polysorbate 80 - MDG:PS80) (**b**), 90:10 (MDG:PS80) (**c**), and 80:20 (MDG:PS80) (**d**) emulsifier ratios and processed at 50% overrun and 250 RPM (not at 100:0 (MDG:PS80), 500 RPM, and 750 RPM.

Figure H.1 - Figure H.7 in **Appendix H** show the drip-through curves and remnant foam images for ice creams made with 75% and 100% overrun across emulsifier ratios.

In the literature, an increase in dasher speed (shear rate) has been shown to increase PC in ice cream (Gelin et al., 1994; Gelin, et al., 1996a, b; Goff et al., 1999; Goff and Jordan,1989; Pelan et al., 1997; Tharp et al., 1998; and Thomsen and Holtsborg, 1998; Walstra, 2003). In

addition, drip-through rate and PC have been shown to have an inverse relationship (Berger and White, 1971; Berger et al.,1972; Segall and Goff, 2002; Muse and Hartel, 2004). As a result, it was expected that as dasher speed increased, drip-through rate would decrease. However, this same trend was not seen in this study. This cannot be explained by partially-coalesced fat since the effect of PC on drip-through rate was found to be statistically significant across all emulsifier ratios ($p < 0.0001$) (no emulsifier added – $p < 0.0001$, 100:0 (MDG:PS80) – $p < 0.0001$, 90:10 (MDG:PS80) – $p < 0.0001$, 80:20 (MDG:PS80) – $p = 0.0031$). Except for ice creams made with no added emulsifiers and 100:0 (MDG:PS80) at 50% overrun, the drip-through rates ranged from 0.18 to 0.33 g/min. It is possible that this range was too narrow to determine the true effect of dasher speed on drip-through rate. There were most likely other interactions between microstructure components that also influenced drip-through rate, not controlled by dasher speed.

Sakuria et al. (1996) and Sofjan and Hartel (2003) both noted a decrease in drip-through rate as overrun increased. This trend was also evident in this study across all emulsifier ratios ($p < 0.0001$) except 80:20 (MDG:PS80) ($p = 0.8768$). The larger volumes of air present in high overrun products caused a reduced rate of heat transfer, which resulted in slower melting rates. This trend was not observed at 80:20 (MDG:PS80) which may be attributed to the large amount of structure created with large amounts of PC with the addition of overrun for these ice creams. Although this trend was observed for the other emulsifier ratios, the ranges for drip-through rates at 90:10 (MDG:PS80) (0.18 to 0.29 g/min) were small when compared to no added emulsifier (0.26 to 1.42 g/min) and 100:0 (MDG:PS80) (0.26 to 1.23 g/min) ice creams. The drip-through (% weight) curves for ice creams processed at 500 RPM across emulsifier ratios and overrun are shown in **Figure 4.32 (a-d)**. **Figure 4.33 (a-d)** displays the remnant foam left atop the screen

after the drip-through test. Ice creams at 50% overrun with no added emulsifiers and 100:0 (MDG:PS80) had faster drip-through rates and less remnant foam than ice creams at 75% and 100%, regardless of dasher speed. Slower drip-through rates and more remnant foam were seen in all ice creams with 75% and 100% overrun, regardless of emulsifier ratio and dasher speed. Ice creams processed at 50% overrun with PS80 also had slower drip-through rates. **Figure H.3 – Figure H.7** in **Appendix H** displays the drip-through curves for ice creams made at 250 RPM and 750 RPM across emulsifier ratios. The corresponding images of the remnant foam left atop the screen after the drip-through test for 250 RPM and 750 RPM can be found in **Figure H.8 – Figure H.11** in **Appendix H**.

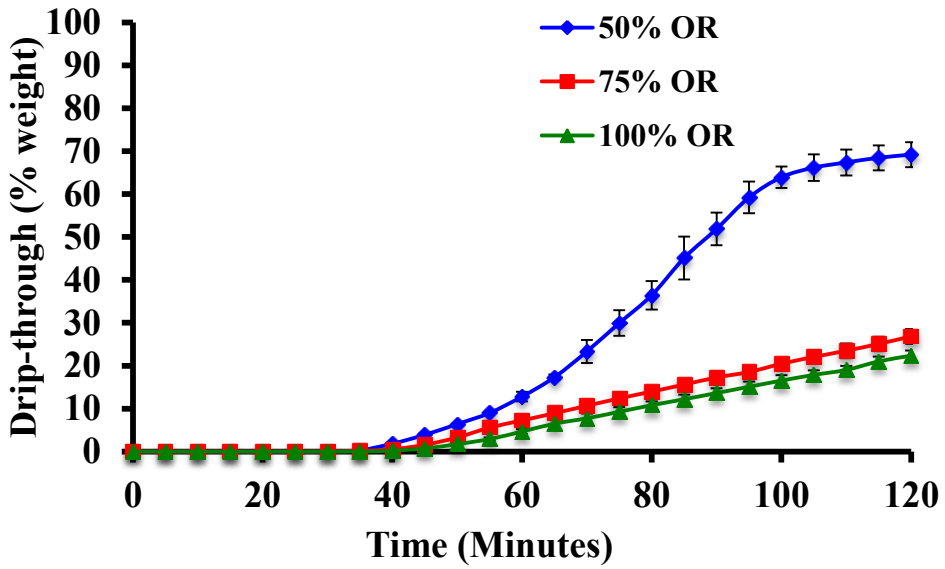

Figure 4.32a: Drip-through (% weight) curves for ice creams made with no added emulsifiers at 500 RPM and 50%, 75%, and 100% overrun (OR). The error bars represent the standard deviations of the mean drip-through (%weight) measured.

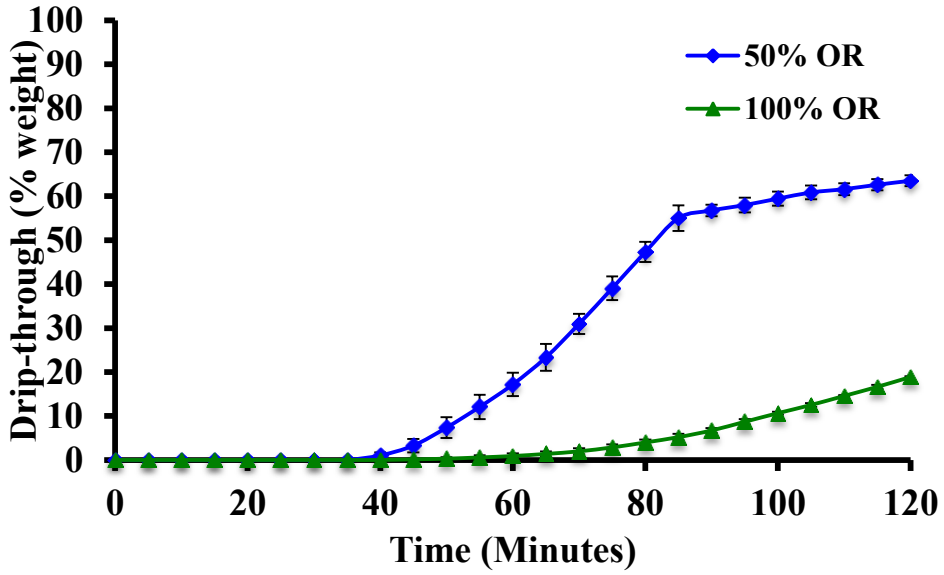

Figure 4.32b: Drip-through (% weight) curves for ice creams made with 100:0 (mono- and diglyceride:polysorbate 80 - MDG:PS80) emulsifier ratio at 500 RPM and 50% and 100% overrun (OR). The error bars represent the standard deviations of the mean drip-through (%weight) measured.

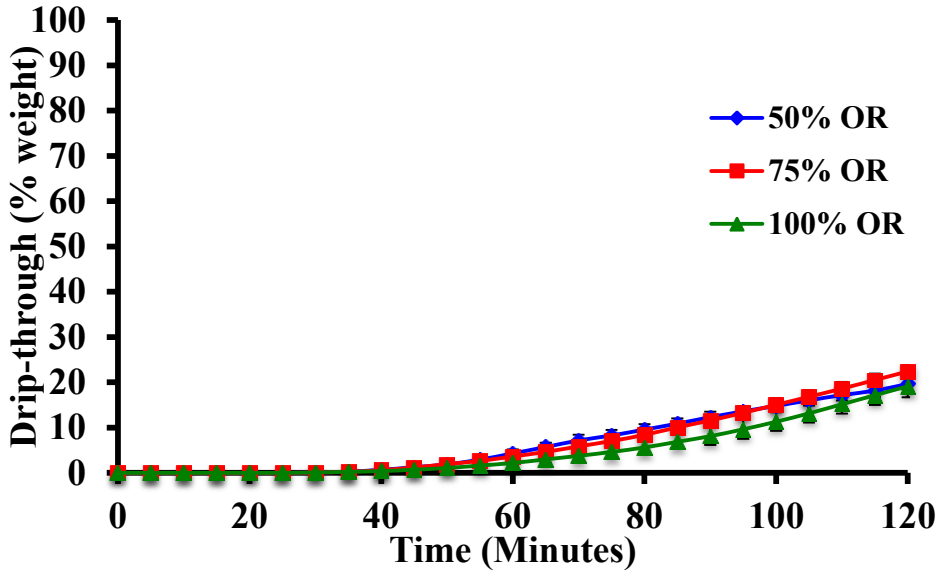

Figure 4.32c: Drip-through (% weight) curves for ice creams made with 90:10 (mono- and diglyceride:polysorbate 80 - MDG:PS80) emulsifier ratio at 500 RPM and 50%, 75%, and 100% overrun (OR). The error bars represent the standard deviations of the mean drip-through (%weight) measured.

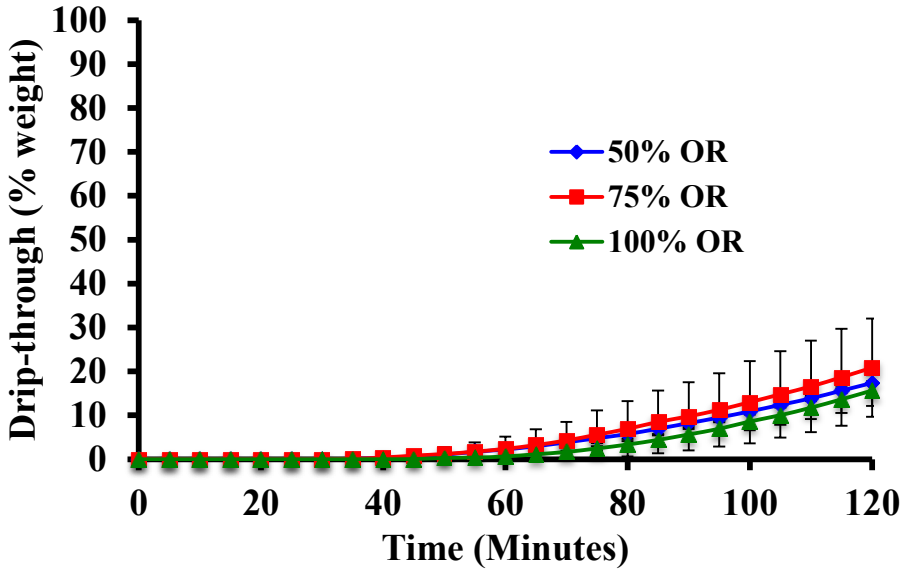

Figure 4.32d: Drip-through (% weight) curves for ice creams made with 80:20 (mono- and diglyceride:polysorbate 80 - MDG:PS80) emulsifier ratio at 500 RPM and 50%, 75%, and 100% overrun (OR). The error bars represent the standard deviations of the mean drip-through (%weight) measured.

At constant overrun and dasher speed, drip-through rates decreased ($p < 0.0001$) with the addition of PS80 at 50% overrun, but this same trend was not seen at 75% and 100% overrun (**Table 4.8** and **Figure 4.34**). More remnant foam was left atop the screen after the drip-through test for ice creams with PS80 at 50% overrun and 500 RPM (**Figure 4.35**). Enough structure must be created at 75% and 100% overrun regardless of dasher speed, which led to minimum collapse in ice cream structure and slow drip- through rates. **Figure H.19** and **Figure H.20** display the drip-through (% weight) curves and images of remnant foam left on top the screen at the end of the drip-through test for ice creams made at 750 RPM and 100% overrun across all emulsifier levels. Differences might have been determined if lower overruns and dasher speeds were used to create the ice creams products.

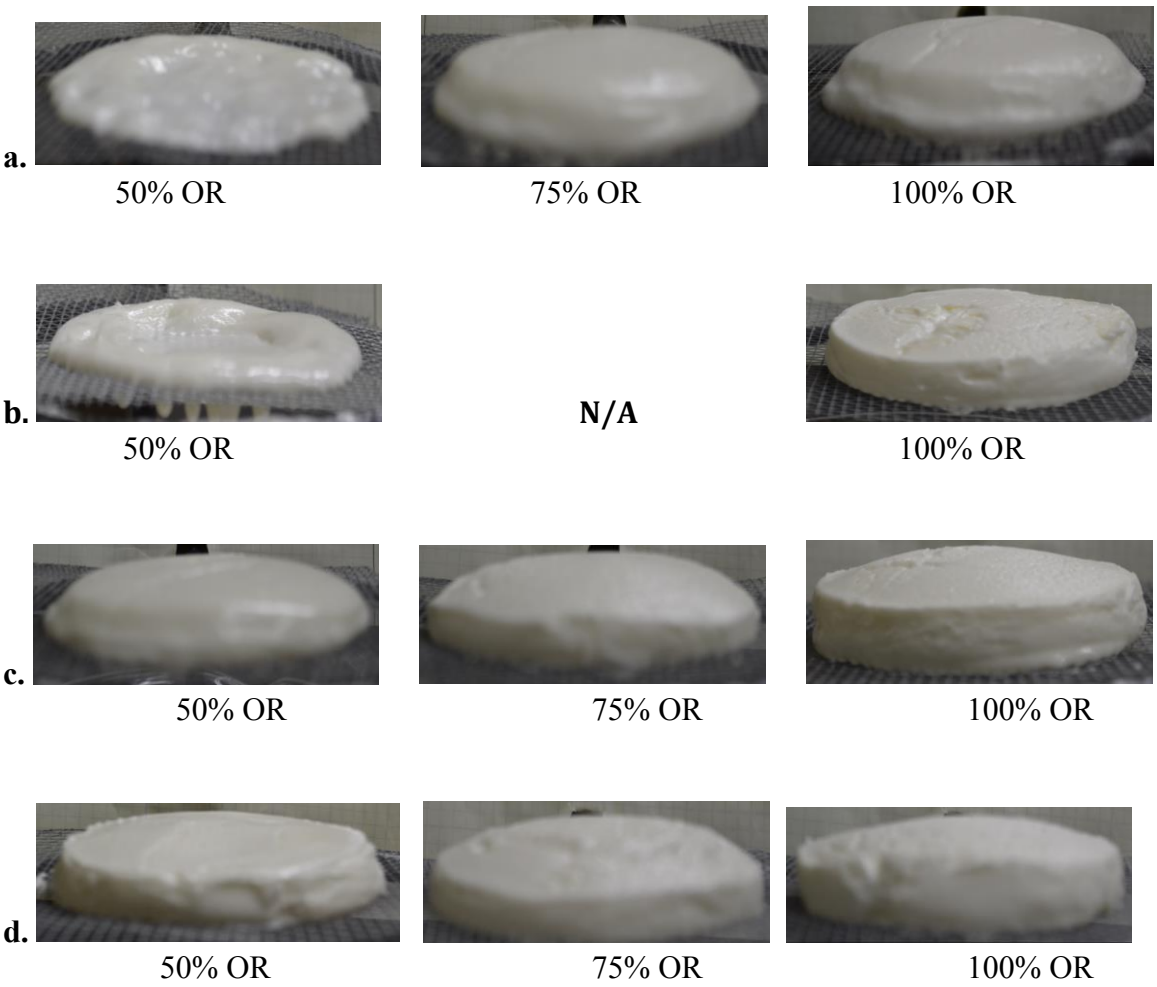

Figure 4.33: Images of ice cream structure left on top of screen at the end of a drip-through test of ice creams made with no added emulsifiers (**a**), 100:0 (mono- and diglyceride:polysorbate 80 - MDG:PS80) (**b**), 90:10 (MDG:PS80) (**c**), and 80:20 (MDG:PS80) (**d**) emulsifier ratios and processed at 500 RPM and 50% (not at 100:0 (MDG:PS80), 75%, and 100% overrun (OR).

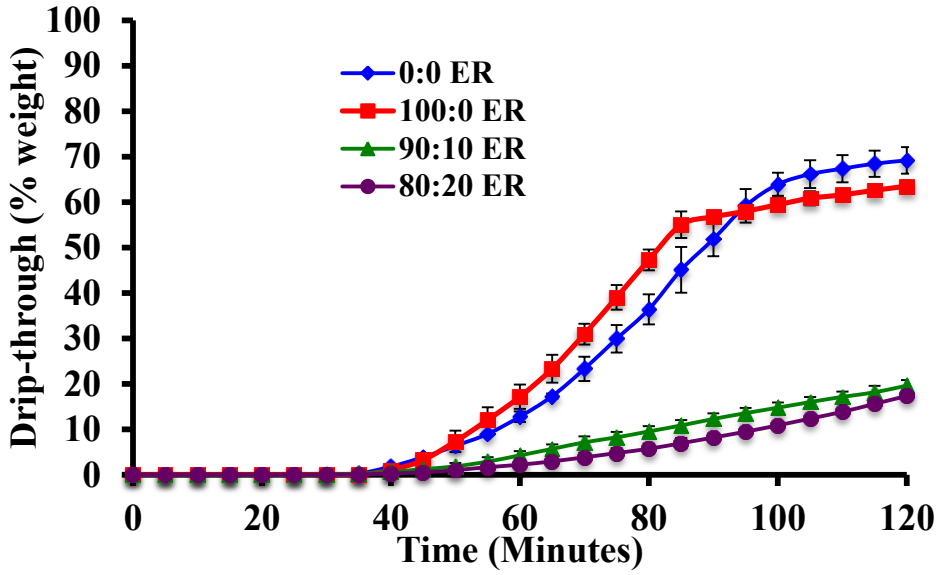

Figure 4.34: Drip-through curves (% weight) for ice creams processed at (0:0 (mono- and diglyceride:polysorbate 80 - MDG:PS80)), 100:0 (MDG:PS80), 90:10 (MDG:PS80), and 80:20 (MDG:PS80) emulsifier ratios (ER) at 50% overrun and 500 RPM. The error bars represent the standard deviations of the mean drip-through (%weight) measured.

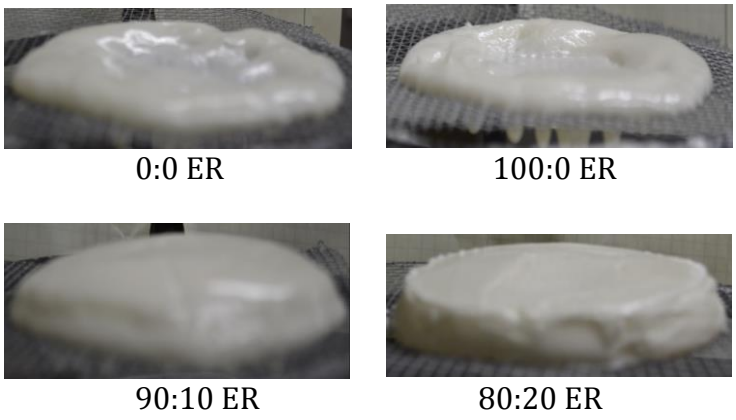

Figure 4.35: Images of ice cream structure left on top of screen at the end of a drip-through test of ice creams made with (0:0 (mono- and diglyceride:polysorbate 80 - MDG:PS80)), 100:0 (MDG:PS80), 90:10 (MDG:PS80), and 80:20 (MDG:PS80) emulsifier ratios (ER) at 50% overrun and 500 RPM.

A two-way ANOVA, using data from ice creams with PS80 (90:10 (MDG:PS80) and 80:20 (MDG:PS80)), showed both dasher speed ($p = 0.0095$) and overrun ($p = 0.0026$) had a statistically significant effect on drip-through rate, with the effect of overrun being more significant. Statistically significant differences were determined between 250 RPM and 750 RPM for dasher speed and between 50% and 100% and 75% and 100% for overrun. However, the interaction between the two parameters was not determined to be significant ($p = 0.0646$).

Mean air cell sizes and ice crystal sizes have been noted to significantly affect drip-through rate. Sofjan and Hartel (2003) found that mean air cell sizes had a direct correlation with drip-through rate. Via a multivariate pairwise comparison test, this observation was seen across all emulsifier levels ($p < 0.0001$) in this study (no emulsifier added – $p < 0.0001$, 100:0 (MDG:PS80) – $p < 0.0001$, 90:10 (MDG:PS80) – $p = 0.0064$, 80:20 (MDG:PS80) – $p < 0.0103$). An increase in ice crystal size resulted in an increase in drip-through rate in a study by Muse and Hartel (2004). However, in this study, mean ice crystal size had a minimal effect on drip-through rate ($p = 0.0544$). This was due to ice crystal sizes being controlled via draw temperature and being very similar across all ice creams analyzed (**Table 4.5**).

4.2.4.1 Predicting Drip-through Rate

Regression was used to determine how the observed physical properties influenced drip-through rate. From the controlled ice cream study, it was determined mean air cell ($p = 0.0546$) and ice crystal size ($p = 0.0071$), overrun ($p = 0.0050$), and the interaction between mean air cell size and overrun ($p = 0.0023$) all significantly influenced the rate of drip for ice creams made with no added emulsifiers across all dasher speeds and overruns. Regression analysis was also performed on ice creams processed with 80:20 (mono- and diglyceride:polysorbate 80

(MDG:PS80) emulsifier ratio across all dasher speeds and overrun. From the regression, no statistical correlations were determined to influence drip-through rate. The differences in the regression analyses could be attributed to the differences in the matrixes in the microstructures formed at no added emulsifiers and at 80:20 (MDG:PS80) emulsifier ratio. For example, in ice creams made with no added emulsifiers, partially-coalesced fat was significantly lower and air cells were significantly larger than ice creams made with 80:20 (MDG:PS80). These variances in the microstructure components affected the drip-through rates and made it difficult to predict the rate of drip based on the microstructure components and their interactions.

4.3 Fat Content Experiment

To determine the effect of fat content on partial coalescence and drip-through rate, ice cream products were made with 6%, 9%, 12%, and 15% fat at an 80:20 emulsifier level. The emulsifier level was properly adjusted for each fat level in order to keep the percent fat to emulsifier ratio constant across ice creams. Products were processed at a dasher speed of 500 RPM and an overrun (OR) of 50%. Various responses were measured including actual overrun, draw temperature, mean ice crystal and air cell size, degree of partial coalescence, and drip-through rate. The measured overruns were close to the target as shown in **Table 4.9**. One target draw temperature, -6^{o}C, was selected for this set of experiments. The actual draw temperatures for the ice creams were close to the target draw temperature (-6.1±0.1^{o}C). All of the analyzed responses are combined in **Table 4.9**.

4.3.1 Mean Ice Crystal Size

One-way ANOVA determined that ice crystal sizes were not statistically different for the ice creams processed with different fat levels ($p = 0.3753$) (**Table 4.9** and **Figure 4.36**). Ice creams were frozen at the same target draw temperature resulting in ice crystals formed with similar size distributions. **Figure 4.37** shows images of ice crystals from ice creams with different fat contents.

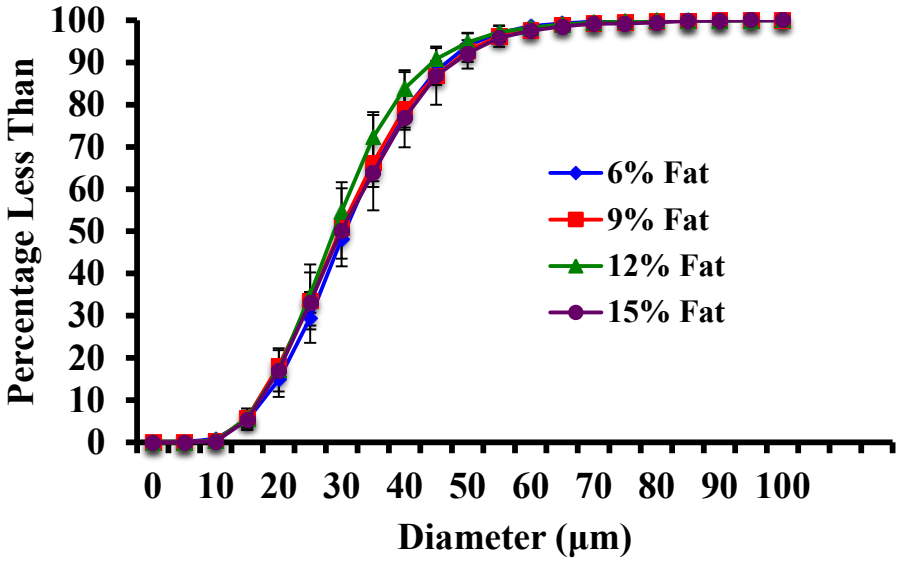

Figure 4.36: Ice crystal size distributions of ice creams made with 6%, 9%, 12%, and 15% fat contents and processed at 500 RPM and 50% overrun. The error bars represent the standard deviations of the mean ice crystal sizes measured for each fat content.

Table 4.9: Means and standard deviations of actual overrun, mean ice crystal size, calculated partial coalescence, mean air cell size, and drip-through rate for ice creams based on 6%, 9%, 12% and 15% fat contents at 80:20 emulsifier ratio (mono- and diglyceride:polysorbate 80 (MDG:PS80), 500 RPM and 50% overrun. The standard deviation (±) represents the variation between replicate means between each variable determined at a set fat content.

% Fat	Emulsifier Level (%)	Actual Overrun (%)	Calculated Partial Coalescence (%)	Mean Air Cell Size (µm)	Mean Ice Crystal Size (µm)	Drip-through Rate (g/min)
6%	0.075	58.1±7.9^{a}	14.4±3.8^{b}	27.2±2.2^{a}	31.5± 1.6^{a}	0.31±0.03^{ab}
9%	0.113	54.6±6.4^{ab}	59.2±7.6^{a}	24.4±1.9^{b}	31.2± 2.7^{a}	0.35±0.04^{a}
12%	0.15	53.1±1.1^{ab}	56.3±9.1^{a}	20.5±0.6^{c}	30.0± 1.6^{a}	0.26±0.04^{bc}
15%	0.188	48.4±1.7^{b}	57.7±5.3^{a}	24.3±1.4^{b}	31.7± 0.7^{a}	0.22±0.03^{c}

^{a,b,c}Means not sharing the same letter are significantly different ($\alpha<0.05$).

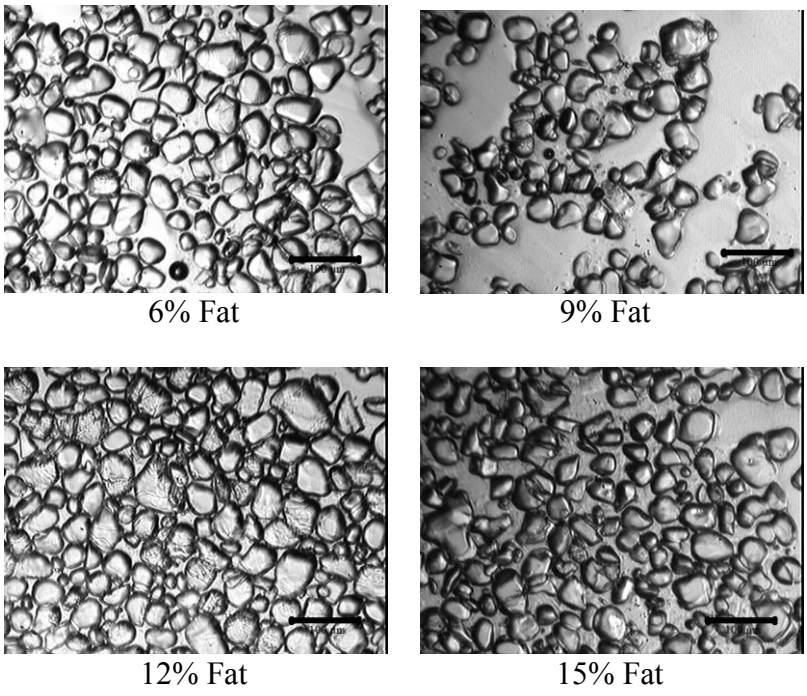

Figure 4.37: Microscope images of ice crystals for ice creams made with 6%, 9%, 12%, and 15% fat at 80:20 (mono- and diglyceride:polysorbate 80 (MDG:PS80) emulsifier ratio, 500 RPM, and 50% overrun (40x magnification, 100 μm scale bar).

4.3.2 Partial Coalescence (PC)

From the one-way ANOVA, fat content had a significant effect on PC ($p < 0.0001$). A Tukey's HSD test indicated that PC increased as fat content increased between 6% and 9% but not between 9%, 12% and 15% fat (**Table 4.9** and **Figure 4.38)**. As discussed in the literature review, the effect of fat content on PC is not fully understood. However, it is known that the extent of fat destabilization is dependent on the fat volume fraction (Hinrichs and Kessler, 1997; Walstra, 2003), so it is not clear why increasing fat did not lead to a continuous increase in partially-coalesced fat. One possible explanation may involve the decrease in water content with increasing fat, as seen in **Table 4.10**. Although the freezing point temperature was constant, the

total ice content on a mass basis would be different during freezing. An increase in shear in the freezer (dasher speed, aeration, ice crystal formation) would lead to an increase in partial coalescence (Gelin et al., 1996a). Although dasher speed and overrun were held constant, with an increase in total solids, the total amount of ice crystals formed decreased as fat content increased. As a result, ice cream products with lower fat content actually underwent more shear (increase in ice crystal content) during the dynamic freezing process than ice creams with higher fat content (decrease in ice crystal content). The increase in fat content/decrease in ice content led to two competing factors during freezing. In one case, PC would be expected to increase with an increase in fat content due to the phase volume effect. On the other hand, PC would be expected to decrease with an increase in fat content due to the reduction in shear. The effect of these competing factors was more evident at 9%-15% fat.

More research is needed in this area to better understand these competing effects. Microscope images of the melted ice creams across fat contents visually confirm the results from the particle size data (**Figure 4.39**).

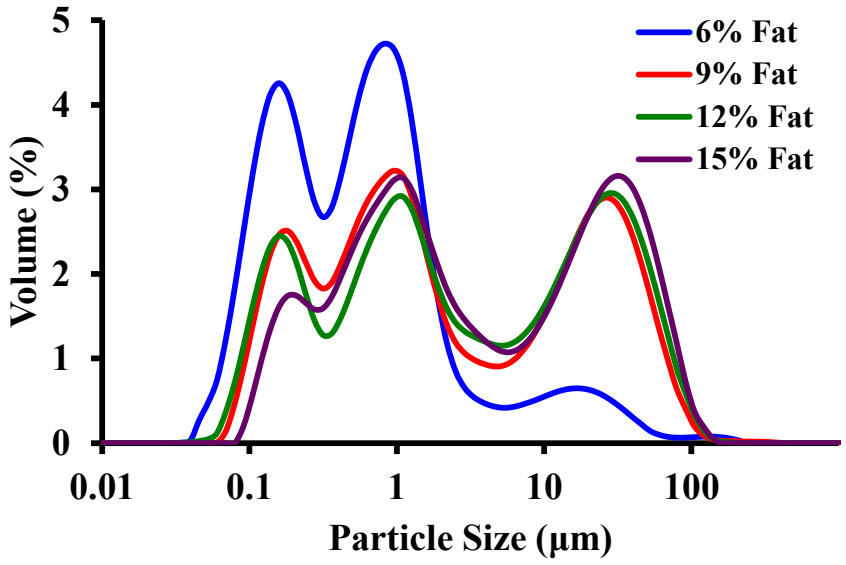

Figure 4.38: Particle size distributions for ice creams made with 6%, 9%, 12%, and 15% fat at 80:20 (mono- and diglyceride:polysorbate 80 (MDG:PS80) emulsifier ratio, 500 RPM, and 50% overrun.

Table 4.10: Total solids (%) for ice creams made with 80:20 (mono- and diglyceride:polysorbate 80 (MDG:PS80) emulsifier ratio at varying fat contents.

Fat Content	Total Solids (%)
6%	34.24
9%	37.61
12%	41.73
15%	44.43

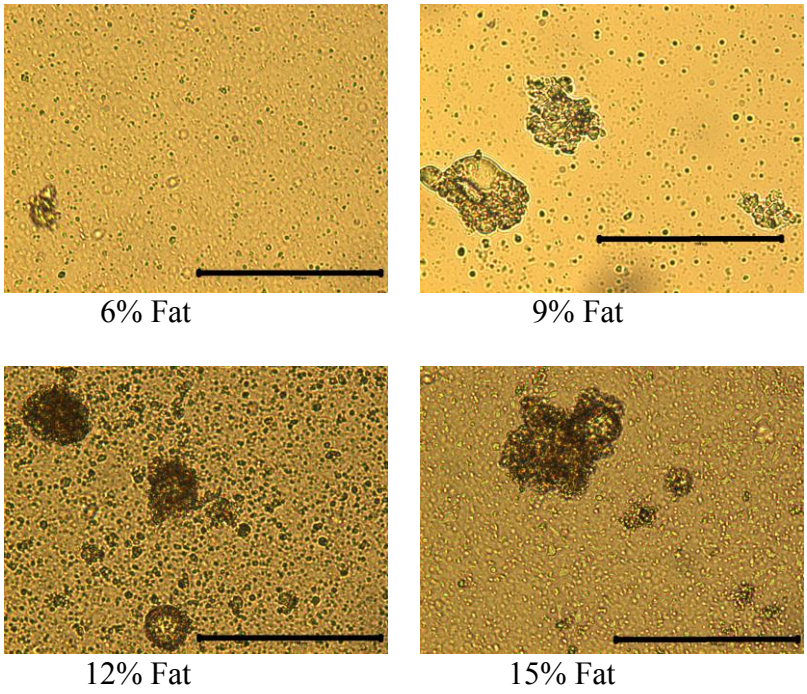

Figure 4.39: Microscope images of melted ice creams made with 6%, 9%, 12%, and 15% fat at 80:20 (mono- and diglyceride:polysorbate 80 (MDG:PS80) emulsifier ratio. Ice creams were processed at 500 RPM and 50% overrun (400x magnification, 100 µm scale bar).

4.3.3 Mean Air Cell Size

Mean air cell sizes for hardened ice creams ranged from 20.5 to 27.2 µm and one-way ANOVA showed that a statistical difference ($p < 0.0001$) was determined for air cell size across fat contents. A Tukey's HSD test determined that mean air cell sizes produced from ice creams made with 6% fat and 12% fat contents were noted to be statistically different from those with 9% and 15% fat contents and from each other (**Table 4.9** and **Figure 4.40**). This does not follow previous literature findings from Chang and Hartel (2002a). In this study, it was determined that fat content had no effect on mean air cell size for freshly made ice creams even though levels of fat destabilization were different. Although an increase in fat content does increase the viscosity of the product inside the freezer (Goff et al., 1994), viscosities were assumed not to be

significantly different at a 14% fat difference in the study by Chang and Hartel (2002a). However, in Chang's study, air cells were measured straight from the batch freezer and not from a hardened ice cream like in this current study. It is possible that air cells were able to change during the hardening process, as shown by Chang and Hartel (2002c) and discussed in **Section 4.2.2**. In this current study, it was assumed that viscosities of the ice creams did slightly increase as fat content increased (Goff et al., 1994), but were similar (9% difference across mixes) and did not have a significant effect on air cells during processing, unlike change in overrun. Since viscosities (same overrun and stabilizers) and ice crystals sizes were similar for each mix, it was assumed that those air cells were the same size upon draw. As a result, air cells could significantly change during the hardening process if not stabilized by enough partially-coalesced fat. The mean air cell size in ice creams produced with 6% fat was slightly larger than the mean air cell size produced from ice creams with 9%, 12%, and 15% fat. The calculated partially-coalesced fat at 6% fat was also significantly lower than all other calculated partially-coalesced fat values (**Table 4.9**). As a result, there was less partially-coalesced fat to act as a barrier and prevent the coalescence of air cells during the hardening process. The 12% fat samples had statistically significant smaller air cell size than 9% and 15% fat, which appears to be an anomalous result, since PC was not significantly different across the three highest fat contents. **Figure 4.41** shows images of air cells from ice creams containing different fat contents.

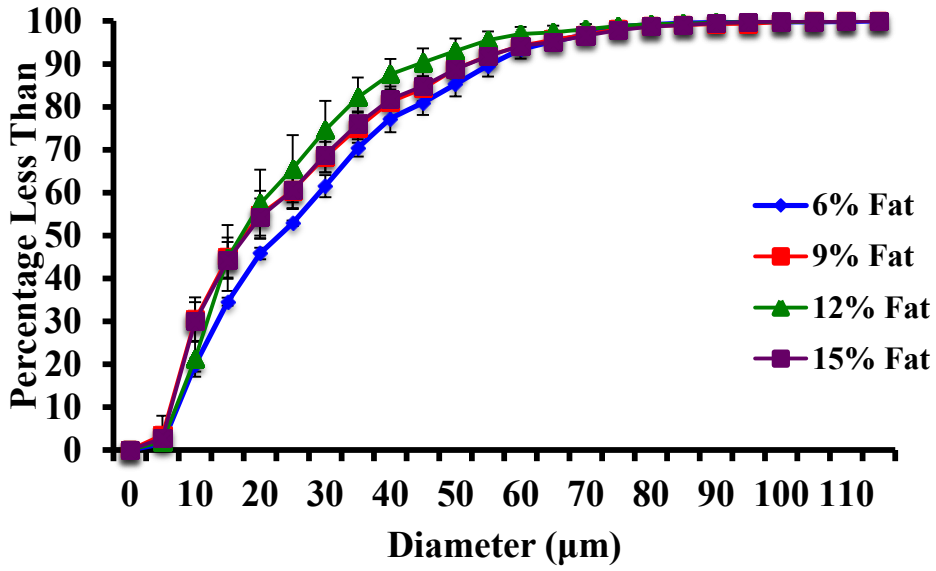

Figure 4.40: Air cell size distributions of ice creams made with 6%, 9%, 12%, and 15% fat at 80:20 (mono- and diglyceride:polysorbate 80 (MDG:PS80) emulsifier ratio, 500 RPM, and 50% overrun. The error bars represent the standard deviations of the mean air cell sizes measured for each fat content.

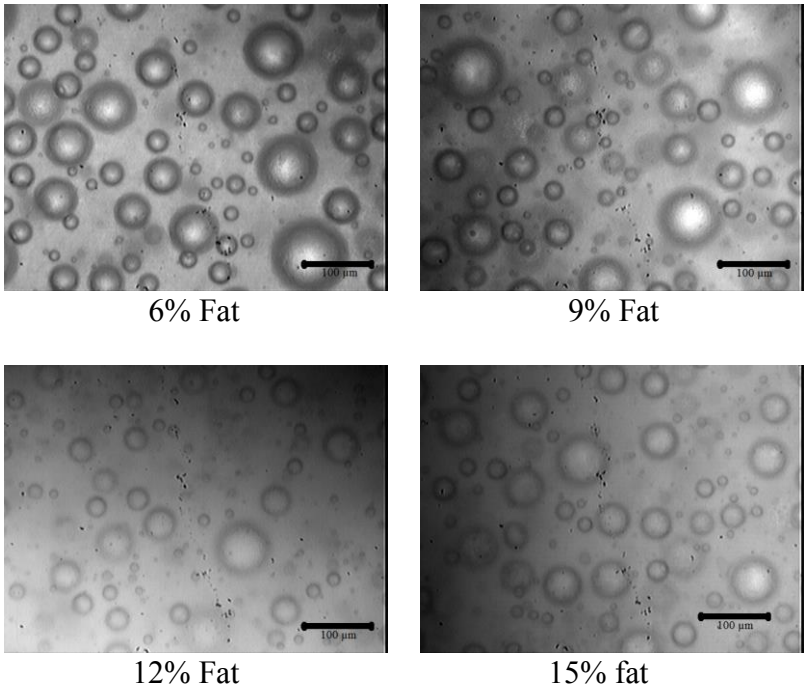

Figure 4.41: Microscope images of air cells for ice creams made with 6%, 9%, 12%, and 15% fat at 80:20 (mono- and diglyceride:polysorbate 80 (MDG:PS80) emulsifier ratio, 500 RPM, and 50% overrun (40x magnification, 100 µm scale bar).

4.3.4 Drip-through Rate

Drip-through rates ranged from 0.22 to 0.35 g/min across fat contents. Previous findings in literature indicated that the lower the total fat, the lower the amount of partially-coalesced fat formed and thus, the slower the drip-through rate (Hinrichs and Kessler, 1997; Walstra, 2003). In this study, a statistically significant difference was determined between fat contents for drip-through rates ($p < 0.0001$). A Tukey's HSD test indicated statistically significant differences between fat contents of 9% and 15%, 9% and 12%, and 6% and 15% (**Table 4.9** and **Figure 4.42**). However, utilizing the multivariate pairwise comparison test, no statistically significant relationship was determined between drip-through rate and partial coalescence ($p = 0.3318$). This statistical finding is evident in ice cream with 6% fat content. Although with lower amount of PC (14.4%), ice creams made with 6% fat had the same drip-through rate as ice creams with higher fat content (**Table 4.9** and **Figure 4.42**). Although not clear, this finding could be related to findings by Koxholt et al. (2001) in which the drip-through rate depended on the critical fat globule diameter and the width of the foam lamellas. In this study, it was shown that if partially-coalesced fat reached a size larger than the width of the foam lamellas, the partially-coalesced fat would be blocked by the air cells. Both the air cells and the partially-coalesced fat would block the drainage of free water and diluted serum phase. As a result, much remnant foam would be present at the end of the drip-through test and a slow drip-through rate would occur. As seen in **Section 4.2.2**, all ice creams processed at 50% overrun and 500 RPM had slow and similar drip-through rates. The combination of 80:20 (MDG:PS80) emulsifier ratio, 50% overrun, and 500 RPM must provide small enough space between the foam lamellas that caused a build up in structures to resist drip and collapse, regardless of fat content and PC. As a result, all four ice creams, despite the different fat contents, had a significant remnant foam left

atop the screen (**Figure 4.43**). Furthermore, neither mean ice crystal size (p = 0.9448) nor mean air cell size (p = 0.1645) were determined to have a statistically significant relationship on drip-through rate for ice creams made with different fat contents.

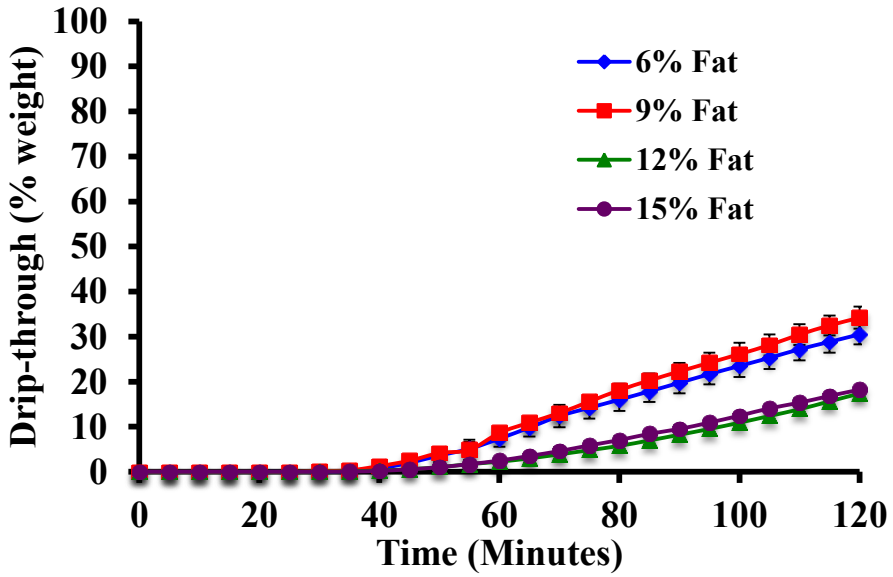

Figure 4.42: Drip-through curves (% weight) for ice creams made with 6%, 9%, 12%, and 15% fat at 80:20 (mono- and diglyceride:polysorbate 80 (MDG:PS80) emulsifier ratio, 500 RPM, and 50% overrun. The error bars represent the standard deviations of the mean drip-through rates measured for each fat content.

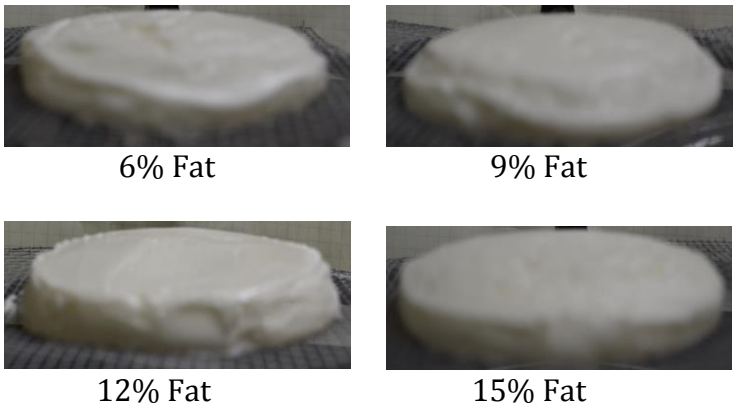

Figure 4.43: Images of remaining ice cream structure left on top of screen at the end of a drip-through test of ice creams made with 6%, 9%, 12%, and 15% fat. Ice creams were processed at 500 RPM and 50% overrun.

4.4 Melt Behavior of Ice Cream

From both the survey on United States commercial ice creams and the study where parameters were controlled, understanding the driving factors that influence drip-through rate would be of great interest. Numerous aspects of the microstructure affect drip-through rate, including those that affect heat transfer, those that affect melting, and those that affect the ability of the melted structure to flow under the pull of gravity. In general, during the drip-through test, a slab of ice cream is set on a mesh screen at ambient temperature and allowed to melt. Heat transfers from the ambient air at room temperature into the ice cream. The increase in temperature due to the heat transfer causes the ice at the surface to melt, generating a cooling effect (latent heat) that slows further heat penetration. The interior of the slab of ice cream gradually warms up, depending on the thermal diffusivity of the matrix.

As the ice melts, the free water combines with the viscous serum phase, causing dilution of the serum. As this occurs, the liquid serum begins to flow down through the matrix of air

cells (between the lamellae), fat globules, partially-coalesced fat globules, and unmelted ice crystals due to natural gravitational force. When sufficient serum reaches the screen, the first drips pass through the mesh (onset of drip-through). Drip-through continues at approximately a constant rate until gradually flow subsides. Some ice creams completely drip-through the mesh screen, leaving no residual of melted ice cream on the screen (**Figure 4.44**). Ice creams like this have 100% change in height (0% height at end of drip-through test) during the drip-through test. Other ice creams exhibit minimal drip-through and leave significant remnant foam atop the screen at the end of the drip-through test, appearing not to melt (**Figure 4.45**). These ice creams have minimal change in height during the drip-through test, leaving a densely packed structure on the screen comprised of air cells and fat globules that prevent further drainage of the serum through the lamellae. Most ice creams fall between these two ends of the drip-through spectrum.

There are many factors that affect how ice cream will melt. Fat, air, ice crystals, the serum phase, and thermal properties (affected by the microstructure matrix) of the ice cream all contribute to the drip-through rate of ice cream. The effects of each of these components are outlined in the sections below.

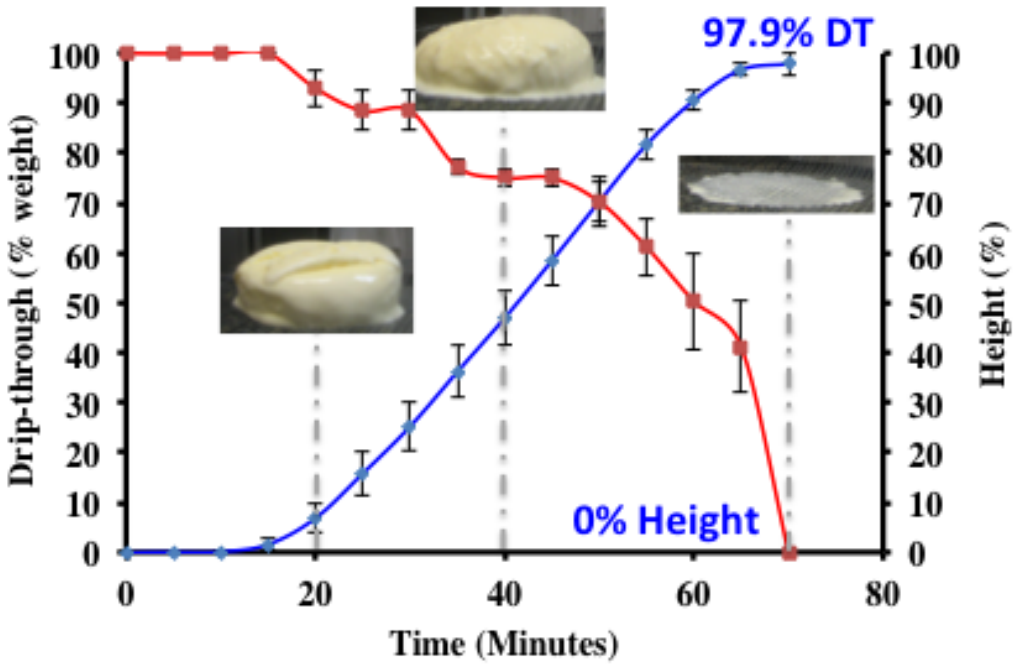

Figure 4.44: Drip-through (% weight) curve (97.9% of sample drip-through (DT) mesh screen) and curve of change in height during the drip-through test for an ice cream with a fast drip-through rate and minimal residual left atop the screen at the end of the drip-through test.

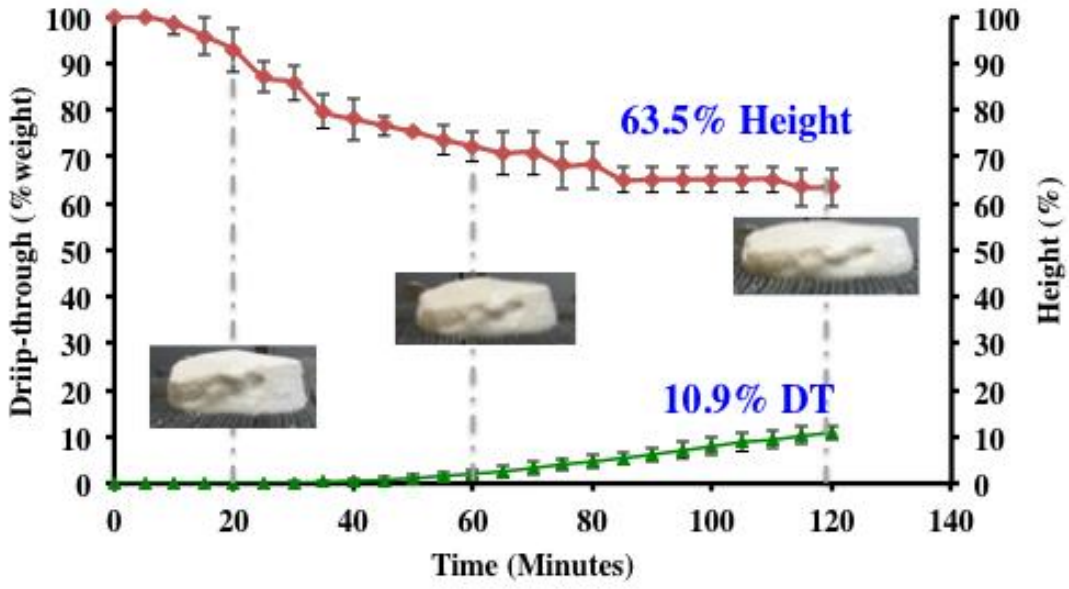

Figure 4.45: Drip-through (% weight) curve (10.9% of sample drip-through (DT) mesh screen) and curve of change in height during the drip-through test for an ice cream with a slow drip-through rate and a large amount of remnant foam left atop the screen at the end of the drip-through test.

4.4.1 Factors that Affect Melt Behavior of Ice Cream

4.4.1.1 Thermal Diffusivity

Thermal diffusivity, the ability for heat to penetrate into the ice cream, is the first parameter to affect drip-through rate. It is influenced by the microstructure of the ice cream, particularly air (overrun and air cell size distribution) and ice (ice content and ice crystal size distribution). Goff and Hartel (2013) indicated that an increase in both the number and dispersion of ice crystals and air cells are expected to reduce thermal diffusivity, and therefore, reduce the onset of drip and the drip-through rate. Typically, high thermal diffusivity (rate of heat transfer) results in a quicker onset of melting and fast drip-through rate. Thermal diffusivity was not specifically studied in either the survey of United States commercial ice creams or the controlled ice cream study, but undoubtedly varied based on the differences in the ice and air phases across the products studied.

4.4.1.2 Serum Phase

Viscosity of the serum phase can also affect the drip-through rate of ice cream products. An increase in viscosity can occur from an increase in fat content, hydrocolloids (stabilizers), and protein content. The viscosity of the serum phase has been noted to have an effect on the drip-through rate of ice cream products with higher mix viscosities giving slower drip-through rates (Muse and Hartel, 2004). It takes longer for a more viscous fluid to flow through the matrix of air cells and fat/partially-coalesced fat globules. Although an increase in protein

content has been noted to increase mix viscosities, Daw and Hartel (2015) determined that this increase in viscosity was protein source dependent. Further, as protein content increased drip-through rates also increased, contrary to the expected trend.

In the survey, viscosities were not measured, but it can be assumed that the viscosities of the commercial ice creams differed as various stabilizers were used to produce those ice cream products. No relationship between viscosity of the mix and drip-through rate could be determined from the survey study, however, as the mix was not available. In the controlled ice cream study, it was assumed that the viscosities were generally the same (except in the fat content (**Section 4.3.3**)) and did not affect the rate of drip.

4.4.1.3 Ice

Ice crystals are an important factor that influences ice cream melting and drip-through rate. Ingredients, processing conditions, and storage can all affect the ice crystal size and the ice phase volume. As a result, the rate of heat transfer into the ice cream is a function of the ice crystal phase (size and phase volume). In general, as the heat transfers into the ice cream, the ice begins to melt, as previously described. However, the rate of melt depends on the size and quantity of ice (ice phase volume). It has been suggested that large ice crystals lead to faster drip-through rate (Muse and Hartel, 2004). This was attributed to the path of flow of melted ice cream (Hartel et al., 2003). It was suggested that with many small ice crystals, the serum phase has more obstacles (numerous ice crystals) to flow through as the ice begins to melt and dilute the serum phase. As a result, the drip-through rate was slower with many smaller ice crystals (Muse and Hartel, 2004). The ice phase volume can also influence the rate of melt. According to Goff and Hartel (2013) an increase in the ice phase volume will lead to a decrease in the drip-

through rate, due to the increase in the number of ice crystals and in surface area. However, Muse and Hartel (2003) did not find ice content to influence rate of melt. The influence of ice phase volume may vary depending on other microstructure components and their interactions.

For the controlled ice cream samples, there was only an 8.5 μm difference in mean ice crystal size between samples and no difference in ice content. As a result, the effect of ice crystal size on drip-through rate was very minimal as the difference between ice crystals was small ($p = 0.0544$) when looking at the effect of emulsifier ratio, dasher speed, and overrun on ice crystal size (**Section 4.2.4**). In addition, for the change in fat content study, ice crystals did not have an effect on drip-through rate ($p = 0.9448$) (**Section 4.3.4**). However, there was a 40.8 μm difference in ice crystal size in the survey of United States commercial ice cream and a statistical correlation was found between ice crystal size and drip-through rate. Ice crystal size had an inverse relationship with drip-through rate ($p < 0.01$) as noted in **Section 4.1.1.2**. One sample that followed this trend was sample 159. It had the smallest mean ice crystal size (26.3 μm) and one of the fastest drip-through rates (1.85 g/min). This sample completely dripped through the mesh screen (100% change in height and 98.2% of sample dripped through) (**Figure 4.46**).

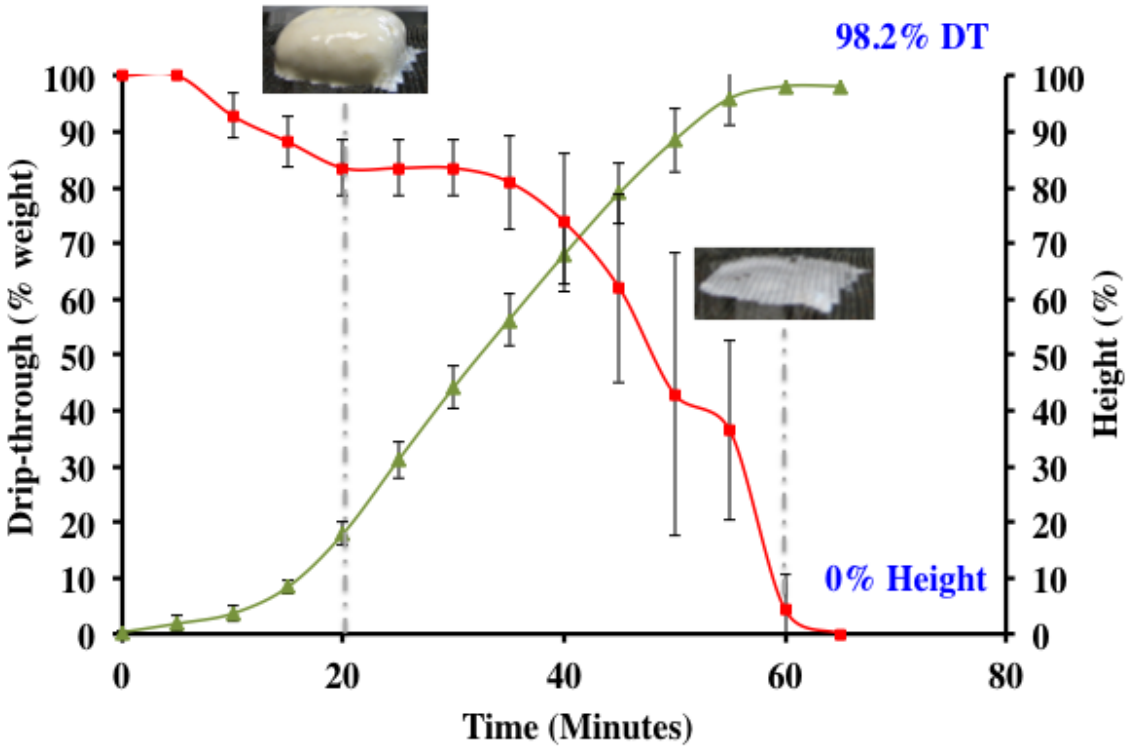

Figure 4.46: Drip-through (% weight) curve (98.2% of sample drip-through (DT) mesh screen) and curve of change in height (100% change in height) during the drip-through test for sample 159 with a fast drip-through rate and minimal residual left atop the screen at the end of the drip-through test.

Sample 880 had the largest ice crystals (67.1μm) and the slowest drip-through rate (0.13 g/min) from the samples surveyed (**Table 4.2**). The drip-through (% weight) and the percent change in height (10.9% drip-through and 63.5% change in height), as seen in **Figure 4.45**. This does not fit the findings of Muse and Hartel (2004). In this study, it was indicated that the flow of the diluted serum (effect from ice crystal size)

rather than the differences in heat transfer influenced the rate of melt. Much of this can be attributed to other components of the microstructure affecting the rate of drip, not just the size of ice crystals.

4.4.1.4 Fat

Fat provides body and texture to ice cream and also plays a critical role in the melt behavior. In general, ice creams containing small and few partially-coalesced fat globules (small clusters) tend to drip-through quickly while those with large and many partially-coalesced fat globules (large clusters) tend to have a slower drip-through rate with more remnant foam at the end of the drip-through test (Berger and White, 1971; Berger et al.,1972; Segall and Goff, 2002; Muse and Hartel, 2004). These clusters play an important role as the diluted serum begins to drain through the lamellae as ice melts. Individual fat globules and small clusters would drain along with the serum. Large clusters would tend to jam more readily, providing a physical barrier to further drainage.

In both the survey of United States commercial ice cream samples and in the controlled ice cream study, most ice creams, but not all, followed this general trend. For instance, from the survey, sample 638 (**Figure 4.44**) had a fast drip-through rate (1.72 g/min) with 97.9% of the product drip-through the screen. In this case, there were an insufficient number of large fat clusters to prevent drainage (5.0% partially-coalesced fat), as shown schematically in **Figure 2.9**. The particle size distribution curves further supported this as the drip-through (the portion of the ice cream that dripped through the mesh screen during the drip-through test) and whole melt (melted ice cream) curves had very similar particle size distributions (**Figure 4.47**). The remnant foam, what little there was, contained only a few clusters.

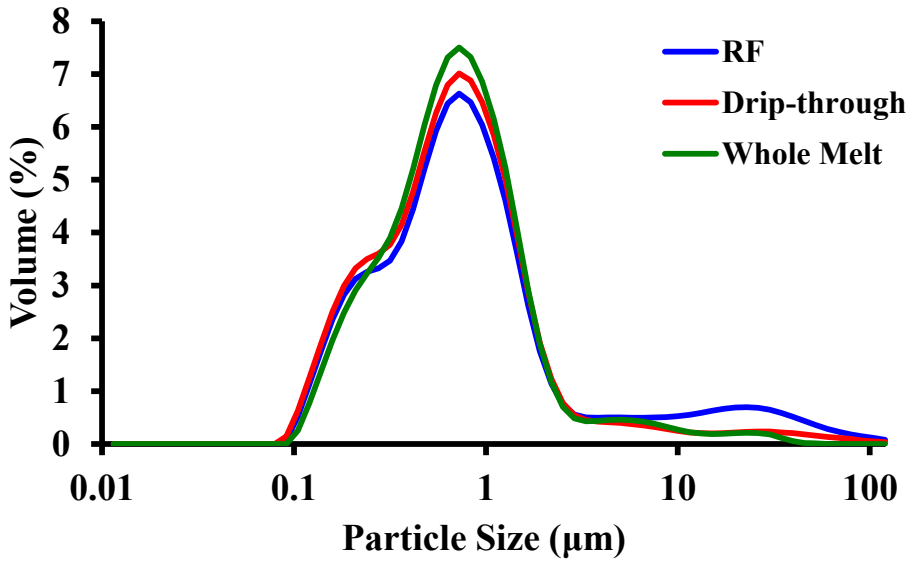

Figure 4.47: Particle size distribution curves representing the Remnant Foam (RF), Drip-through, and Whole Melt portions of sample 638.

Sample 880 from the survey on United States commercial ice creams is an example of an ice cream with large percentage of partially-coalesced fat globules (40.4%) and a slow drip-through rate (0.13 g/min). This occurrence can most likely be attributed to the large size (67.6 µm) of the partially-coalesced fat in the product, which was too large to flow between the lamellae and other partially-coalesced fat globules. At the end of 120 minutes of the drip-through test, all of the ice was melted into water, yet 89.1% of that product stayed in the remnant foam with only 10.9% of the product dripping through the screen (**Figure 2.10** and **Figure 4.45**). **Figure 4.48** shows the particle size distributions for the remnant foam (RF), melted ice cream (Whole Melt), and the portion of sample that dripped through the mesh screen (Drip-through). As indicated by the Drip-through and RF curves, the majority of the partially-coalesced fat globules were left in the remnant foam (RF), and what little dripped through contained almost none.

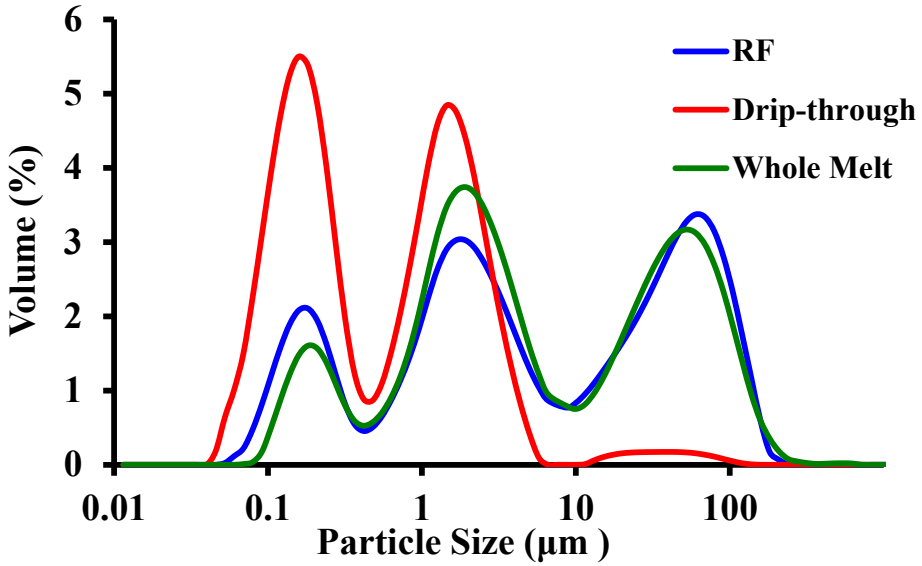

Figure 4.48: Particle size distribution curves representing the Remnant Foam (RF), Drip-through, and Whole Melt portions of sample 880.

There were, however, ice creams that did not follow this general trend. For example, from the survey, sample 215 only had 7.8% partially-coalesced fat with an average cluster size of 21.4 µm. With this low amount of partially-coalesced fat globules, it may have been expected that sample 215 would have a fast drip-through rate (0.67 g/min). From the particle size curves in **Figure 4.49**, the remnant foam (RF) contained more partially-coalesced fat globules than the melted ice cream (Whole Melt) and more than the product that dripped through the mesh screen (Drip-through). These particle size curves confirm the theory that fat globules were held up and not able to flow and drip out of the ice cream, despite the small percentage of partially-coalesced fat. **Figure 4.50** displays the percent change in height and drip-through (% weight) curve during the drip-through test for sample 215. At the end of the drip-through test, 54.5% of the sample had dripped-through the screen and there was a 47.0% change in height. From the remnant foam

particle size curve, it can be seen that very large partially-coalesced fat globules (210 µm average size) were left atop the screen at the end of the drip-through test (**Figure 4.49**). These particles, which were more concentrated in the remnant foam, were too large to drip-through the lamellae, despite the small amount of partially-coalesced fat found in the ice cream (whole melt).

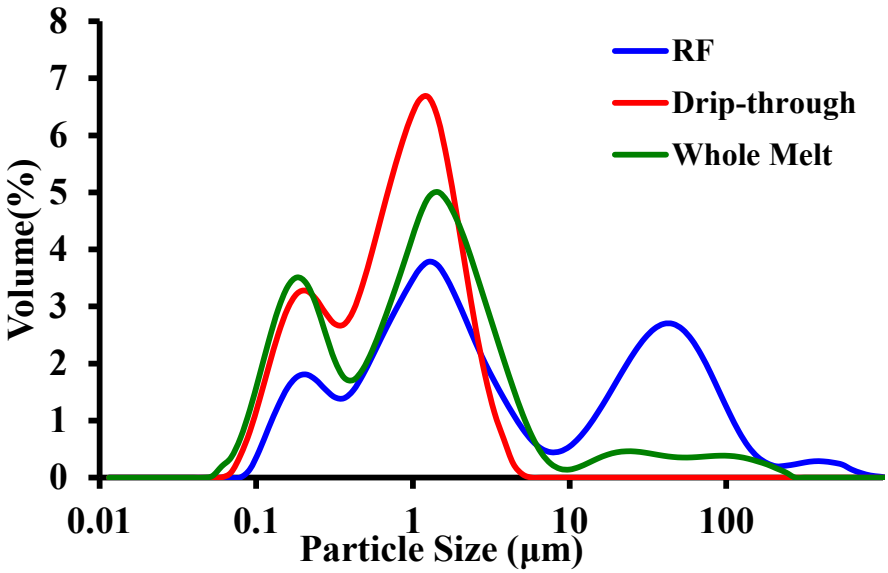

Figure 4.49: Particle size distribution curves representing the Remnant Foam (FR), Drip-through, and Whole Melt portions of sample 215.

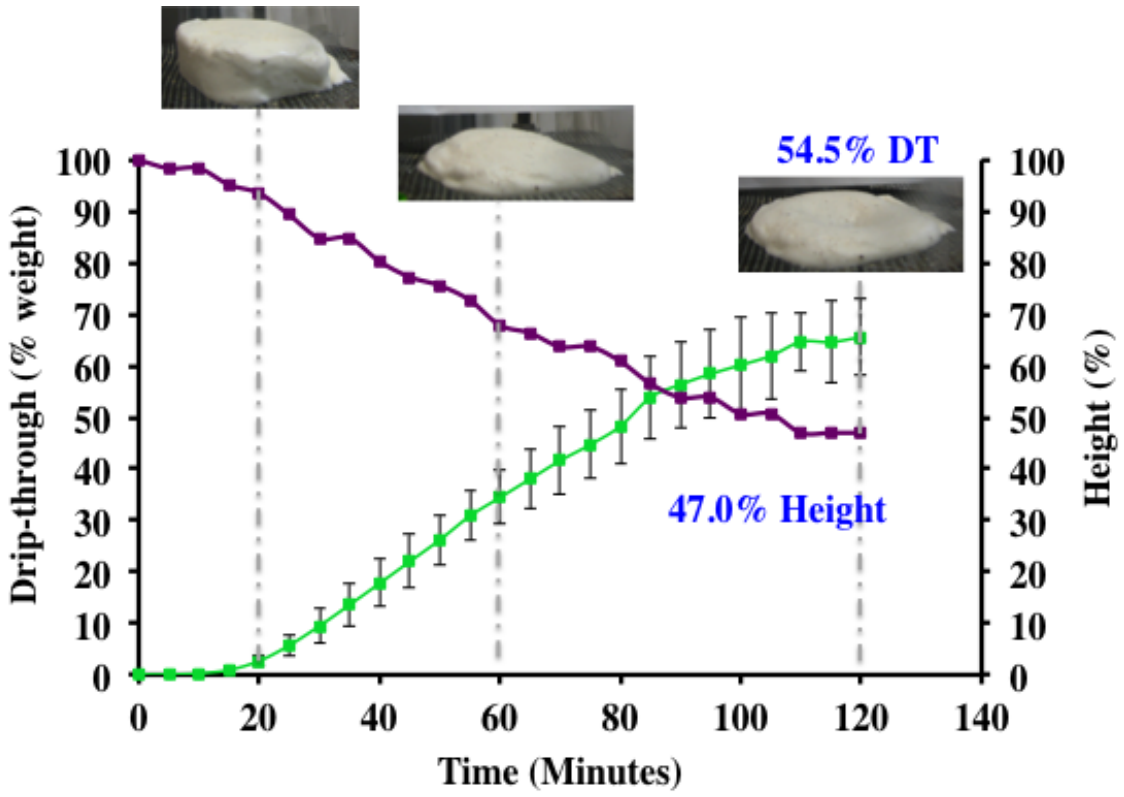

Figure 4.50: Drip-through (% weight) curve (54.5% of sample drip-through (DT) mesh screen) and curve of change in height (47.0% change in height) during the drip-through test for sample 215 with a fast drip-through rate and minimal residual left atop the screen at the end of the drip-through test.

4.4.1.5 Air

During the continuous freezing process, air is injected into ice cream, typically targeting a specific overrun. Air is an insulator and as a result it influences the rate at which ice cream melts. An increase in air (higher overrun) results in an increase in insulation in the ice cream and a decrease in thermal diffusivity (Goff and Hartel, 2013). As a result, it is expected that with an increase in overrun, there is a decrease in time for onset of drip and drip-through rate, as seen by Sofjan and Hartel (2003) and Sakurai et al. (1996). In addition, an increase in overrun causes a

decrease in the thickness of the lamellae, the space between the air bubbles. With higher overrun, there are more air cells in a given volume causing the air cells to be closer together, shrinking the lamellae.

From the survey on United States ice creams, overrun was not was not found to have a correlation with drip-through rate ($p = 0.5757$). However, there were some samples that fit the expected trend (higher overrun, slower drip-through rate). For example, sample 652 from the survey on United States commercial ice creams is an example of an ice cream with high overrun (72.2%) and a drip-through rate of 0.44 g/min. Sample 313 had a low overrun (26.9%) and a drip-through rate of 1.40 g/min (**Table 4.2**).

In the controlled ice cream study, there were many samples that also fit this trend. For instance, utilizing one-way ANOVA ($\alpha = 0.05$), the ice creams made with no added emulsifiers were found have a statistically-significant correlation with drip-through rate ($p < 0.0001$). Ice cream processed at 750 RPM and 50% overrun had a drip-through rate of 1.13 g/min. It is assumed that once ice began to melt, it mixed with and diluted the serum phase. The diluted serum phase then flowed through the matrix of the ice cream via natural gravitational force. There was limited structure holding up the flow of the diluted serum phase and as a result, little remnant foam was left atop the screen (**Figure 4.31a**). It can be assumed that the matrix of the air cells and fat globules did not hinder the flow, similar to sample 638 in the survey study. However, with an increase in overrun, large differences in the drip-through rate were observed. For example, ice cream made with no added emulsifiers at 750 RPM and 100% overrun had a drip-through rate of 0.29 g/min, similar to sample 652 from the survey. As described above, the ice began to melt and mix with and dilute the serum phase. However, unlike the 50% overrun samples with no added emulsifiers, a large amount of remnant foam was

left atop at the end of the drip-through test. In this case, the serum phase was not able to flow through the microstructure components, which were composed of air cells, partially-coalesced fat, and fat globules (shown schematically in **Figure 2.10)**. This matrix greatly hindered the serum flow due to the size, arrangement, and quantity of components. There were a sufficient number of particles larger than the gap between the lamellae, resulting in particles jamming together at the start of collapse, preventing any further collapse of the product. As a result, the majority of the partially-coalesced fat globules stayed in the remnant foam as seen in the particle size curves of the portions of the drip-through test (**Figure 4.51**). The majority of the ice cream products produced in this study had similar melt behaviors, including ice creams made with no added emulsifiers at 75% overrun. **Figure 4.52** shows the particle size curves of the portions of the drip-through test for an ice cream made with 90:10 (mono- and diglyceride:polysorbate 80 - MDG:PS80) at 750 RPM and 75% overrun. This sample had larger particles in the remnant foam (RF) than that in **Figure 4.51**, but resulted in similar melt behavior.

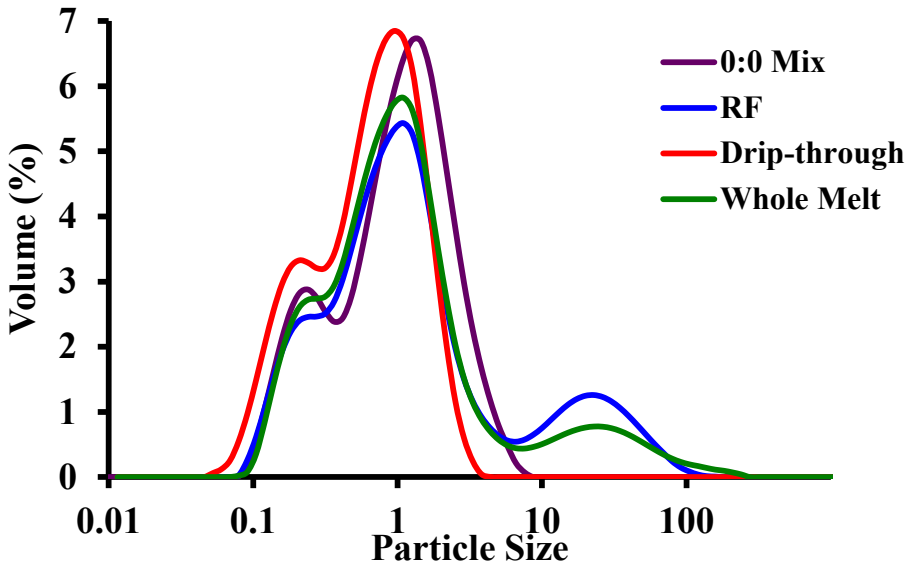

Figure 4.51: Particle size distributions for ice cream mix made with no added emulsifiers and curves representing portions from the drip-through test (Remnant Foam (FR), Drip-through, and Whole Melt) from ice cream processed at dasher speed of 500 RPM and 100% overrun.

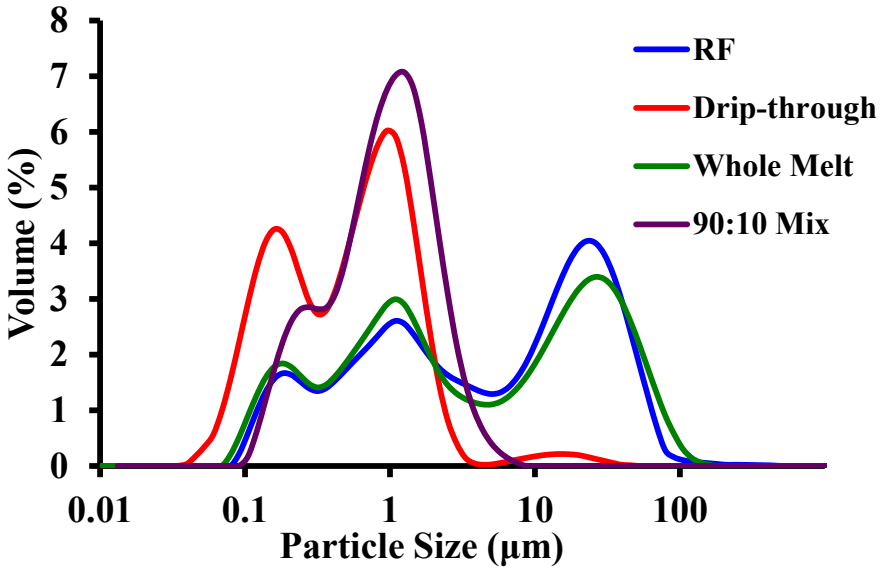

Figure 4.52: Particle size distributions for ice cream mix made with 90:10 (mono- and diglyceride:polysorbate 80 - MDG:PS80) emulsifier ratio and curves representing portions from the drip-through test (Remnant Foam (FR), Drip-through, and Whole Melt) from ice cream processed at dasher speed of 750 RPM and 75% overrun.

There were also samples that did not follow this trend. For example, sample 638 (**Figure 4.44** and **Figure 4.47**) actually had high overrun (97.5%) but had a fast drip-through rate (1.72 g/min) as previously indicated. Despite the high overrun, the rate of drip was driven more by the small partially-coalesced fat globules (2.9 μm average cluster size) than the effect of thermal diffusivity for this sample. It can be assumed that the gap between the lamellae were large enough that once the ice started to melt, the free water was able to diffuse into and dilute the serum phase, it was able to flow through the matrix of the microstructure.

4.4.2 Predicting Drip-Through Rate

As described in the sections above, there were ice creams that followed the expected trends in drip-through based on their microstructure components, but there were also samples that did not follow the expected trends. This made understanding and predicting drip-through rate difficult since there were various factors that interacted to influence the rate of drip as described in **Section 5.4.2.1**. For example, even though a sample had high overrun, fast drip-through rate might occur if it had either no partial coalescence (intact fat globules) or small partially-coalesced fat globule clusters. Furthermore, even though a sample had low amounts of partially-coalesced fat, slow drip-through rate might occur if it had high overrun (small spaces between the lamellae). Thus, it is difficult to predict drip-through rate as a slight change in the microstructure could alter the influences on drip-through rate, even in the controlled ice cream study.

5. Conclusions and Recommendations

5.1 Survey of United States Commercial Ice Cream Products

From the survey, it is clear that there exists a wide range of compositional and structural attributes in the United States commercial ice cream products that were analyzed. Some instrumental measurements were good predictors and indicators of sensorial attributes of ice cream products. Overrun and mean air cell size distribution were good predictors of breakdown and denseness while percent fat destabilization was a good indicator of greasiness. Total fat content and percent fat destabilization were also good predictors of the overall perception of creaminess. However, not all physical and compositional attributes correlated with the sensorial measurements; for example, mean ice crystal size and iciness or drip-through rate and melt rate. In general, full fat ice creams were only distinguishable from the low fat and nonfat products by their fat content and percent destabilized fat. There were numerous interdependent components within the structural, compositional, and sensorial properties that make it difficult to determine how ice cream products will behave, regardless of the fat phase. This present work proves that the interactions between physical and compositional parameters cause complexities in understanding the influences on the behavior of ice cream products. There is potential for greater knowledge of these interactions and how ice cream products are perceived in terms of sensory, by understanding the complete relationship between physical and compositional parameters and sensory attributes.

5.2 Effect of Dasher Speed, Overrun, and Emulsifier Ratio on Microstructure and Physical Properties of Ice Cream

5.2.1 Ice Crystals

Since ice creams were frozen to a similar draw temperature (-6.1±0.1^{o}C), it was not expected for there to be statistical differences in ice crystals as dasher speed, overrun, and emulsifier ratios changed. However, statistical differences were determined in ice crystals sizes for ice creams made with 80:20 (MDG:PS80) at 75% and 100% overrun as dasher speed increased. In addition, significant differences in ice crystal sizes were noted as overrun increased for ice creams made with no added emulsifiers at 500 RPM and at 250 RPM for ice creams made with 80:20 (MDG:PS80). These differences, although statistically significant, were very small. Controlling the draw temperature during freezing allowed for the control of ice crystal sizes, despite the increase in dasher speed and overrun.

5.2.2 Partial Coalescence (PC)

In the controlled ice cream study, it was determined that partial coalescence increased with an increase in dasher speed, overrun, the addition of emulsifiers, and an increase in PS80. This follows the expected trends previously observed by Goff, 1997; 2002; Goff and Hartel, 2013; Walstra, 2003; Goff et al. (1987), Gelin et al. (1994), Gelin (1996a, b), Goff and Jordan (1989), Pelan et al. (1997), Tharp et al. (1998), Thomsen and Holtsborg (1998), Goff et al.

(1999), and Bolliger et al. (2000). In general, ice creams with no added emulsifiers had the lowest amounts of partially-coalesced fat while ice creams made with 80:20 (MDG:PS80) had the highest amounts of partially coalesced fat.

5.2.3 Air Cells

In this study, the direct effect of dasher speed and overrun on air cell size was not determined as the sizes of air cells were measured on hardened ice cream products not at draw. However, it was determined that smaller air cells were found with an increase in partially-coalesced fat, in general. As dasher speed increased, no statistically significant correlation was determined in mean air cell sizes for ice creams made with no added emulsifiers or 100:0 (MDG:PS80). However, with the addition of PS80, dasher speed was noted to have a significant effect on air cell size. Although emulsifiers were not thought to affect air cell sizes during the freezing process, in this study, air cell sizes significantly decreased in hardened ice creams with the addition of PS80. This can be attributed to an increase in partial coalescence, inhibiting air cells from coalescing during the hardening process, as observed by Chang and Hartel (2002a). Significant differences between mean air cell size as overrun increased was also observed, mostly between the 50% overrun when compared to 75% and 100% overrun settings. This trend was generally seen across emulsifier ratios and dasher speeds.

5.2.4 Drip-through Rate

Drip-through rate could not be predicted or controlled in this study. In addition, the range in drip-through rates was not as large as expected in this study. Much of this is due to the combination of the parameters set and the freezer utilized. In general, the melt behavior of ice

cream products did not correlate with partial coalescence. This is likely because of other microstructure components and their interactions that govern melt behavior (overrun, air cell size, number density of air cells and partially-coalesced fat). Ice creams produced with no added emulsifiers and 100:0 (MDG:PS80) at 50% overrun across all dasher speeds had the fastest drip-through rates. This is most likely due to the limited build up of structure in these ice creams.

In general, the effect of dasher speed on drip-though rate was not significant across emulsifier ratios and overrun. Ice creams made with 75% and 100% overrun had the slowest drip-through rates, regardless of dasher speed and emulsifier ratio. For 50% overrun, the addition of PS80 resulted in slower melting rates, although, at 75% and 100% overrun, this effect was not seen. Ice creams with faster drip-through rates also had less remnant foams left atop the screen at the end of the drip-through test. As expected, more remnant foam was seen in ice creams with slower drip-through rates.

5.3 Fat Content Experiment

An increase in fat content did not lead to a decrease in drip-through rate as expected. This can be attributed to drip-through rate being influenced by the lamella size more so than the amount of fat present in the system.

An increase in fat content only led to an increase in partial coalescence between 6% and 9% fat and not between 9%, 12%, and 15% fat. This is likely due to two competing factors during freezing. Since more fat results in less water (decrease in ice content during freezing) these products under went less shear during freezing. On the other hand, ice cream with higher fat had higher collision rates (phase volume effect) of fat globules during freezing. It would be

expected that partial coalescence increased with an increase in fat content due to the phase volume effect. On the other hand, partial coalescence would be expected to decrease with an increase in fat content due to the reduction in shear.

5.4 Recommendations

Controlling melt behavior was difficult in this study due to the manufacturing parameters used during freezing. Future work in this area could better describe drip-through rate with a broader range of parameters used. The results from this experiment were freezer dependent, as a result, utilizing a different scraped surface heat exchanger could also produce a range of different results that could better describe the physical and transport properties of ice cream melting. In addition, the standard drip-through test, which has been used and accepted for years, may need to be revaluated as it does not correlate with the effects of melt rate in the mouth. Also, there might be other factors affecting melt that the drip-through test does not clearly show. Utilizing scanning electron microscopy (SEM), magnetic resonance imaging (MRI), and/or x-ray tomography to see inside of ice cream could lead to better understanding of the space between the lamellae and the possible influence of the lamella during melt. Furthermore, much work has focused on the effect of fat globules and partially-coalesced fat on drip-through rate. Additional research needs to be done on the effect of air cells (number density, size, etc.), in combination with partial coalescence, on drip-through rate. Furthermore, the impact of the microstructure on thermal diffusivity is not widely understood and should be further studied to better understand

drip-through rate. Further research in these areas would help with better understanding the effect of the microstructure and their interactions on drip-through rate as well as provide information to develop and more concrete model of melting.

References

Adleman, R., Hartel, R.W. 2001. Lipid crystallization and its effect on the physical structure of ice cream. In: Garti, N., Sato, K. (eds) **Crystallization processes in fats and lipid systems**. Marcel Dekker, New York, NY. pp 381–427.

Aime, D.B., Arntfield, S.D., Malcolmson, L.J., Ryland, D. 2001. Textural analysis of fat reduced vanilla ice cream products. Food Research International. 34(2–3):237–46.

Arbuckle, W. S. 1977. **Ice Cream. 3rd ed**. Avi Publisher Company. Westport, CT.

Arbuckle, W.S. 1986. **Ice Cream. 4th ed.** AVI Publishing Company, Westport, CT.

Barfod, N.M., Krog, N., Larsen, G., Buchheim, W. 1991. Effects of emulsifiers on protein-fat interaction in ice cream mix during aging. Fat Science Technology. 93:24–35.

Berger, K. G. 1997. Ice Cream. In: Friberg, S.E., Larsson, K. (eds) **Food Emulsions. 3rd ed**. Marcel Dekker, Inc., New York, NY. pp 413-490.

Berger, K.G., Bullimore, B.K., White, G.W., Wright, W.B. 1972. The structure of ice cream. Dairy Industries. 37:419–425, 493–497.

Berger, K.G., White, G.W. 1971. An electron microscopical investigation of fat destabilization in ice cream. Journal of Food Technology. 6: 285–294.

Bolliger, S., Goff, H.D., Tharp, B.W. 2000. Correlation between colloidal properties of ice cream mix and ice cream. International Dairy Journal. 10:303–309

Boode, K. 1992. Partial Coalescence in Oil-in-Water Emulsions, Ph.D. Thesis. Wageningen, Agricultural University.

Brooker, B. E., Anderson, M., Andrews, A. T. 1986. The development of structure in whipped cream. Food Microstructure. 5:277–285.

Campbell, I.J., Pelan, B.M.C. 1998. The influence of emulsion stability on the properties of ice cream. In: Buchheim, W. (eds), **Ice Cream**. Proceedings of the International Symposium held in Athens, Greece, 19-19 September 1997. Brussels, Belgium: International Dairy Federation. pp 25-36.

Chang, Y., Hartel, R.W. 2002a. Development of air cells in a batch ice cream freezer. Journal of Food Engineering. 55:71-78.

Chang, Y., Hartel, R.W. 2002b. Measurement of air cell distribution in dairy foams. International Dairy Journal. 12:463-472.

Chang, Y., Hartel, R.W. 2002c. Stability of air cells in ice cream during hardening and storage. Journal of Food Engineering. 55:59–70.

Code of Federal Regulations. 2014.Title 2 Food and Drugs, Part 135 Frozen Desserts.

Conforti FD. 1994. Effect of fat content and corn sweeteners on selected sensory attributes and shelf stability of vanilla ice cream. Journal of Dairy Technology. 47:69–75.

Cook, K.L.K., Hartel, R.W. 2010. Mechanisms of ice crystallization in ice cream production. Comprehensive Review Food Science Food Safety. 9(2):213–22.

Daw, E., Hartel, R.W. 2015. Fat destabilization and melt-down of ice creams with increased protein content. International Dairy Journal. 43:33-41.

Dickinson, E. 1993. In: Goddard, E.D., Ananthapadmanabhan, K.P. (eds.), **Interactions of Surfactants with Polymers and Proteins**. CRC, Boca Raton, FL, pp. 295.

Donhowe, D.P., Hartel, R.W., Bradley, R.L. 1991. Determination of ice crystal size distribution in frozen desserts. Journal of Dairy Science. 74: 3334-3344.

Drewett, E.M., Hartel, R.W. 2007. Ice crystallization in a scraped surface freezer. Journal of Food Engineering. 78:1060-1066.

Eisner, M.D., Wildmoser, H., Windhab, E.J. 2004. The different role of emulsifiers in conventionally freezered and ultra-low-temperature-extruded ice cream. In Tharp, B., editor. Ice cream II. Proceedings of the 2nd IDF International Symposium on Ice Cream; 2003 May 14–16; Thessaloniki, Greece, pp. 178–89.

Ergun, R. 2011. Fat crystallization and mechanism of partial coalescence. Ph.D. Thesis. University of Wisconsin-Madison.

Flores, A. A., Goff, H. D. 1999. Ice crystal size distributions in dynamically frozen model solutions and ice cream as affected by stabilizers. Journal of Dairy Science. 82:1399–1407.

Fredrick, E., Walstra, P., Dewettinck, K. 2010. Factors governing partial coalescence in oil-in-water emulsions. Advances in Colloid and Interface Science. 153:30-42.

Gelin, J.-L., Poyen, L., Courthadon, J. -L., Le Meste, M., Lorient, D. 1994. Structural changes in oil-in-water emulsions during the manufacture of ice cream. Food Hydrocolloids. 8:299-308.

Gelin, J.-L., Poyen, L., Rizzotti, R., Le Meste, M., Courthadon, J.-L., & Lorient, D. 1996a. Interactions between food components in ice cream. Part 1. Unfrozen emulsions. Food Hydrocolloids. 10:385-393.

Gelin, J.-L., Poyen, L., Rizzotti, R., Dacremont, C., Le Meste, M., & Lorient, D. 1996b. Interactions between food components in ice cream. Part 2. Structure-texture relationships. Journal of Texture Studies. 27:199-215.

Giermanska, J., Thivilliers, F., Backov, R., Schmitt, V., Drelon, N., Leal-Calderon, F. 2007. Gelling of Oil-in-Water Emulsions Comprising Crystallized Droplets. Langmuir. 23:4792-4799.

Goff, H.D. 1992. Examining the milk solids-not-fat in frozen dairy desserts. Modern Dairy. 7(3):16-17.

Goff, H.D. 1997. Colloidal aspects of ice cream—a review. International Dairy Journal 7:363–373.

Goff, H.D. 2002. Formation and stabilisation of structure in ice cream and related products. Current Opinion Colloid Interface Science. 7:432–437 .

Goff, H.D., Davidson, V.J., Cappi, E. 1994. Viscosity of Ice Cream Mix at Pasteurization Temperatures. Journal of Dairy Science. 77(8): 2207 – 2213.

Goff, H.D., Hartel, R.W. 2013. **Ice Cream**. 7th ed. Springer, New York, NY.

Goff, H.D., Liboff, M., Jordan, W.K., Kinsella, J.E. 1987. The effects of Polysorbate 80 on the fat emulsion in ice cream mix: evidence from transmission electron microscopy studies. Food Microstructure. 6:193–198.

Goff, H.D., Jordan, W.K. 1989. Action of emulsifiers in promoting fat destabilization during the manufacture of ice cream. Journal of Dairy Science. 72:18–29.

Goff, H. D., Vega, C. 2007. Structure-engineering of ice-cream and foam-based foods. In: D. J. McClements, D.J. (ed.), **Understanding and Controlling the Microstructure of Complex Foods**. CRC Press, Boca Raton, FL, pp. 557-574.

Goff, H. D., Verespej, E., Smith, A. K. 1999. A study of fat and air structures in ice cream. International Dairy Journal. 9:817–829.

Govin, R., Leeder, J.G. 1971. Action of emulsifiers in ice cream utilizing the HLB concept. Journal of Food Science. 36:718-722.

Guinard, J.X., Zoumas-Morse, C., Mori, L., Uatoni, B., Panyam, D., Kilara, A. 1997. Sugar and fat effects on sensory properties of ice cream. Journal of Food Science. 62(5):1087–94.

Hartel, R.W., Muse, M.R., Sofjan, R. 2003. Effects of structural attributes on hardness and melting rate of ice cream. In: Goff, H. D., Tharp, B. W. (eds). **Ice cream II**. Special issue 401. Brussels: International Dairy Federation, pp 124–39.

Hinrichs, J., Kessler, H.G. 1997. Fat content of milk and cream and effects on fat globule stability. Journal of Food Science. 62:992.

Goff, H.D., Hartel, R.W. 2006. Ice cream and frozen desserts. In: Hui, Y.H. (ed) **Handbook of food science, technology, and engineering Volume 4**. CRC Press. Boca Raton, FL. pp 154-27–154-28.
Hyvönen, L., Linna, M., Tuorila, H., Dijksterhuis, G. 2003. Perception of Melting and Flavor Release of Ice Cream Containing Different Types and Contents of Fat. Journal of Dairy Science, 86:1130–1138

Kabalnov, A. S. 1998. Coalescence in emulsions. In Binks, B. P. (ed.). **Modern aspects of emulsion science**. The Royal Society of Chemistry. Cambridge, UK.

Kabalnov, A.S., Wennerström, H. 1996. Macroemulsion stability: the oriented wedge theory revisited. Langmuir. 12:276-292.

Kaylegian, K.E., Lindsay, R.C. 1994. Application of milk fat fractions in foods. In Handbook of Milk Fat Fraction and Technology and Applications. American Oil Chemists' Society Press. Champaign, lL.

King, N. 1950. The physical structure of ice cream. Diary Industries. 15:1052-1055.

Koxholt, M.M.R., Eisenmann, B., Hinrichs, J. 2001. Effect of the fat globule sizes on the meltdown of ice cream. Journal of Dairy Science. 84:31–37.

Kroezen, A. B. 1988. Flow properties of foam in rotor–stator mixers and distribution equipment. Ph.D. Thesis. University of Twente, The Netherlands.

Lin, P.M., Leeder. J.G. 1974. Mechanism of emulsifier action in an ice cream system. Journal of Food Science. 39:108-111.

Lopez, C., Bourgaux, C., Lesieur, P., Bernadou, S., Keller, G., Ollivon, M. 2002. Thermal and Structural Behavior of Milk Fat: 3. Influence of Cooling Rate and Droplet Size on Cream Crystallization. Journal of Colloid Interface Science. 254:64.

Morris, C.E. 1992. Balancing act: engineering flavors for low fat foods. **Chilton's Food Engineering**. 68:77–81.

Muhr, A. H., Blanshard, J. M. V. 1986 Effect of polysaccharide stabilizers on the rate of growth of ice. Journal of Food Technology. 21:683-710.

Muse, M.R. 2003. A structural model to explain melting rate and hardness of ice cream. Masters Thesis. University of Wisconsin-Madison.

Muse, M.R., Hartel, R.W. 2004. Ice Cream structural elements that affect melting rate and hardness. Journal of Dairy Science. 87:1-10.

Pawar, A.B., Caggioni, M., Hartel, R.W., Spicer, P.T. 2012. Arrested coalescence of viscoelastic droplets with internal microstructure. Faraday Discussion. 158:341–350.

Pelan, B.M.C., Watts, K.M., Campbell, I.J., Lips, A. 1997. The stability of aerated milk protein emulsions in the presence of small molecule surfactants. Journal of Dairy Science. 80: 2631–2638.

Prindiville, E. A., Marshall, R.T., Heymann, H. 1999. Effect of Milk Fat on Sensory Properties of Chocolate Ice Cream. Journal of Dairy Science, 82:1425–1432.

Regand, A., H. D. Goff. 2003. Structure and ice recrystallization in frozen stabilized ice cream model systems. Food Hydrocolloids. 17:95–102.

Roland, A.M., Phillips, L.G., Boor, K.J. 1999. Effects of fat content on the sensory properties, melting, color, and hardness of ice cream. Journal of Dairy Science. 82:32–8.

Rossa, P.N., Burin, V.M., Bordignon-Luiz, M.T. 2012. Effect of microbial transglutaminase on functional and rheological properties of ice cream with different fat contents. LWT-Food Science and Technology. 48:224–230.

Russell, A.B., Cheney, P.E., Wantling, S.D. 1999. Influence of freezing conditions on ice crystallization in ice cream. Journal of Food Engineering. 39:179-191

Sakurai, K., Kokubo, S., Hakamata, K., Tomita, M., Yoshida, S. 1996. Effect of production conditions on ice cream melting resistance and hardness. Milchwissenschaft. 51(8):451–454.

Segall, K.I., Goff, H.D. 2002. A modified ice cream processing routine that promotes fat destabilization in the absence of added emulsifier. International Dairy Journal. 12:1013–1018.

Sofjan, R.P., Hartel, R.W. 2004. Effects of overrun on structural and physical characteristics of ice cream. International Dairy Journal. 14(3):255–262.

Stampanoni Koeferli, C.R., Piccinali, P., Sigrist, S. 1996. The influence of fat, sugar and non-milk solids on selected taste, flavor and texture parameters of vanilla ice-cream. Food Quality and Preference. 7(2):69–79.

Tharp. B. W., Forrest, B., Swan, C., Dunning, L., Hilmoe, M. 1998. Basic factors affecting ice cream meltdown. In: **Ice Cream.** In: Buchheim, W. (eds), **Ice Cream**. Proceedings of the International Symposium held in Athens, Greece, 19-19 September 1997. Brussels, Belgium: International Dairy Federation. pp. 54–64.

Thivilliers, F., Laurichesse, E., Saadaoui, H., Leal-Calderon, F. 2010. Shear-induced instabilities in oil-in-water emulsions comprising partially crystallized droplets. Langmuir. 26 (22):16782-16790.

Thivilliers, F., Laurichesse, E., Saadaoui, H., Leal-Calderon, F., Schmitt, V. 2008. Thermally Induced Gelling of Oil-in-Water Emulsions Comprising Partially Crystallized Droplets: The Impact of Interfacial Crystals. Langmuir. 24:13364-13375.

Thomas, E. L. 1981. Structure and properties of ice cream emulsions. Food Technology. 35(1):41–48.

Thomsen, M., Holtsborg, J. 1998. The effect of homogenization pressure and emulsifier type on ice cream mix and finished ice cream. In: Buchheim, W., **Ice Cream**. Special Issue 9803. Brussels, Belgium: International Dairy Federation. pp. 105–111.

Torza, S., Cox, R.G., Mason, S.G. 1972. Particle motions in sheared suspensions. XXVII. Transient and steady deformation and burst of liquid drops. Journal of Colloid Interfacial Science. 38:395-411.

Vanapalli, S.A., Coupland, J.N. 2001. Emulsions under shear – the formation and properties of partially-coalesced lipid structures. Food Hydrocolloids. 15(4-6):507-512.

Vanapalli, S.A., Palanuwech, J., & Coupland, J.N. 2002. Influence of fat crystallization on the stability of flocculated emulsions. Journal of Agricultural and Food Chemistry. 50(18):5224-5228.

van Boekel, M.A.J.S. 1980. Influence of fat crystals in the oil phase on stability of oil-in- water emulsions, Ph.D. Thesis. Wageningen, Agricultural University.

Walstra, P. 1983. "Formation of Emulsions," In: **Encyclopedia of Emulsions Technology Vol 1**, Marcel Dekker Inc., New York.

Walstra, P. 1996. Dispersed systems: Basic considerations. In: Fennema, O.R. (ed). **Food Chemistry 3rd ed.** Marcel Dekker, Inc., New York, NY. pp. 95-155.

Walstra, P. 1989. Principles of foam formation and stability. In Wilson, A.J. (ed) **Foams: Physics, Chemistry and Structure.** Springer, Berlin. pp. 1-15.

Walstra, P. 2003. **Physical Chemistry of Foods.** Marcel Dekker, Inc, New York, NY. pp. 529-534.

Walstra, P., Becher, P. ed. 1996. **Encyclopedia of emulsion technology, vol. 4. Chapter 1**. Marcel Dekker, Inc., New York, NY.

Walstra, P., Jenness, R. 1984. **Dairy Chemistry and Physics**. Wiley, New York.

Walstra, P., Jonkman, M. 1998. The role of milk fat and protein in ice cream. In: Buchheim, W. (eds), **Ice Cream**. Proceedings of the International Symposium held in Athens, Greece, 19-19 September 1997. Brussels, Belgium: International Dairy Federation. pp. 17-24.

Appendix A1: Drip-through (% weight) curves of the 18 commercial ice creams.

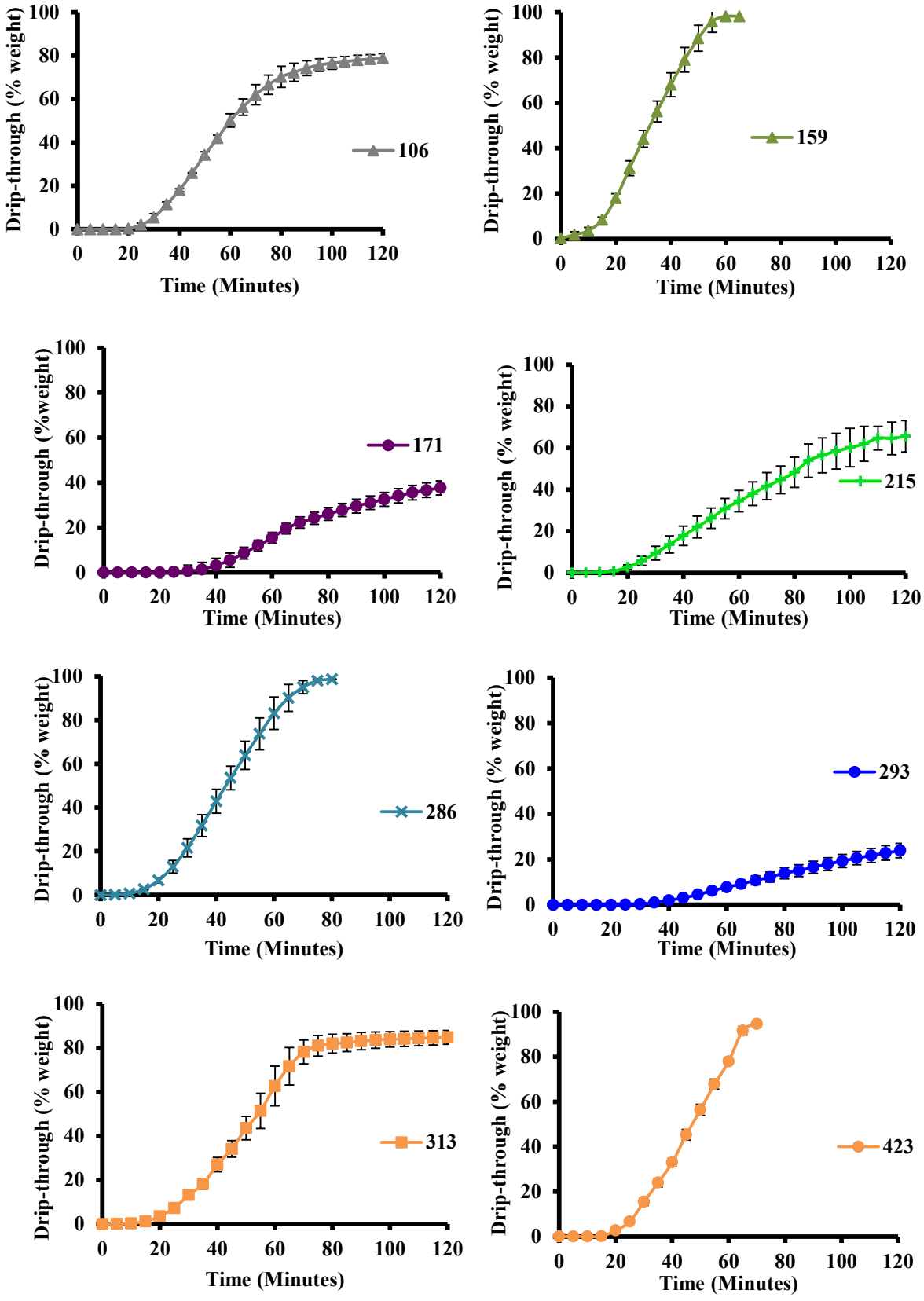

Appendix A1 continued

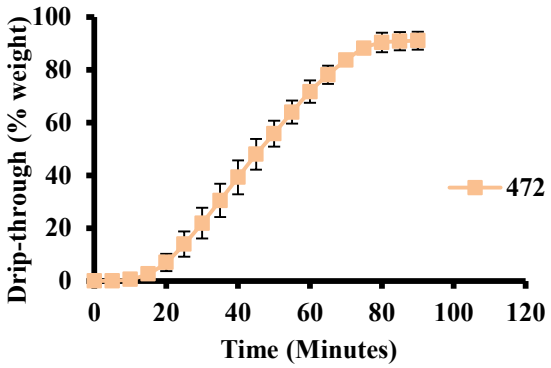

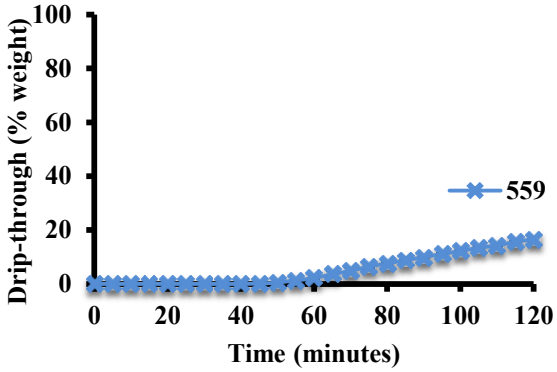

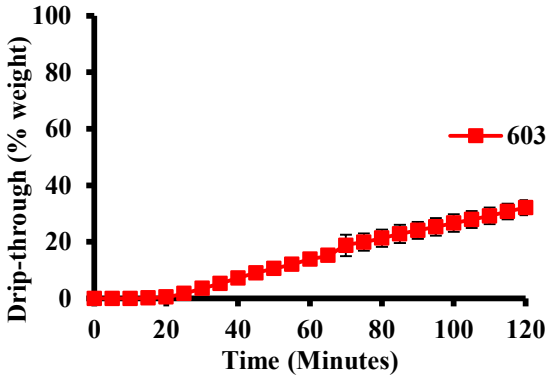

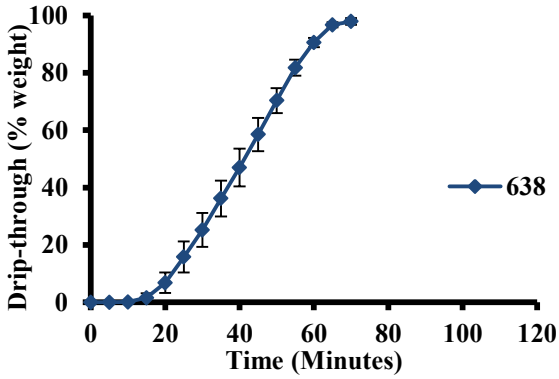

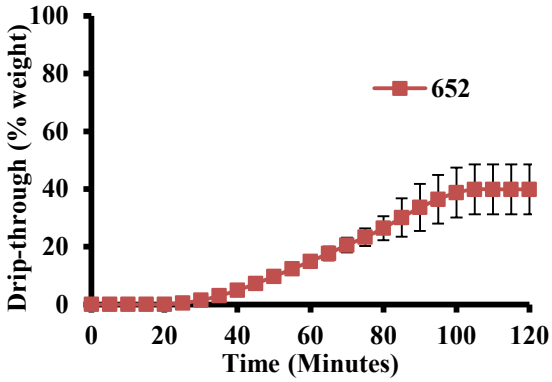

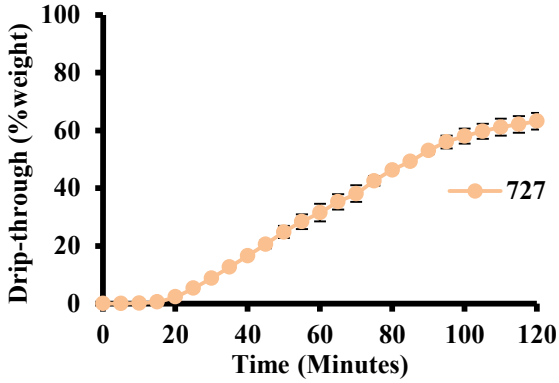

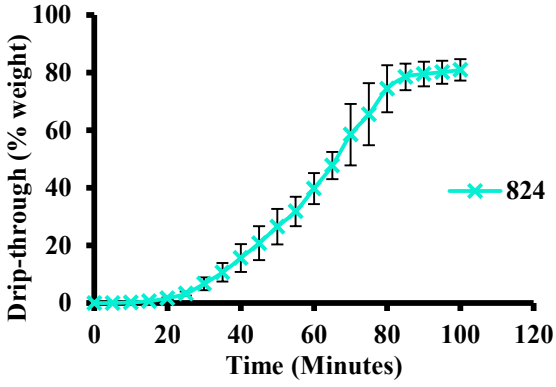

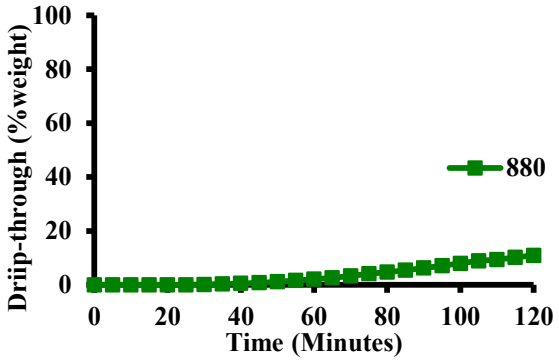

Appendix A1 continued

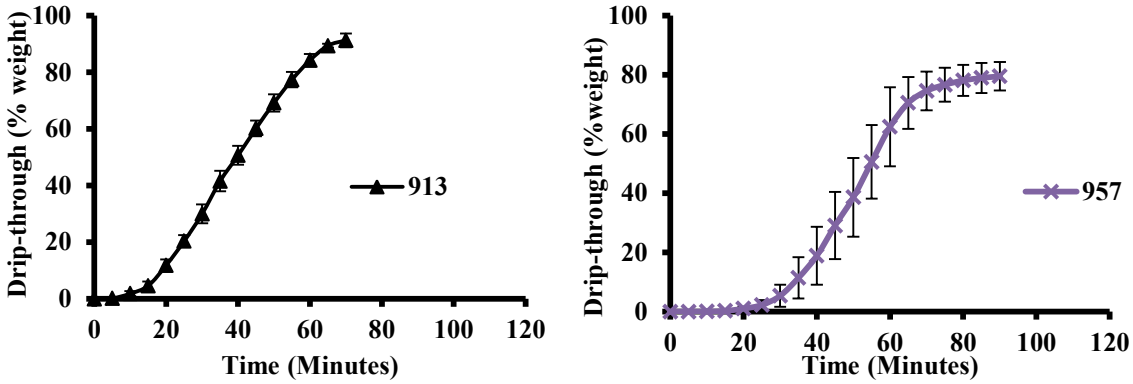

Figure A.1: Drip-through (% weight) curves of the 18 commercial ice creams surveyed. The error bars represent the standard deviations of the drip-through (% weight) measured.

Appendix A2. Structure left atop the screen at the end of the drip-through test.

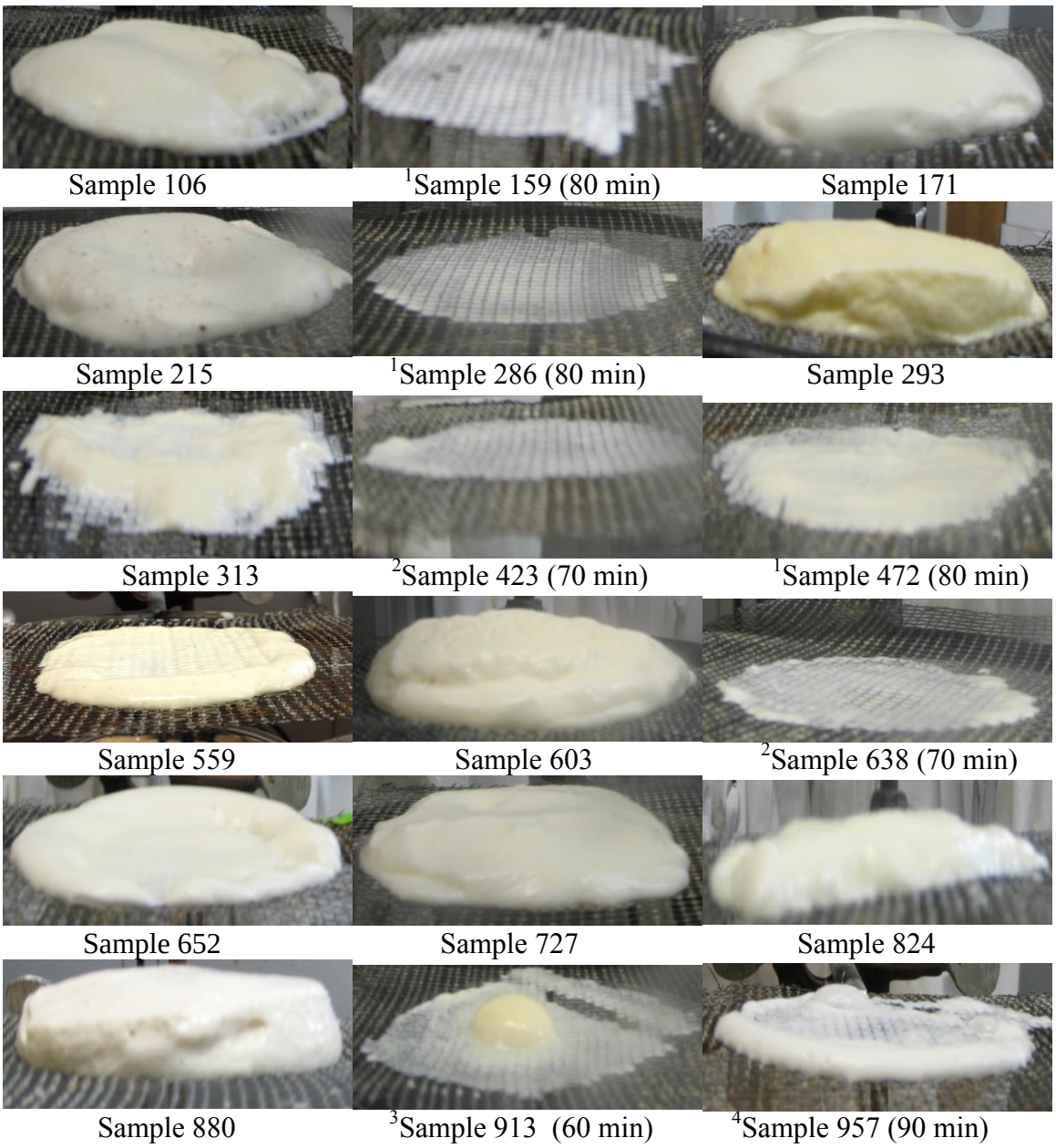

Figure A.2: Images and visual comparison of ice cream structure left on top of screen at the end of a drip-through test of all 18 commercial ice cream samples surveyed. All samples completed at 120 minutes, unless indicated otherwise.
[1]Ice cream samples that ended drip-through test at 80 minutes
[2]Ice cream samples that ended drip-through test at 70 minutes
[3]Ice creams samples that ended drip-through test at 60 minutes
[4]Ice cream samples that ended drip-through test at 90 minutes

Appendix B: Images of ice crystals under the microscope.

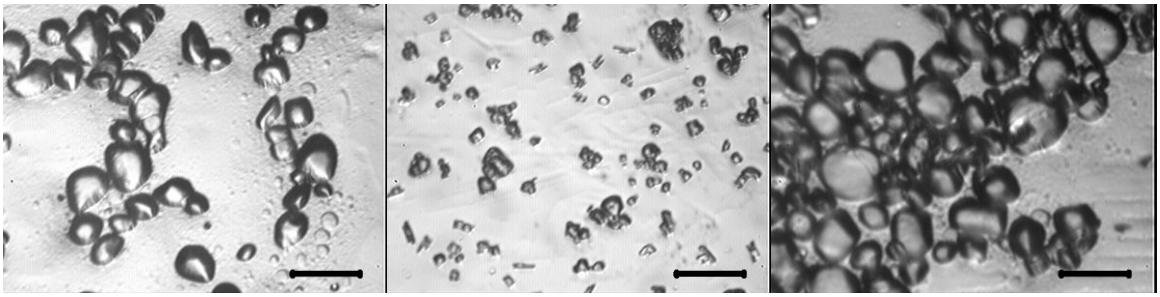

Sample 106 Sample 159 Sample 171

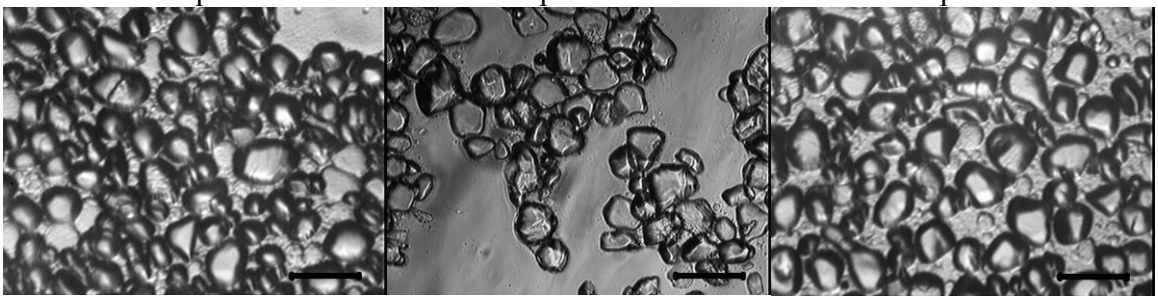

Sample 215 Sample 286 Sample 293

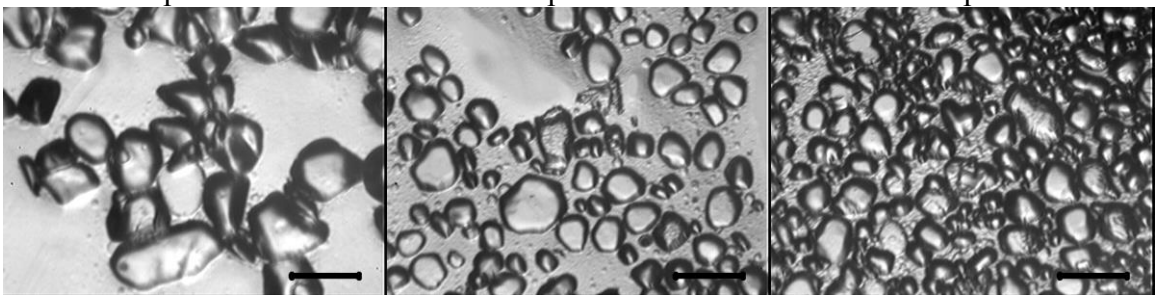

Sample 313 Sample 423 Sample 472

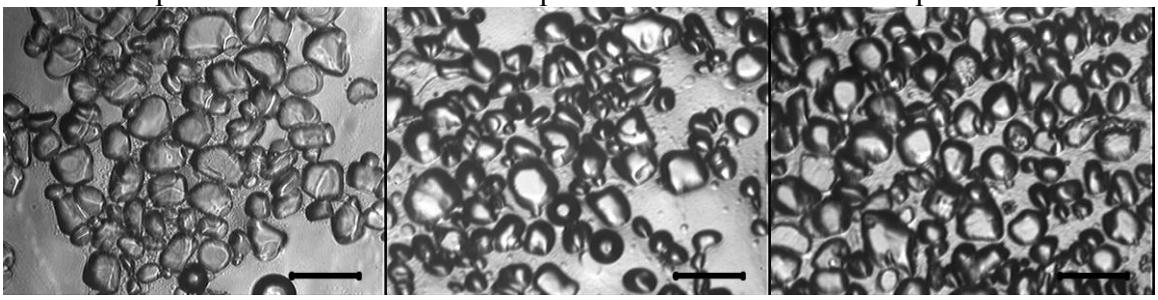

Sample 559 Sample 603 Sample 638

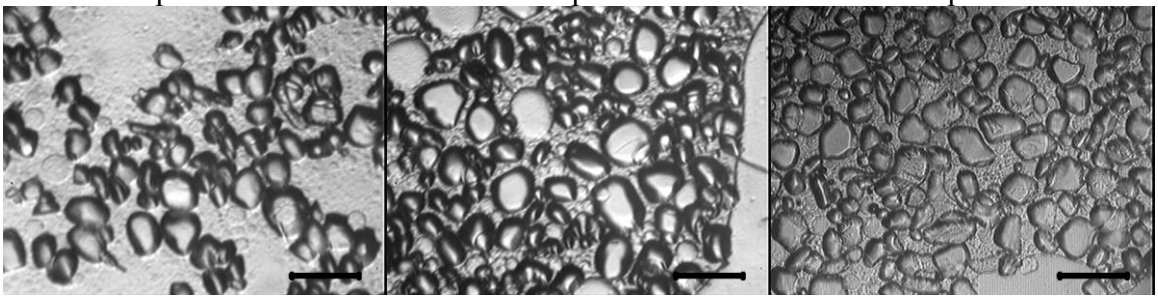

Sample 652 Sample 727 Sample 824

Appendix B continued

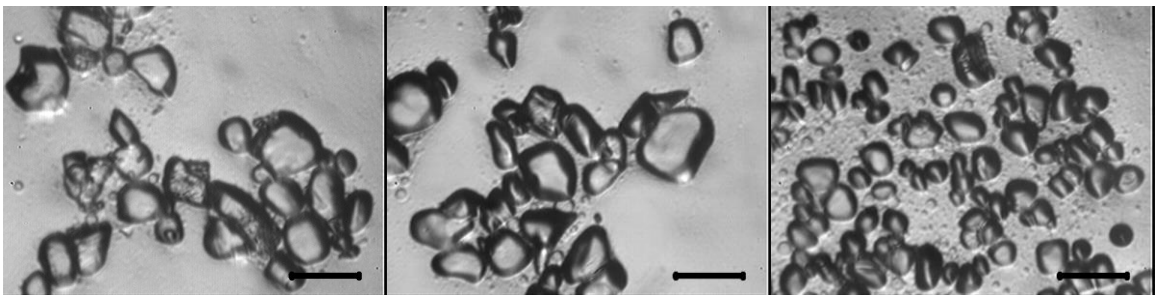

Sample 880 Sample 913 Sample 957

Figure B: Microscope images of ice crystals from the United States commercial ice creams surveyed (40x magnification, 100 μm scale bar).

Appendix C1. Particle size distribution curves of the 18 commercial ice cream products.

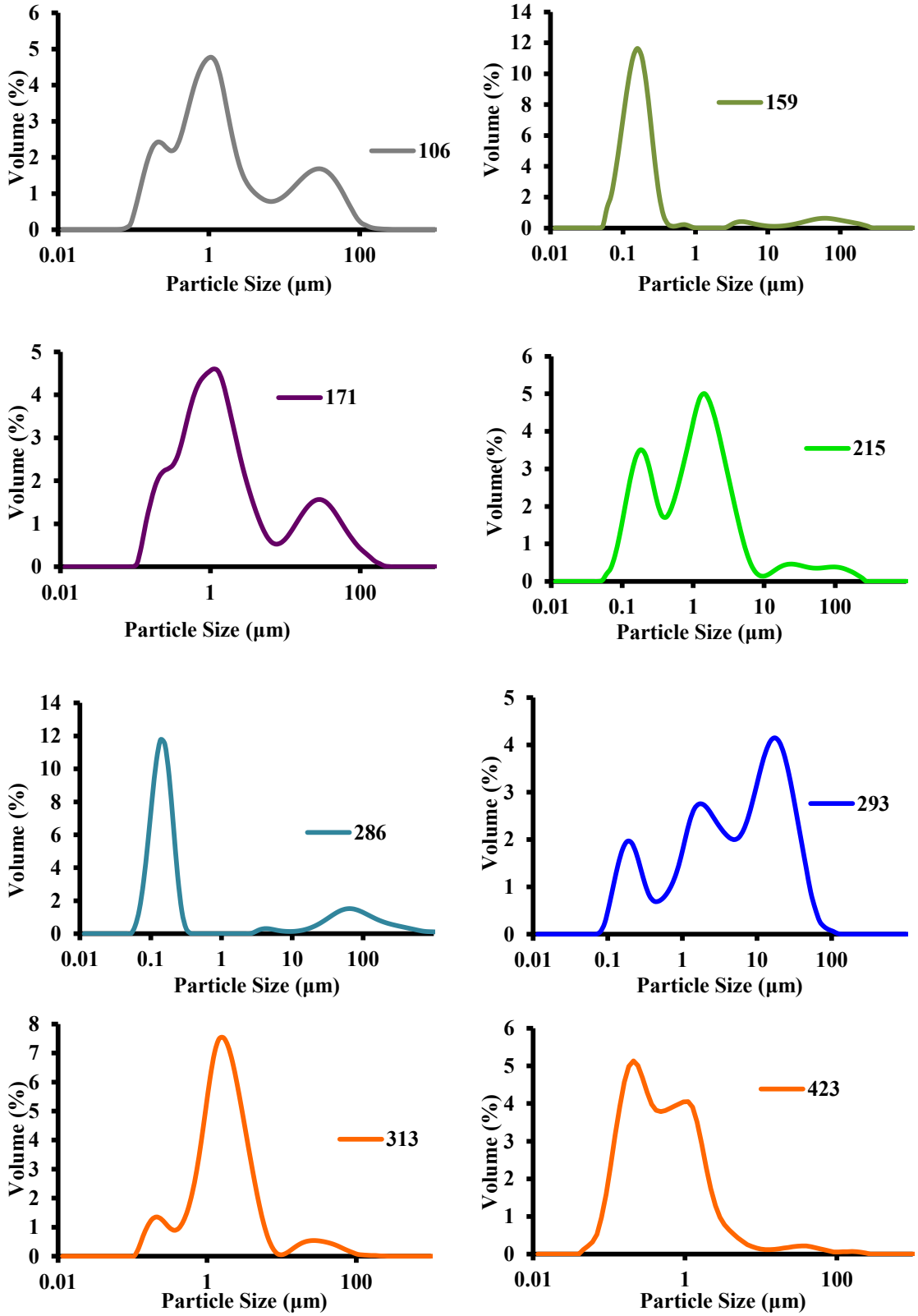

Appendix C1 continued

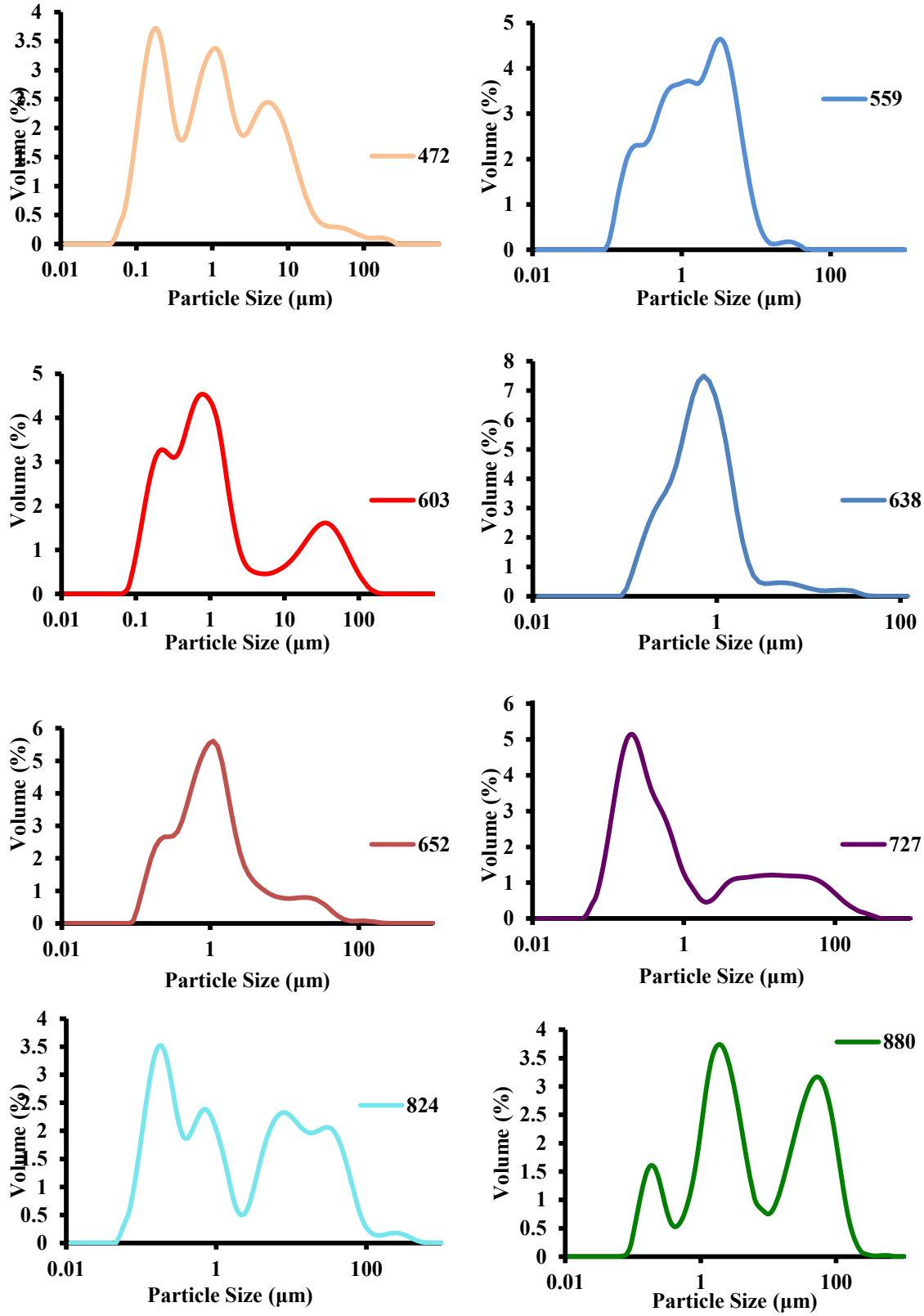

Appendix C1 continued

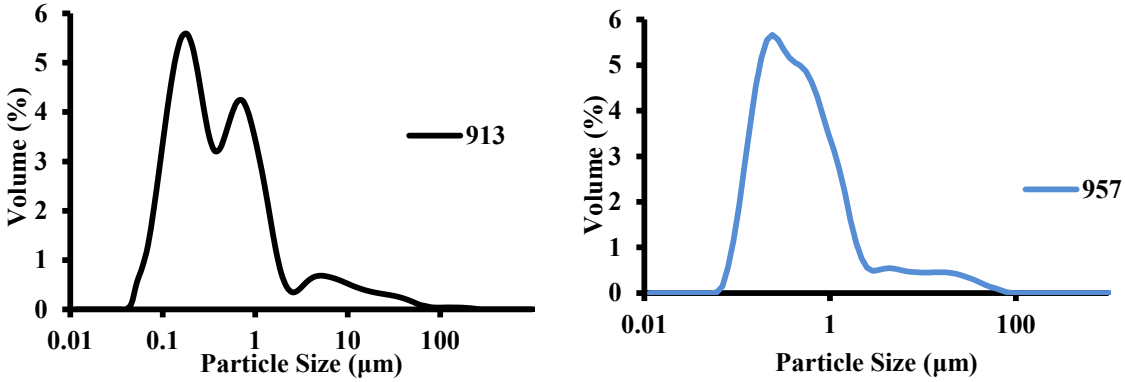

Figure C.1: Particle size distribution for the 18 commercial ice creams surveyed.

Appendix C2. Microscopy images of the 18 melted commercial ice cream products.

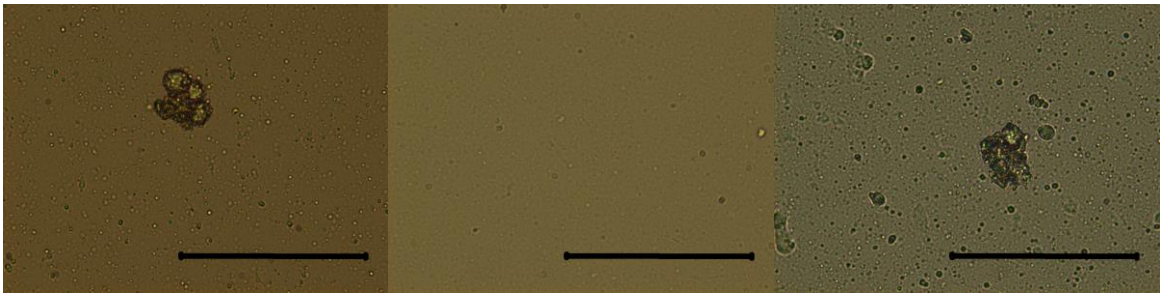

Sample 106 Sample 159 Sample 171

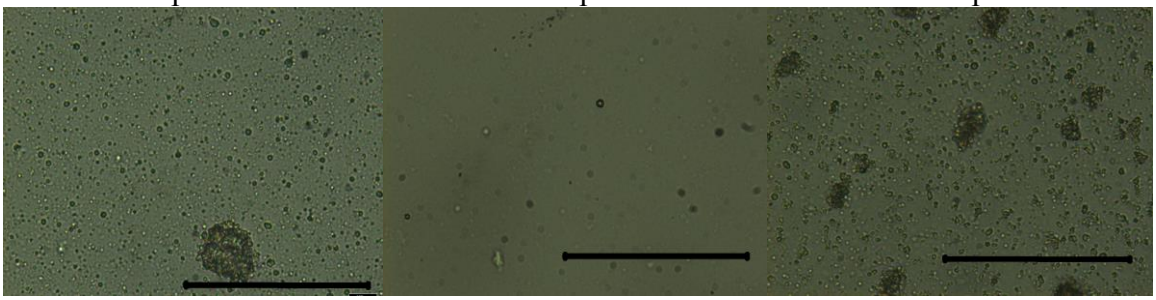

Sample 215 Sample 286 Sample 293

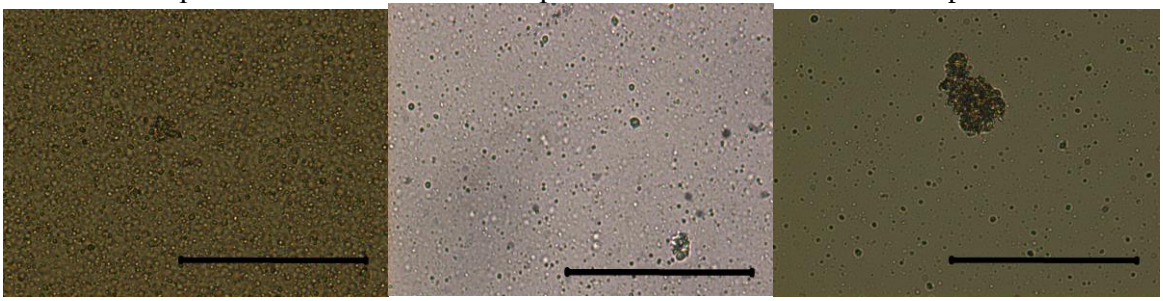

Sample 313 Sample 423 Sample 472

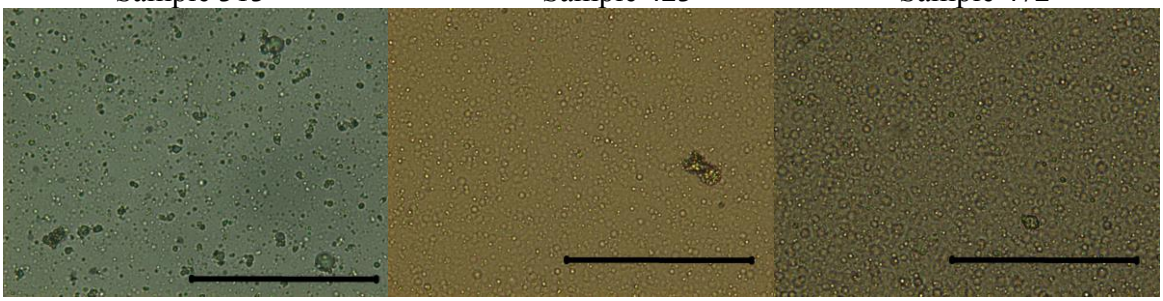

Sample 559 Sample 603 Sample 638

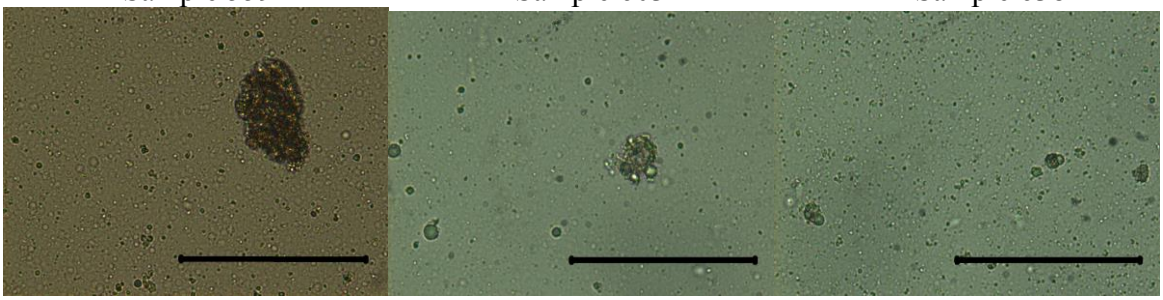

Sample 652 Sample 727 Sample 824

Appendix C2 continued

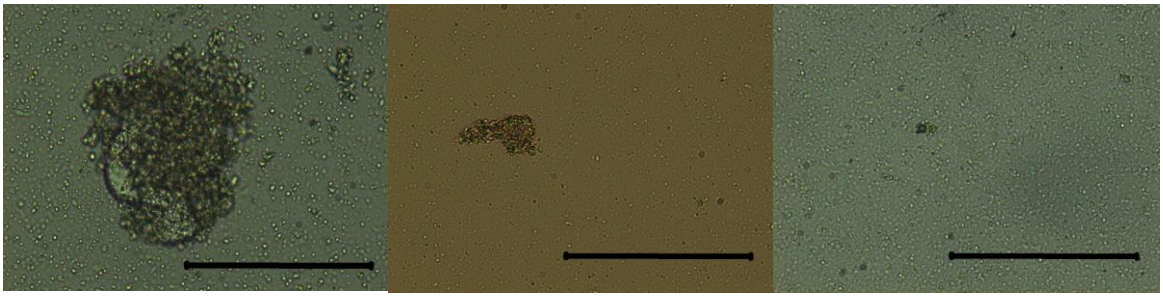

Sample 880 Sample 913 Sample 957

Figure C.2: Microscopy images of melted ice creams from the 18 commercial ice creams sampled (400x magnification, 100 μm scale bar).

Appendix D: Images of air cells under the microscope from the 18 commercial ice creams surveyed.

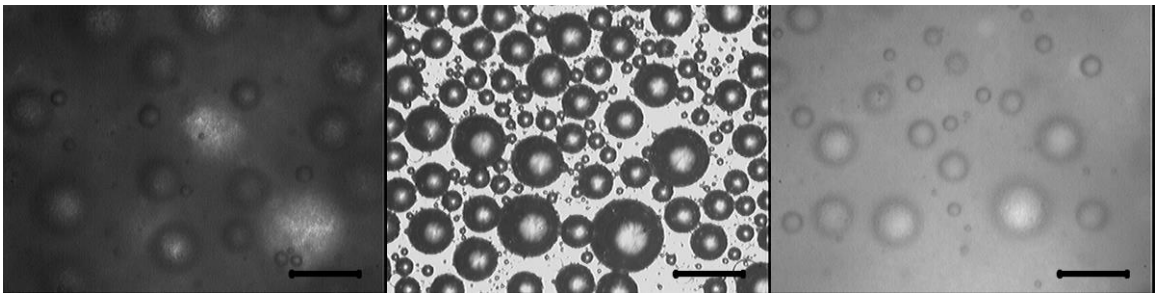

Sample 106 Sample 159 Sample 171

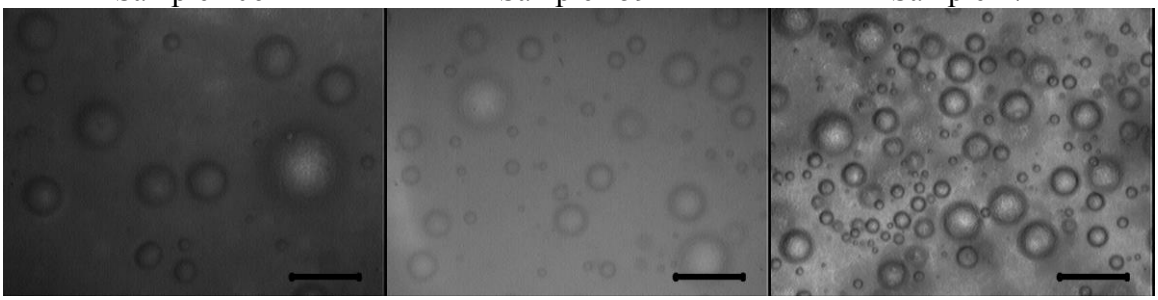

Sample 215 Sample 286 Sample 293

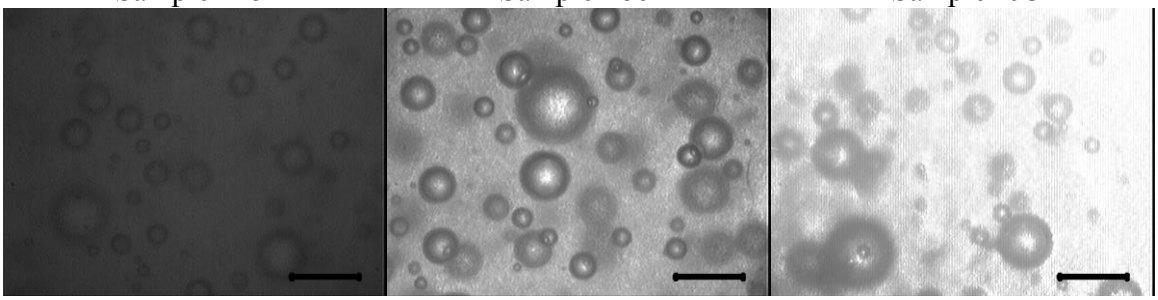

Sample 313 Sample 423 Sample 472

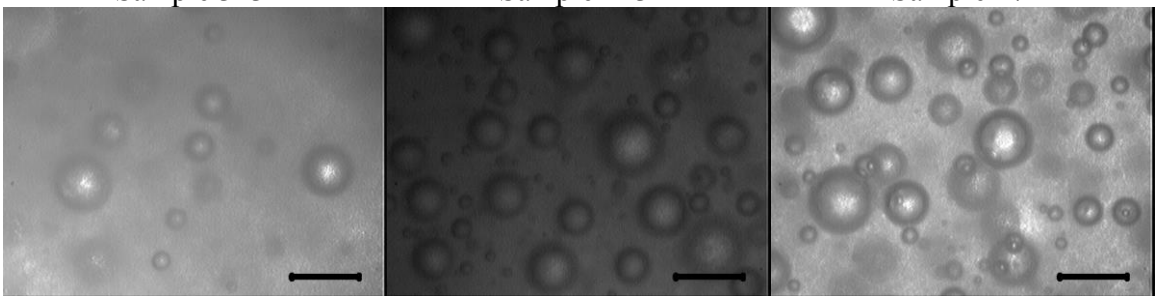

Sample 559 Sample 603 Sample 638

Appendix D continued

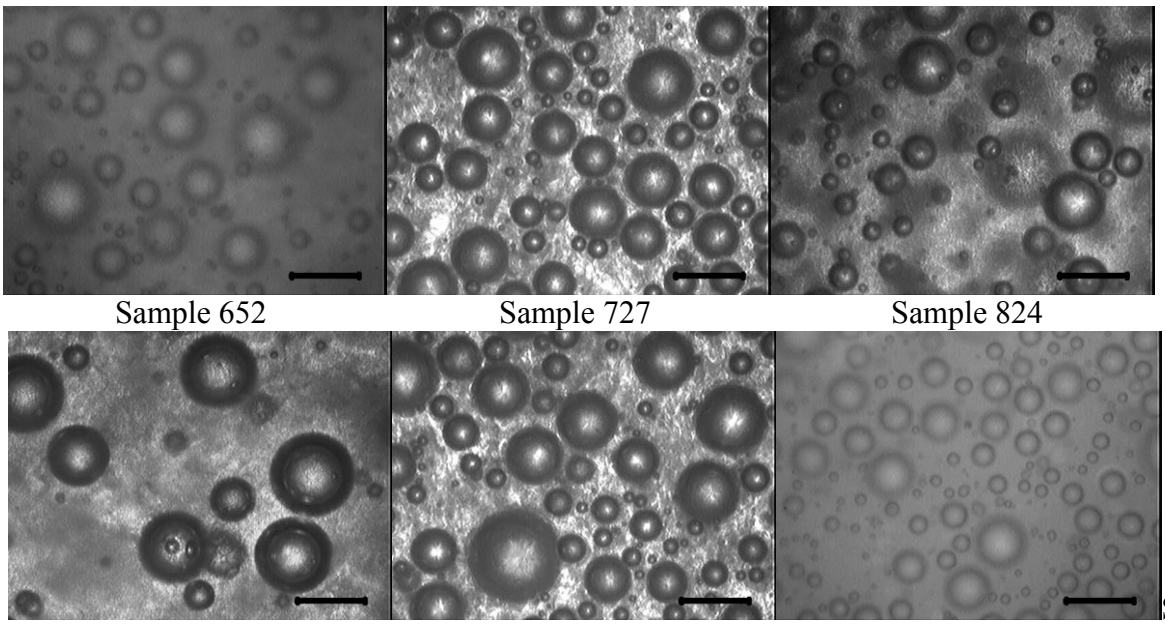

Figure D.1: Microscope images of air cells from the United States commercial ice creams surveyed (40x magnification, 100 μm scale bar).

Appendix E1. Sensory lexicon

ICE CREAM REFERENCE AND SCALING

Directions: Rinse mouth with water to cleanse palette. Evaluate ice cream.
Record the intensity score of each attribute using values between 0 to 15 in the box provided.

In Mouth

Melt Rate

Using small plastic spoon, place 1 cube of ice cream on tongue. Close mouth. Ice cream rests on tongue, mouth should be relaxed. Evaluate rate of ice cream melt. Expectorate the sample.

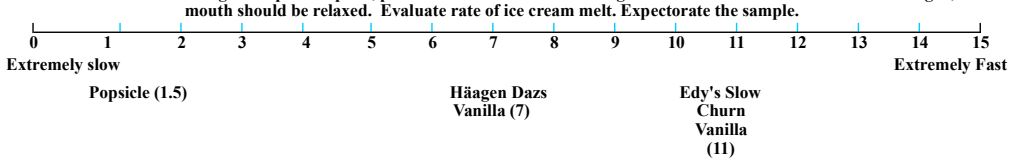

Breakdown

Manipulate ice cream sample between tongue & palette 3-5 times. Evaluate the amount of force required to manipulate the sample. Take the average of the amount of force required to manipulate sample prior to melt. Expectorate the sample.

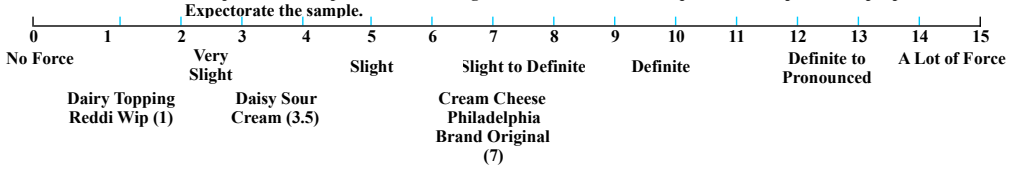

Size of Ice Particulate

During manipulation of sample, you may feel particulates. Particulate may or may not melt. Ice particulate will melt. Evaluate the size of the ice particulates. There may be more than one size of ice particulate in sample. Expectorate the sample.

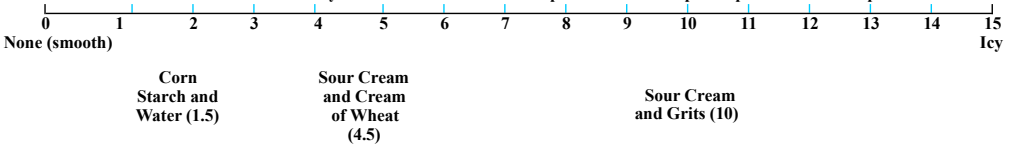

Denseness

The compactness of the cross section
Place sample between molars and compress once. Expectorate the sample.

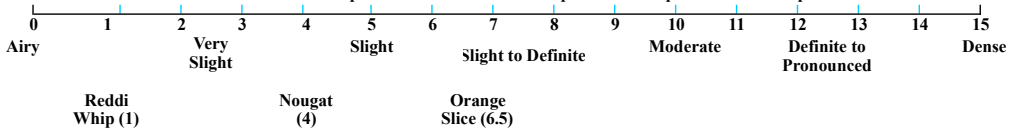

Residual

Greasiness

Degree of greasy mouth coating or amount of oil left on the mouth surfaces.
Allow sample to melt and warm in mouth. Expectorate the sample.

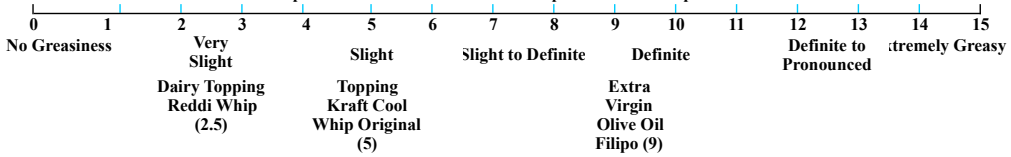

Texture & Flavor

Overall Creaminess

Flavors and aromas associated with creamy, milky products. Allow sample to melt and warm in mouth. Expectorate the sample.

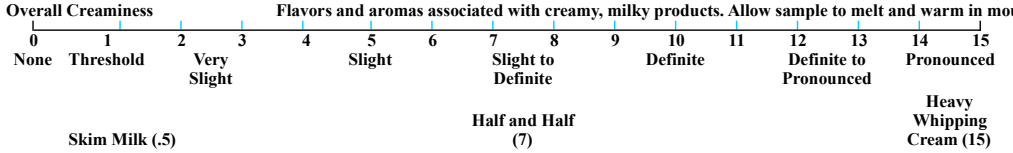

Figure E.1: The lexicon used to determine the sensorial attributes of the ice creams surveyed.

Appendix E2. Ice cream sensory ballot

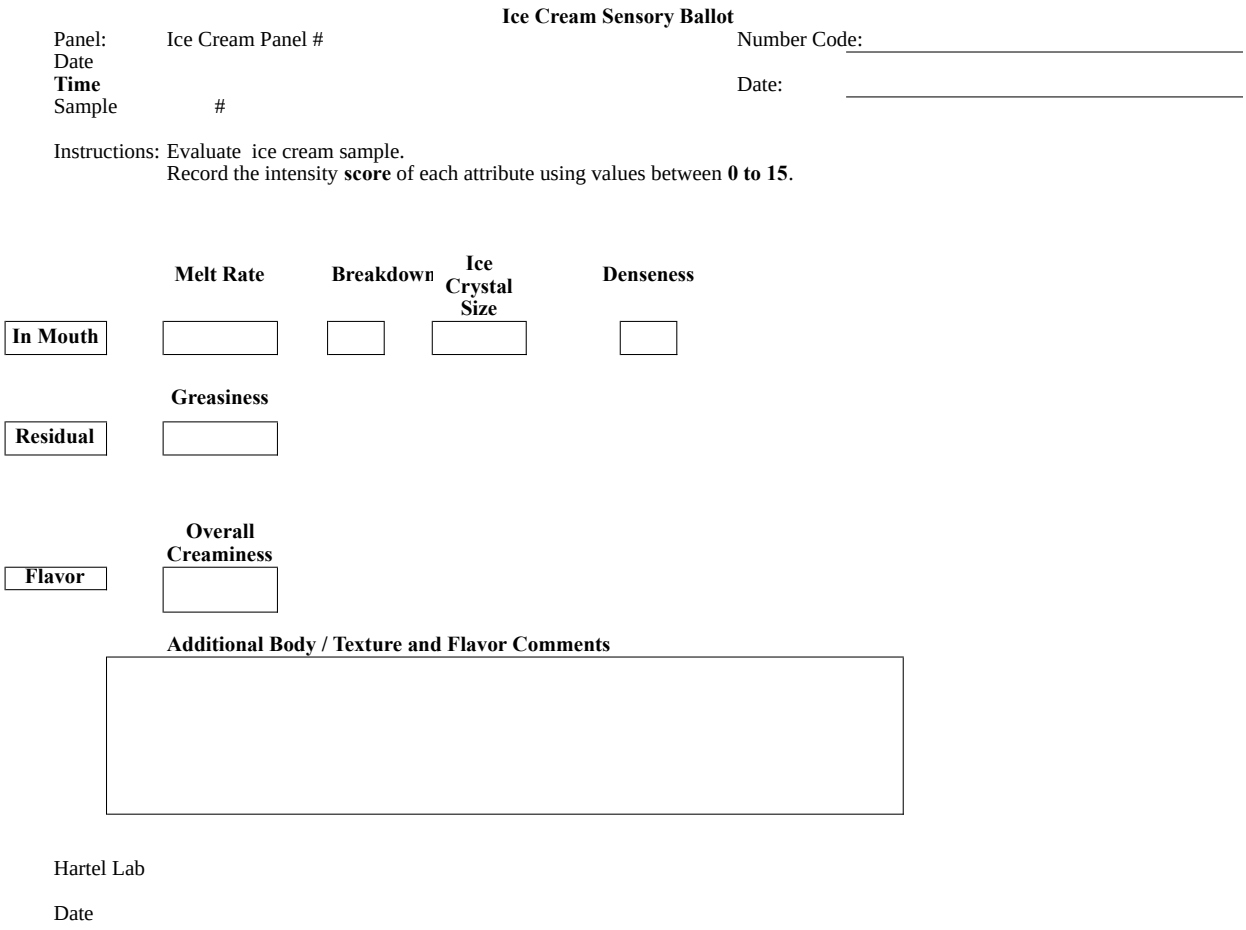

Ice Cream Sensory Ballot

Panel: Ice Cream Panel # Number Code: _____

Date

Time Date: _____

Sample #

Instructions: Evaluate ice cream sample.
Record the intensity **score** of each attribute using values between **0 to 15**.

	Melt Rate	Breakdown	Ice Crystal Size	Denseness
In Mouth				

	Greasiness
Residual	

	Overall Creaminess
Flavor	

Additional Body / Texture and Flavor Comments

Hartel Lab

Date

Figure E.2: Example of ice cream sensory ballot used during sensory testing.

Appendix F: Mean ice crystal size distributions and microscopy images of ice creams.

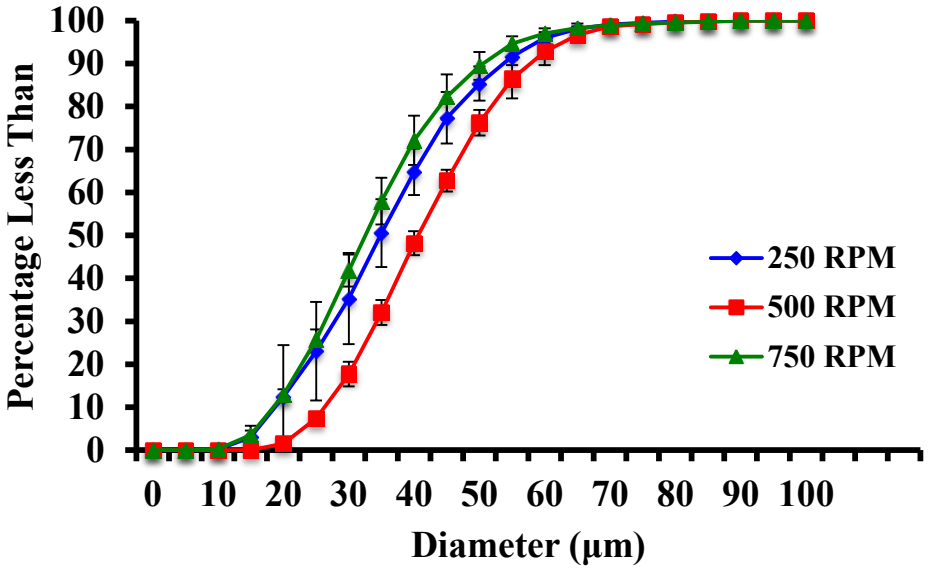

Figure F.1: Ice crystal size distributions of ice creams made with no added emulsifiers at dasher speeds of 250 RPM, 500 RPM, and 750 RPM at 50% overrun. The error bars represent the standard deviations of the mean air cell sizes measured.

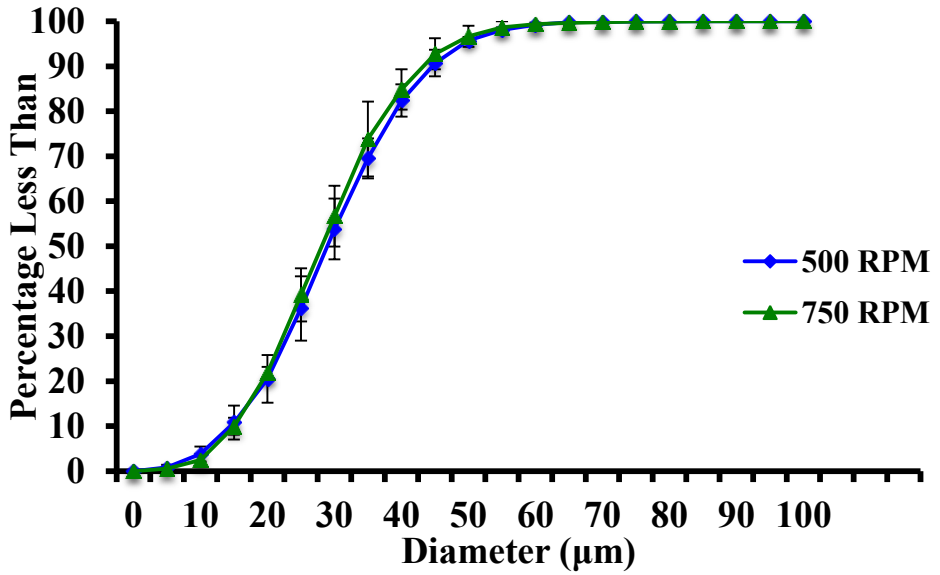

Figure F.2: Ice crystal size distributions of ice creams made with 100:0 (mono- and diglyceride:polysorbate 80 - MDG:PS80) emulsifier ratio at dasher speeds of 500 RPM and 750 RPM at 50% overrun. The error bars represent the standard deviations of the mean air cell sizes measured.

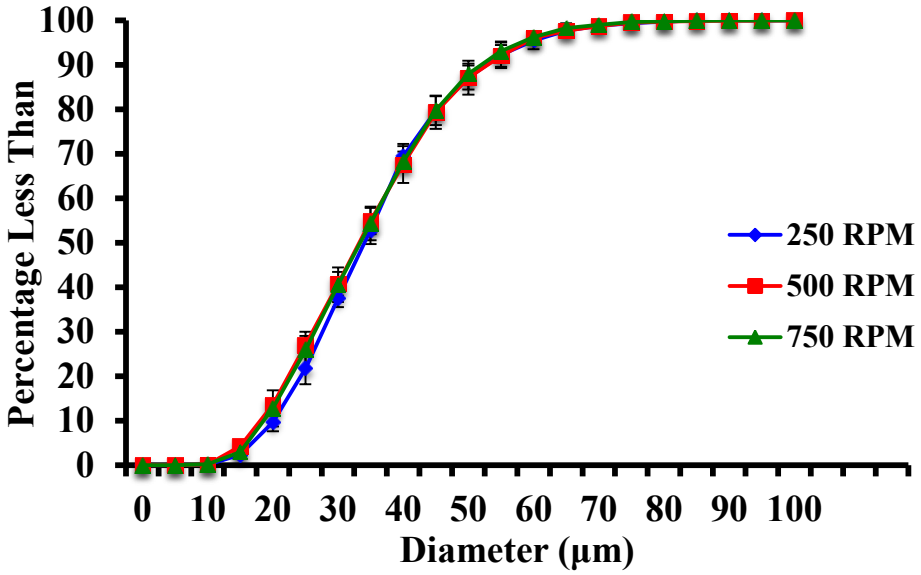

Figure F.3: Ice crystal size distributions of ice creams made with 90:10 (mono- and diglyceride:polysorbate 80 - MDG:PS80) emulsifier ratio at dasher speeds of 250 RPM, 500 RPM, and 750 RPM at 50% overrun. The error bars represent the standard deviations of the mean air cell sizes measured.

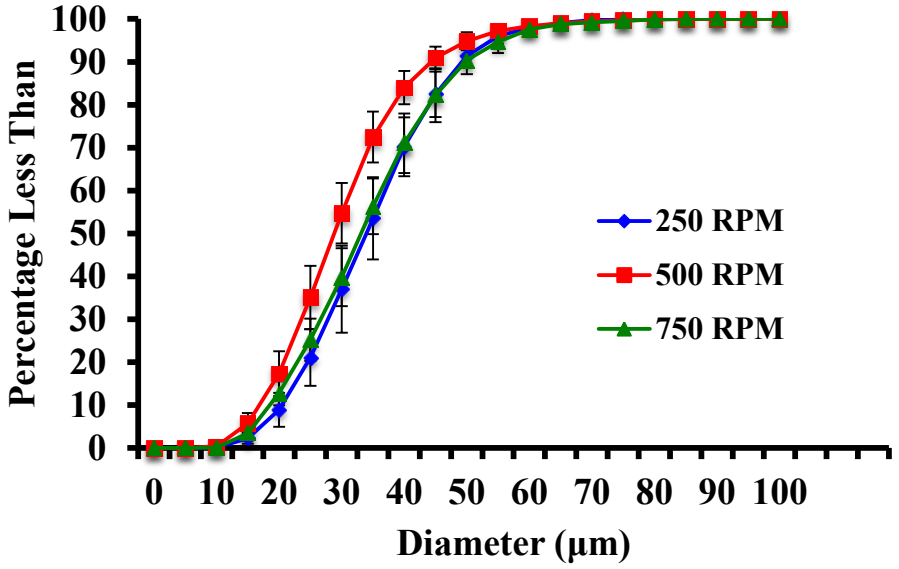

Figure F.4: Ice crystal size distributions of ice creams made with 80:20 (mono- and diglyceride:polysorbate 80 - MDG:PS80)at dasher speeds of 250 RPM, 500 RPM, and 750 RPM at 50% overrun. The error bars represent the standard deviations of the mean air cell sizes measured.

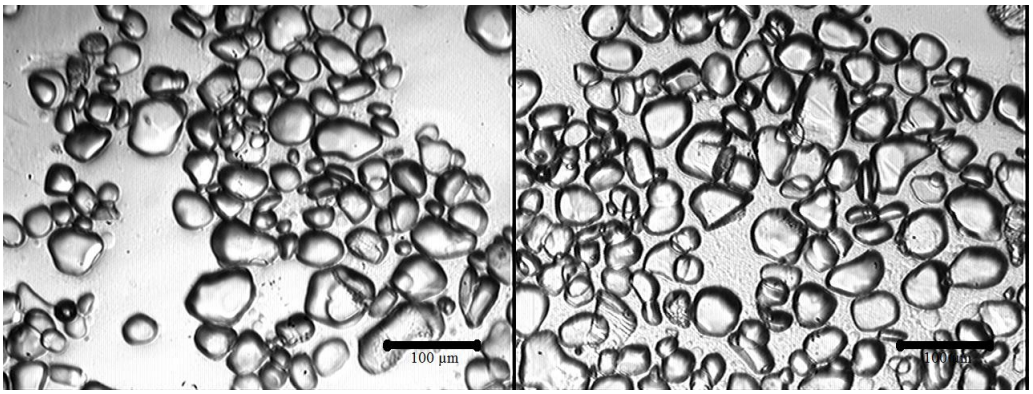

250 RPM 500 RPM

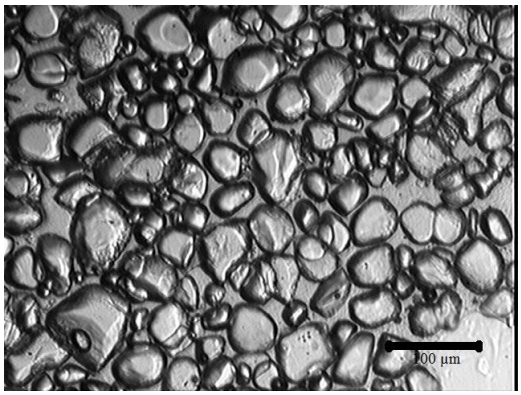

750 RPM

Figure F.5.: Microscope images of ice crystals in ice creams made with no added emulsifiers. Ice creams were processed at 250 RPM, 500 RPM, and 750 RPM at 50% overrun (40x magnification, 100 µm scale bar).

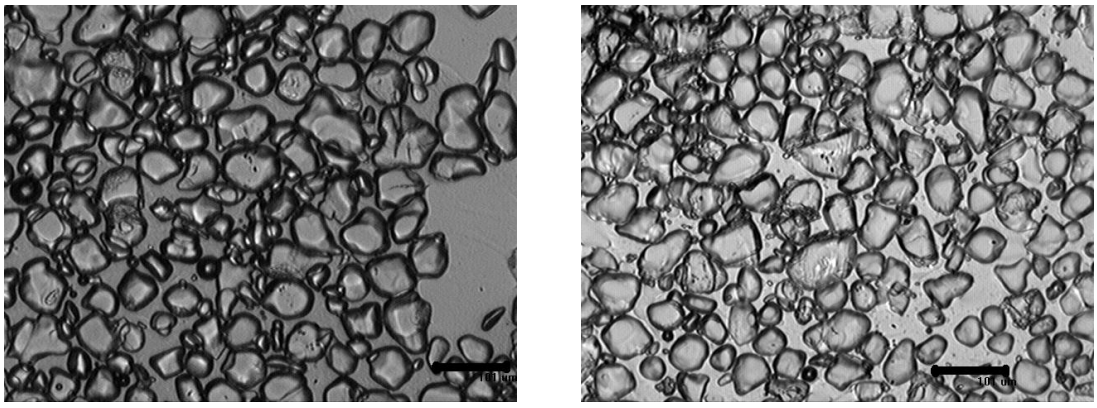

500 RPM 750 RPM

Figure F.6: Microscope images of ice crystals for ice creams made with 100:0 (MDG:PS80) (mono- and diglyceride:polysorbate 80 - MDG:PS80) emulsifier ratio and processed at 50% overrun at 500 and 750 RPM (40x magnification, 100 µm scale bar).

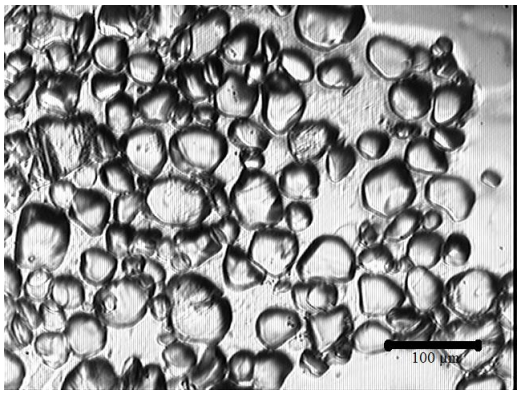

250 RPM

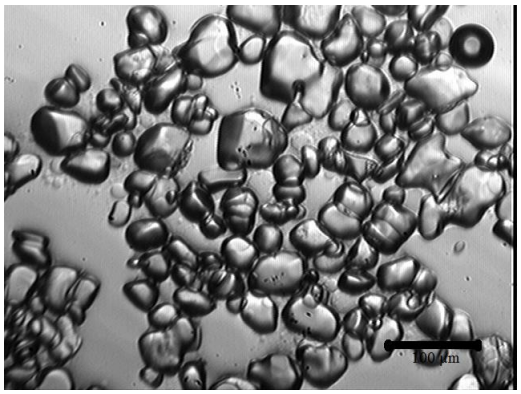

500 RPM

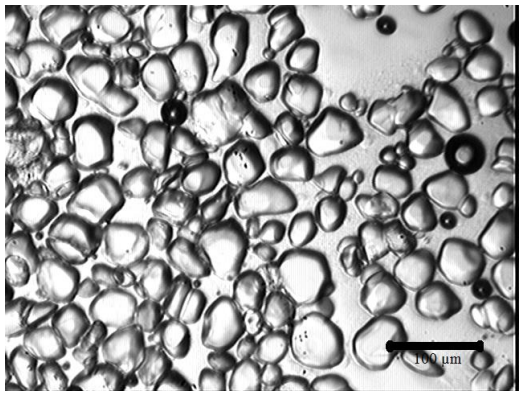

750 RPM

Figure F.7: Microscope images of ice crystals for ice creams made with 90:10 (mono- and diglyceride:polysorbate 80 - MDG:PS80) emulsifier ratio at 250 RPM, 500 RPM, and 750 RPM at 50% overrun (40x magnification, 100 µm scale bar).

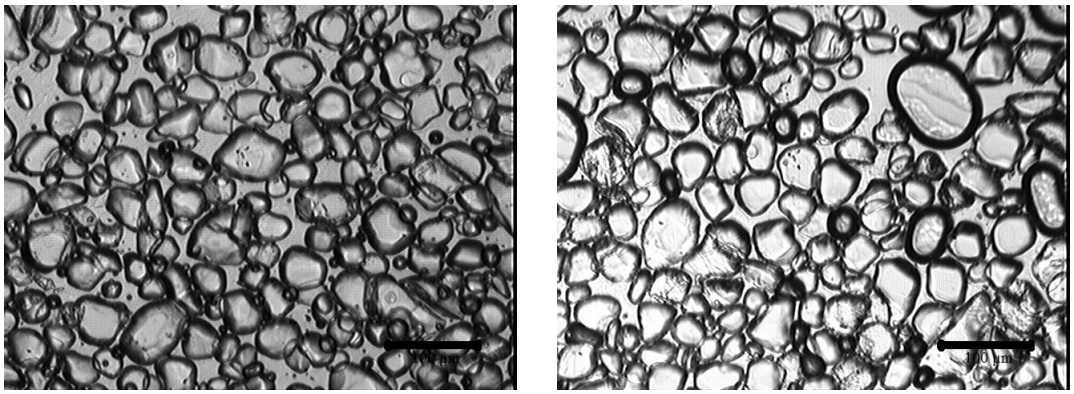

250 RPM 500 RPM

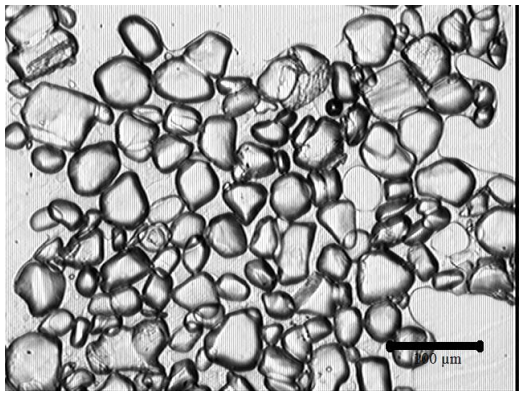

750 RPM

Figure F.8: Microscope images of ice crystals in ice creams made with 80:20 (mono- and diglyceride:polysorbate 80 - MDG:PS80) emulsifier ratio at 250 RPM, 500 RPM, and 750 RPM at 50% overrun (40x magnification, 100 μm scale bar).

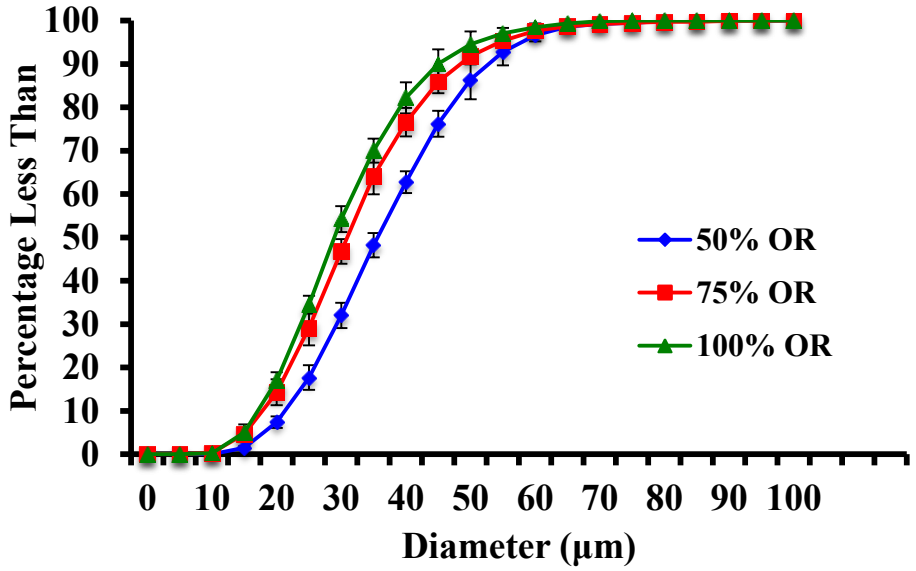

Figure F.9: Ice crystal size distributions of ice creams made with no added emulsifiers at 50%, 75%, and 100% overrun (OR) overrun and 500 RPM. The error bars represent the standard deviations of the mean ice crystal sizes measured.

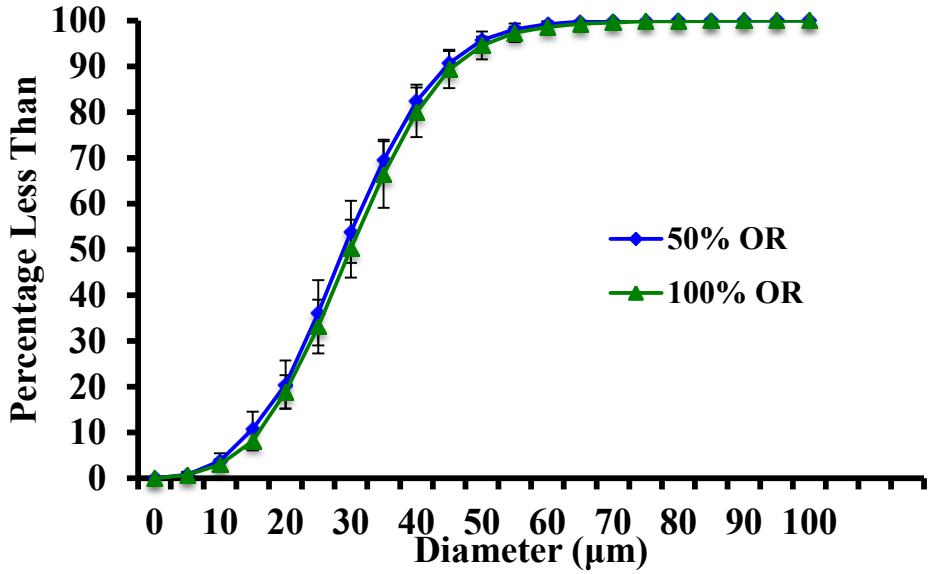

Figure F.10: Ice crystal size distributions of ice creams made with 100:0 (mono- and diglyceride:polysorbate 80 - MDG:PS80) emulsifier ratio at 50% and 100% overrun (OR) overrun at 500 RPM. The error bars represent the standard deviations of the mean ice crystal sizes measured.

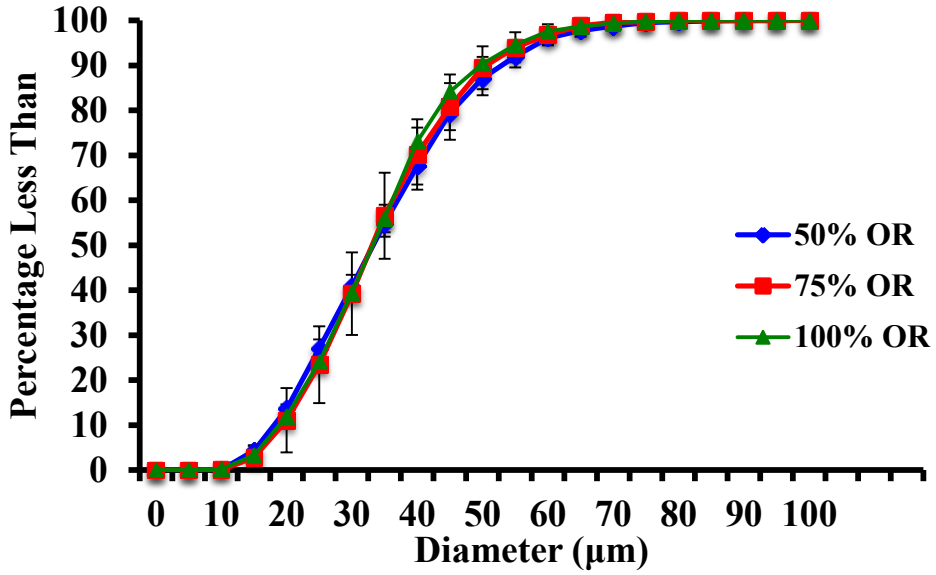

Figure F.11: Ice crystal size distributions of ice creams made with 90:10 (mono- and diglyceride:polysorbate 80 - MDG:PS80) emulsifier ratio at 50%, 75%, and 100% overrun (OR) overrun and 500 RPM. The error bars represent the standard deviations of the mean ice crystal sizes measured.

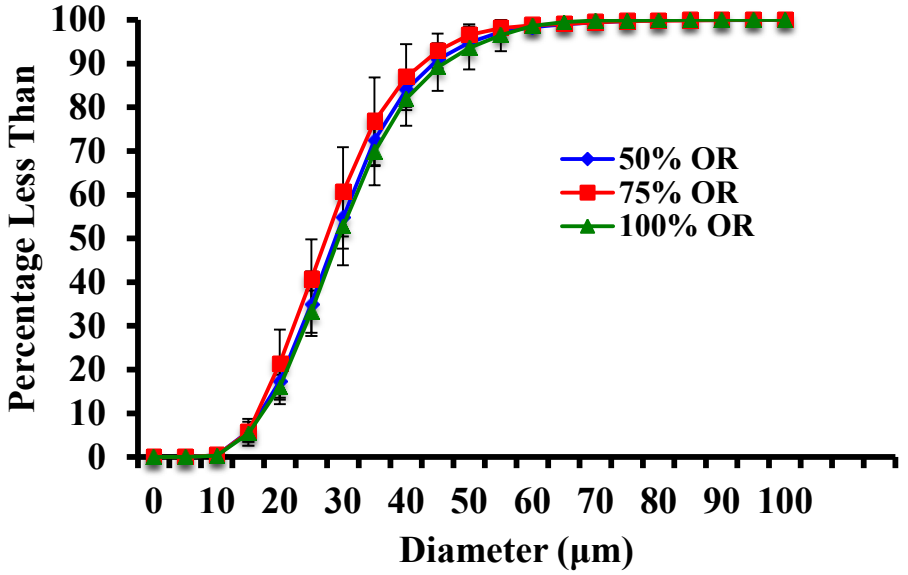

Figure F.12: Ice crystal size distributions of ice creams made with 80:20 (mono- and diglyceride:polysorbate 80 - MDG:PS80) emulsifier ratio at 50%, 75%, and 100% overrun (OR) overrun and 500 RPM. The error bars represent the standard deviations of the mean ice crystal sizes measured.

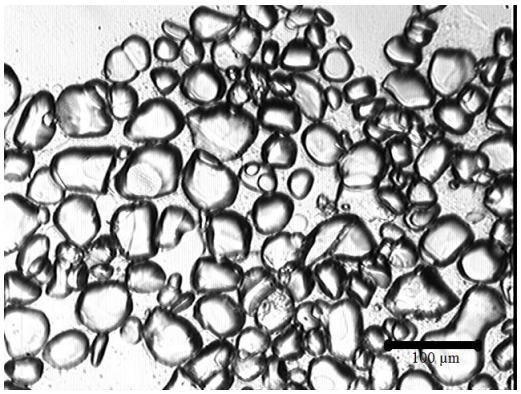

50% OR

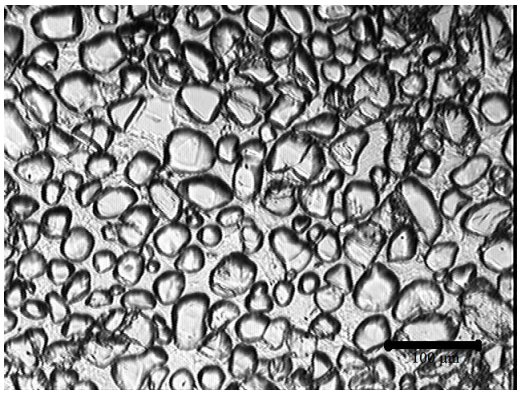

75% OR

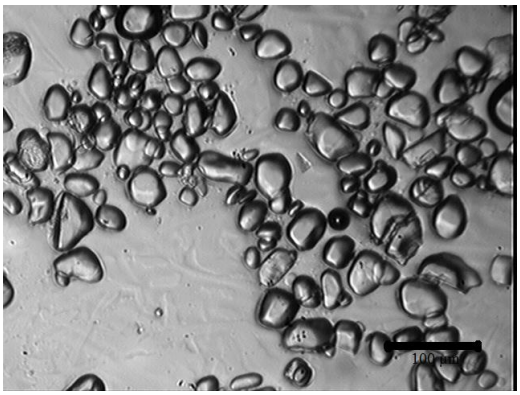

100% OR

Figure F.13: Microscope images of ice crystals from ice creams made with no added emulsifiers at 50%, 75%, and 100% overrun (OR) at 500 RPM (40x magnification, 100 µm scale bar).

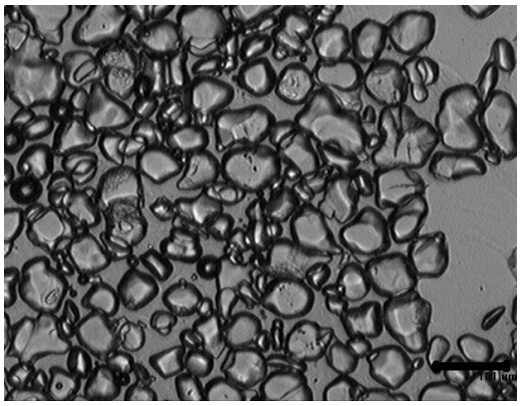

50% OR

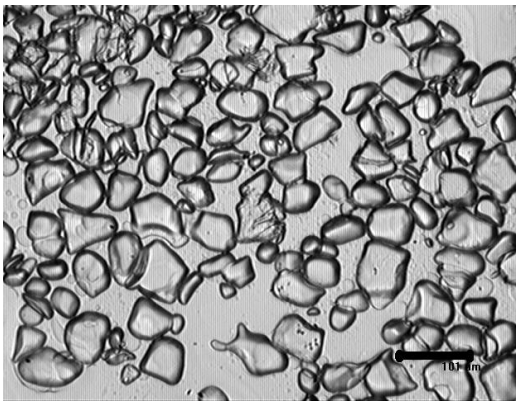

100% OR

Figure F.14: Microscope images of ice crystals for ice creams made with 100:0 (mono- and diglyceride:polysorbate 80 - MDG:PS80) emulsifier ratio and processed at 500 RPM at 50% and 100% overrun (OR) (40x magnification, 100 µm scale bar).

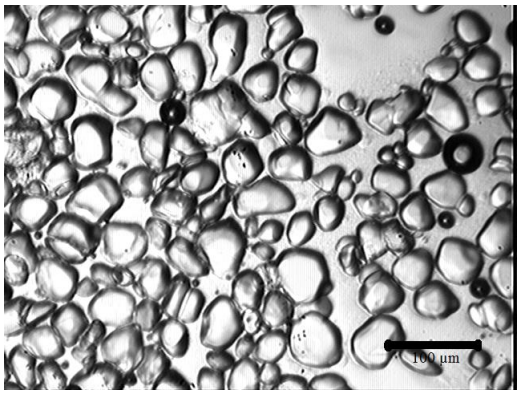

50% OR

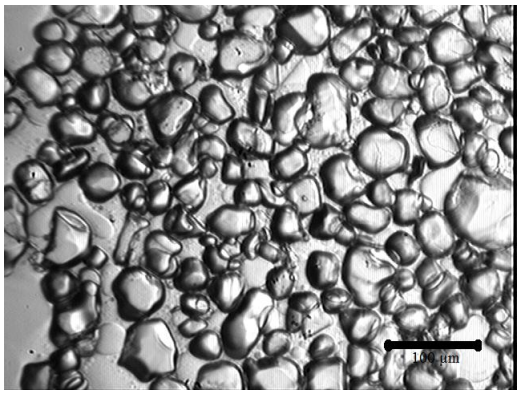

75% OR

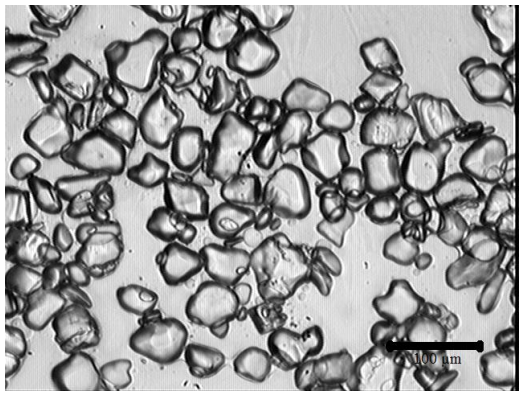

100% OR

Figure F.15: Microscope images of ice crystals in ice creams processed with 90:10 (mono- and diglyceride:polysorbate 80 - MDG:PS80) emulsifier ratio at 50%, 75%, and 100% overrun (OR) at 500 RPM (40x magnification, 100 µm scale bar).

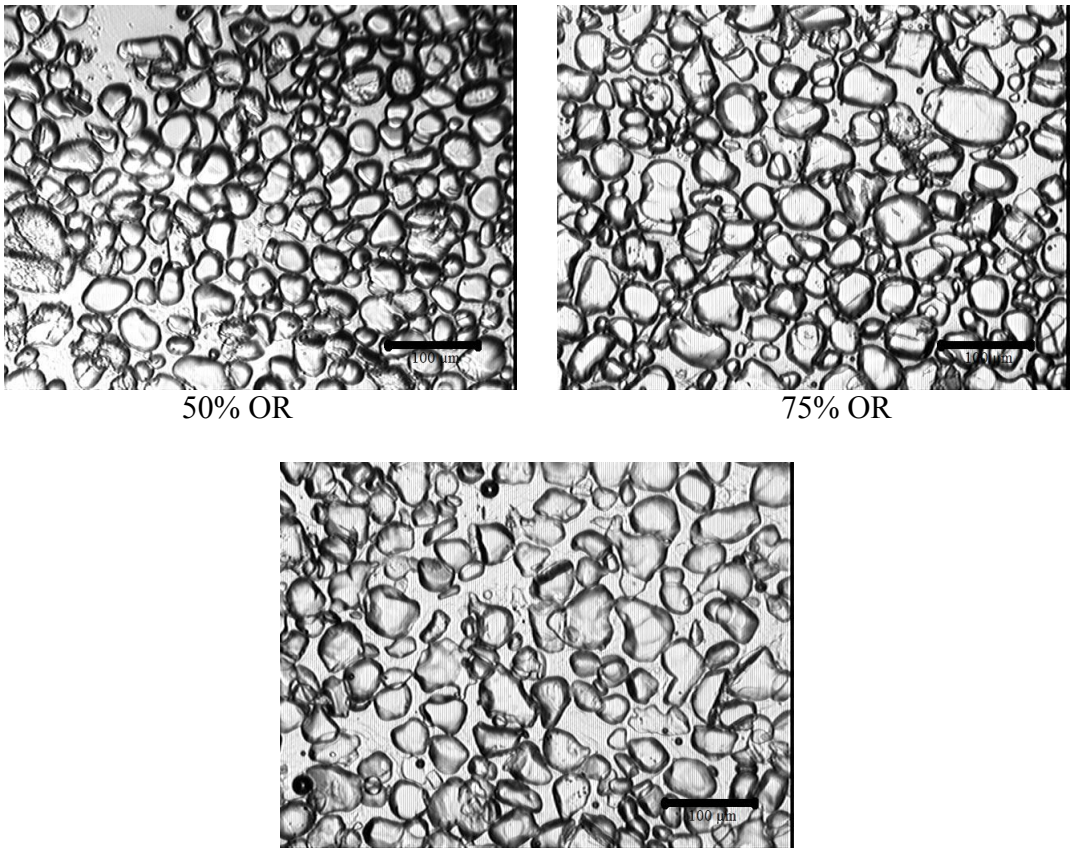

50% OR 75% OR

100% OR

Figure F.16: Microscope images of ice crystals from ice creams made with 80:20 (mono- and diglyceride:polysorbate 80 - MDG:PS80) emulsifier ratio at 50%, 75%, and 100% overrun (OR) at 500 RPM (40x magnification, 100 µm scale bar).

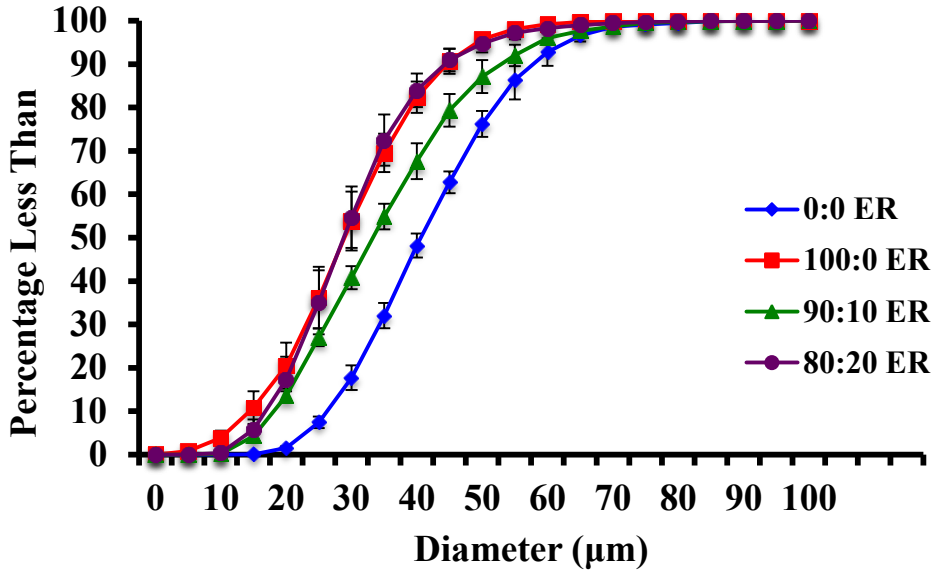

Figure F.17: Ice crystal size distributions of ice cream made with no added emulsifiers (0:0 (mono- and diglyceride:polysorbate 80 - MDG:PS80)), 100:0 (MDG:PS80), 90:10 (MDG:PS80), and 80:20 (MDG:PS80) emulsifier ratios (ER) at 100% overrun and 750 RPM. The error bars represent the standard deviations of the mean ice crystal sizes measured.

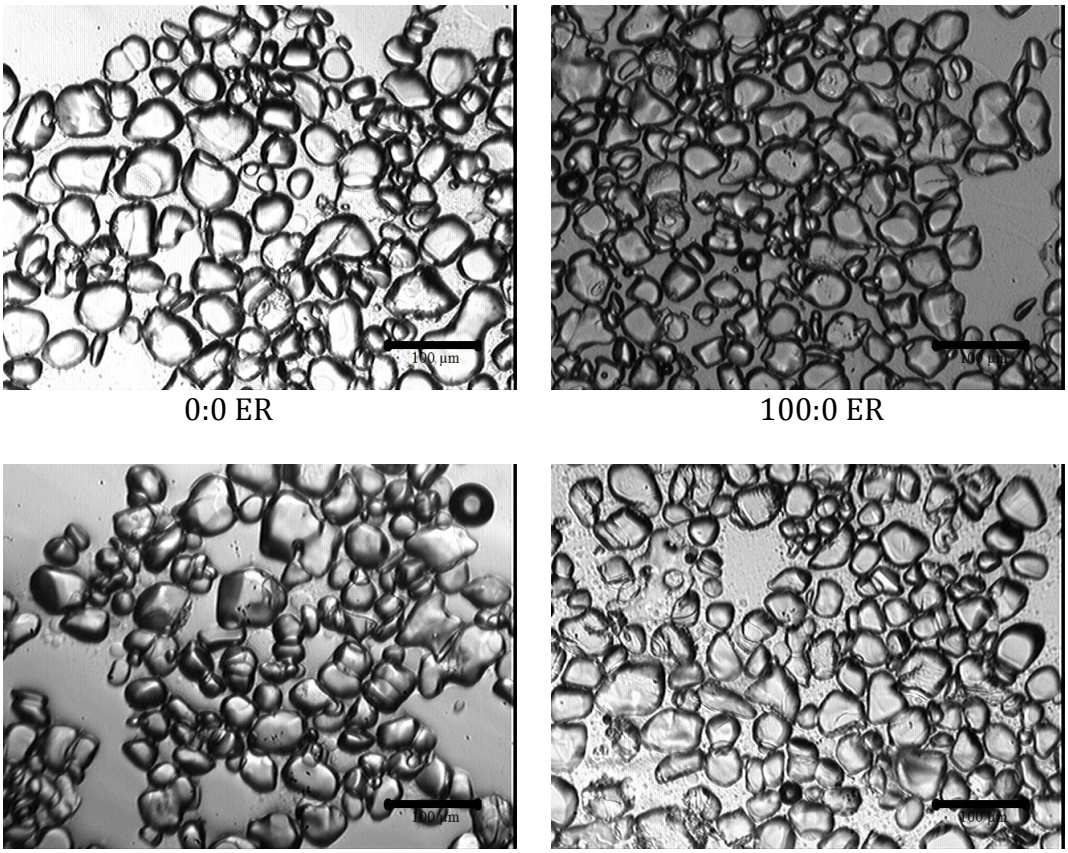

Figure F.18: Microscope images of ice crystals from ice cream made with no added emulsifiers (0:0 (mono- and diglyceride:polysorbate 80 - MDG:PS80)) 100:0 (MDG:PS80), 90:10 (MDG:PS80), and 80:20 (MDG:PS80) emulsifier ratios (ER) at 500 RPM and 50% overrun and 750 RPM and 100% overrun.

Appendix G: Particle size distributions for 75% and 100% overrun and 250 RPM and 750 RPM across all dasher speed at each emulsifier ratio.

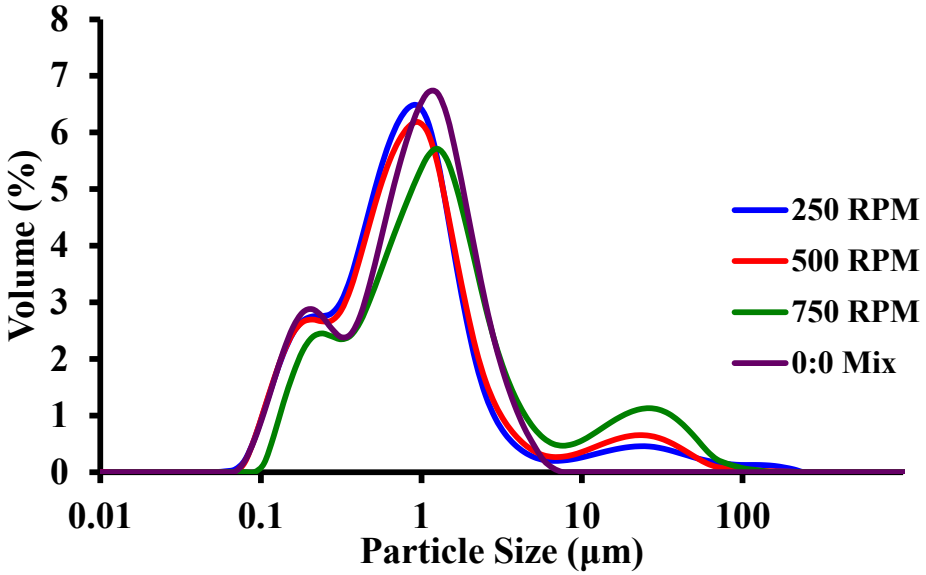

Figure G.1: Particle size distributions for ice cream mix made with no added emulsifiers and ice creams processed at 75% overrun and at set dasher speeds of 250 RPM, 500 RPM, and 750 RPM.

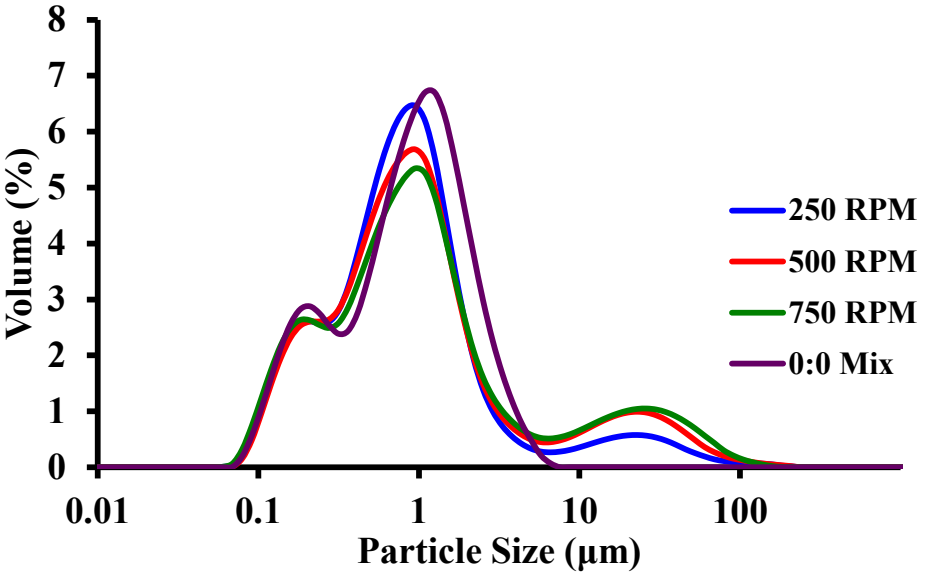

Figure G.2: Particle size distributions for ice cream mix made with no added emulsifiers and ice creams processed at 100% overrun and at set dasher speeds of 250 RPM, 500 RPM, and 750 RPM.

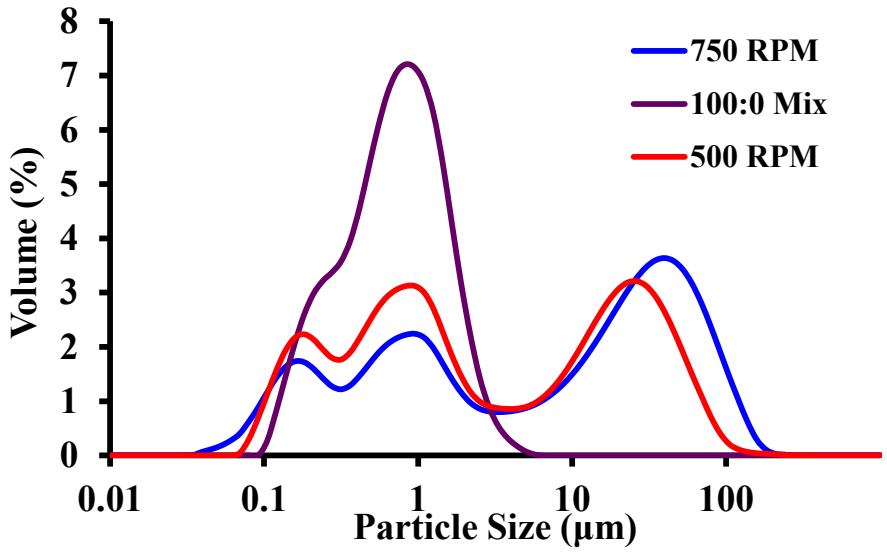

Figure G.3: Particle size distributions for ice cream mix made 100:0 (mono- and diglyceride:polysorbate 80 - MDG:PS80) and ice creams processed at 100% overrun and at set dasher speeds of 500 RPM and 750 RPM.

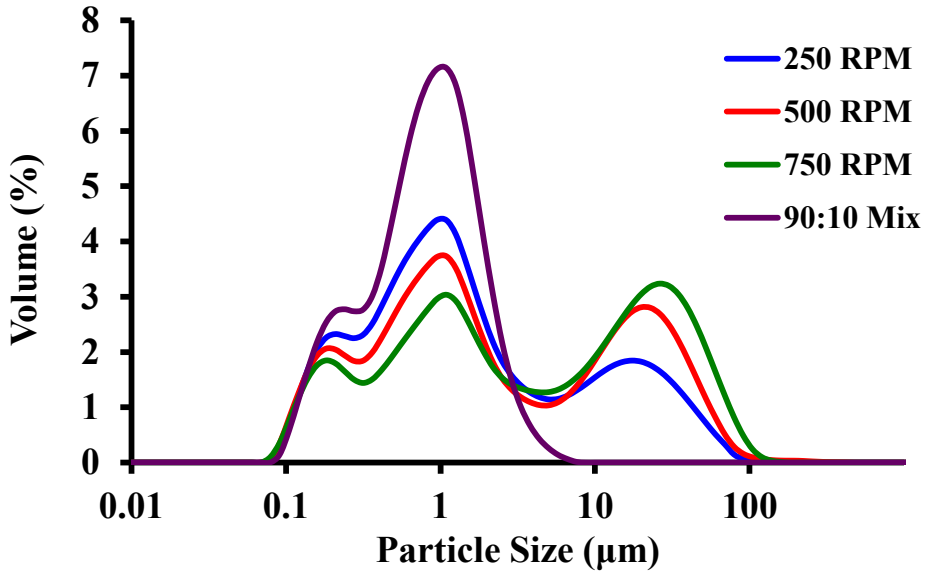

Figure G.4: Particle size distributions for ice cream mix made with 90:10 (mono- and diglyceride:polysorbate 80 - MDG:PS80) and ice creams processed at 75% overrun at dasher speeds of 250 RPM, 500 RPM, and 750 RPM.

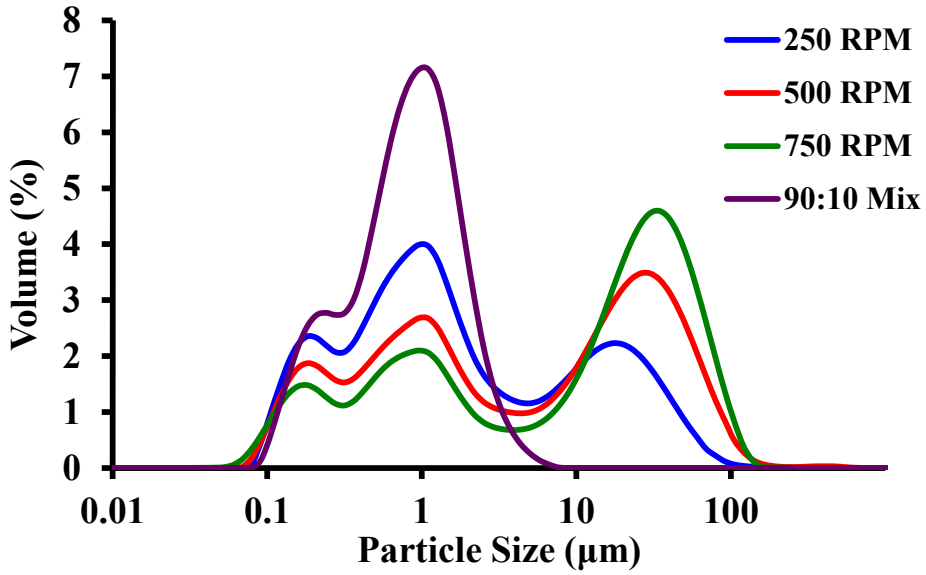

Figure G.5: Particle size distributions for ice cream mix made with 90:10 (mono- and diglyceride:polysorbate 80 - MDG:PS80) and ice creams processed at 100% overrun at dasher speeds of 205 RPM, 500 RPM, and 750 RPM.

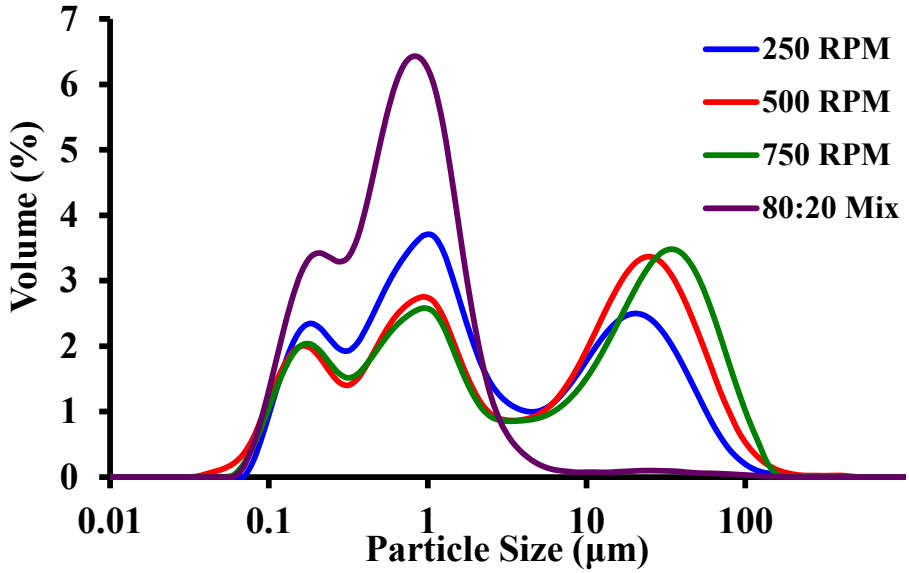

Figure G.6: Particle size distributions for ice cream mix made with 80:20 (mono- and diglyceride:polysorbate 80 - MDG:PS80) and ice creams processed at 75% overrun and at set dasher speeds of 250 RPM, 500 RPM, and 750 RPM.

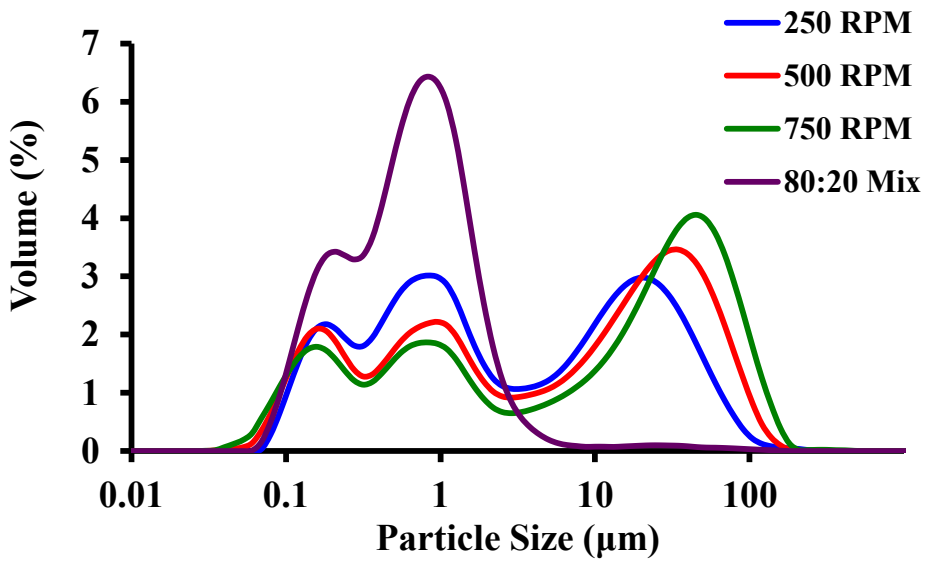

Figure G.7: Particle size distributions for ice cream mix made with 80:20 (mono- and diglyceride:polysorbate 80 - MDG:PS80) and ice creams processed at 100% overrun and at set dasher speeds of 250 RPM, 500 RPM, and 750 RPM.

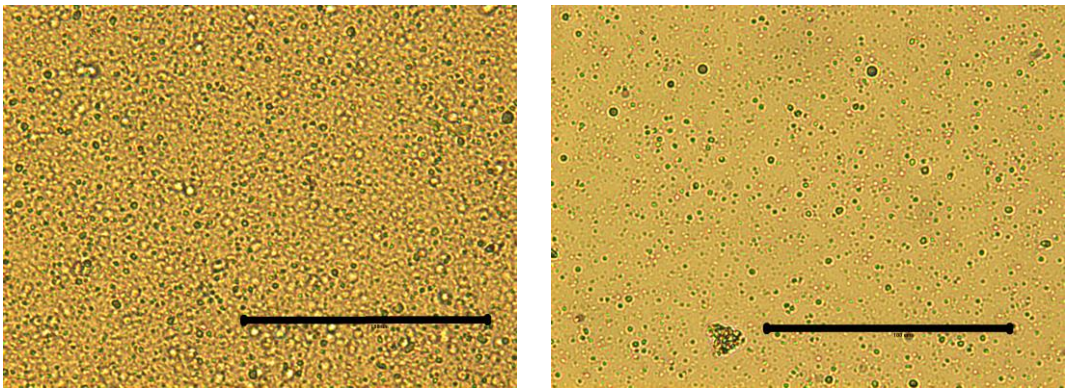

a.1: 250 RPM, 75% OR **a.2:** 250 RPM, 100% OR

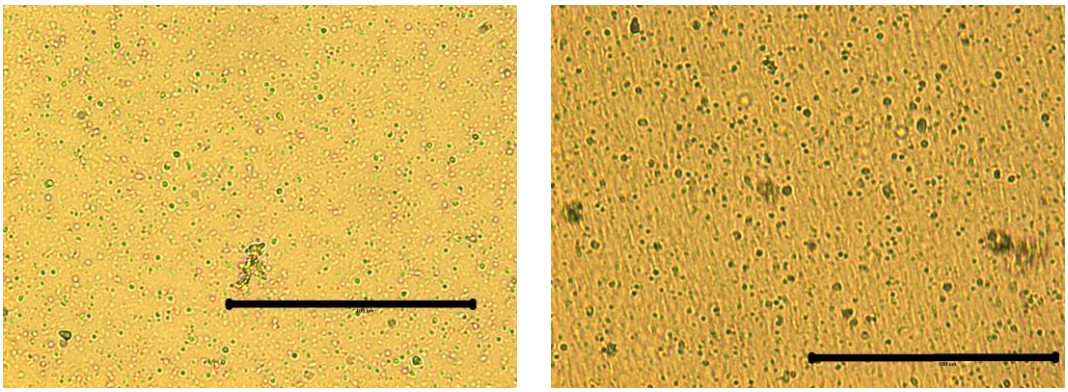

b.1: 500 RPM, 75% OR **b.2:** 500 RPM, 100% OR

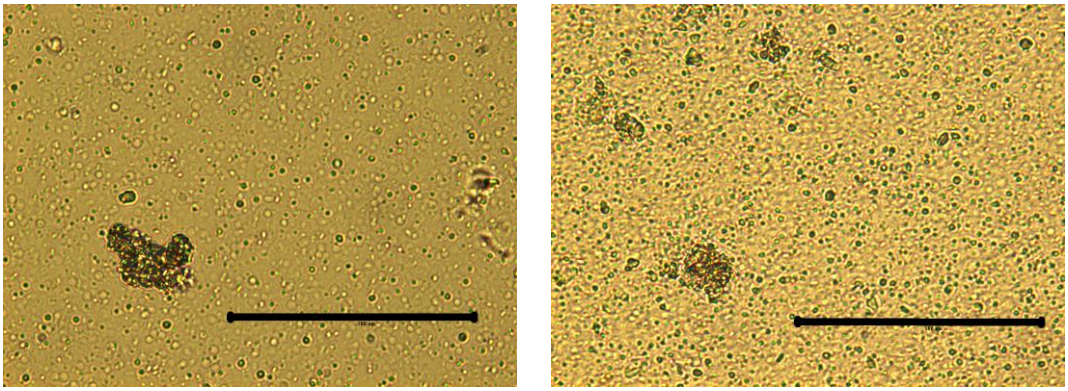

c.1: 750 RPM, 75% OR **c.2:** 750 RPM, 100% OR

Figure G.8: Microscope images of melted ice creams made with no added emulsifiers at dasher speeds of 250 RPM (**a**), 500 RPM (**b**), and 750 RPM (**c**) and at 75% (**1**) and 100% (**2**) overrun (OR) (400x magnification, 100 μm scale bar).

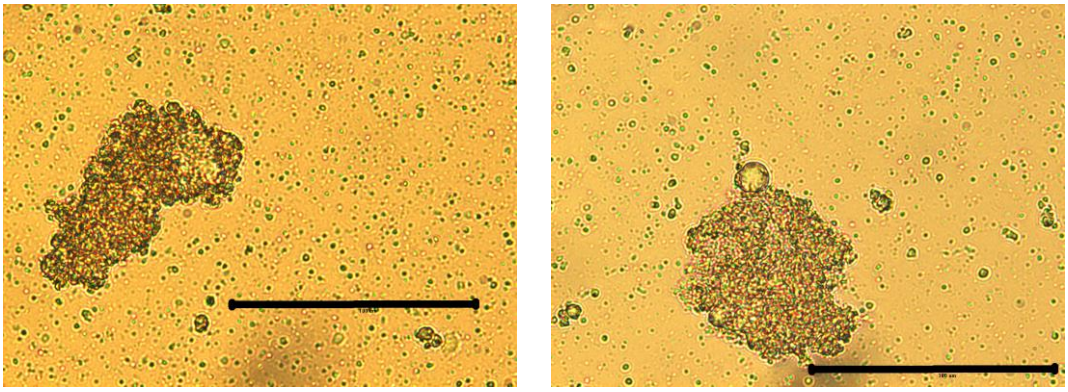

500 RPM 750 RPM

Figure G.9: Microscope images of melted ice creams made with 100:0 (mono- and diglyceride:polysorbate 80 - MDG:PS80) at 100% overrun and dasher speeds of 500 RPM and 750 RPM (400x magnification, 100 μm scale bar).

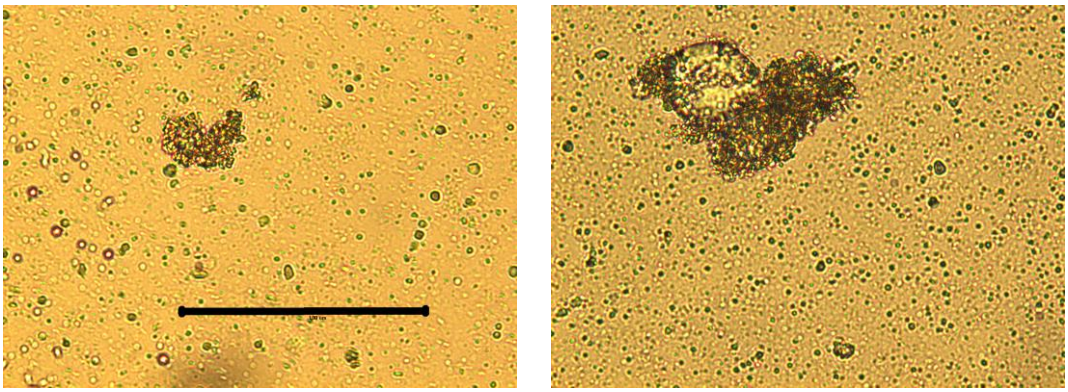

a.1: 250 RPM, 75% OR

a.2: 250 RPM, 100% OR

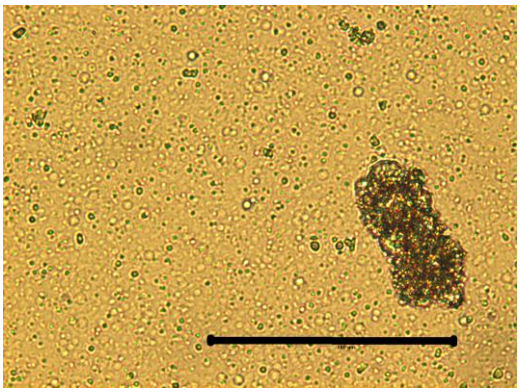

b.1: 500 RPM, 75% OR

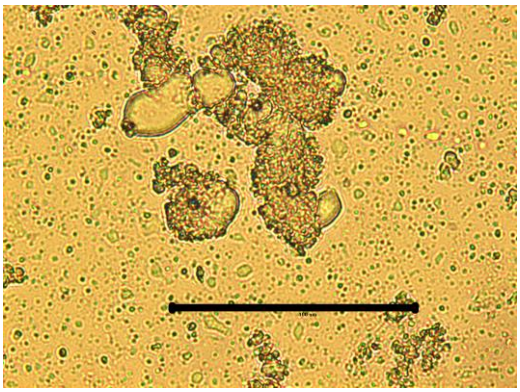

b.2: 500 RPM, 100% OR

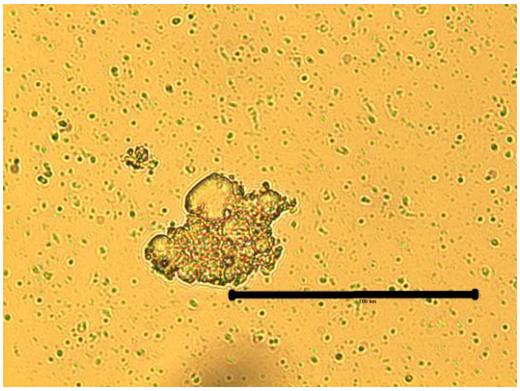

c.1: 750 RPM, 75% OR

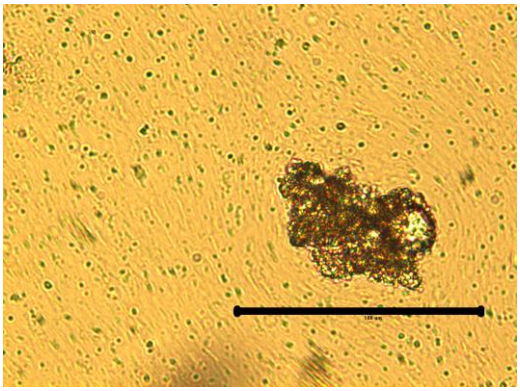

c.2: 750 RPM, 100% OR

Figure G.10: Microscope images of melted ice creams made with 90:10 (mono- and diglyceride:polysorbate 80 - MDG:PS80) at dasher speeds of 250 RPM (**a**), 500 RPM (**b**), and 750 RPM (**c**) and at 75% (**1**) and 100% (**2**) overrun (OR) (400x magnification, 100 μm scale bar).

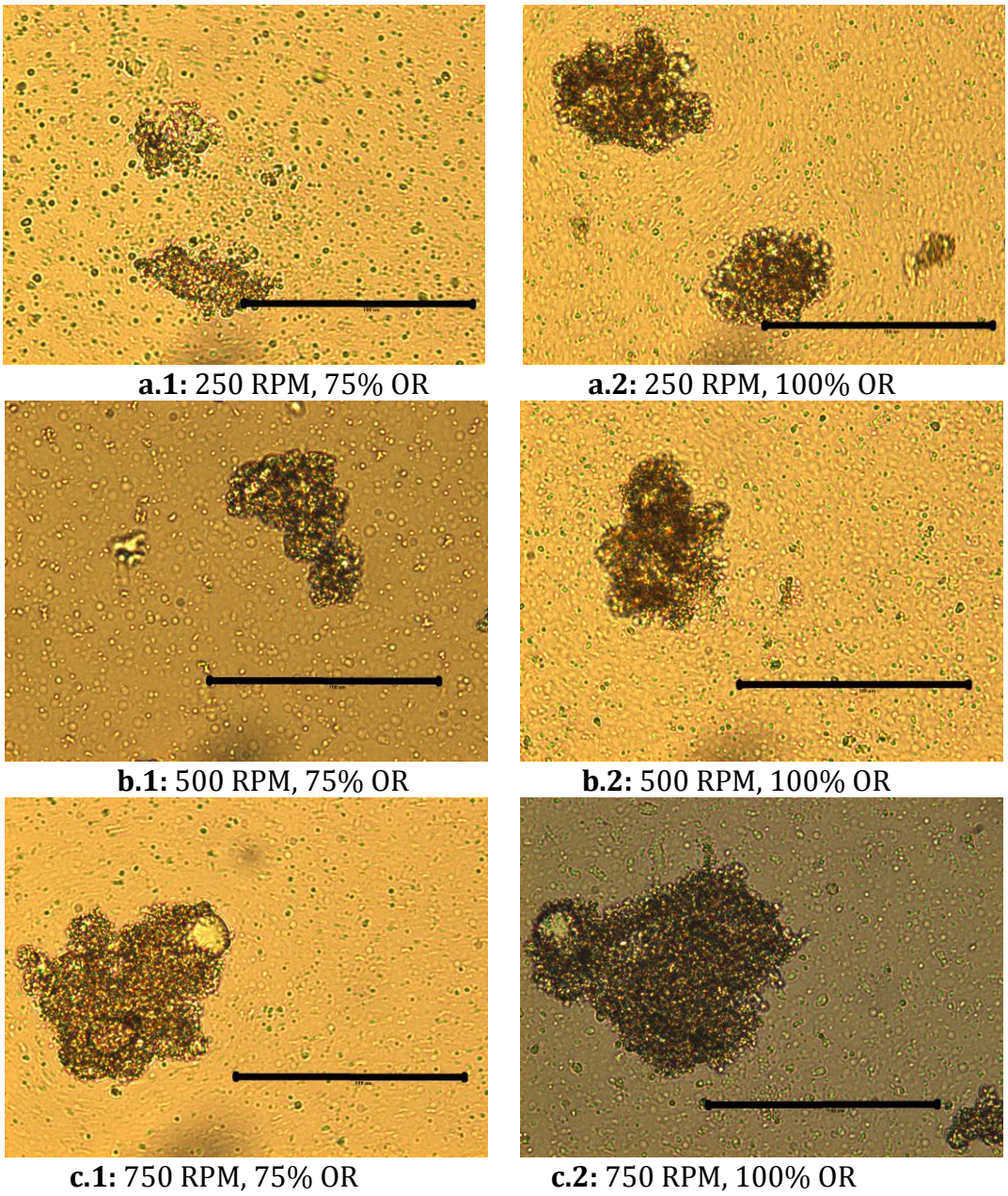

Figure G.11: Microscope images of melted ice creams made with 80:20 (mono- and diglyceride:polysorbate 80 - MDG:PS80) at dasher speeds of 250 RPM (**a**), 500 RPM (**b**), and 750 RPM (**c**) and at 75% (**1**) and 100% (**2**) overrun (OR) (400x magnification, 100 μm scale bar).

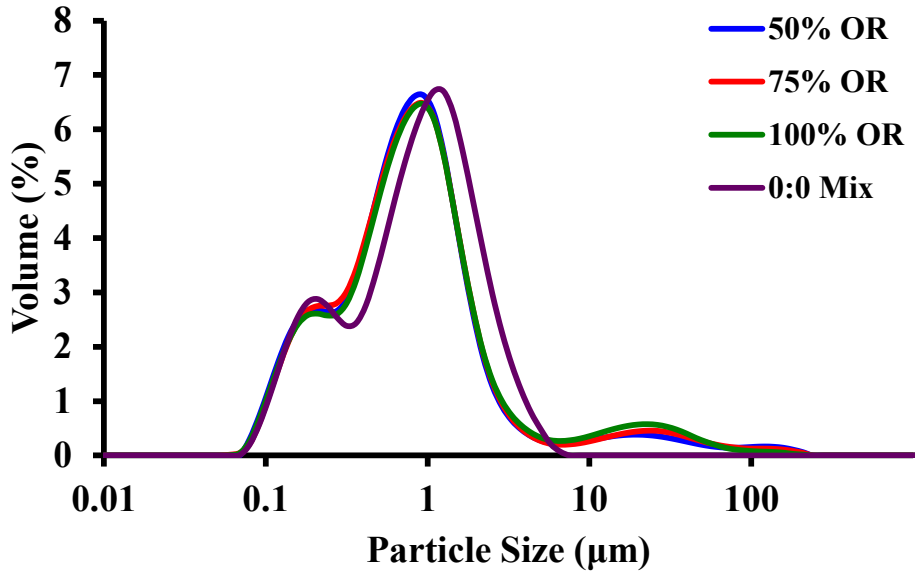

Figure G.12: Particle size distributions for ice cream mix made with no added emulsifiers and ice creams processed at dasher speed of 250 RPM with overruns (OR) of 50%, 75%, and 100%.

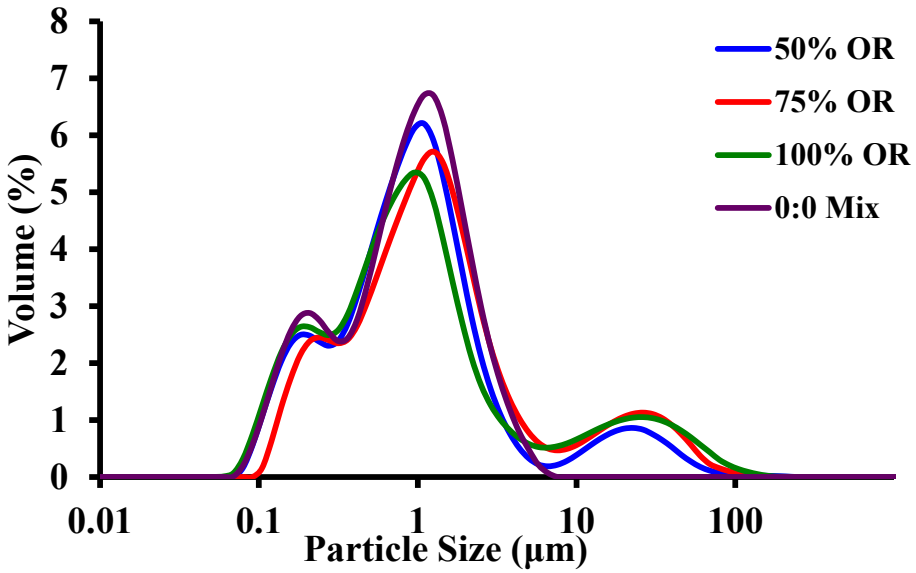

Figure G.13: Particle size distributions for ice cream mix made with no added emulsifiers and ice creams processed at dasher speed of 750 RPM with overruns (OR) of 50%, 75%, and 100%.

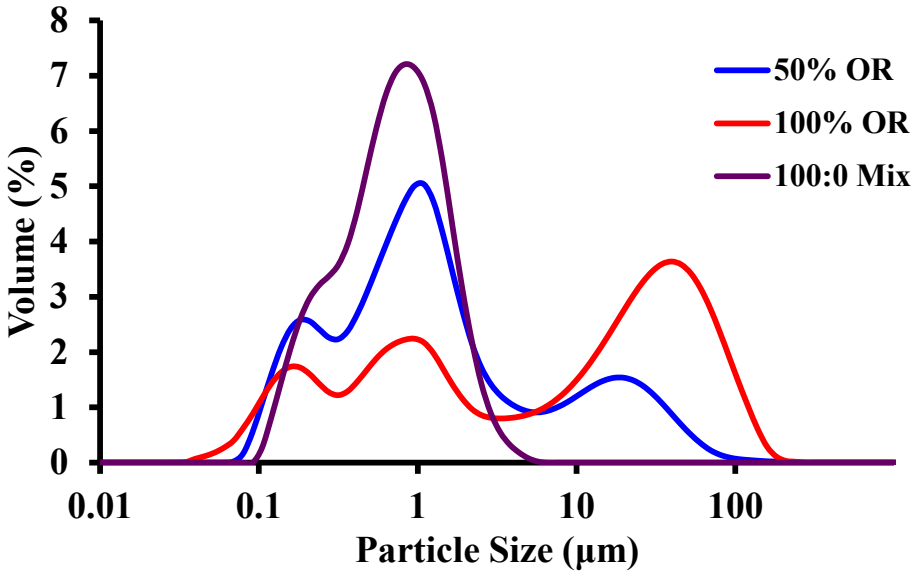

Figure G.14: Particle size distributions for ice cream mix made with 100:0 (mono- and diglyceride:polysorbate 80 - MDG:PS80) and ice creams processed at dasher speed of 750 RPM and overruns (OR) of 50% and 100%.

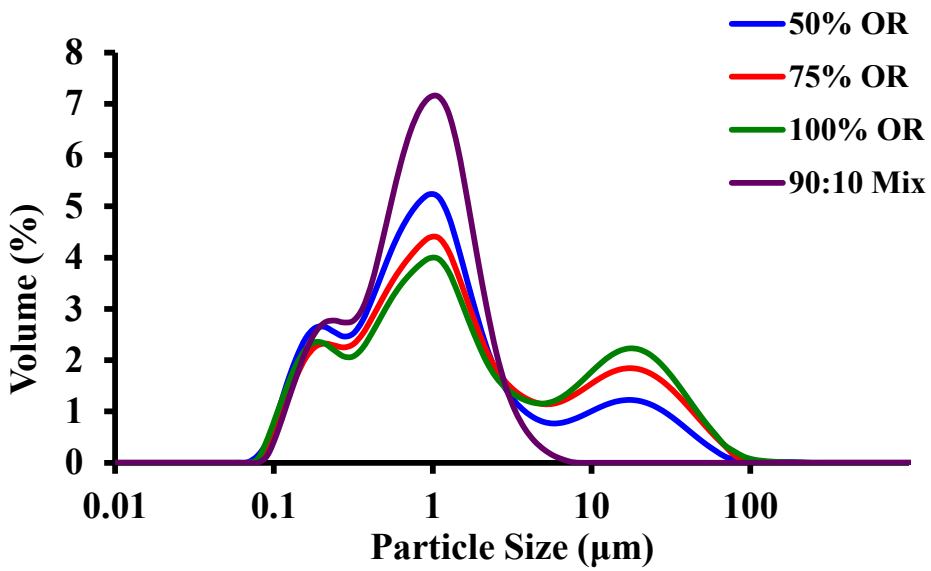

Figure G.15: Particle size distributions for ice cream mix made with 90:10 (mono- and diglyceride:polysorbate 80 - MDG:PS80) and ice creams processed at dasher speed of 250 RPM and overruns (OR) of 50%,75%, and 100%.

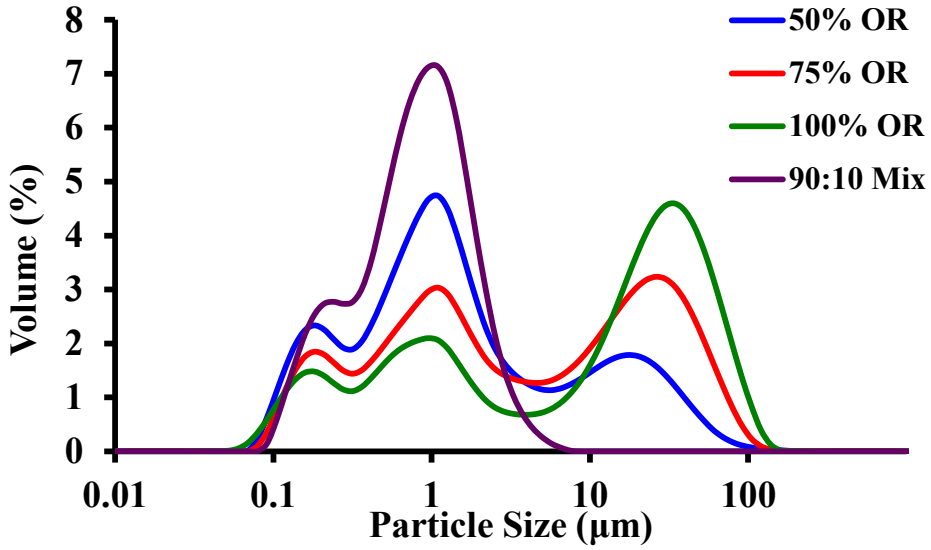

Figure G.16: Particle size distributions for ice cream mix made with 90:10 (mono- and diglyceride:polysorbate 80 - MDG:PS80) and ice creams processed at dasher speed of 750 RPM and overruns (OR) of 50%,75%, and 100%.

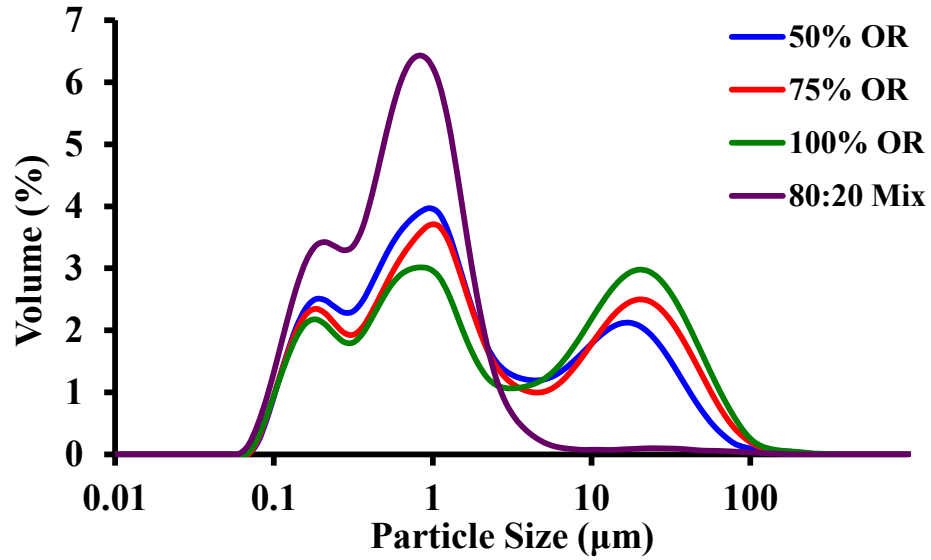

Figure G.17: Particle size distributions for ice cream mix made with 80:20 (mono- and diglyceride:polysorbate 80 - MDG:PS80) and ice creams processed at dasher speed of 250 RPM and overruns (OR) of 50%,75%, and 100%.

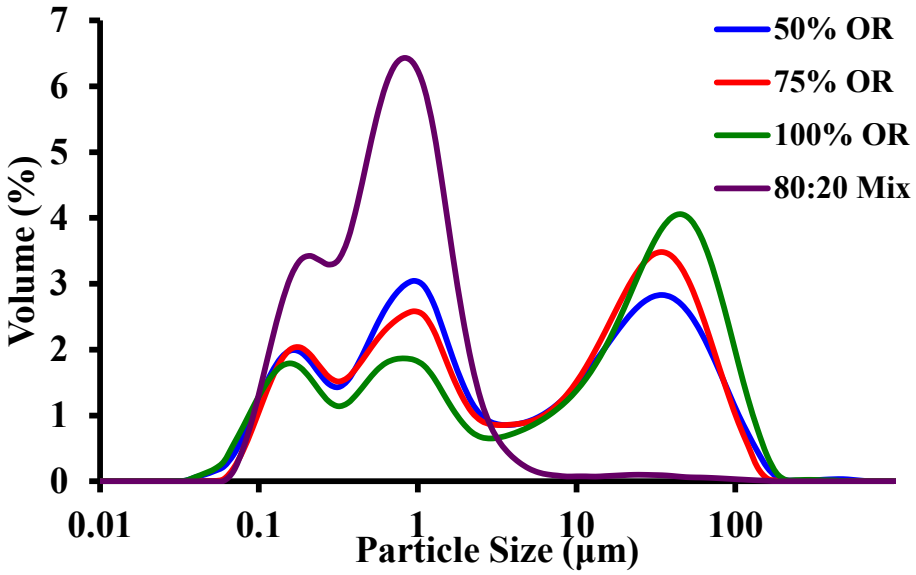

Figure G.18: Particle size distributions for ice cream mix made with 80:20 (mono- and diglyceride:polysorbate 80 - MDG:PS80) and ice creams processed at dasher speed of 750 RPM and overruns (OR) of 50%,75%, and 100%.

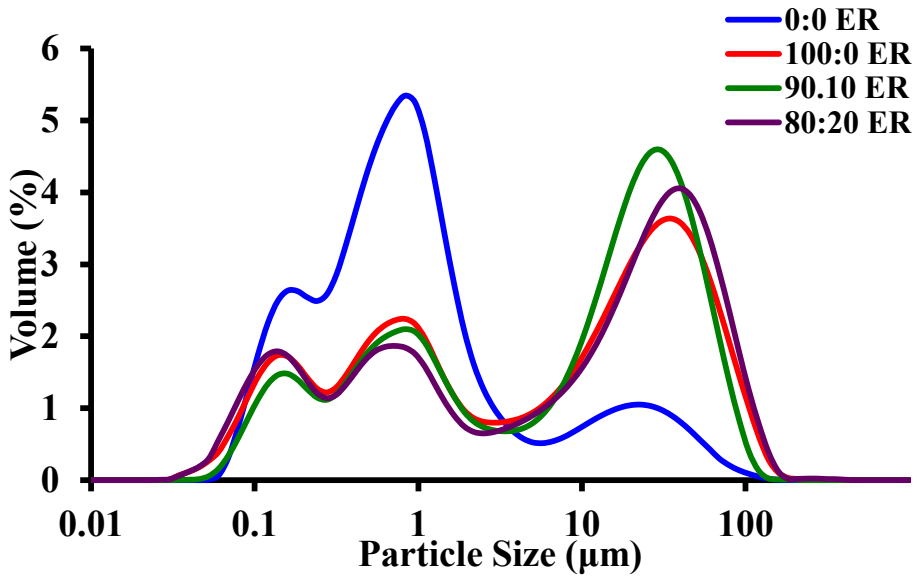

Figure G.19: Particle size distributions for ice creams processed at 750 RPM, 100% overrun, and with no added emulsifiers (0:0 ((mono- and diglyceride:polysorbate 80 - MDG:PS80)), 100:0 (MDG:PS80), 90:10 (MDG:PS80), and 80:20 (MDG:PS80) emulsifier ratio (ER).

Appendix H: Drip-through curves (% weight) and images of remnant foam left atop the screen at the end of the drip-through test.

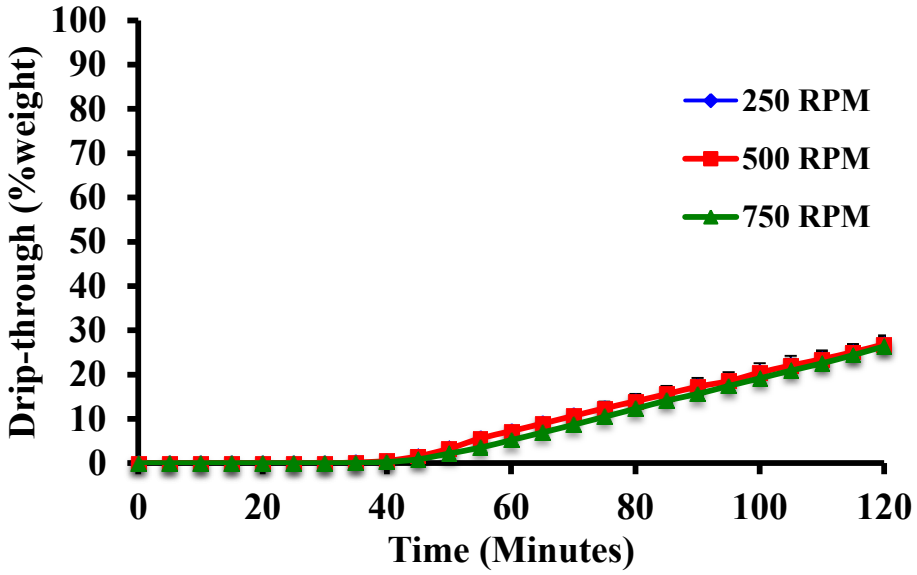

Figure H.1: Drip-through (% weight) curves for ice creams made with no added emulsifiers at 75% overrun and 250 RPM, 500 RPM, and 750 RPM. The error bars represent the standard deviations of the mean drip-through (%weight) measured.

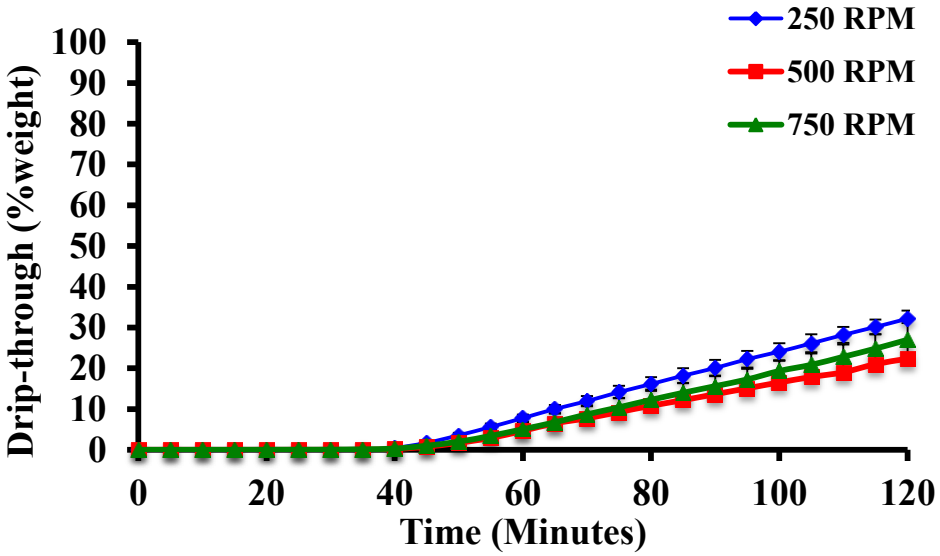

Figure H.2: Drip-through (% weight) curves for ice creams made with no added emulsifiers at 100% overrun and 250 RPM, 500 RPM, and 750 RPM. The error bars represent the standard deviations of the mean drip-through (%weight) measured.

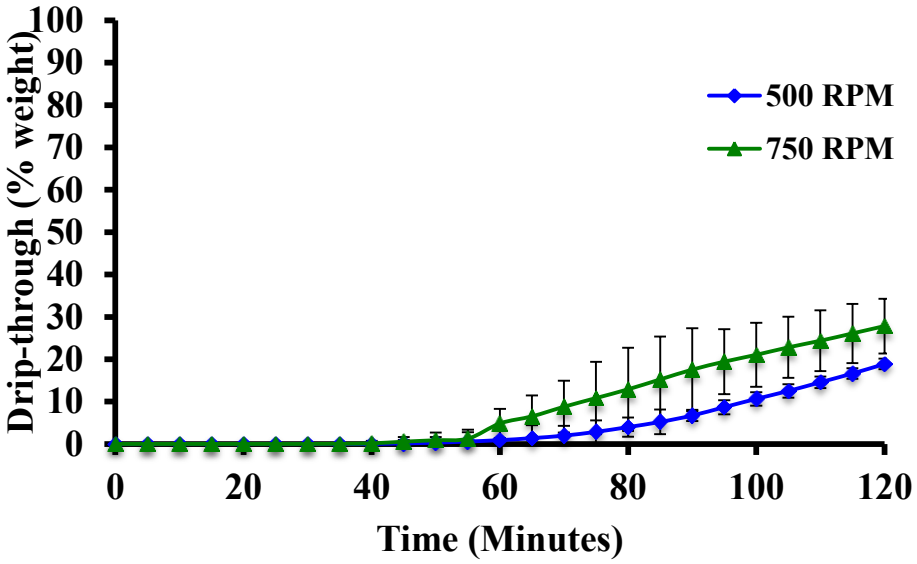

Figure H.3: Drip-through (% weight) curves for ice creams made with 100:0 (mono- and diglyceride:polysorbate 80 - MDG:PS80) emulsifiers at 100% overrun and 500 RPM and 750 RPM. The error bars represent the standard deviations of the mean drip-through (%weight) measured.

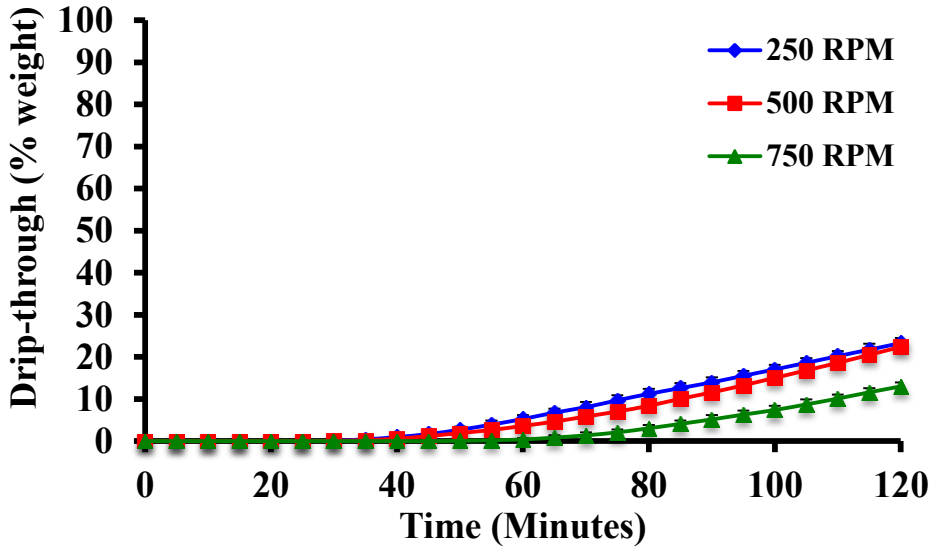

Figure H.4: Drip-through (% weight) curves for ice creams made with 90:10 (mono- and diglyceride:polysorbate 80 - MDG:PS80) emulsifiers at 75% overrun and 250 RPM, 500 RPM, and 750 RPM. The error bars represent the standard deviations of the mean drip-through (%weight) measured.

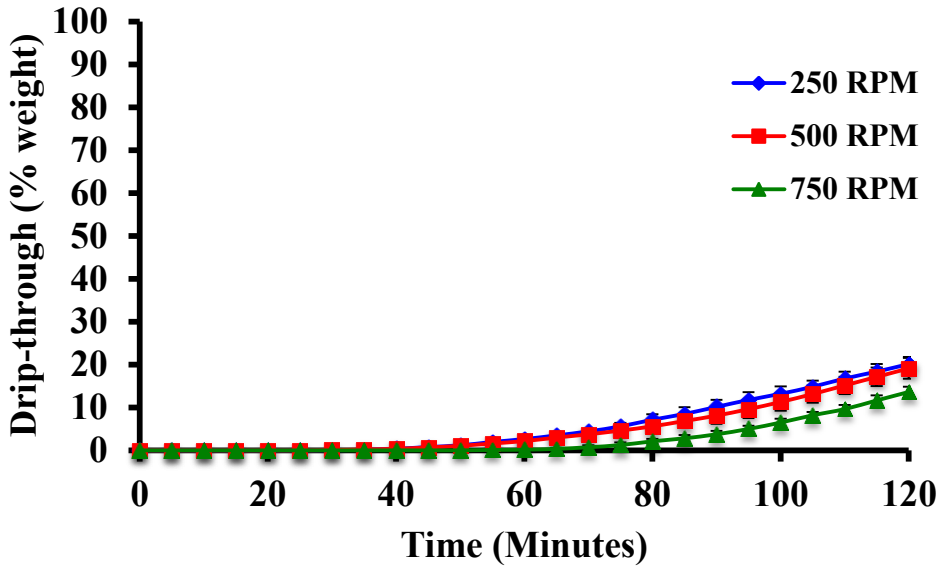

Figure H.5: Drip-through (% weight) curves for ice creams made with 90:10 (mono- and diglyceride:polysorbate 80 - MDG:PS80) emulsifiers at 100% overrun and 250 RPM, 500 RPM, and 750 RPM. The error bars represent the standard deviations of the mean drip-through (%weight) measured.

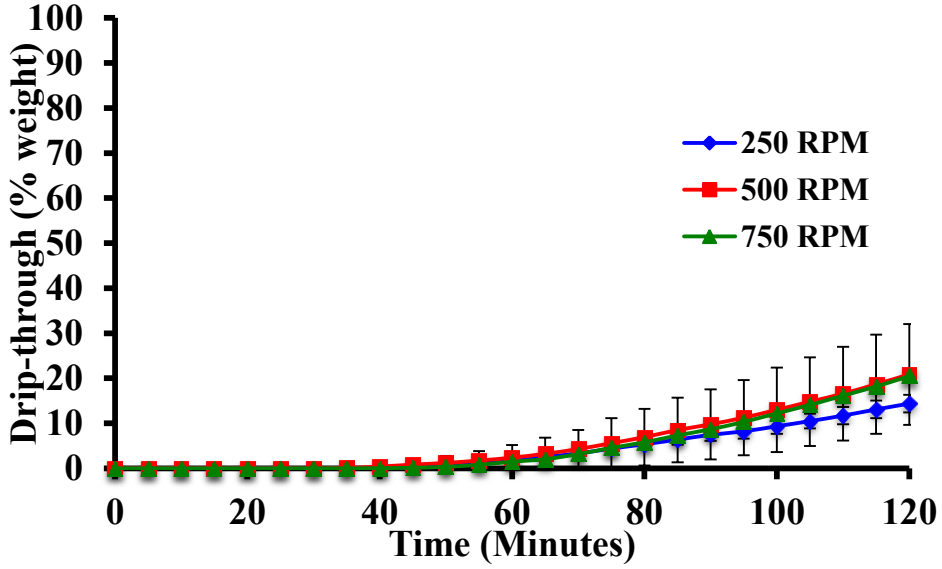

Figure H.6: Drip-through (% weight) curves for ice creams made with 80:20 (mono- and diglyceride:polysorbate 80 - MDG:PS80) emulsifiers at 75% overrun and 250 RPM, 500 RPM, and 750 RPM. The error bars represent the standard deviations of the mean drip-through (%weight) measured.

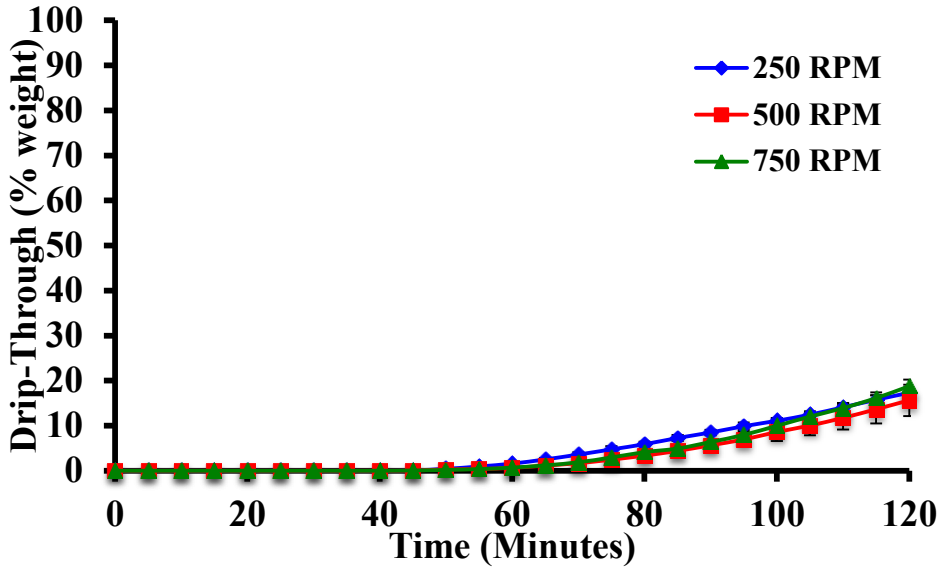

Figure H.7: Drip-through (% weight) curves for ice creams made with 80:20 (mono- and diglyceride:polysorbate 80 - MDG:PS80) emulsifiers at 100% overrun and 250 RPM, 500 RPM, and 750 RPM. The error bars represent the standard deviations of the mean drip-through (%weight) measured.

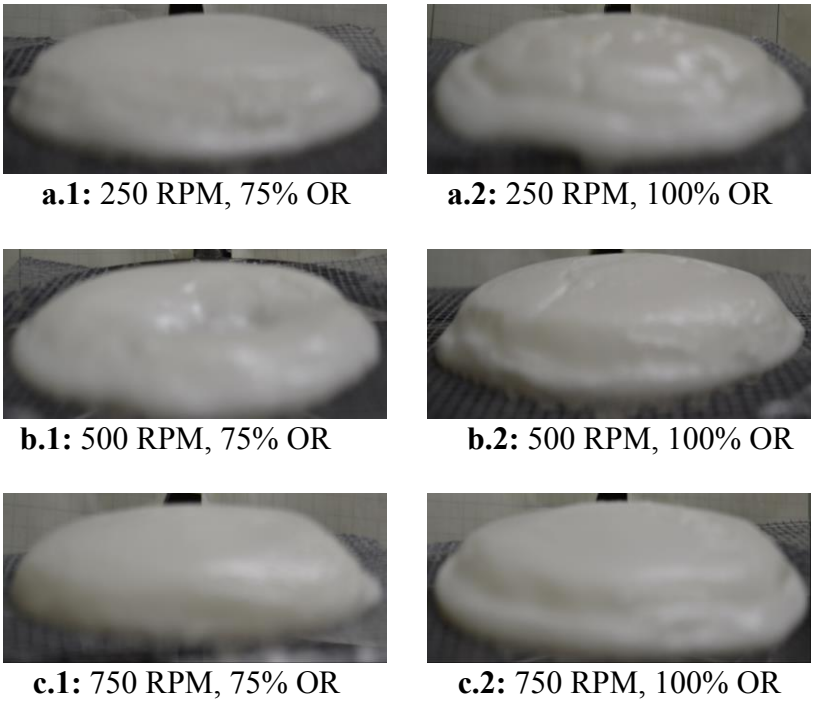

a.1: 250 RPM, 75% OR **a.2:** 250 RPM, 100% OR

b.1: 500 RPM, 75% OR **b.2:** 500 RPM, 100% OR

c.1: 750 RPM, 75% OR **c.2:** 750 RPM, 100% OR

Figure H.8: Images of ice cream structure left on top of screen at the end of a drip-through test of ice creams made with no added emulsifiers at dasher speeds of 250 RPM (**a**), 500 RPM (**b**), and 750 RPM (**c**) and at 75% (**1**) and 100% (**2**) overrun (OR).

500 RPM 750 RPM

Figure H.9: Images of ice cream structure left on top of screen at the end of a drip-through test of ice creams made with 100:0 (mono- and diglyceride:polysorbate 80 - MDG:PS80) at 100% overrun and dasher speeds of 500 RPM and 750 RPM.

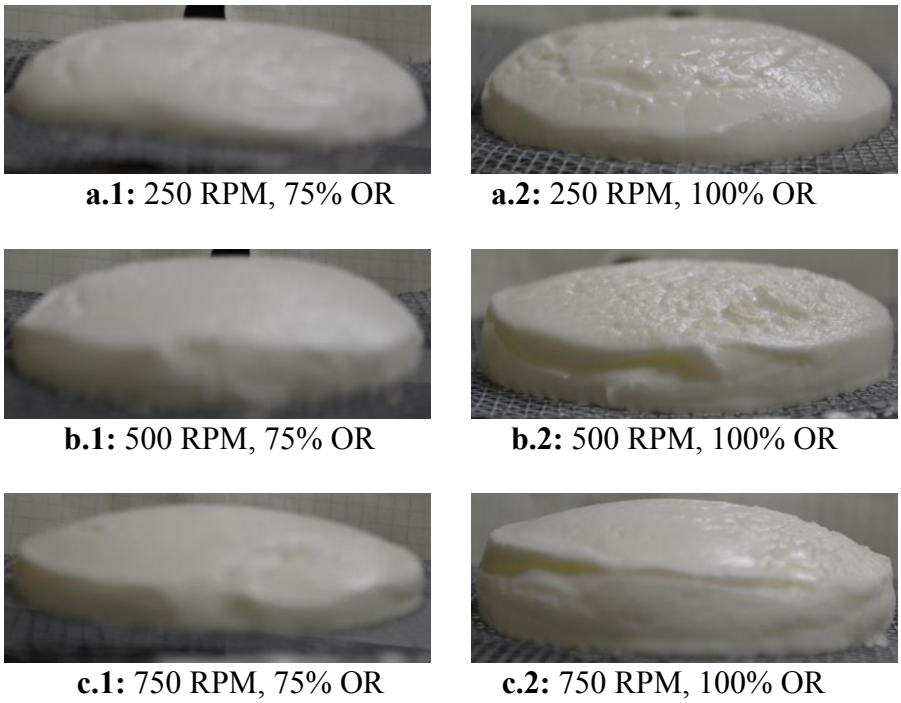

a.1: 250 RPM, 75% OR **a.2:** 250 RPM, 100% OR

b.1: 500 RPM, 75% OR **b.2:** 500 RPM, 100% OR

c.1: 750 RPM, 75% OR **c.2:** 750 RPM, 100% OR

Figure H.10: Images of ice cream structure left on top of screen at the end of a drip-through test of ice creams made with 90:10 (mono- and diglyceride:polysorbate 80 - MDG:PS80) emulsifier ratio at 100% overrun and at dasher speeds of 250 RPM (**a**), 500 RPM (**b**), and 750 RPM (**c**) and at 75% (**1**) and 100% (**2**) overrun (OR).

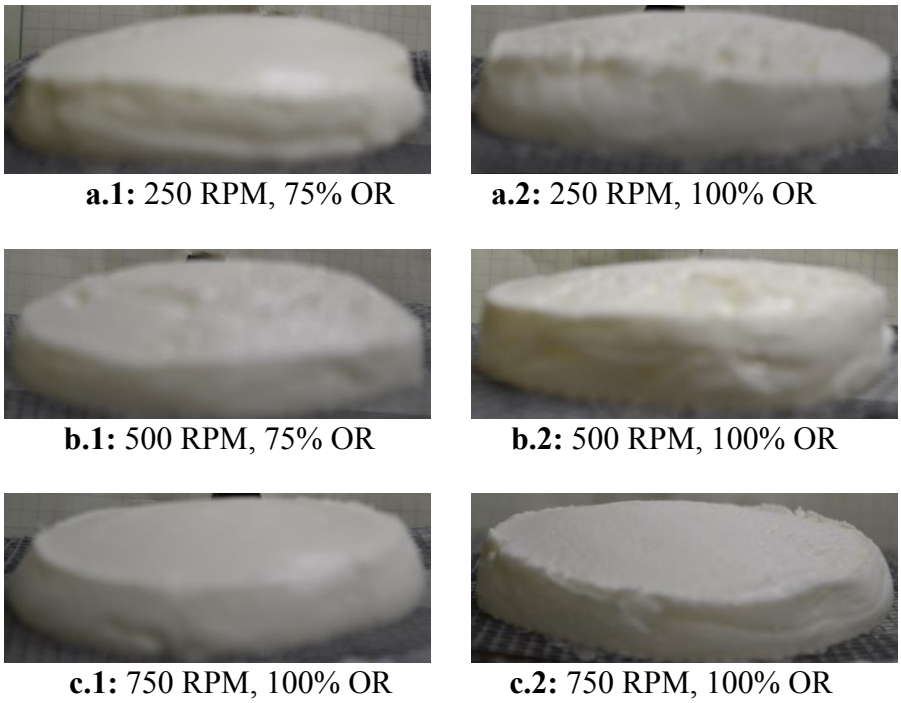

Figure H.11: Images of ice cream structure left on top of screen at the end of a drip-through test of ice creams made with 80:20 (mono- and diglyceride:polysorbate 80 - MDG:PS80) emulsifier ratio at 100% overrun and at dasher speeds of 250 RPM (**a**), 500 RPM (**b**), and 750 RPM (**c**) and at 75% (**1**) and 100% (**2**) overrun (OR).

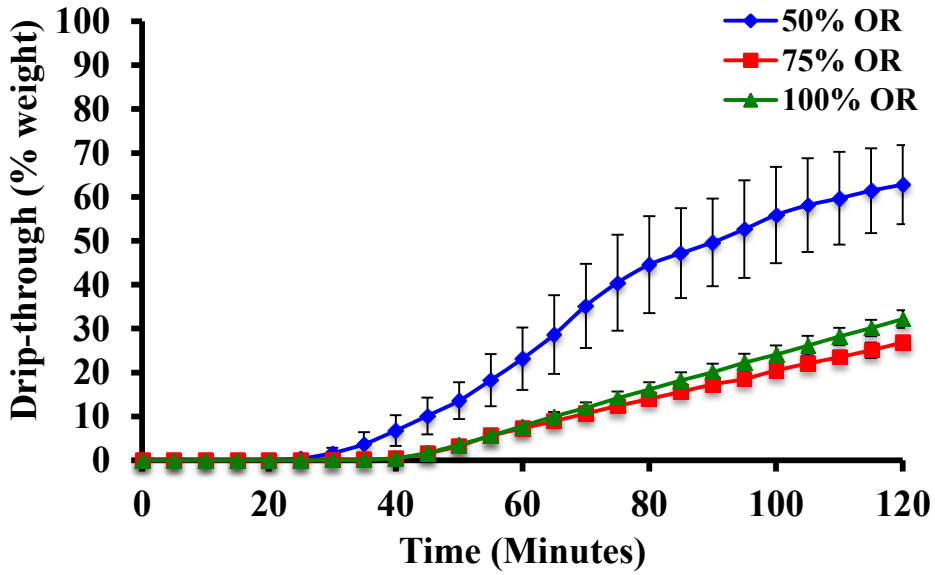

Figure H.12: Drip-through (% weight) curves for ice creams made with no added emulsifiers at 250 RPM and 50%, 75%, and 100% overrun (OR). The error bars represent the standard deviations of the mean drip-through (%weight) measured.

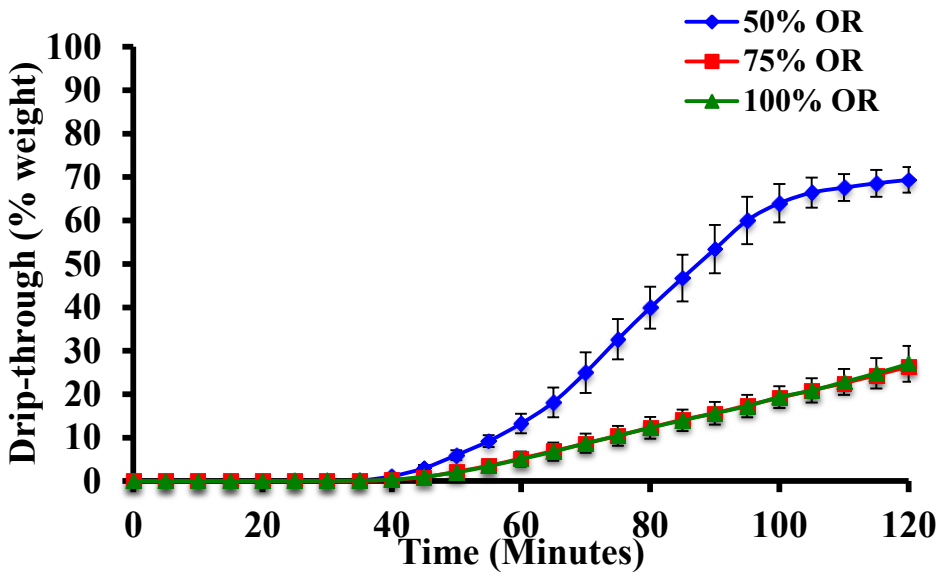

Figure H.13: Drip-through (% weight) curves for ice creams made with no added emulsifiers at 750 RPM and 50%, 75%, and 100% overrun (OR). The error bars represent the standard deviations of the mean drip-through (%weight) measured.

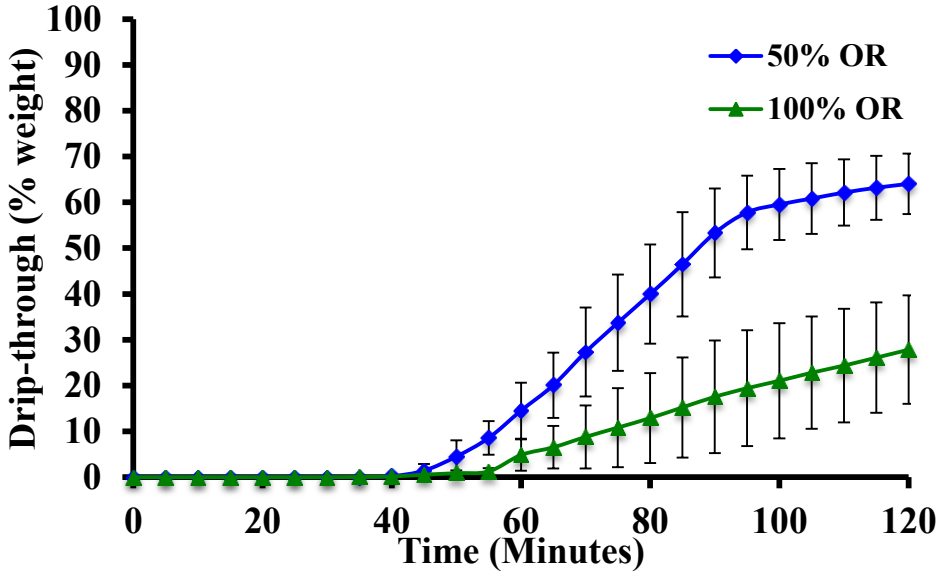

Figure H.14: Drip-through (% weight) curves for ice creams made with 100:0 (mono- and diglyceride:polysorbate 80 - MDG:PS80) emulsifier ratio at 750 RPM and 50% and 100% overrun (OR). The error bars represent the standard deviations of the mean drip-through (%weight) measured.

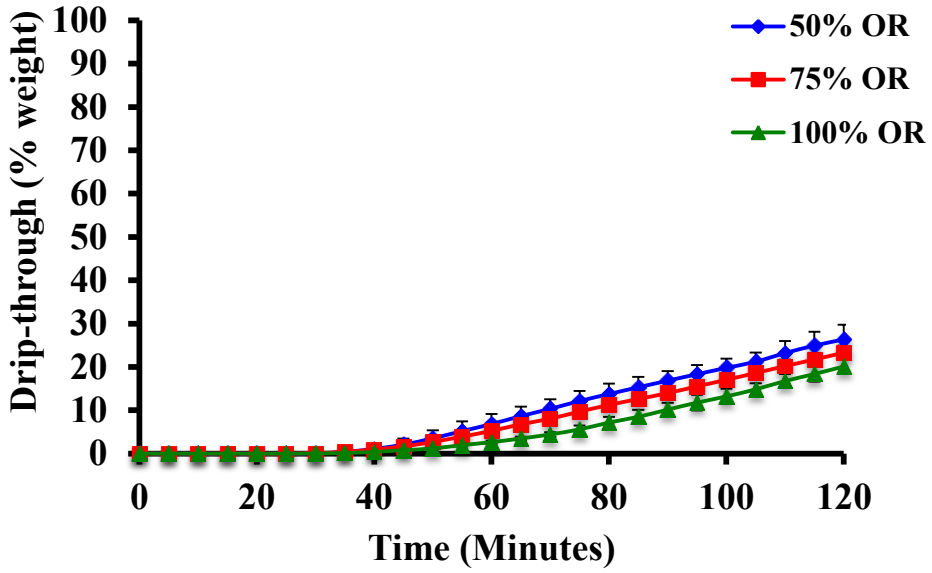

Figure H.15: Drip-through (% weight) curves for ice creams made with 90:10 (mono- and diglyceride:polysorbate 80 - MDG:PS80) emulsifier ratio at 250 RPM and 50%, 75%, and 100% overrun (OR). The error bars represent the standard deviations of the mean drip-through (%weight) measured.

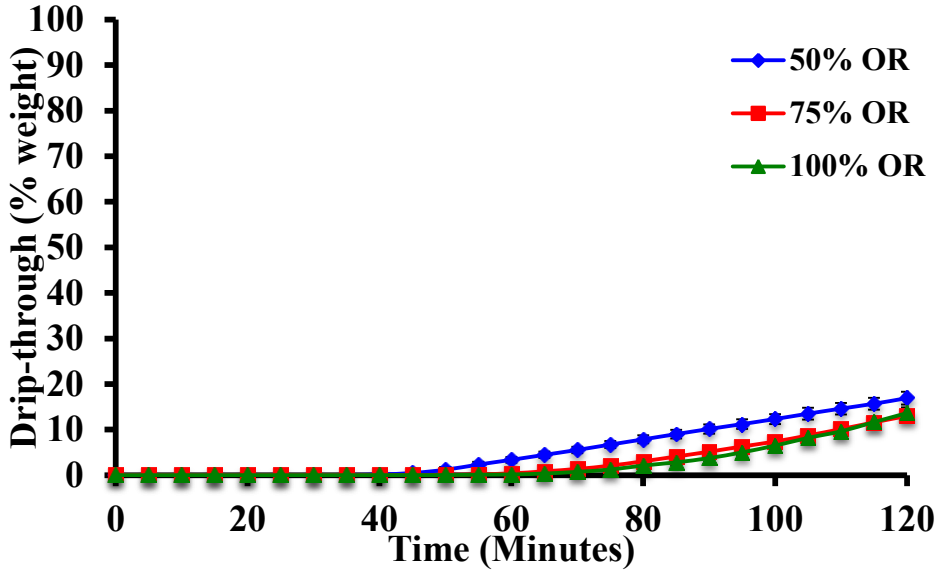

Figure H.16: Drip-through (% weight) curves for ice creams made with 90:10 (mono- and diglyceride:polysorbate 80 - MDG:PS80) emulsifier ratio at 750 RPM and 50%, 75%, and 100% overrun (OR). The error bars represent the standard deviations of the mean drip-through (%weight) measured.

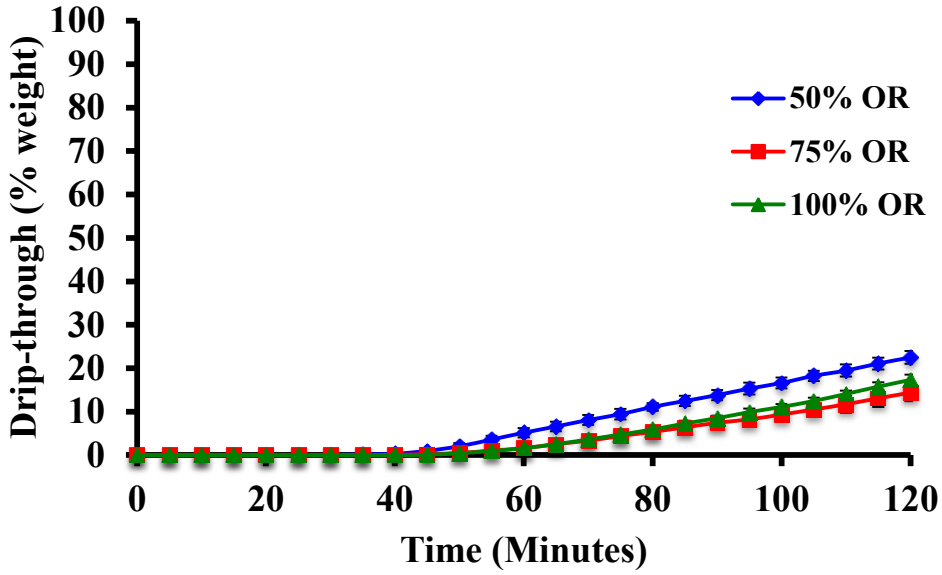

Figure H.17: Drip-through (% weight) curves for ice creams made with 80:20 (mono- and diglyceride:polysorbate 80 - MDG:PS80) emulsifier ratio at 250 RPM and 50%, 75%, and 100% overrun (OR). The error bars represent the standard deviations of the mean drip-through (%weight) measured.

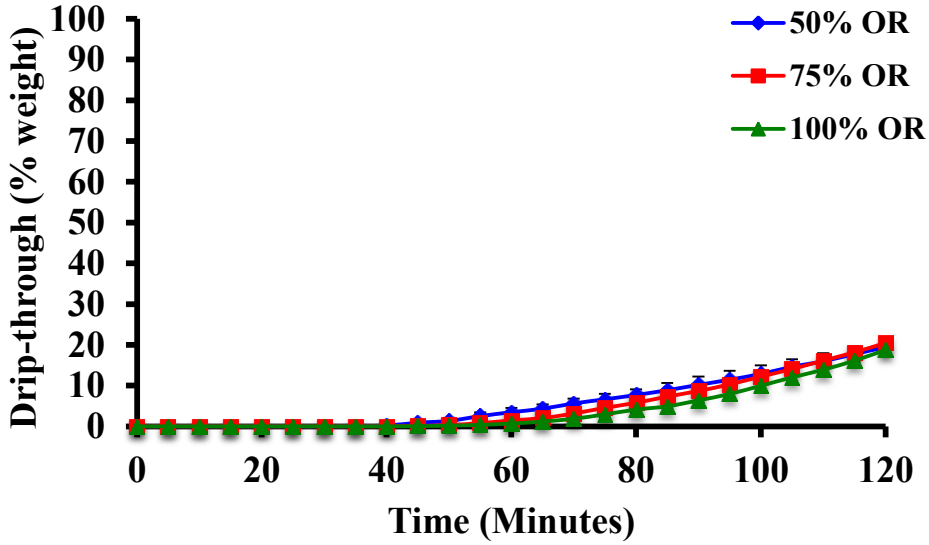

Figure H.18: Drip-through (% weight) curves for ice creams made with 80:20 (mono- and diglyceride:polysorbate 80 - MDG:PS80) emulsifier ratio at 750 RPM and 50%, 75%, and 100% overrun (OR). The error bars represent the standard deviations of the mean drip-through (%weight) measured.

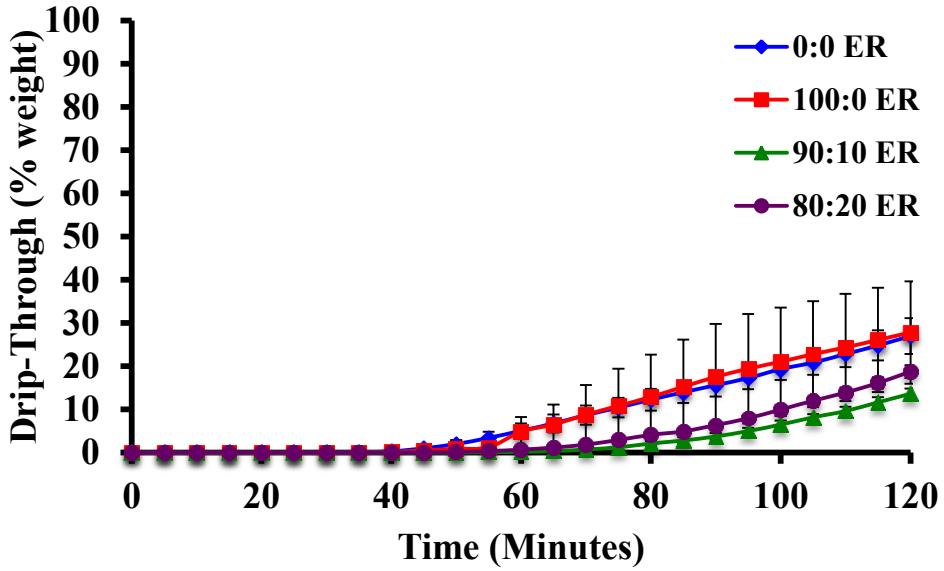

Figure H.19: Drip-through curves (% weight) for ice creams processed at (0:0 (mono- and diglyceride:polysorbate 80 - MDG:PS80)), 100:0 (MDG:PS80), 90:10 (MDG:PS80), and 80:20 (MDG:PS80) emulsifier ratios (ER) at 100% overrun and 750 RPM. The error bars represent the standard deviations of the mean drip-through (%weight) measured.

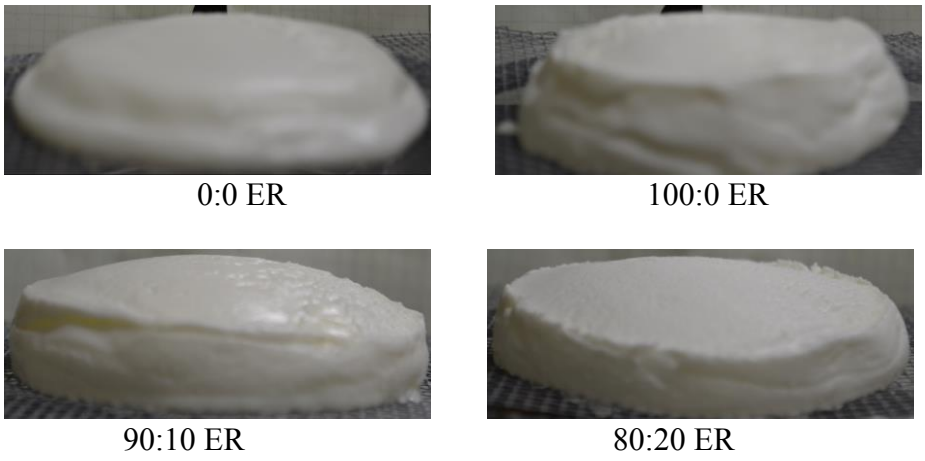

Figure H.20: Images of ice cream structure left on top of screen at the end of a drip-through test of ice creams made with (0:0 (mono- and diglyceride:polysorbate 80 - MDG:PS80)), 100:0 (MDG:PS80), 90:10 (MDG:PS80), and 80:20 (MDG:PS80) emulsifier ratios (ER) at 100% overrun and 750 RPM.